Behaviour of Prefabricated Modular Buildings Subjected to Lateral Loads

Tharaka Gunawardena

ORCID: 0000-0001-6958-1470

A thesis submitted in total fulfilment of the requirements for the degree of Doctor of Philosophy

Department of Infrastructure Engineering

The University of Melbourne

October 2016

Abstract

Prefabricated Modular Buildings are increasingly becoming a highly sort after technology to achieve cost effective and speedy construction in the construction industry. This increasing trend for prefabricated modular buildings has now spread into multi-storey applications since they can provide a much faster output for the ever increasing urban construction demand. In this regard the effect of lateral loads become critical as the height of the buildings increase. Therefore, the design of lateral load resisting systems is vital for these structures to perform effectively.

However, there is an absence of detailed scientific research or case studies that investigate into the structural performance of modular buildings. This knowledge gap has resulted in a lack of confidence in Structural Engineers to optimise the designs of modular buildings. This has resulted in modular buildings being uneconomically over-designed in order to ensure structural stability and safety.

This thesis will therefore formulate a methodology for modular buildings to be analysed and designed against lateral loads according to globally accepted methods. The knowledge gained about the structural behaviour and performance against lateral loads of modular buildings will be used to propose key design principals that Engineers can use in designing modular buildings. It will also lead to an understanding on how modular structures can be optimised to achieve a more economical solution without compromising the structural stability and safety at the expected performance levels.

In order to achieve these objectives global analysis of multi storey modular buildings is conducted with a newly proposed structural system that successfully addresses many shortcomings of modular structural systems that are presently being used. This new structural system is first analysed using global analysis models using nonlinear static pushover analysis and nonlinear time history analysis techniques. The module to module connections that are critical in transferring the lateral loads to stiffer members of the structure are then studied in detail using finite element

modelling and laboratory experiments. The results of these analyses and experiments are critically evaluated in order to present a better understanding of the behaviour of multi-storey modular buildings under lateral loads. The thesis introduces the critical modes of failure that were identified for the module to module connections through the aforementioned analyses and explains how the structural design of the connections as well as the overall structure shall be approached.

In addition to the design methodology, practising Engineers would also require a solid technique to analyse these structures using commercially available analysis software. In this regard, this thesis produces a methodology that can be used to estimate the overall stiffness of the module to module connections so that these values of stiffness can be used in modelling the connection as spring or link elements in a global model. This information would be quite useful for engineering applications as many of the commercially available software provide this capability in modelling connections as spring or link elements but lack guidance on how the value of stiffness needs to be estimated.

Therefore, this thesis provides a preliminary knowledge-base for a new modular structural system to be established with a sound understanding on how it behaves under lateral loads and how the analysis and design of the overall structure can be approached confidently. Additionally recommendations are provided to take this research forward in developing the technology further with a much broader understanding on various loading conditions and applications.

Declaration

This is to certify that;

i) the thesis comprises only my original work towards the PhD,

ii) due acknowledgment has been made in the text to all other material used,

iii) the thesis is less than 100,000 words in length, excluding tables, maps, bibliographies and appendices.

Tharaka Gunawardena

October 2016

Acknowledgement

At the completion of my candidature, I wish to express my sincere and heartfelt gratitude to my supervisors Associate Professor Tuan Ngo, Professor Priyan Mendis, Associate Professor Lu Aye and Dr Robert Crawford. They have helped immensely in creating a welcoming and supportive environment to carry out my research from the beginning to the end. I wish to acknowledge that their expert knowledge and experience which was shared with me without reservations was key to the success of my research.

I am also thankful to all former PhD students, post-doctoral researchers and lecturers at the Department of Infrastructure Engineering, The University of Melbourne for their continuous support throughout my candidature. I wish to specially acknowledge the support of the administration staff at the department for their kind and helpful efforts in providing valuable assistance with daily operations as well as other formalities.

I am thankful to The University of Melbourne in granting me the Australian Postgraduate Award – Industry (APA-I) scholarship and providing me with all necessary facilities for a worthwhile engineering research. The Thesis Bootcamp which was organised by the Melbourne School of Engineering was especially helpful in preparing me and getting me started with my thesis.

I am also thankful to my former lecturers from the University of Moratuwa, Sri Lanka for their valuable advice and guidance which provided me with the basic knowledge I needed to start my engineering career. In the same note I am also thankful to my former employer Eng. Shiromal Fernando for mentoring me throughout my career.

Eventually I wish to dedicate this thesis to my parents, my wife, my grandmother, my parents-in-law, my sister and my siblings-in-law whom I am in debt for providing me with love, encouragement and understanding which guided me to achieve greater heights.

Contents

List of Figures

List of Tables

List of Notations

ABSSUM	Absolute sum
ADRS	Acceleration-displacement response spectrum/spectra
AEC	Architectural, Engineering and Construction industry
AISC	American Institute of Steel Construction
APEC	Asia-Pacific Economic Corporation
ASCE	American Society of Civil Engineers
ATC	Applied Technology Council
BIM	Building Information Modelling
CMP	Consecutive modal pushover procedure
CQC	Complete quadratic quotients
CSI	Computers and Structures Incorporated
CTBUH	Council on Tall Buildings and Urban Habitat
CUREe	California Universities for Research in Earthquake Engineering
DBLSUM	Double sum
FEM	Finite element model
FEMA	Federal Emergency Management Agency
GFRP	Glass-fibre reinforced polymers
GMC	General modal combination

HIC-HLRN	Habitat International Coalition - Housing and Land Rights Network
MCE	Maximum considered earthquake
MDOF	Multi degree of freedom
MEP	Mechanical electrical and plumbing
MMI	Modified Mercalli Intensity scale
MMP	Multi-mode pushover procedure
MMPA	Modified modal pushover analysis
MMS	Moment Magnitude Scale
MPA	Modal pushover analysis
MSB	Modular steel buildings
MWN	Mercalli-Wood-Newman scale
NRC	Nuclear Regulatory Commission
OSM	Off-site Manufacturing
PBSD	Performance based seismic design
PDHRE	People's Movement for Human Rights Education
PEER	Pacific Earthquake Engineering Research Centre
PFC	Parallel flange channel
PGA	Peak ground acceleration
PGD	Peak ground displacement
PGV	Peak ground velocity
PRC	Pushover results combination method
RC	Reinforced concrete

RHS	Rectangular hollow section
SAC	Joint venture of SEAOC, ATC and CUREe
SDOF	Single degree of freedom system
SEAOC	Structural Engineers Association of California
SHM	Structural health monitoring
SHS	Square hollow section
SPT	Standard penetration test
SRSS	Square root of sum of squares
UA	Universal angle
UNDRO	United Nations Disaster Relief Organisation
USGS	United States Geological Survey
A	Maximum excursion (amplitude) on the Wood-Anderson seismograph
A_0	Bolt shank area
A'_0	Empirical function that depends on the distance to the epicentre from the station (δ)
A_s	Tensile stress area of the bolt
a_e	Minimum distance from the ply edge to the centre of the hole in the direction of the bearing load
$\underline{C}$	Damping matrix
C_0	Modal participation factor
C_1	Factor to account for increased displacement of short period structures
C_2	Modification factor to account for hysteresis shape
C_3	Factor to account for second order effects

d	Diameter of the bolt hole
d_f	Bolt diameter
E	Modulus of elasticity
e	Width across corners
e_{nut}	Width across corners of the nut
f_{uf}	Minimum tensile strength of the bolt
f_{up}	Minimum tensile strength of the ply
G	Shear modulus
g	Gravitational acceleration
I	Second moment of area
$\underline{K}$	Stiffness matrix
k	Thickness of bolt head
k_b	Factor for bolt hole type (1.0 for standard holes, 0.85 for oversize holes and short slots and 0.70 for long slotted holes)
k_{br}	Combined stiffness of the bolted connection against combined shear and tension
k_m	Stiffness of the clamped material
k_p	Probability factor as per Table 3.1 of AS 1170.4: 2007
k_{slip}	Stiffness of the connection at elastic slip stage
k_r	Reduction factor for length of bolt line (bears a value of 1.0 for connections other than lap connections)
k_τ	Stiffness of the connection against shear
L	Grip length of the bolt

$\underline{M}$	Mass matrix
M_0	Seismic moment
M_L	Richter scale
M_W	Moment magnitude scale
M_1^*	Effective modal mass for the fundamental mode of vibration
m	Thickness of standard nut
m_j	Lumped mass at the j^{th} floor level
N_{tf}	Nominal tensile capacity of the bolt
N_{tf}^*	Design tensile force of the bolt
N_{ti}	Minimum pretension imparted on the bolts during installation
n_{ei}	Number of shear planes
n_x	Number of shear planes in the unthreaded region
R	Response of a structure (shear, deflection etc.)
R^2	Coefficient of determination
R_i	Response of an individual mode of a structure (e.g. modal deflection)
$R_{i\,max}$	Maximum response of an individual mode of a structure (e.g. maximum modal deflection)
R_{max}	Maximum response of a structure (maximum shear, maximum deflection etc.)
RZ	Participation of the modal mass to rotational movement about Z (vertical) axis
$\underline{S}$	Matrix that represents the inelastic strength with respect to the hysteretic behaviour
$S_a \left({}^{T_e}/_{2\pi}\right)^2$	Response spectral displacement

s	Width across flats
s_{nut}	Width across flats of the nut
T_e	Effective natural period
T_n	Natural period
t_p	Thickness of the ply
U_N	Roof displacement
UX	Participation of the modal mass to translational movement in X direction
UY	Participation of the modal mass to translational movement in Y direction
u	Displacement vector
$\dot{u}$	Velocity vector
$\ddot{u}$	Acceleration vector
$\ddot{u}_g$	Gravitational acceleration
V_b	Base shear
V_b	Bearing capacity of the ply
V_f	Nominal shear capacity of the bolt
V_f^*	Design shear force of the bolt
V_p	Tear-out capacity of the ply
V_{sf}	Slip resistance of the bolted connection
β_j	Damping ratio for the j^{th} mode
δ	Distance to the epicentre from the measuring station
δ_t	Peak displacement
ϵ_{ij}	Modal correlation coefficient

θ_p	Angle of principal stress
μ	Ductility
μ	Coefficient of friction between plies
σ_e	Equivalent (von Mises) stresses
σ_x	Normal stresses in the x direction
σ_y	Normal stresses in the y direction
τ	Influence vector for ground displacement
τ_{max}	Maximum shear stress
τ_{xy}	Shear stress
Ø	Capacity reduction factor as per Table 3.4 of AS 4100: 1998
ϕ_{j1}	j^{th} floor element of the fundamental mode
φ_m	Maximum curvature
φ_y	Yield curvature
ω_i	Natural frequency

Chapter 1 Introduction

1.1. Background

Prefabrication and modularisation have both separately and jointly been a part of building construction for many years in various forms. Prefabricated dry wall systems, roof trusses, beams, rebar cages etc. and modularised furniture, plumbing systems etc. are such examples. Similarly, the demand to complete building constructions within a short time period while continuing to improve the quality of the output has also been a critical performance criteria that the Architectural, Engineering and Construction (AEC) industry has been striving to achieve.

The concept of prefabricated modular structures has arisen in recent times as an effective solution to the AEC industry to achieve both speedy construction as well improved and sustainable quality of the final product. Prefabricated building modules (such as apartments, office spaces, stair cases etc.) can be fully constructed with architectural finishes and services inside a quality controlled factory environment, ready to be delivered and assembled on site to form a safe and stable structure. Most manufacturers will nowadays cater for any architectural design with innovative modular units accordingly. Such building modules are mass produced in factories where the intense labour which would have otherwise been required at a conventional building site is replaced with specialist workmanship and machine handling in a mass production facility.

As more innovative and unconventional designs are generated through modern architecture, prefabricated modules with different shapes and sizes will be demanded. A building designer is free to lay out a building in the conventional manner to suit a client's desire and the requirements of the market. The building would then be adjusted and divided into units that are in width and length suitable for transportation and lifting into position by a crane on site.

Although the technology in using prefabricated modular structures is fairly new, it is becoming increasingly popular in the AEC industry due to its many attractive features that serve well for designers, builders as well as the ultimate dwellers.

This project was sponsored by Australian Research Council through a Linkage Grant. The research direction and methodology were planned and implemented through close consultation with the industry.

1.1.1. Applications of Prefabricated Modular Structures

Modular technology has already been used on many low rise structures around the world and is gaining popularity in being used for multi-storey medium to high rise buildings as well. Some of the notable applications of this technology is described below;

Little Hero Building in Melbourne, Australia

The low rise apartment building 'Little Hero' in Melbourne, Australia (Figures 1.1 and 1.2) is a great example among many others. The building consists of 58 single-storey apartment modules and 5 double-storey apartment modules.

Figure 1. 1. A conceptual image of the modular building 'Little Hero' in Melbourne, Australia

Figure 1. 2. An image from the modular building 'Little Hero' after being built and occupied (Left) and one during its on-site assembly (Right)

The 8 modular stories were assembled with finishes within 8 days and the building was constructed in a site with a very narrow access road demonstrating many advantages of modular construction. This is also a noteworthy construction as it is one of the earliest multi-storey modular constructions in Australia and the world.

SOHO Apartment Building in Darwin, Australia

Figure 1. 3. SOHO Apartments in Darwin, Australia (IrwinConsult, n.d.)

This 32 storey building (Figure 1.3) is presently the tallest modular building in the world. This building was completed in September 2014 and consists of 21 modular storeys. The modules have used concrete floors as a special feature in this construction. The concrete floors have been used as an alternative to any light-weight material to better cater for the high humidity in the tropical Northern Territory of Australia and also provides an improved fire rating.

Student Housing Building in Wolverhampton, UK

This 25 storey apartment building (Figure 1.4) has been completed with only 27 weeks of on-site work. Lawson et al. (2012) explain that this has resulted in a 50 per cent saving from the on-site construction time estimated for a conventional site-intensive project. The productivity has been estimated in terms of savings in man-hours to an 80 per cent improvement from a site-intensive construction. In addition, Lawson et al. (2012) state that modular construction can reduce site wastage up to 70 per cent compared to site-intensive construction methods.

Figure 1. 4. A 25 storey modular building in Wolverhampton, UK (Lawson et al., 2012)

Therefore, not only have modular structures proven time-efficient, but they have also proven to be more environmentally friendly, providing energy-efficient solutions. As discussed by

Lawson et al. (2012) in general prefabricated modular buildings have proven to reduce construction waste considerably and this is mainly through means of minimised off-cuts (Osmani et al., 2006).

One9 Apartment Building in Melbourne, Australia

'One9 Apartments' is a ten storey modular building built in one of the inner suburbs of Melbourne, Australia that consists of 34 apartments which are designed for energy efficiency and comfortable liveability. The above ground modular floors as shown in Figure 1.5 were assembled on site in as few as five days. The site (Figure 1.6) was constrained by a nearby large shopping mall which was not to be disturbed. Modular technology proved to be the best solution to cater for the client's need in constructing a ten storey building in only a few days which helped to save a significant cost that the client would have otherwise foregone in dealing with a construction in a heavily congested suburb with a difficult set of constraints that limited the work flow on site.

Figure 1. 5. 'One9 Apartments' modular building in Melbourne, Australia

Figure 1. 6. One9 Apartments during construction (Hickory Group, 2014)

The 'One9 Apartments' development also has secured a 6-star rating from Green Star Australia for its many features that promote sustainable construction by example. Modular construction has proven its value in many avenues in this project especially considering the fact that it was built in a land as small as 277 square metres.

In addition to many examples where modular structures have been used for commercial use, they have also been quite a productive solution for post disaster relief operations. Some post disaster housing reconstruction programmes where prefabricated modules were used are discussed below;

Post Katrina Housing in Mississippi, USA

Due to the large housing demand which followed the Hurricane Katrina disaster in 2005, much research has gone into improving the previously used 'FEMA Trailers' and to implement modular construction for temporary housing. A design by Architect. Marianne Cusato inspired this modular house, which was named the 'Katrina Cottage'. It was designed to be installed with a floor area of 27.8 square metres. However this was improved to incorporate a more permanent housing solution with 20 different cottage models that allowed for future extensions (McIntosh, 2013).

Reconstruction after Haiti Earthquake in 2010, Haiti

Following the Haiti earthquake in 2010, the Canadian Embassy in Haiti had carried out the installation of 46 modular housing units as temporary shelter for 75 individuals. This was however carried out as a temporary housing solution to serve for the immediate needs of disaster victims until more permanent housing solutions were arranged.

1.2. Significance of the Research

When observing the existing modular structures, two main types of modules can be identified in the form of load bearing modules and corner supported modules which are described in detail in Chapter 2. Load bearing modules are more suited for single and double storey applications where the structure would need to withstand primarily gravity loads. However, the lateral load resisting mechanisms become more critical in taller buildings. Therefore the corner supported modules are a more viable option for multi storey applications as their connections are capable of connecting elements both vertically and laterally unlike those in load bearing type modules.

It is observed that there is a significant knowledge gap in the understanding of the structural behaviour of corner supported modules and therefore many of the buildings are essentially over designed to ensure their safety and structural stability. This knowledge gap becomes more significant in medium to high rise applications where the lateral loads are more critical.

In this regard, the understanding of the behaviour against both wind and earthquake forces are essential. It is also necessary to investigate into the makeup of the key elements of the lateral load resisting mechanisms that are used in modular structures. The connections that transfer these lateral loads are critical in the safety and stability of the system when subject to lateral forces. The research was therefore motivated by the many problems that can be solved by bridging this knowledge gap, and was focused to establish the role and performance of the connections in modular buildings in the overall lateral load resisting mechanism.

Wind and earthquake loads are the main lateral loads resisted by a structure. Wind loads are generally evaluated through quasi-static linear analysis methods and analysis is quite straightforward. However, earthquake analysis methods are more complicated and usually involve nonlinear dynamic analysis techniques. Therefore, this thesis will focus on earthquake analysis and design. However, the findings are generally applicable to both earthquake and wind loads.

It is also observed that most multi-storey modular buildings use a central concrete core to act as the main lateral load resisting system. Some of those structures also include many in-situ cast elements that complete the structure. This practice is well demonstrated through Figure 1.7. The tendency to secure the structure with critical elements that are not pre-cast modular elements will deprive the structure of the many advantages that the modular

Figure 1. 7. An example of current practice in multi-storey modular construction

technology offers. It would effectively make the structure not completely modular. The thesis therefore introduces a new structural system which caters to this problem and provides a solution where a completely modular structure would be possible. This concept is described in detail in Chapter 4. The thesis will continue to use this newly introduced system as the main structural system for the case study models used to produce the analytical results. The thesis hopes to introduce this structural system as a viable and structurally efficient solution for future multi-storey modular construction.

1.2.1. Aims and Objectives

It is understood that the module-module connections are critical in resisting lateral loads and transferring them to stiffer vertical elements. The main aim of the research is to identify the role of these connections between corner supported modules in the overall lateral load resisting system. By identifying this, it is then possible to further optimise the design of these connections and introduce more innovative structural systems. The following objectives are set out in this regard;

- Identifying the general structural behaviour and load transfer mechanisms of a corner supported modular structure by analysing a 3D computer model, under gravity loads as well as earthquake and wind loads
- Identifying the contribution of connections in the performance of the lateral load resisting system
- Introduction of a new structural system where stiffer walls are used as parts of strategically selected modules. The lateral load resisting system is to be studied in detail for this concept and the contribution of the modules with stiffer wall elements is to be established in the overall lateral load resisting system.
- Evaluating the behaviour of a module to module connection subjected to a lateral load through a detailed finite element analysis. Comparing these computer generated results with laboratory testing results for validation.

- Using the validated finite element model to identify critical failure criteria of the module to module connection and thereby proposing a suitable approach to design the connection for strength and serviceability criteria. In addition, providing the theoretical background to the necessary idealisations in preparing global structural models to analyse modular buildings using commercially available software.

1.3. Research Scope and Methodology

The thesis will be focused on achieving the aims and objectives that were set out in section 1.2.1. The methodology that is set out to carry out the research from the beginning is presented as a flow chart in Figure 1.8.

The results and conclusions presented in the thesis will only cover corner supported type modules and bear a larger focus on the 'Advanced Corner Supported Modular Structural System' that is newly introduced with this thesis. The load bearing elements and the connections that make up the modular systems studied in this thesis shall all be considered to have been constructed in steel.

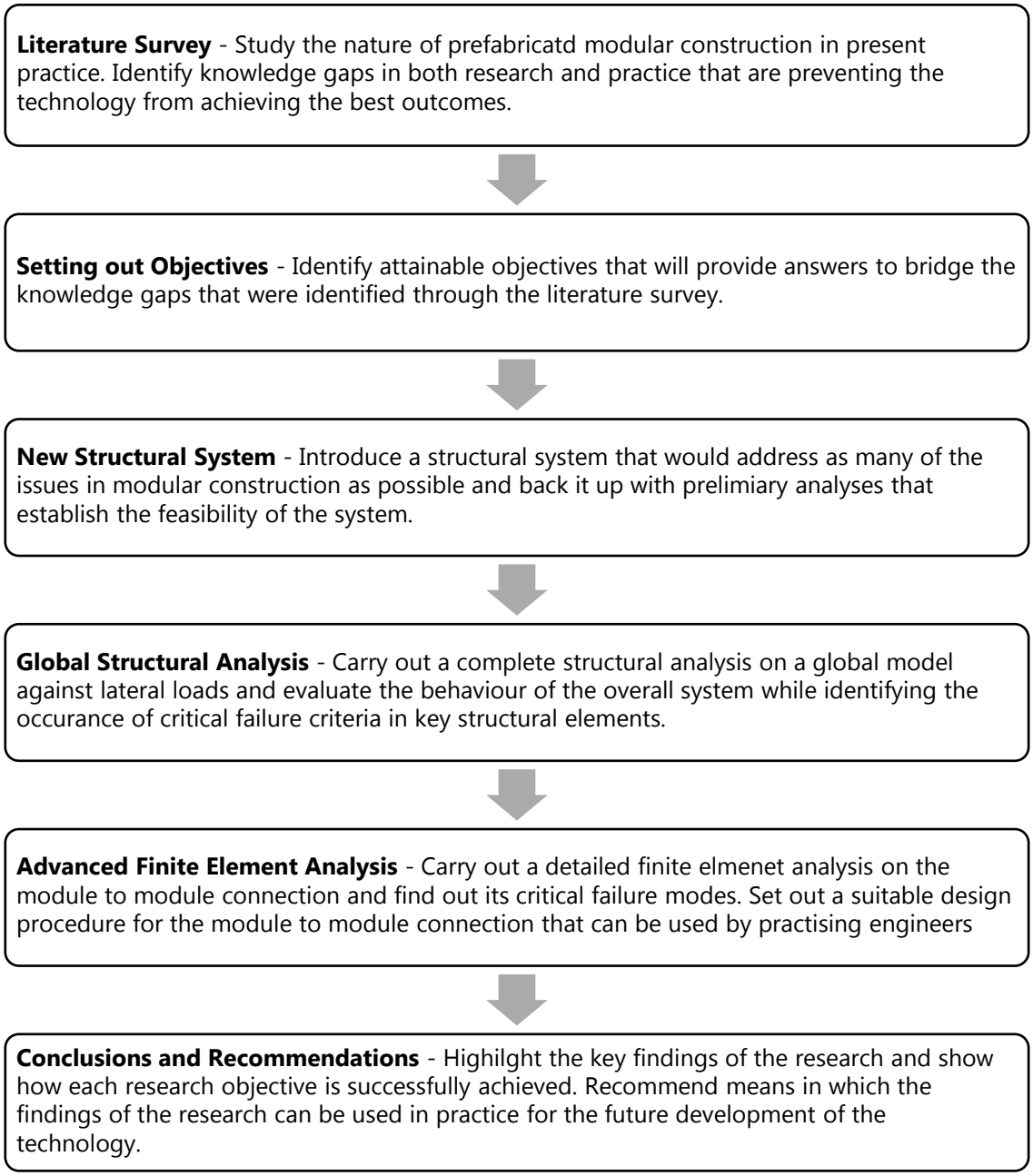

Figure 1. 8. Action plan for the research presented through a flow chart

1.4. Thesis Layout

The thesis consists of eight chapters. A brief introduction into these eight chapters is presented below;

Chapter 1 will be a general introduction into Prefabricated Modular Buildings and the progress of the technology through the years. The chapter will illustrate the popularity of the technology in the property development industry through examples of successfully completed modular buildings. A list of the key aims and objectives of the research will be presented and the significance of this research for the future of the modular construction will be emphasised in this chapter.

Chapter 2 will be a detailed literature review on Prefabricated Modular Buildings in terms of the current practice and different structural systems that are available. The chapter will discuss various ways in which modular buildings and prefabricated construction can be categorised. Many publications that have presented research on the existing prefabricated modular buildings will be critically discussed. The chapter will also discuss literature on research that has been carried out about different connections that are used in corner supported modules. Since the research focuses on steel bolted connections, this chapter will critically evaluate various literature that highlight different theoretical, analytical and experimental findings on the behaviour of such connections when subjected to lateral loads.

Chapter 3 is a review on the earthquake analysis techniques as relevant for the research objectives. The theoretical background of earthquake loads using earthquake ground motions and other resources will be discussed in this chapter. The chapter will also discuss further about different analytical methods that are carried out to investigate the behaviour of structures subjected to earthquake forces.

Chapter 4 will be mainly an introduction with analytical results to the newly introduced 'Advanced Corner Supported Modular Structural System' for multi-storey modular buildings. This will be presented through the journal paper, "An Innovative Flexible Structural System Using Prefabricated Modules" which is published in the Journal of Architectural Engineering.

Additional discussions that highlight the usefulness of this concept will also be presented in this chapter.

Chapter 5 will discuss the results of the global model carried out on a multi-storey modular building, and will discuss the behaviour and performance under earthquake loads. The analysis will be presented mainly through results generated using the software RUAUMOKO 3D. A discussion will be presented where the results of the performance of the structural system will be critically evaluated.

Chapter 6 will discuss the finite element analysis carried out on one of the module to module connections using the software ANSYS. This chapter will also discuss the outcome of the laboratory experiment that was carried out with the primary intention of validating the analysis results from ANSYS. The results will be compared and further discussions will be presented on the validation of the model.

Chapter 7 will present further analytical results from the finite element analysis which will develop an understanding on the behaviour of the bolts in each of the connection designs that are examined. The output results will be discussed in detail to arrive at a better understanding of the critical failure modes and the required details for the structural design of the connection.

Chapter 8 will explain the conclusions from the research findings and include recommendations on how the structural systems with prefabricated modules should be modelled, analysed and designed. Suggestions on future research needs will also be presented in this chapter.

1.5. List of Publications

The following journal papers have been published in the Open House International Journal's special issue on Post Disaster Housing Reconstruction, the American Society of Civil Engineers' (ASCE) Journal of Architectural Engineering and the Earthquakes and Structures Journal respectively:

- Gunawardena, T., Ngo, T., Aye, L., Mendis, P. & Crawford R. (2014), Time Efficient Post Disaster Housing Reconstruction with Prefabricated Modular Structures. *Open House International*, 39(3): pp.59-66.
- Gunawardena, T., Mendis, P. & Ngo, T., (2016). Innovative Flexible Structural System Using Prefabricated Modules. *Journal of Architectural Engineering*, 22(2), American Society of Civil Engineers.
- Gunawardena, T., Mendis, P. & Ngo, T., (2016). Behaviour of Multi-storey Prefabricated Modular Buildings under Seismic Loads. *Earthquakes and Structures: Special Issue for Australian Network of Structural Health Monitoring*, 11(6): pp. 1061-1076, Techno Press.

The following conference papers have also been published;

- Gunawardena, T., Ngo, T., Aye, L. & Mendis, P. (2011). *Innovative Prefabricated Modular Structures - An Overview and Lifecycle Energy Analysis*. International Conference on Structural Engineering, Construction & Management. Kandy, Sri Lanka

  10 min presentation on the above paper during the conference on 19th December 2011
- Gunawardena, T., Ngo, T., Aye, L. & Mendis, P. (2012). *Structural Performance under Lateral Loads of Innovative Prefabricated Modular Structures.* Australian Conference on the Mechanics of Structures and Materials. Sydney, Australia
- Gunawardena, T., Ngo, T., Aye, L., Mendis, P. & Crawford, R. (2012). *A Holistic Model for Designing and Optimising Sustainable Prefabricated Modular Buildings*. International Conference on Sustainable Built Environment. Kandy, Sri Lanka

10 min presentation on the above paper during the conference on 15th December 2012

- Gunawardena, T., Ngo, T., Mendis, P. & Alfano, J. (2014). *Sustainable Prefabricated Modular Buildings*. International Conference on Sustainable Built Environment. Kandy, Sri Lanka

  20 min presentation on the above paper during the conference in the special event held to introduce the Sri Lankan chapter of the Council on Tall Buildings and Urban Habitat (CTBUH) on 13th December 2014

- Gunawardena, T., Karunaratne, R., Mendis, P. & Ngo, T. (2016). *Prefabricated Construction Technologies for the Future of Sri Lanka's Construction Industry*. International Conference on Sustainable Built Environment. Kandy, Sri Lanka

Chapter 2 Literature Review

2.1. Background to Modular Construction

The idea of prefabricated modular construction has been used in buildings around the world for many years. Not only has this concept covered buildings specifically, but has been in use in many other related and unrelated fields such as furniture, computer hardware and automobiles.

The concepts of prefabrication and modularisation in connection to building construction targets a variety of outcomes as benefits to the Client of a project.

Some of the many benefits and features of prefabricated modular construction are as follows:

- The modules can incorporate all components of a building including stairs, lift shafts, facades, corridors and services
- The modules are mass produced in a quality controlled production facility. A unit's length, width and height can vary from project to project. It is even possible to build units of various shapes and sizes where the only limiting factor would be the transportability.
- There is minimal work on site to complete the buildings as the façade and interiors themselves form part of modules. This enables the construction process to move away from a labour oriented process to a more process oriented production and assembly process, resulting in building sites with less congestion and pollution.
- The modules are able to be removed from the main structure for future reuse or relocation. The reusability of prefabricated modules adds a large impact on modular buildings having a much lower life cycle energy (Aye et al., 2012).

- Modular construction at present reduces construction time by over 50% from a site-intensive building (Lawson et. al., 2012). The projects mentioned in section 1.1.1 are evidence for the achievement of such fast construction outputs. This ensures that the Client of the project starts generating revenue from the project much faster and invests the opportunity costs of having a different construction technology in earning further income.

2.2. Categorisation of Prefabricated Modular Types

Modular construction has gained a lot of popularity in the recent few years, and from what is already constructed it is evident that there are various types of prefabricated modules as well as various structural systems that are employed in constructing buildings out of them. This section will systematically categorise the various types of prefabricated modules according to their load transfer mechanisms, structural systems, production type and predominant building materials.

Lawson et al., (2012) identified two different types of building modules according to their load transfer mechanisms as;

1. Corner supported modules – where loads are transferred from edge beams to the supporting corner columns to the ground or a podium floor
2. Load bearing modules – where the loads are transferred from the side walls of the module to the ground

Where load bearing modules are mainly used in 1 to 2 storey buildings, it is the corner supported modules that are being used for most of the taller buildings. However, a third mechanism where an advanced corner supported system inclusive of stiff wall elements is introduced through this thesis. Therefore, according to their load transfer mechanisms prefabricated modules can be categorised into 3 types namely;

1. Corner supported modules (Figure 2.1)
2. Load bearing modules (Figure 2.1)

3. Advanced Corner Supported Modular Structural System – Where gravity loads are transferred though the side walls of the modules and lateral loads are transferred through lateral column to column connections as those in corner supported modules.

Figure 2. 1. A corner supported module (Left) and a Load Bearing Module (Right)

Lusby-Taylor et al., (2004) identified prefabricated construction in 5 categories according to the way it is manufactured and assembled on site as;

1. Modular (Volumetric) construction: production of three dimensional units in controlled factory conditions prior to transportation to site.
2. Panelised construction: Flat panel units are produced in a factory and assembled on-site to produce a three dimensional structure.
3. Hybrid (Semi-volumetric) construction: combines both panelised and modular approaches. Typically, modular units (also known as "Pods") are used for the highly serviced and more repeatable areas such as kitchens and bathrooms, with the remainder of the dwelling or building constructed using panels
4. OSM (Off-site manufacturing) sub-assemblies and components: covers approaches that fall short of being classified as systemic OSM but which utilise several factory fabricated innovative subassemblies or components in an otherwise traditionally built structural fabric, e.g. roof cassettes, pre-cast concrete foundation assemblies, but excluding window, door sets, roof trusses.
5. Non-OSM: This category is intended to encompass schemes utilising innovative housing building techniques and structural systems that fall outside the OSM categories.

The existing prefabricated modular buildings can also be categorised according to the structural system that has been used as follows;

1. Load bearing System: As described previously, this type of modular buildings use load bearing modules, and are typically 1 to 2 stories in height and occasionally slightly taller. The gravity loads of each stack of modules are run down through the side walls down to the foundation. The neighbouring modules do not share loads or transfer any lateral loads from one to the other.
2. System with Central RC Core and modules that are connected to the core directly: Here the system consists mainly of corner-supported modules as introduced previously. The gravity loads are directly transferred down to the foundation through the perimeter or corner columns of each module. One vertical stack of modules acts as one block of vertical loads. This system can go up to any height, and typically have resulted in structures of 8 to 10 stories high. The lateral load resisting system is essentially managed by the central core that is made out of reinforced concrete. The modules are connected laterally to the central core either directly or through neighbouring modules. The lateral loads are expected to be transferred to the foundation mainly through the central core.
3. System with Central RC core where modules are stacked up in rows and the floor levels are eventually poured with concrete: The poured concrete fills up the vertical gap between the roofs of a certain level of modules and the floors of the level of modules directly above it. Once hardened this concrete membrane acts as a rigid diaphragm which is continuous and connected to the core and is able to transfer all of the lateral loads to the core. However, this results in an excessive use of material in the form of concrete, where the floors and roofs of each module is already in place. It also hinders the ability of the modules to be removed and reused in a different location. In practice this system has been used in buildings that go up to 25 to 30 stories high.
4. Advanced Corner Supported Modular System with stiff modules: This is a system where the dependency of the central core is no longer a constraint to the structural system. This system is described with more details in Chapter 4.

Prefabricated modules also differ from the construction materials used in building them. Various different materials such as concrete, steel, timber and GFRP (glass fibre reinforced polymers) have been used in manufacturing prefabricated modules. Since prefabricated construction is developing at a rapid rate, new and innovative materials are being experimented to be used for various elements such as facades, bathroom fittings, plumbing, and insulation etc. in prefabricated modules. Examples of some of the main construction materials used are shown below in Figures 2.2 to 2.4;

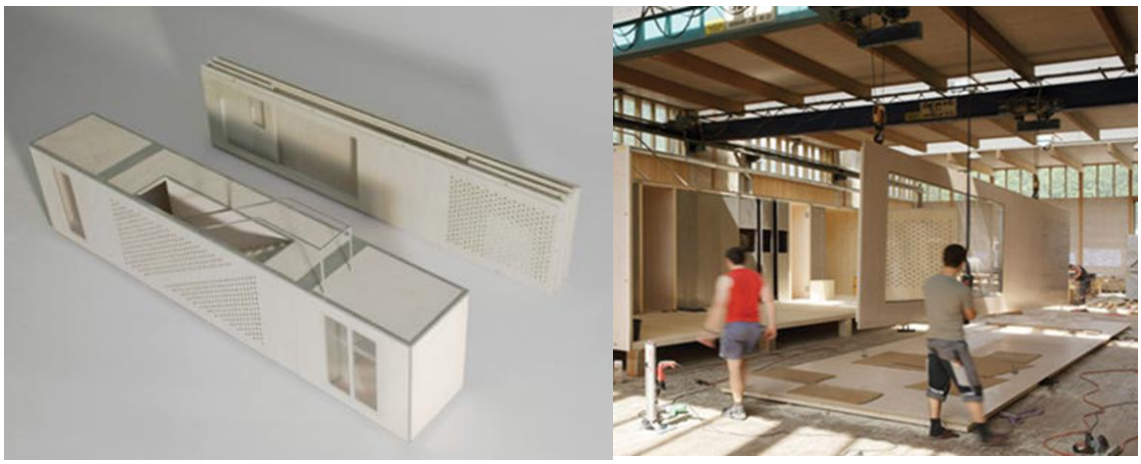

Figure 2. 2. Prefabricated modules made with timber

Figure 2. 3. Prefabricated modules made with concrete

Figure 2. 4. Prefabricated modules made with steel

2.3. Review of Literature on Structural Behaviour of Prefabricated Modular Buildings

It must be noted that the research on modular construction has thus far been focused mainly on topics such as energy efficiency, sustainability, construction technology and economic and financial aspects. Only a handful of noteworthy research on the structural behaviour of modular buildings have been reported. In that regard it must also be noted that this thesis aims at filling that knowledge gap which exists due to the lack of comprehensive research related to the structural behaviour of modular buildings.

The research work done on Modular Steel Buildings (MSB) by Annan et al. (2009a) is one rare research into the behaviour of modular systems that are subjected to lateral loads. The mentioned paper specifically analyses a typical floor of a modular building made up of six modules that are connected horizontally via filed bolted clip angles which are welded to the floor beams. This is the first instance in published literature that the use of horizontal steel connections are identified with regard to the overall design of a modular building. The methodology adopted in this research (Figure 2.5) in connecting the modules horizontally closely resembles a pure corner supported system with minor differences. For example, concrete is poured on-site on top of the horizontal connection after the bolting of clip angles from two neighbouring modules. It provides a key insight into the principles adopted in modelling the steel joint in a global analysis model. The lateral connections are modelled as

spring or link elements at the common joint to allow independent rotation of the connected modules. These connections are assumed to be rigid connections for the purpose of forming the computer model. This research has provided a valuable insight mainly into the modelling of the horizontal steel connections.

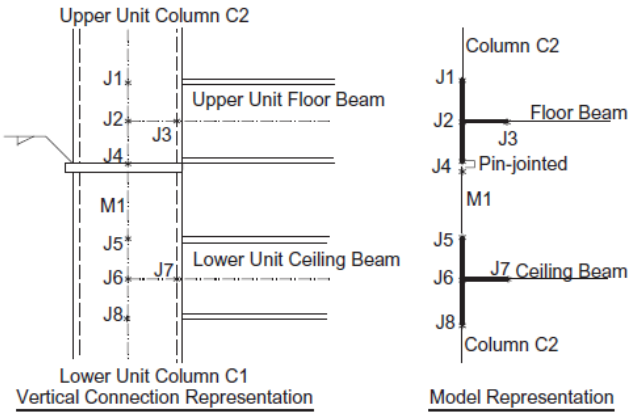

Figure 2. 5. Modelling idealisation for module to module connections proposed by Annan et al. (2009a)

In addition, Annan et al. (2009b) conducted a seismic assessment of several typical modular steel buildings. Specimens of 2-storey, 4-storey and 6-storey modular buildings in a braced system showed predominantly first-mode response with some sensitivity to higher modes against earthquake forces. Where the maximum drifts in the elastic region were shown in the top stories, highest concentration of inelasticity was shown in the first floor level. The authors concluded that this was due to the limited redistribution of internal forces from one story level to the other, and the inelastic behaviour of braces within the modules that occur as a result.

Studying a set of modular steel frames which were fitted with double skin steel walls against applied cyclic loading, Hong et al. (2011) presented some important findings on the structural performance of steel modules which are stiffened by double skinned steel walls. It was mentioned that the double skin steel walls were made with two layers of corrugated steel panels sandwiched between steel plates and soldered at connecting ends. It was found that the lateral stiffness of the steel modules that were fitted with double skin steel walls were 4 times higher than that of the steel modules without double skin steel walls. Further, the

double skin steel wall panels yielded before the yielding of the internal columns of the modules which ensures that the modules will show warning signs before failure at ultimate state. The results had also been validated by a nonlinear structural analysis, however, the modelling details were not presented in too much clarity.

Both these research projects are highly relevant for the subject matter and useful in identifying the used test procedures and how test results are validated using computer models. Annan et al. (2009a) in addition used structural period and modal participation factors to demonstrate and to an extent validate the structural behaviour of the modular steel-braced frames.

Further, Lawson et al. (2008 and 2010) briefly discussed structural stability and robustness of modular structures. They show the robustness of modular structures in the form of providing an alternative load path in two ways. Firstly, if one of the corner supports of a module fails, the tying action of connections keeps the failed module in equilibrium with a stressed skin action acting on the walls. Where the supports are continuously removed the walls undergo in-plane shear forces resembling the action of a deep beam. Although this is a detailed discussion of robustness and structural stability of modular structures there are no recommendations to solve the problem or how to improve the system after identifying these characteristics.

2.4. Other Attributes of Modular Construction

As previously discussed, although there is a considerable lack of research done in establishing the structural behaviour of modular buildings there has been a number of notable publications that have investigated into many other aspects of modular construction. Some of those publications are discussed here.

2.4.1. As Temporary Structures

Prefabricated modules have been used around the world as temporary housing solutions for various situations. Post disaster reconstruction programmes are the leading employer of this method of temporary housing. It is observed that in recent times especially after the tsunami disaster in Japan in 2012, many hundreds of prefabricated modules were used as single and multi-unit temporary houses that were deployed with a short period of notice. The advantage was that the units could be made available for deployment in a very short period and they did not require additional construction to be carried out after being deployed to the sites.

Another form of temporary accommodation is construction site offices. It is a common observation that many modular type units are used in construction sites as offices, toilets, kitchens etc. They provide many advantages such as;

- low cost establishment of a site office,
- quick setting up so that it does not disrupt the construction process going on in the site
- ability to be reused in many more construction projects

All these minor uses can be incorporated into a major project that is constructed mainly out of prefabricated modules.

2.4.2. As Permanent Post-disaster Housing

As explained in section 2.4.1, the practice up to now has been to employ prefabricated modular units as temporary housing for post-disaster reconciliation activities. However, the nature of the prefabricated modular construction process provides the unique ability for it to be used as permanent housing as well, which will significantly reduce the time taken to provide solutions to disaster-affected communities.

Many houses can be simultaneously built through mass production facilities and also simultaneously installed on-site, which will cut down construction time. This time saving means that the affected communities can recommence their livelihoods much sooner.

Further, the funding for the project will also make greater savings by avoiding time fluctuations in material and labour costs and exchange rates.

a) Resource Availability and Integration

Yan et al. (2010) categorised resources as "*Government-driven, Market-driven and Donor-driven*" prior to identifying the related issues. They have identified that although government-driven operations have an initial advantage of price and rate interventions from the government, eventually they succumb to economic factors such as inflation of material prices and rises in wages. Donor-driven processes have shown a lack of capacity in having resources available. Market-driven processes are seen as the most desirable in terms of performance and results, but they lack support from the other parties involved, such as governments and humanitarian agencies.

In a later study, Yan et al. (2011) identified five main types of factors that affect resource availability in post-disaster reconstruction, namely:-

- Market- related factors
- Logistics-related factors
- Project-related factors
- Organisation-related factors
- Environment-related factors

Tas et al. (2010 & 2011) have reported that almost 16 different contractors were involved in the reconstruction process after the Kocaeli earthquake in Turkey. This is a large number of different firms working on the same project, which would eventually require a good platform of integration.

Solutions from Modular Housing

Although modular construction as a technology may not solve the resource availability issue, it has the potential to considerably reduce the burden of finding resources. Many logistics-related factors as stated by Yan et al. (2011) can be reduced by having almost all of the

operations running under one manufacturing plant; whereas in a site-intensive construction different resources would need to be called upon at different times by different contractors.

Arshad & Athar (2013), in their study on the rehabilitation after the Kashmir earthquake, have pointed out that engaging a limited number of parties in the reconstruction process is a key success factor. Modular construction by its character involves a minimum number of parties, as the house is already built by the time it arrives on site. Most of its construction is done as pre-organised mass production, which is streamlined and will mostly not be affected by the nature of the situation. Most processes are already integrated before modular units are assembled on site. Modern integration techniques, such as Building Information Modelling (BIM), can also be easily incorporated to support the design and planning process of modular construction.

b) Availability and Skills of Workforce

The number of houses that need reconstruction after a large-scale natural disaster can be extremely large. This requires an appreciably large workforce, which may be unrealistic to be found at once. Arshad & Athar (2013) also acknowledged the fact that lack of knowledge and/or skills of the locals assisting was a key issue during the reconstruction process in Pakistan.

Solutions from Modular Housing

The expertise needed for the construction of a modular housing unit is mostly needed inside the manufacturing facility. Once the modules arrive on site, they will only require a minimum amount of labour for the installation process. As mentioned previously, it is observed that local communities volunteer during many housing reconstruction processes, and the expertise needed in the on-site construction of modular houses is minimal where they can provide a better and more efficient service. The activity needed on-site can be as minimal as tightening a few nuts and bolts, and local volunteers with minimum work experience could be trained easily to carry out these tasks.

c) Lack of Expertise in Planning

As previously mentioned through publications of institutions such as Oxfam (2003) and Roosli et al. (2012) identified a lack of expertise and knowledge in the relevant authorities about the process of housing reconstruction as a major setback in the housing reconstruction process. They also identified the importance of all approaches and plans being integrated as a universal plan, which is lacking in many large-scale post-disaster housing operations.

Solutions from Modular Housing

A high percentage of the construction process of a modular structure is a pre-planned process carried out in a factory environment. The process to construct a module from its raw materials does not need any drastic changes even during a post-disaster reconstruction scenario.

External parties would only get involved in the on-site construction and for integrating the infrastructure. Modular units are generally built with provisions for services and it is only a matter of connecting them on-site once the modules are assembled. Further, since the interiors as well as façades, roofs, etc. are all pre-constructed into the modules, the planning required becomes much simpler. This provides a more workable platform for institutions of various disciplines, such as contractors, governmental institutions, non-governmental organisations and humanitarian agencies, to work together and produce better results.

d) Overall Quality of Houses and End User Satisfaction

Eventually, the satisfaction of the end users is a key concern. Although the affected individuals may eventually be thankful for the resettlement of their livelihoods after possibly losing all their possessions, it must be understood that they are entitled to have their own opinion on the quality of the finished product. For this reason institutions such as FEMA, APEC and UNDRO have set standards for post-disaster housing reconstructions.

Structural Engineers Association, Washington (2011) with respect to the post-disaster operations in Japan, suggests that having timely solutions to housing will reduce the burden on social services, and the stress on affected individuals by living in temporary shelters. To satisfy this requirement fully, the housing solutions will need to cater to most of the

requirements of those individuals which will then reduce their grievances by having minimal defects and desires not fulfilled.

Solutions from Modular Housing

The production of a housing module is done in a highly quality controlled environment. The quality checks inside a mass production facility will be more reliable compared to an on-site construction, especially in a post-disaster scenario where on-site construction will be under heavy pressure for rapid delivery.

Further, modules can be adjusted to suit the needs of the end users, and as the construction is highly time efficient, the parties involved can take time to analyse the situation and to plan for the specific requirements of the affected community. This will make sure that the final product suits them with respect to both structural stability and liveability.

Other Benefits

Modular construction requires minimum access roads as on-site construction will be minimal. Modular units can be shipped in or transported on trucks and placed on-site using mobile cranes. This is a very convenient and practical method of construction, especially in a disaster struck area where vehicle access could be a key limiting factor.

Modular structures have proven to be more environmentally friendly than conventional steel or concrete buildings. Far less waste is generated by modular construction, thereby giving it an edge in having a smaller impact on the environment, which may result in time and cost savings over reduced expenses in dealing with waste disposal. In further studies, Aye et al. (2012) have found that more than 80% of the embodied energy in an original steel modular system can be saved by reusing the modules. It is important to notice the advantage provided by modular units by its ability to be easily dismantled and relocated as and when the need arises. This can provide a great deal of flexibility in a post-disaster housing operation.

Modules can also be easily dismantled for relocation. If the tenants are unhappy with where they are located the relevant agencies can help them relocate with the houses they have been provided with. This adds value to the operation by being more oriented towards the human needs as suggested through HIC-HLRN and PDHRE human rights requirements.

2.4.3. Other Applications and Benefits

Prefabricated modules are seen in many other minor yet demanding uses as follows;

- Granny flats – prefabricated annexes to existing houses which can be ordered and assembled on-site and have the whole construction completed in a matter of days
- Service pods – separate wet and dry spaces such as toilets, kitchens, storage rooms etc. that can be attached to existing structures
- Enclosures – internal fixes that can be brought in and installed inside an existing structure such as office spaces for factories

Therefore, it is clear that modular construction techniques are very useful in laying out the landscape for the future of construction in both large scale as well as small scale building projects and building components. It is required now to fill the knowledge gaps that exist in the structural analysis and design of modular buildings to make sure their benefits can be made fully available to the society.

Chapter 3 Earthquake Analysis and Design

3.1. Background

As discussed in Chapter 1, the focus of this thesis is the seismic performance of the considered modular structural system. The seismic performance can be evaluated in many ways. As per the Australian Standard AS1170.4: 2007, the analysis can be carried out as a quasi-static analysis as well as a dynamic analysis. The dynamic analysis could follow the dynamic response spectra given in the standard or apply a dynamic earthquake time history.

Seismic analyses can be categorised in many ways. According to how the analysis is carried out, they can be divided into two categories as static and dynamic earthquake analyses. It could also be categorised as force-based and displacement-based according to the principles that govern the limiting criteria. The force-based approach follows the commonly practiced limit state analysis which is produced through many design standards around the world. Displacement-based analysis focuses more on the performance aspects of the structure in relation to its target displacements or drifts under a given earthquake force. For this reason, displacement-based earthquake designs are more commonly known as Performance Based Seismic Design (PBSD).

The response of a building to dynamic forces that are applied on it are dependent on the modal characteristics of the building. The dominant modes in terms of their mass participation ratios, will bear a larger influence on the actual response of the structure to an applied lateral force. Static earthquake analysis procedures that are proposed in design standards follow a much simplified method to calculate the resulting forces and displacements. However, they still refer to a structural period that is generated as a function

of generic mass and stiffness based characteristics of the building. However, since the static analysis procedures do not take the inertial effects into consideration they are also known as Quasi-static Analyses.

The categorisation can be summarised as follows;

- Linear static analysis
- Nonlinear static analysis
- Linear dynamic analysis
- Nonlinear dynamic analysis

While the earthquake analysis methods have a wide variety, earthquakes themselves differ from each other by a number of parameters, namely;

- Intensity
- Depth
- Duration
- Peak Ground Acceleration (PGA)
- Peak Ground Velocity (PGV)
- Peak Ground Displacement (PGD)
- Energy Released
- Damage Caused

Several scales are used in practice around the world to categorise earthquakes according to their 'magnitude' which is a measure of the intensity of an earthquake and the energy released during the event. Such scales used to estimate the magnitude are;

- Richter Intensity Scale (M_L)
- Moment Magnitude Scale (M_W/MMS)
- Mercalli Intensity Scale and Modified Mercalli Intensity Scale (MMI)

These different scales that measure magnitude and the parameters used to calculate them are briefly discussed below;

Richter Intensity Scale (M_L)

$$M_L = \log_{10} A - \log_{10} A'_0(\delta) = \log_{10}[A/(A'_0(\delta)])$$ Eq. 3.1

Where, M_L = Richter Intensity

A = Maximum excursion (amplitude) on the Wood-Anderson seismograph (USGS, 1989)

A'_0 = Empirical function that depends on the distance to the epicentre from the station (δ)

δ = Distance to the epicentre from the measuring station

Richter Intensity Scale is the first intensity scale that was available to measure the intensity of earthquakes in the world. It was a stepping stone to further advancements in the field.

Moment Magnitude Scale (M_W)

$$M_W = \frac{2}{3}\log_{10} M_0 - 6.07$$ Eq. 3.2

Where, M_0 = Seismic moment in Nm

The constants that are applied on the Moment Magnitude Scale (2/3 and 6.07) are applied in order to make the scale more compatible with Richter Intensity Scale values.

The observed effects of different range of values of the Moment Magnitude Scale (Similar values would result from the Richter Intensity Scale) are listed in Table 3.1 as shown below;

Table 3. 1 Classification of Earthquakes according to their Magnitudes on Moment Magnitude Scale and their Estimated Frequency of Occurrence (Average Annually)

Magnitude (Assuming M_W~M_L)	Description	Observed Effects	Estimated Frequency of Occurrence – Avg. Annually (USGS, 2012)
Less than 2.0	Micro	Recorded by Seismographs but not generally felt by humans	-
2.0 -2.9	Minor	Felt by some sensitive humans but no damage to man-made structures	1,300,000
3.0-3.9		Felt by humans often but no damage to man-made structures, however shaking of domestic objects can be noticed	130,000

4.0-4.9	Light	Felt by humans and makes rattling noises indoors and shaking of objects and at times falling over or toppling. Damage to man-made structures is minimal to none.	13,000
5.0-5.9	Moderate	Felt by everyone. Can cause minor damage to poorly constructed structures, but minimal to no damage to other man-made structures.	1319
6.0-6.9	Strong	Strong violent shaking can be felt closer to epicentre where the shaking effects can be felt over a wider area even hundreds of kilometres. Can cause severe damage to poorly built buildings, and slight to moderate damage to well-designed buildings.	134
7.0-7.9	Major	Felt across greater distances. Can severely damage or collapse poorly built buildings and cause considerable damage to well-designed structures.	15
8 and above	Great	Can completely destroy communities closer to the epicentre.	1

Mercalli Intensity Scale and Modified Mercalli Intensity Scale (MMI)

The Mercalli Intensity Scale is developed primarily to measure the intensity of an earthquake by considering both qualitative and quantitative measures. In other words, the scale takes into account both magnitude as well as observed effects that the earthquake has on earth surface, humans, natural objects and man-made structures. The scale is quantified from I to XII after a modification in 1902.

The 12 degree Mercalli Intensity Scale was later modified in 1931 by Harry O. Wood and Frank Neumann as the Mercalli–Wood–Neumann (MWN) scale. This was again modified by Charles Richter (creator of Richter Intensity Scale) and was thereafter named the Modified Mercalli Intensity (MMI) Scale. The basic outlook of the scale remains the same with the same 12 degrees of intensity as the Mercalli Intensity scale.

Since the observed effects of an earthquake varies vastly as the distance from epicentre increases, the same earthquake can result in many MMI values depending on the location it is estimated for.

The values of Modified Mercalli Intensity (MMI) Scale are listed below in Table 3.2 against the perceived effects of the earthquakes.

Table 3. 2 Classification of Earthquakes according to their Magnitudes on Modified Mercalli Intensity Scale (UPSeis, n.d.)

Magnitude (MMI)	Equivalent Richter Intensity	Observed Effects
I	1.0 – 2.0	Not felt by many, barely noticeable
II	2.0 - 3.0	Felt by few people especially on upper floors
III	3.0 – 4.0	Noticeable on upper floors
IV	4.0	Felt by many indoors and a few outdoors. Sensations similar to a heavy truck passing by.
V	4.0 – 5.0	Felt by almost everyone, some people awakened if at night. Small objects moved. Trees and poles may shake.
VI	5.0 – 6.0	Felt by everyone. Difficult to stand. Some heavy furniture moved, wall plasters may fall and some chimneys may get damaged.
VII	6.0	Slight to moderate damage in well-built ordinary structures. Considerable damage to poorly built structures. Walls may collapse.
VIII	6.0 – 7.0	Little damage in specially built structures and considerable damage to ordinarily built structures. Poorly-built buildings will have severe damage. Walls may collapse.
IX	7.0	Considerable damage to specially built structures. Ground cracked noticeably. Wide spread destruction.
X	7.0 – 8.0	Most masonry and frame structures and their foundations destroyed. Ground badly cracked. Landslides and wide spread destruction.
XI	8.0	Complete damage. Few if any structures left standing. Bridges destroyed. Wide cracks on ground. Waves can be seen on ground.
XII	8.0 and greater	Total damage. Waves seen on ground. Objects thrown up into the air.

Several parameters are estimated in an earthquake as peak ground parameters. The following is a brief description of such parameters;

Peak Ground Acceleration (PGA)

The peak ground acceleration (PGA) is a parameter that is dependent primarily on the magnitude, epicentre distance (including mechanical properties of the travel path), and the soil conditions at the site. This value is measured directly from an accelerogram. This is also

a measurement taken directly from the instrument at a station as against a "felt measurement".

Peak Ground Velocity (PGV)

The peak ground velocity (PGV) is calculated by the integration of an accelerogram record. It is therefore the maximum value of the rate of change of ground displacements of a reference point during the passing of earthquake waves. The ratio of PGA/PGV has been studied by several researchers (Mohraz, 1976; Seed et al., 1974) and this has been introduced in an attempt to characterise the frequency content of the ground motion using a single parameter. Ground motions closer to an epicentre tend to show high peak acceleration-to-velocity ratios, whereas those on softer soils or at larger distances from the epicentre show comparatively lower values.

Peak Ground Displacement (PGD)

Peak ground displacement (PGD) records are usually obtained from the double integration of accelerograms. Consequently, reliable PGD values are more difficult to obtain, particularly since a base line correction technique is usually adopted to overcome residual drift effects (Mohraz, 1976). The PGD is a useful measurement in carrying out displacement-based designs and realistic values are important in ensuring the long period components of the design response spectra are accurate.

3.2. Basic Principles of Earthquake Analysis and Design

The seismic response of a building depends on dominant modes of vibration of the building which are defined through its mass and stiffness, the ground motion at the foundation, and the mode of soil structure interaction. The motion of a very stiff building is more similar to the ground motion whereas that of a very flexible building can be quite different. The response will be based on criteria such as the natural frequency, the damping ratio of the structure, the behaviour of the foundation, the ductility of the structure, the duration of the earthquake etc.

As discussed previously earthquake analysis procedures for buildings can take the form of either force-based design or performance-based design. Traditionally, earthquake design of buildings has been based primarily on forces. However, the large social and economic losses resulting from several earthquakes, have prompted the Engineers to embrace the concept of performance-based seismic design (PBSD). Although the basic objective of PBSD is to produce structures that respond in a more reliable manner during earthquakes, many Engineers associate PBSD with overall improved performance.

With further depth, force-based and performance-based design procedures can be categorised as linear static analysis, non-linear static analysis, linear dynamic analysis, and non-linear dynamic analysis as mentioned previously.

Detailed descriptions of each of these procedures are presented in the following section.

3.3. Force Based Methods of Earthquake Analysis

The effects of an earthquake on a structure can be evaluated in many ways. Design codes that are used around the world for Engineering practice categorise these analysis techniques into two main types namely, static and dynamic analyses. There are many different ways to analyse the response of a structure to earthquake loads that are applied according to these two main categories and some of the common methods are as follows;

3.3.1. Linear Static Analysis

Linear static analysis is carried out with equivalent static forces to simulate the dynamic action of an earthquake on the structure. Structural Engineers continue to use static analysis procedures for earthquake designs based on the notion that buildings designed this way have performed well in the past during earthquakes (Herath, 2011). Therefore, for a convenient yet justifiable design, an earthquake is applied in the form of an equivalent static force acting horizontally on the building and is intended to represent the inertial force, which

is mass times acceleration, occurring at the critical instant of maximum deflection and zero velocity during the largest cycle of vibration as the structure responds to the earthquake motion (Taranath, 1988).

Linear static analysis is a simple yet useful tool for earthquake design and produces reasonable results for low- to medium-rise regular buildings where the response is dominated by first mode. However, in the design of tall buildings, there is a significant impact on the responses from higher modes; therefore, this method would not be very appropriate in such applications.

Though a similar framework is adopted in the force-based design of buildings in different design codes, the coefficients and the distribution of lateral loads along the height of the building are different from one to the other.

3.3.2. Nonlinear Static Analysis

Certain static analysis techniques are widely used in checking structures for their nonlinear behaviour against larger lateral loads. These analysis techniques are discussed below;

Nonlinear Static Pushover Analysis

As a static nonlinear analysis, pushover analysis is one of the most used and popular methods in earthquake engineering as this method follows after a response spectrum analysis. This analysis technique provides a load versus deformation relationship of the structure, starting from a state of rest and continuing onto the ultimate failure of the structure. A horizontal load, that is representative of the equivalent static load of a particular mode of vibration of a structure, which may be conveniently taken as the total base shear of the structure, is applied to push the structure from rest to failure. Similarly, the deformation may be obtained for any storey of a building but is commonly taken at the top storey as it would usually produce the worst deformation.

Pushover analysis could be either force controlled or displacement controlled. In the force controlled method, the lateral static force is applied incrementally and deformations will result as the dependent variable. While the load increments push the building to incrementally larger deformations, the stiffness matrix of the building will change once these deformations transform the building from the elastic state to the inelastic state. In the displacement controlled method, the displacement of the top storey of the building is increased in increments such that the required horizontal force pushes the building laterally, following the fundamental horizontal translational mode of the building in the direction of the lateral load. The stiffness matrix of the building will change as before, when the building moves from elastic state to inelastic state. However, the displacement controlled method is preferred over the force controlled method, since the analysis can be carried out to the target level of displacement. Figure 3.1 shows a simple explanation of how a pushover analysis is carried out.

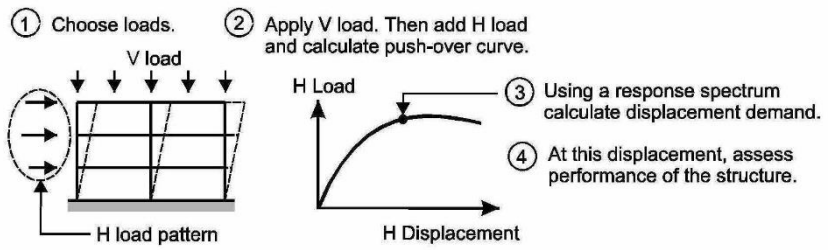

Figure 3. 1. Main steps followed in static push-over analysis (Powell, 2013)

Although the simple pushover procedure is adequate for structures with dominant first modes, more complex structures such as high rise buildings require a method that includes higher mode effects as well. In that regard, Poursha et al. (2009) presented a modified pushover procedure that account for higher mode effects. This method has aptly been named the Consecutive Modal Pushover (CMP) procedure. The CMP procedure utilises multi-stage and single-stage pushover analyses where the final structural responses are deduced by enveloping the results of the multi-stage and single-stage pushover analyses.

On a similar pursuit, a Multi-mode Pushover (MMP) method was proposed by Sasaki et al. (1998), but the earthquake demands were not clearly quantified. More recently, the Pushover

Results Combination (PRC) method (Moghada, 2002) was proposed, in which the maximum seismic response was derived from combining the results of several pushover analyses where mode shapes were considered as load patterns in each analysis. The final response was calculated as a weighted sum of the results from each pushover analysis using modal participation factors.

Chopra & Goel (2002) developed the Modal Pushover Analysis (MPA) with a similar approach to Moghada (2002). In this method the earthquake demands were separately determined for each of the modal pushover analyses and then combined using an appropriate modal combination rule. The research concluded that the MPA procedure would be adequately accurate in practical analysis and design applications. Nevertheless, the plastic hinge rotations were considerably underestimated (Chopra & Goel, 2002; Chopra & Goel, 2004; Poursha et al., 2010) even though a large number of modes were considered. A modified version of the MPA (modified modal pushover analysis-MMPA) (Rakesh, 2004 & 2005) was then proposed, in which the seismic demands of the structure were obtained by combining the inelastic response of first-mode pushover analysis with the elastic response of higher modes. Another investigation (Chopra et al., 2004) on MMPA showed that it provided a more accurate estimate of the seismic demand for structures where MPA underestimated demand relative to non-linear response history analysis.

Several more researchers (Jan et al., 2004; Sasaki et al., 1998) have proposed enhanced pushover procedures to account for higher mode effects while retaining the simplicity of invariant load patterns. The adaptive modal combination procedure (Kalkan & Kunnath, 2006) also accounts for higher mode effects by combining the response of individual modal pushover analyses and it further incorporates the effects of varying dynamic characteristics during the inelastic response via its adaptive feature.

The upper bound method which was proposed by Jan et al. (2004) reasonably predicted the non-linear behaviour and seismic demand of tall buildings. However, this procedure has a tendency to overestimate the seismic demand at the upper stories and underestimate them at lower stories. Further, in an effort to overcome the limitations of the currently used non-linear static procedures an enhanced site specific spectrum-based pushover procedure was

proposed by Gupta & Kunnath (2000). The additional feature in this method was the recognition of soft stories in the base or lower third of the buildings.

In addition, according to FEMA 450 (2003), the non-linear static pushover procedure is not appropriate for structures where higher mode effects are significant, unless a linear dynamic procedure is performed as well. To determine if higher modes are significant, a modal response spectrum analysis is proposed to be performed for the structure, using sufficient modes to capture 90% mass participation; and a second response spectrum analysis to be performed considering only the first-mode response. Further, a comparison of the pushover analysis with load distributions in FEMA and the modal pushover analysis for tall buildings showed that both methods have shortcomings over these methods in predicting important response parameters in buildings (Poursha et al., 2010).

Further, Martino & Kingsley (2004), Grierson (2006) and Moehile (2006) have also observed that non-linear pushover procedures may not be appropriate for structures such as tall buildings where higher mode effects have a significant impact on the overall behaviour of the building. In addition, this method of analysis does not seem to accurately compute the local response quantities, such as hinge plastic rotations (Chopra & Goel, 2002). However, this method is adequately accurate and simple to be performed on low to medium rise structures with simple floor arrangements where there is a dominant first mode in a given direction.

Displacement Coefficient Method

The displacement coefficient method is based on the displacement demand and the displacement capacity at the top of a building. In this method, the displacement capacity of the building in consideration is obtained by carrying out a pushover analysis as explained previously in this chapter. Failure is deemed to occur when performance limits based on the strength capacity or deformation capacity are exceeded in a member or a joint. A guideline to determine deformation associated with different structural materials is provided in FEMA 273 (1997).

The peak displacement demands recommended in FEMA 273 (1997) are based on the product of a series of coefficients that are associated with the spectral displacements of an elastic oscillator. The peak displacement estimate is given by:

$$\delta_t = C_0 C_1 C_2 C_3 S_a \left({}^{T_e}/_{2\pi}\right)^2 \qquad \text{Eq. 3.3}$$

Where;

$C_0 = Modal\ participation\ factor$
$C_1 = Factor\ to\ account\ for\ increased\ displacement\ of\ short\ period\ structures$
$C_2 = Modification\ factor\ to\ account\ for\ hysteresis\ shape$
$C_3 = Factor\ to\ account\ for\ second\ order\ effects$
$S_a \left({}^{T_e}/_{2\pi}\right)^2 = Response\ spectral\ displacement\ where\ T_e\ is\ the\ effective\ natural\ period$

A detailed study by Whitaker et al. (1998) using 20 earthquake ground motions compatible with the code spectrum demonstrated that the coefficient method produced reasonably accurate results for structures with periods greater than the predominant site period. However, for structures with shorter periods, the mean inelastic displacements may exceed those predicted by Eq. 3.3. A perceived shortcoming of the method is the use of an effective stiffness calculated at relatively low strains to estimate the ultimate displacements of a structure that has experienced significant inelastic excursions (Wilson, 2000). However, the displacement coefficient method is restricted to a single-mode response and therefore, it is more suitable for low-rise buildings where the behaviour is dominated by the fundamental mode of vibration.

Capacity Spectrum Method

The capacity spectrum method was originally proposed by Freeman et al. (1975) as a rapid evaluation procedure for assessing the seismic vulnerability of buildings. This method was thereafter recommended for the seismic evaluation, design and retrofitting of buildings in ATC 40 (1996). This method assumes that the displacement response of a non-linear system can be estimated from the response of an elastic system possessing reduced stiffness and increasing damping. The procedure compares the capacity of the structure (in the form of a

pushover curve) with the earthquake demands on the structure (in the form of a response spectrum). The two curves are then plotted in a spectral acceleration versus spectral displacement graph, which is better known as the acceleration displacement response spectra (ADRS). By converting the base shears and roof displacements from a non-linear pushover to equivalent spectral accelerations and displacements and superimposing an earthquake demand curve, the non-linear pushover is converted to a capacity spectrum.

The capacity spectrum is converted from a pushover curve as described previously using the modal properties of the first-mode. The following equations (from Eq. 3.4 to 3.7.) are used for this conversion;

$$A = {V_b}/{M_1^*} \quad \text{Eq. 3.4}$$

$$D = {U_N}/{\Gamma_1} \quad \text{Eq. 3.5}$$

$$\Gamma_1 = \frac{\sum m_j \phi_{j1}}{\sum m_j \phi_{j1}^2} \quad \text{Eq. 3.6}$$

$$M_1^* = \frac{\left[\sum m_j \phi_{j1}\right]^2}{\sum m_j \phi_{j1}^2} \quad \text{Eq. 3.7}$$

Where;

$V_b = Base\ shear$
$U_N = Roof\ displacement$
$M_1^* = Effective\ modal\ mass\ for\ the\ fundamental\ mode\ of\ vibration$
$m_j = Lumped\ mass\ at\ the\ j^{th}\ floor\ level$
$\phi_{j1} = j^{th}\ floor\ element\ of\ the\ fundamental\ mode$

The earthquake demand curve is developed by response spectra, plotted with different levels of “effective” or “surrogate” viscous damping (e.g. 5%, 10%, 15%, 20%, and sometimes 30%) in order to approximate the reduction in structural response due to the increasing levels of damage). Typically, acceleration response spectra curves are plotted as a function of period. The spectral displacement corresponding to each period is obtained from the following equation (Eq. 3.8) to convert it to the ADRS format (Mahaney et al., 1993).

$$D = \frac{T_n^2}{4\pi^2} A$$ Eq. 3.8

Where;

$T_n = Natural\ period$
$A = Spectral\ acceleration$

A graphical representation of the conversion of the pushover curve and earthquake response spectrum to ADRS format in order to generate the capacity and demand diagrams is demonstrated through Figure 3.2. The resulting capacity spectrum and the determination of the performance point is shown in Figure 3.3.

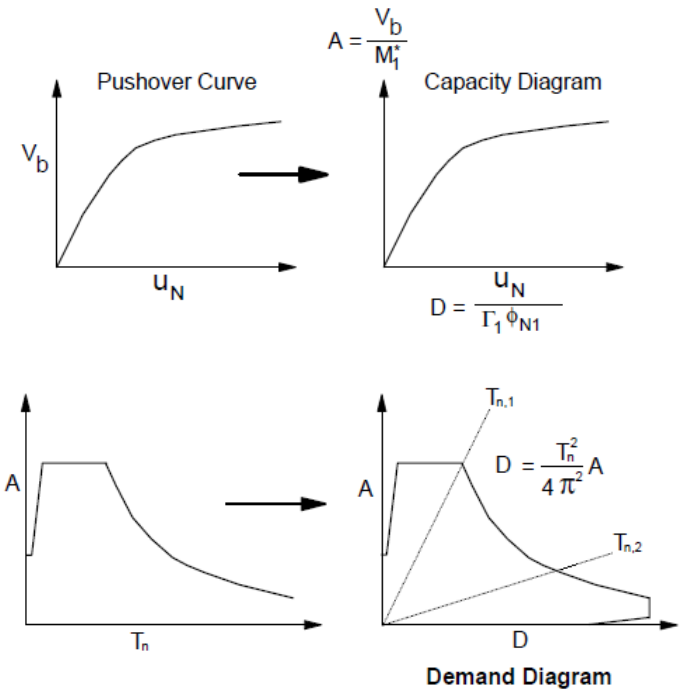

Figure 3. 2. Developing the Capacity and Demand diagrams (Chopra et al., 1999)

In the capacity spectrum approach, the pseudo-acceleration relationship has to be assumed when constructing the elastic demand spectrum. This assumption may result in erroneous outcomes for long period structures with high damping ratios, thus the conventional demand spectra require a substitute elastic structure. However, in order to extend the conventional

demand spectra to a bilinear model, secant stiffness needs to be used to calculate the effective period (Jie et al., 2007).

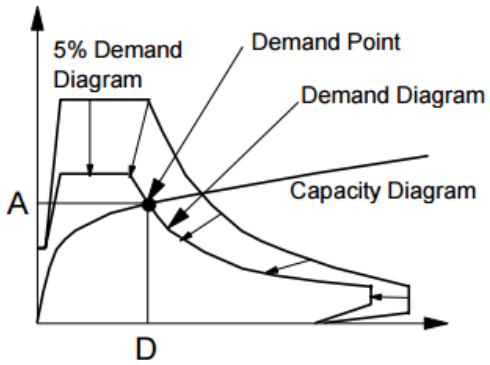

Figure 3. 3. Determination of demand (performance) point by capacity spectrum method (Chopra et al., 1999)

At low values of ductility, equivalent linear parameters given in ATC 40 (1996) lead to significant errors in estimating the performance point. Therefore, a higher order fit of the data at lower ductility values is necessary. To mitigate this issue, a new methodology has been developed to evaluate effective linear parameters that can improve the estimation of the performance point considerably (Guyader & Iwan, 2006).

However, the ATC 40 (1996) method has been found to underestimate the deformation of inelastic systems for a wide range of period and ductility values. In an attempt to solve this issue, an improved capacity demand diagram method that uses the well-known constant ductility design spectrum to develop the demand diagram has been developed by Chopra & Goel (1999, 2000).

This performance-based procedure is generally limited to fundamental modes of vibration. However, for tall buildings, higher mode participation is significant, and procedures for including higher mode effects have been presented that are based on the capacity spectrum method concept (Paret et al., 1996; Sasaki et al., 1998). A useful resource for developing and verifying performance-based procedure is the use of building response records (Gilmartin et al., 1998). By carefully studying recorded building motion records, modal responses can be filtered out and pushover characteristics can be identified as real outcomes.

By comparing the discussed displacement coefficient method and the capacity spectrum method, it has been shown that the target displacement is overestimated by the displacement coefficient method and underestimated by the capacity spectrum method. Further, the relationships between the damping model can be used in the capacity spectrum method with the use of stiffness degradation (Lin & Miranda, 2004).

By analysing the available literature it is seen that Capacity Spectrum Method is a useful tool for a simple building with ductility values that are not too low. The method proves to be a simple yet effective tool to establish a preliminary understanding of the building's performance under earthquake forces.

Over the years, performance-based design procedures have developed significantly from their humble beginnings. However, these very complex, codified performance-based design procedures takes the focus away from attributes and behaviour of an individual building. Therefore, engineers require a method with sufficient latitude to arrive at the best estimate of a building's capacity. The capacity spectrum method stands up well when compared to other performance-based design procedures, and it has the added advantage of giving an engineer the opportunity to visualise the relationship between demand and capacity (Freeman, 2004). However, differences between the various methodologies have more to do with unknowns in material behaviour and quantification of energy dissipation, than in the method of analysis (Freeman, 1998).

N2 Method

The earthquake design of a new buildings and earthquake evaluation of an existing buildings require a method that provides an accurate estimate of demand in terms of structural stiffness, strength, ductility and energy dissipation. The design and analysis procedures provided in most of the design codes are based on the assumption of linear elastic structural behaviour, however they fail to meet the above mentioned requirement. On the other hand, the non-linear dynamic time-history analysis using multi-degree-of-freedom (MDOF) mathematical models is not practical for everyday design use. Such an analysis requires

additional information (time-histories of several ground motions and the hysteretic behaviour of structural members) and the results are not necessarily more reliable, due to uncertainties and possibility of various values in the input data. Therefore, a simplified method for the non-linear seismic damage analysis of planar building structures, referred to as the N2 method (where N stands for non-linear, and 2 stands for two mathematical models), has been developed by Fajfar & Gaspersic, (1996) and Fajfar (1999).

This method estimates the global seismic demand for structures that vibrate primarily in the fundamental mode fairly accurately and has the ability to detect design weaknesses such as a weak storey mechanism or excessive deformation demands. Further, the influence of different ground motions and structural parameters on the structural response can also be easily studied. However, for structures where higher mode effects are significant, some demand quantities determined by the N2 method may be underestimated.

Secant Stiffness Method

The direct displacement method based on the secant stiffness of a structure was developed over the last couple of decades in order to mitigate the deficiencies in existing force-based methods. In direct displacement-based design, the structure is represented by a substitute structure with a single-degree-of-freedom system, and the performance is based on the peak displacement response with the secant stiffness rather than the initial stiffness of the structure. The design procedure determines the strength required at designated plastic hinge locations in order to achieve the design aims in terms of defined displacement targets. Then it is combined with the capacity design procedures to ensure that plastic hinges occur only where previously intended.

Although this method was derived for simple structures such as walls, frames, wall framed structures and bridges, the application of this method for other structural types should be investigated (Sullivan et al., 2006).

Nonlinear static analysis is very sensitive to the pattern used for lateral loading on the structure. Seismic loading applied on the computer model should be as similar as possible to the actual loading which occurs during an earthquake. This is how critical cases of

deformation and internal forces can be accurately identified in the model. For this reason, FEMA suggests at least two types of lateral load distributions be applied to the structure. In this respect Goltabar et al. (2008) have presented a PBSD on a concrete frame for varying percentages of symmetry in the structure. The nonlinear analysis has been carried out using SAP2000 and ETABS software. The study recommends that higher symmetry results in better performance or easy achievement of pre-defined performance levels. This is useful in arranging critical structural elements of a modular structure.

3.3.3. Linear Dynamic Analysis

Under the linear dynamic procedure, design seismic forces and the corresponding internal forces and displacements of the structure are determined using a linear elastic dynamic analysis. Most earthquake design codes provide similar methods for this type of analysis.

Code Based Response Spectrum Analysis

A response spectrum is a simple yet effective method to represent the different frequencies that are contained in earthquake ground motions. It is a representation of how the peak response of a single-degree-of-freedom (SDOF) system varies with the natural period and damping of the system.

The equation of motion for a SDOF system is shown below, where the mass is 'm', inertia force is 'c' and the stiffness of the system is 'k'.

$$m\ddot{u} + c\dot{u} + ku = -m\ddot{u}_g \qquad \text{Eq. 3.9}$$

The system is represented in the schematic diagram shown in Figure 3.4 below;

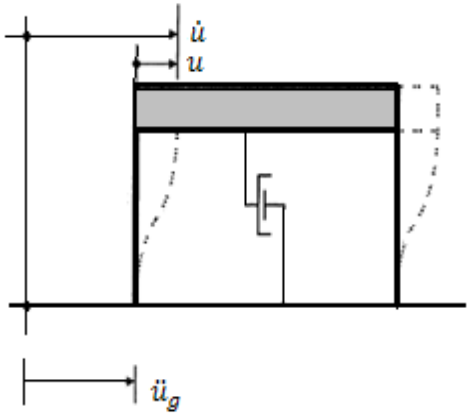

Figure 3. 4. A schematic representation of a single degree of freedom (SDOF) system

The design response spectra used for structural engineering designs and specified in seismic design codes are developed by enveloping many representative earthquake spectra (Newmark & Hall, 1982). Since factors such as magnitude, source, distance to epicentre, travel path and site conditions change the shape of response spectra, a series of new relationships were developed for defining the target spectrum (Idriss, 1990). These approaches have been modified and put to practical use by considering geological parameters such as the soil type, shear velocity of the crust etc. and produced in various seismic design codes such as AS1170.4 (2007) and ASCE-7(2010).

Many seismic design codes including the Australian code 1170.4 (2007) require a response spectrum analysis for medium to high rise structures. As per AS1170.4 (2007) all structures taller than 50m above ground require a linear dynamic analysis to determine their response to earthquake forces. An earthquake response spectrum is defined according to the soil type in the site and the desired return period and probability of occurrence with respect to the importance level and occupancy category of the structure.

The key factors that determine the response of a building are the properties of its dominant modes (those with higher modal mass participation factors) and the overall seismic weight of the building.

Software such as RUAUMOKO, SAP2000 and ETABS carry out the calculations to establish the modal properties such as period/frequency, mass participation and modal displacements. Peak response for the applied acceleration for each mode must be estimated separately. However, for the overall result, these peak responses need to be combined according to the mass participation of each model. The principles which are followed in the modal analysis and the subsequent modal combinations in order to obtain the above mentioned overall response are explained under the next subheading. The above mentioned computer programmes are capable of using these modal combination methods to provide the overall response of the analysed structure.

This procedure includes the response spectrum modal analysis method and the time-history method for the multi-degree-of-freedom systems.

The equation of motion considered for these analyses can be written as:

$$\underline{M}.\ddot{\underline{u}} + \underline{C}.\dot{\underline{u}} + \underline{K}.\underline{u} = -\underline{M}.\underline{\tau}.\ddot{u}_g \qquad \text{Eq. 3.10}$$

Where;

$\underline{M} = Mass\ matrix$
$\underline{C} = Damping\ matrix$
$\underline{K} = Stiffness\ matrix$
$\ddot{u} = Acceleration\ vector$
$\dot{u} = Velocity\ vector$
$u = Displacement\ vector$
$\tau = Influence\ vector\ for\ ground\ displacement$
$\ddot{u}_g = Gravitational\ acceleration$

Modal Analysis and Modal Combination Methods

Modal analysis is one of the most commonly adopted methods of designing structures for earthquakes in order to obtain estimates of structural response, both in terms of design forces and displacements. The first step of the procedure is to perform an eigen-value analysis of the structure with a given seismic mass and elastic stiffness in order to identify its modal characteristics. The characteristics of particular importance are the modal periods and

modal shapes. The natural frequencies,ω_i are calculated from the solution of the following determinant:

$$\left|\underline{K} - \omega_i^2 . \underline{M}\right| = 0 \qquad \text{Eq. 3.11}$$

The modal combinations and directional combinations can be carried out using various methods such as;

- SRSS method (Square Root of Sum of Squares)
- CQC method (Complete Quadratic Quotients)
- Absolute Sum method
- General Modal Combination method (GMC)
- 10 Percent Method of Nuclear Regulatory Commission (NRC 10%)
- Double Sum

A brief description for some of the above mentioned modal combination methods is given below where R is a given response value of the structure (shear, deflection etc.);

Absolute Sum Method (ABSSUM)

$$R_{max} = \sum |R_i|_{max} \qquad \text{Eq. 3.12}$$

It is assumed here that all modal peaks occur at the same time and the representative maximum of a single independent response value is obtained by considering the sum of absolute maximum values of the individual modal responses.

Square Root of Sum of Squares Method (SRSS Method)

$$R_{max} = \sum [R_{i\,max}^2]^{0.5} \qquad \text{Eq. 3.13}$$

The representative maximum value of a particular response of interest subjected to a single independent directional component of an earthquake is obtained by calculating the square root of the sum of the squares of corresponding maximum values of the individual modal responses.

Double Sum Method (DBLSUM Method)

$$R_{max}^2 = \sum R_k^2 + 2\sum\sum \in_{ij} R_i R_j \qquad \text{Eq. 3.14}$$

Where there are modes that are in-phase, the maximum values of individual modes occur simultaneously and hence their combined effect can be obtained by adding the individual modal responses. Further, the estimate of the maximum value obtained by SRSS rule can significantly underestimate the combined response in the case of modes whose responses are correlated (Nukala, 1999). The effect of such modes can be calculated assuming that each of the separate modes are correlated to one another and the maximum response can be expressed as shown in Eq. 3.14 where ϵ_{ij} is the modal correlation coefficient.

The coefficient ϵ_{ij} can be calculated using many methods such as the method by Rosenblueth & Elorduy's (1969), method by Gupta & Cordero (1981) and the method by Der Kiureghian (1980). Where the coefficient is calculated using the latter, it is known as the Complete Quadratic Quotients method (CQC Method).

Complete Quadratic Quotients Method (CQC Method)

$$R_{max} = \sum\sum\left[R_{i\,max}.\beta_{ij}.R_{j\,max}\right]^{0.5} \qquad \text{Eq. 3.15}$$

Eq. 3.15 shows the CQC method calculation where β_j is the damping ratio for the j^{th} mode.

The CQC method treats the modal damping more accurately than the double sum method and the coefficient calculation proposed by Rosenblueth and Elorduy (Bezler et al., 1990). Therefore, out of all the modal combination methods, CQC method seems to be the most accurate and is recommended to be used by many software such as CSI ETABS and CSI SAP2000.

The approximate inelastic response of structures to earthquake excitation can be estimated using inelastic response spectra. Inelastic spectra can be obtained from the design spectra by dividing by the period-dependent R factor. The example of an assumed relationship between the elastic and inelastic response is representative of the equal-displacement rule. However, the use of inelastic response spectra for MDOF systems is approximate and assumes that the elastically derived mode shapes, modal periods and mass participation

factors are similar for the system responding in the inelastic range. Therefore, this method is reasonable for regular structures with low ductility; but significant differences may be obtained for the inelastic response behaviour of irregular and very ductile structures (Wilson, 2000).

3.3.4. Nonlinear Dynamic Analysis

The non-linear dynamic procedure involves a time-history dynamic analysis to directly calculate the seismic responses. The equation of motion here is for an elastic multi-degree of freedom (MDOF) structure and is written in a similar form to the equation for an elastic SDOF system (Eq. 3.9) as follows;

$$\underline{M}\ddot{u} + \underline{C}\dot{u} + \underline{S}u = -\underline{M}.\underline{\tau}.\ddot{u}_g \qquad \text{Eq. 3.16}$$

Where;

$\underline{S} = Matrix\ that\ represents\ the\ inelastic\ strength\ with\ respect\ to\ the\ hysteretic\ behaviour$

For MDOF systems, the explicit damping matrix needs to be defined. An estimate of the damping matrix can be obtained by Rayleigh damping method. In this method of dynamic analysis, the ground motions are directly applied to the base of the structural model which is created through a computer software that is capable of dynamic nonlinear analysis. However, the complexity of the inelastic model may vary from a SDOF substitute structure to a detailed three dimensional (3D) finite element model, depending on the objectives of the analysis and the available resources.

Nonlinear Time History Analysis

Nonlinear time-history analysis is the most reliable method at present for determining or verifying the response of a designed structure to the design level of intensity, and the number of records to be used for the analysis is defined by many codes.

There are two alternatives defined by the codes EC 8 (2004), IBC (2009) and ASCE-7 (2010) for the number of accelerograms to be used in design verifications. The first option involves

using a minimum of three spectrum compatible records, with the design response being taken as the maximum from the three records for the given response parameter (displacement, shear force, etc.) investigated. The second option requires a minimum of seven spectrum compatible records, with the average value being adopted for the response parameter considered.

There are three methods for obtaining spectrum compatible accelerograms as follows:

- amplitude scaling of acceleration records from real earthquakes to provide a best fit to the design spectrum over the period range of interest
- generating artificial spectrum compatible records using special purpose programs
- manipulating existing real records to match the design spectrum over the full range of periods.

The ground motion time-history is most commonly obtained from records of past earthquakes. Databases are available in the literature, for example, the PEER Ground Motion Database (PEER, 2014). The earthquake characteristics and local site conditions should be carefully specified in the selection of time-history records. When the records are obtained from amplitude scaling of existing records, the scatter between records is likely to be large, and hence, a larger number of records may be needed to obtain a reliable average. However, it is seen that at periods longer than the fundamental period, displacements of the scaled spectrum are significantly lower than the design spectrum. According to ASCE-7 (2010), the scale factors are selected through trial-and-error, such that the average of response spectra from the scaled motions does not fall below the target design response spectrum over the period range $0{\cdot}2T$ through $1{\cdot}5T$, where T is the fundamental period of vibration of the building. Further, when the scaling approach is used, scale factors should not be too large (approximately two). Large scaling factors tend to bias non-linear response towards the high side (i.e. increase non-linear response relative to that which would be obtained using records whose peaks naturally match the target spectrum) (Luco & Bazzurro, 2004).

Response spectra associated with maximum considered earthquake (MCE) hazard levels (e.g. 2%/50 yrs) are often the result of a combination of a large event and an unusually large

motion at the period of interest for that event (sometimes referred to as positive epsilon, where epsilon is defined as the number of standard deviations above or below the median ground motion level for the magnitude and distance that are required to match the probabilistic spectrum). If a motion is selected without approximately the same value of epsilon, and it is subsequently scaled up to the MCE spectrum, it will tend to overestimate the non-linear response (Baker, 2005).

However, when ground motions are scaled to response spectra with significant differences in fault-normal and fault-parallel directions, it is preferable to scale the individual components to their individual target spectra rather than the vectors of the two components, although it is not specified by most codes or guidelines (Stewart et al., 2001).

When the motions are scaled, they would need to be selected such that all significant structural periods are representative. Moreover, the motions should have some broad-band content or more time-histories would be needed, as the structures will have non-linear behaviour and structural periods will shift and likely lengthen during earthquake excitation. However, this would require that the non-linear response history analyses be performed for much more than the minimum of three or seven time-history sets currently used for tall building design. Alternatively, a Monte Carlo analysis could be performed with many ground motion simulations (Lew et al., 2008).

Artificially generated accelerograms are the second alternative and these can be matched to the design spectrum for the full period range with comparatively small error. To obtain a meaningful average using artificial records, a less number of records are required. An objection that commonly exists with artificial records is that they are too overestimated, that real records are not spectrum compatible over the full period range, and that artificial records typically have a longer duration than real records (Priestley et al., 2007).

The third option is the manipulation of existing recorded accelerograms to obtain full spectrum matching. This method has the advantage over pure artificial records where the essential character of the original record is avoided. However, to obtain the required spectrum matching, the duration of the record typically has to be extended, opening the method to the same objection as directed against artificial records.

However, given an accurate force-deformation relationships and a representative ground motion time-history, calculation from the non-linear time-history method is often recognised as the "exact solution" in structural dynamics problems. However, assumptions, restrictions and simplifications may always be included. Further, the lengthy computation times and expensive resources are some of the major drawbacks which are somewhat diminishing with the advanced capabilities of modern computers. Validation of the analysis results is another important issue, and the information obtained is difficult to be understood directly without further treatment. However, in many codes of practice around the world, 3D time-history analysis has been recommended as the best option for the dynamic analysis procedure.

The calculated response of the structure from this time-history analysis is highly sensitive to the characteristics of individual ground motions. Therefore, the selection and characteristics of accelerograms to be used for the analysis requires careful consideration as mentioned previously.

3.4. Displacement Based Earthquake Analysis

Displacement based earthquake analysis which is also known as performance-based seismic design (PBSD) is a significant improvement over prescriptive code-based approaches that permit engineers to complete designs without a sufficient understanding of a building's likely performance. A performance-based design provides the designer and the building owner with greater insight into the likely response of the building to ground shaking. If such a design is performed carefully, and thoughtfully peer reviewed, the resulting design is likely to be a much safer and a more serviceable building (Willford et al., 2008).

As one of the pioneering steps into PBSD, Structural Engineers Association of California SEAOC (1999) proposed the following framework (Table 3.3) with performance levels for the design and verification of new constructions of buildings:

Table 3. 3 Framework proposed by SEAOC (1999) for performance based seismic design

Earthquake Design Levels	Earthquake Performance Level				
		Fully Operational	Immediate Occupancy	Life Safety	Collapse Prevention
	Frequent (50 Years)	Basic Objective	**Unacceptable**	**Unacceptable**	**Unacceptable**
	Occasional (72 Years)	Essential/Hazardous Objective	Basic Objective	**Unacceptable**	**Unacceptable**
	Rare (475 Years)	Safety Critical Objective	Essential/Hazardous Objective	Basic Objective	**Unacceptable**
	Very Rare (2475 Years)	Uneconomical	Safety Critical Objective	Essential/Hazardous Objective	Basic Objective

Dowrick (2009) gives a detailed introduction for PBSD where he explains that the initial concepts for PBSD arose in the 1980s with a growing awareness of the fact that building codes in general do not minimise property damage in moderate and small earthquakes although they provide a good level of life-safety. Dowrick (2009) explains that a performance objective is a coupling of an expected performance level with expected levels of earthquake ground motions.

Dalal Sejal et.al. (2011) have given a very useful introductory insight into PBSD. It explains the concepts with reference to the guidelines Vision 2000 (SEAOC, 1995), ATC40 (1996), FEMA273 (1997), and SAC/FEMA350 (2000). The authors identify two methods in which the conceptual design phase could be carried out for PBSD, namely;

- Traditional force-based design methods followed by checks for pre-determined performance objectives
- Direct design aiming at the pre-quantified performance objectives

The latter is identified as the most effective method where the design may begin directly targeting pre-quantified drift levels and yield mechanisms as the key performance indicators.

Kappos & Panagopoulos (2004) presented how PBSD could be carried out through inelastic static and dynamic analyses. The analysis here has been carried out as a dynamic time-history

analysis on equivalent single degree of freedom (SDOF) systems using SAP2000 software. The three key features of the procedure are;

- Two distinct performance objectives, 'serviceability' (or damage limitation), typically associated with an earthquake with 50%/50 yr probability, and 'life safety', typically associated with an earthquake with 10%/50 yr probability, are explicitly considered, and the basic strength level of the structure is not defined on the basis of life safety criteria (as in most existing procedures, code-type or otherwise), but on the basis of serviceability criteria. A third performance objective ('collapse prevention'), typically associated with an earthquake with 2%/50 yr probability, is accounted for in the design for shear and the detailing of members, although no separate analysis is made for this performance objective.
- Explicit consideration of inelasticity is made in the analysis, but is only restricted to those members that are selected as seismic energy dissipating zones (plastic hinge zones) by the designer; the selection of these zones follows the well-established capacity design principles (e.g. Paulay & Priestley, 1992).
- Detailing of critical members for confinement is performance-based, i.e. it is controlled by post-yield deformation requirements predicted from the inelastic analysis.

3.5. Stiffness of Bolted Steel Connections

Corner supported modular systems rely heavily upon their module to module connections to resist lateral loads. As discussed previously, these connections exist in many forms made out of various materials. However, for the purpose of this research considering the Advanced Corner Supported Modular Structural System only steel bolted connections shall be considered for analysis and experiments.

The behaviour of these connections are characterised mainly by the stiffness and strength properties. Strength of the connection depends on the characteristic strength of the steel materials which the bolts and plates are made up of. However, estimating the overall stiffness of the connection is not as straightforward.

The tensile stiffness of the connection can be calculated in the form of k=EA/L according to Hooke's Law as provided in design standards such as the Eurocode (EC3, 1993). However, as concluded from many experimental research carried out (van Gaasbeek, 2005 and Lee, 2011) this value can be far from accurate since it applies only to the bolt. In reality the stiffness of a bolted connection relies on factors such as the bolt arrangement with respect to the load path, the nature of bolt holes and the length of the threaded and non-threaded parts of the bolts and many other physical properties such as the modulus of elasticity of the material.

There are few computational approaches to calculate the stiffness of a bolted connection introduced by some notable researchers. The approach suggested by Wileman et al. (1991) to establish these values of stiffness is one of the most widely used theoretical computational methods used in estimating the stiffness of bolted connections as per Musto and Konkle (2006). A few noteworthy methods of estimating the stiffness of a bolted connection including that of Wileman et al. are discussed below;

Wileman et al. (1991)

According to Wileman et al. (1991) the stiffness of the clamped material (k_m) is expressed in the following form through an exponential relationship;

$$k_m = AEd\mathrm{e}^{B(d/L)} \qquad \text{Eq. 3.17}$$

Where;

$E = Modulus\ of\ Elasticity\ of\ the\ material$
$d = diameter\ of\ the\ bolt\ hole$
$d/L = Aspectratio\ of\ the\ joint\ where\ L\ is\ the\ grip\ length\ of\ the\ bolt$
$A = Numerical\ dimensionless\ constant\ depending\ on\ the\ material\ and\ carries\ a\ value\ of\ 0.78715\ for\ steel$
$B = Numerical\ dimensionless\ constant\ depending\ on\ the\ material\ and\ carries\ a\ value\ of\ 0.62873\ for\ steel$

Where more than one material or member is clamped the connection shall be considered as a combination of springs connected in series and the overall stiffness shall be calculated as;

$$\frac{1}{k_m} = \frac{1}{k_1} + \frac{1}{k_2} + \cdots + \frac{1}{k_n} \qquad \text{Eq. 3.18}$$

This formula for stiffness is used in the theoretical calculations of connection stiffness in this thesis. However, the following empirical formulae introduced by various researchers must also be noted.

Shignley & Mischke (2006)

In this method Shingley & Mischke (2006) proposed that the overall deformations relate to the stress distribution below a fastener that takes the shape of a conical frustum. They recommended an angle of 30 degrees to be taken as the sloping angle of the frustum and this resulted in a simplified equation for the stiffness as shown below;

$$k_m = \frac{0.577\pi Ed}{2ln\left(5\frac{0.577L + 0.5d}{0.577L + 2.5d}\right)}$$

Eq. 3.19

Where;

$$E = Modulus\ of\ Elasticity\ of\ the\ material$$
$$d = diameter\ of\ the\ bolt\ hole$$

Various research work carried out by Haidar et al. (2011), Musto and Konkle (2006) and Al-Huniti (2005) have established a close comparison among all these empirical formulae. However, due to the comprehensive nature of the formula introduced by Wileman (1991) it has been chosen as the most suitable for the purpose of this thesis.

3.6. Stress Calculations to Evaluate Failure Criteria of Steel Bolts

Chapters 6 and 7 of this thesis focus on the behaviour of a proposed module to module steel bolted connection to an applied lateral load. The failure criteria is measured through the stresses that are developed in each of the components of the connection.

There are many theories in which stresses are calculated. Measuring the principal stresses would be adequate for a uniaxial load application. However, the connection in question undergoes stresses in more than one direction during the loading history. Therefore, the overall failure of the connection will need to follow a more comprehensive stress analysis

method even though the different individual contributions to the failure can be included by studying the principle stresses. Listed below are a few theories which are typically used to carry out stress analyses;

Maximum Normal Stress Theory

The 'Maximum Normal Stress Theory' states that a material will fail either in tension or compression once the maximum normal stress in a given direction reaches the yield tensile or compressive stress respectively. It must be noted here that the yielding compressive stress is a difficult value to determine as it is different failure criteria that most materials go through during compression.

Maximum Principal Stress Theory (Rankine Theory)

If explained simply, the maximum and minimum normal stresses that occur in a defined principle directions are termed as principal stresses. For normal stresses in a given principal plane, the principal stresses can be demonstrated as shown in Figure 3.5 and be calculated as shown in Eq. 3.20.

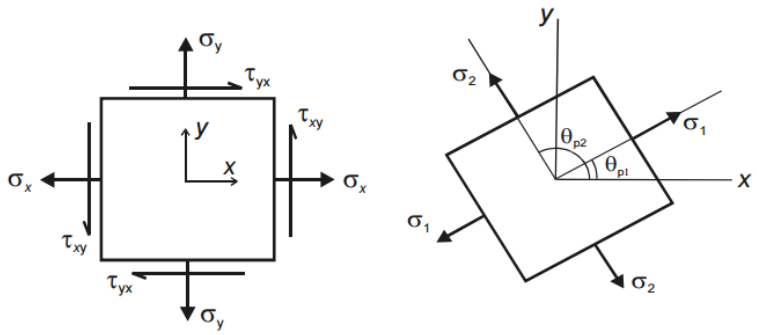

Figure 3. 5. An illustration of principal stresses found out by the normal stresses in a 2D plane

$$\sigma_{1,2} = \frac{\sigma_x+\sigma_y}{2} \pm \sqrt{\left(\frac{\sigma_x-\sigma_y}{2}\right)^2 + \tau_{xy}^2} \qquad \text{Eq. 3.20}$$

Where, σ_x and σ_y are the normal stresses and τ_{xy} is the shear stress and the angle of principal stress θ_p is found as;

$$\tan 2\theta_p = \frac{2\tau_{xy}}{\sigma_x - \sigma_y}$$

Eq. 3.21

Similarly, a finite element in a 3D space would have three principal stresses.

The 'Maximum Principal Stress Theory' states that a brittle material ruptures once the maximum principal stress in the material reaches a limiting stress value. This critical value could is taken as the tensile strength of the particular material measured by carrying out a uniaxial tension test.

Although both these theories are straightforward they do not provide comprehensive solutions to ductile materials and situations where a combination of shear and axial stresses exist.

Maximum Shear Stress Theory (Tresca)

Similar to the normal and principal stress theories, Tresca's 'Maximum Shear Stress Theory' states that a material will fail once the shear stress in a given direction reaches a limiting stress known as the 'yielding shear stress'.

The maximum shear stress for a 2D plane is given as;

$$\tau_{max} = \sqrt{\left(\frac{\sigma_x - \sigma_y}{2}\right)^2 + \tau_{xy}^2} = \frac{\sigma_1 - \sigma_2}{2}$$

Eq. 3.22

Distortion Energy Theory (von Mises)

Often referred to as the 'von Mises Yield Criterion', the Distortion Energy Theory was developed for predicting the yielding of materials primarily assuming they are isotropic. This theory unlike the maximum stress theories show a high suitability to estimate the yielding stresses of ductile material such as steel.

This theory is based on the value 'equivalent stress' also known as the 'von Mises stress' calculated as follows;

$$\sigma_e = \sqrt{\frac{(\sigma_1-\sigma_2)^2+(\sigma_2-\sigma_3)^2+(\sigma_3-\sigma_1)^2}{2}} \qquad \text{Eq. 3.23}$$

According to this theory the yielding occurs when the distortion energy reaches a critical value for the particular material. Effectively, this occurs when the equivalent stress, σ_e reaches the yield (tensile) strength of the material and failure occurs when the equivalent stress reaches the ultimate tensile strength of the material.

Bruneau et al. (2011) illustrate the yield surfaces defined through the von Mises theory and Tresca theory (Figure 3.6). Accordingly certain yielding actions fall outside the maximum shear stress and maximum principal stress criteria that are covered by the 'Mises ellipse'. Since the maximum principal stress theory too does not cover ductile materials fully, the von Mises stress criterion is considered to be the most suitable stress calculation method to estimate the limiting stresses in the module to module connection that is discussed in the thesis.

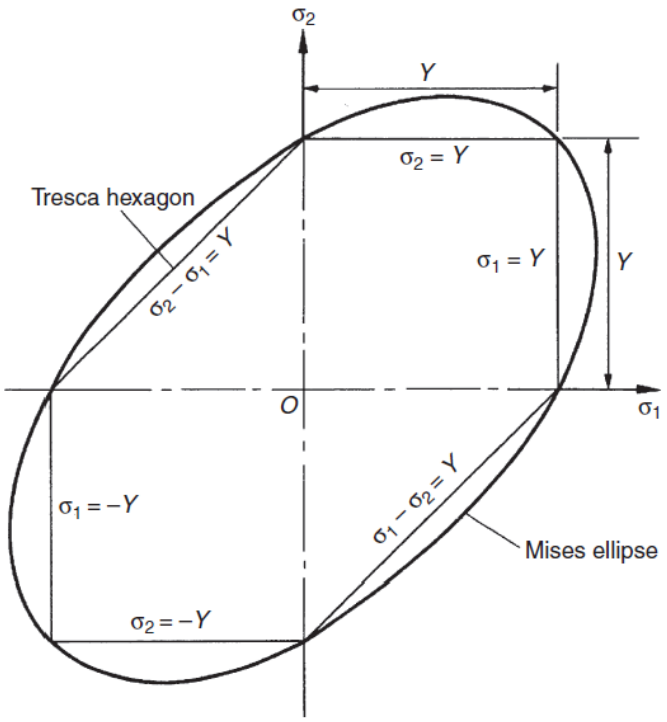

Figure 3. 6. Tresca and von Mises yield surfaces in a σ_1, σ_2 space (Bruneau et al., 2011)

Interaction Method for Combined Loading

Since there could be a combination of shear and bearing stresses that form simultaneously in the bolts that have hole clearances in the connection discussed in the thesis, an interaction of the different stresses need to be considered.

The interaction method uses mathematical relationships that represent the loading condition at yield or at failure of a structural member subjected to two or more simultaneously applied loads. Equations that represent the interaction relationships can be found in design manuals and codes of practice. Different codes of practice provide factors of safety on top of the allowable stress limits.

Such interaction equations are defined in the form of;

$$\bar{R} = R_1^X + R_2^Y + R_3^Z \qquad \text{Eq. 3.24}$$

Where R_1, R_2 and R_3 are load ratios (defined in the form of R = Applied load/ Allowable load) of various components such as tension, bending, torsion and shear and X, Y and Z are the exponents that define the interaction relationship.

The Australian standard AS 4100: 1998 provides the interaction relationship for tension and shear for bolts in a similar form in the form of an inequality as follows;

$$\left(\frac{V_f^*}{\emptyset V_f}\right)^2 + \left(\frac{N_{tf}^*}{\emptyset N_{tf}}\right)^2 \leq 1 \qquad \text{Eq. 3.25}$$

Where;

$V_f^* = Design\ shear\ force\ of\ the\ bolt$
$V_f = Nominal\ shear\ capacity\ of\ the\ bolt$
$N_{tf}^* = Design\ tensile\ force\ of\ the\ bolt$
$N_{tf} = Nominal\ tensile\ capacity\ of\ the\ bolt$
$\emptyset\ = 0.8\ which\ is\ the\ capacity\ reduction\ factor\ as\ per\ Table\ 3.4\ of\ AS\ 4100{:}\ 1998$

Chapter 4 An Advanced Corner Supported Modular Structural System

4.1. Background

Almost all multi-storey modular buildings that are constructed in the world to date comprise of corner supported modules. The main reason for this is that taller buildings demand an efficient lateral load transfer mechanism which the corner supported system is capable of providing. On the other hand, a load bearing modular system is not equipped to provide such performance. However, as discussed in Chapter 1, it is observed that these corner supported systems either directly connect the corner supported modules to a reinforced concrete shear core or effectively do so by pouring concrete in-situ as a floor slab after placing the modules in a particular floor (see Figure 1.7).

This practice eliminates the chances of the building being a complete modular structure. Effectively it reduces the amount of benefits such as reusability and reduction of construction waste that a fully modular solution would otherwise present to the end user.

4.2. Introduction to the Advanced Corner Supported Modular Structural System

As a solution to the above issue, a new structural system is introduced through this thesis. This system is a self-sustained system as far as the lateral load resistance is concerned. The modules themselves are allowed to incorporate stiff wall elements and placed strategically on a building plan to ensure effective lateral load resistance. This work is published in the Journal of Architectural Engineering of the American Society of Civil Engineers (ASCE) (Gunawardena et al., 2016).

In this new structural system a cast-in-situ or prefabricated core is not the predominant lateral-load-resisting component of the superstructure. The elevator core in this system is intended to be formed with steel elements as a part of some of the prefabricated modules themselves and therefore will not be the central component in the lateral-load-resisting system. The prefabricated modules are stacked vertically and connected horizontally through bolted plates. The lateral congruity for lateral load transfer is provided by these connections and improved greatly through the introduction of modules with stiff concrete walls. Because these stiff modules, which are strategically placed in the main structure, resist the majority of lateral loads and transfer them down to the foundation, the need for a stiff central core becomes less critical. The structure can now act as a purely modular system.

This technology has the potential to reduce construction time significantly by completely eliminating the time and costs incurred in building the traditional core of a low-rise building. The elevator shafts and staircases can be accommodated in the prefabricated modules themselves. It also gives the opportunity for the stiffer walls to be constructed using innovative materials, such as composites and high-strength concrete and steel. Concrete walls can be built by filling after the modules are placed. Vertically running building services that are traditionally housed in the central concrete core can also be accommodated in prefabricated modules.

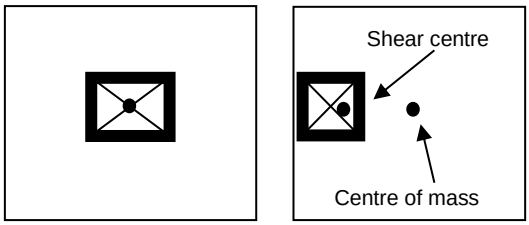

Figure 4. 1. Placement of the core in conventional buildings; (a) concentric core where torsional forces are minimized, (b) eccentric core where higher torsions apply on the structure

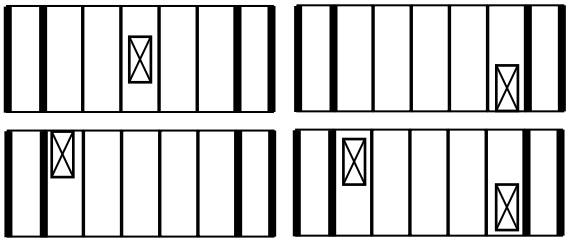

Figure 4. 2. Four different conceptual placements of the elevator shaft (on plan view) made possible with the new system

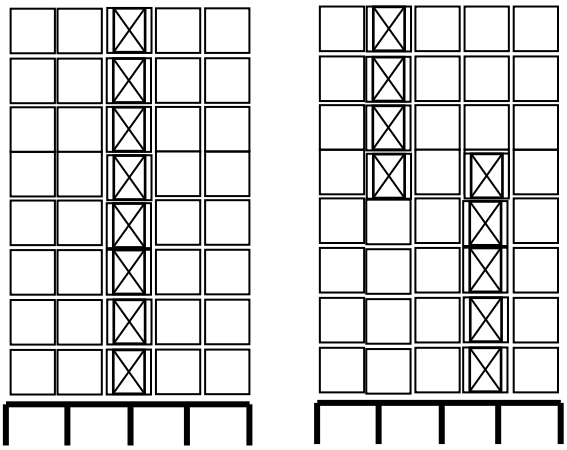

Figure 4. 3. Two different conceptual arrangements of the lift core made possible with the new system, on elevation view

More importantly, the new system provides architects with a great amount of freedom with a structure that is not restricted by the placement of a core. In conventional structures, the core would ideally be situated in the centre so that the shear centre of the structure coincides with the centre of mass, reducing torsional forces. Figure 4.1 illustrates this phenomenon.

Because the stiffer modules take the lateral loads, the elevator core can be moved around in the building as the Architect pleases while considering the vertical transportation requirement. Figure 4.2 shows different plan arrangements that are possible with the new system.

The elevator core can even be staggered vertically. Thus, Architects will have further freedom to change the placement of the elevator core at different levels of the building (Figure 4.3), which is not normally possible in conventional construction because the elevator core is required to transfer the loads to the foundation.

With its potential to further reduce construction time and cost and to be a significant addition to the range of innovations

that Architects can work with, this new system shows great promise in being developed as an economical and sustainable solution for modern construction. Therefore, the preliminary case study was carried out to understand the structural feasibility of this system and it is presented in the following sections;

4.3. Preliminary Structural Analysis

4.3.1. Methodology

A 20-story medium-rise building was modelled as a modular structure (Figure 4.4) using the computer program ETABS. ETABS is widely used around the world for the analysis of buildings, especially to analyse behaviour against lateral loads. Two types of modules were used for each story in the model; Type 1 had stiffer reinforced concrete walls of 100 mm thickness, and Type 2 had lightweight wall panels without such reinforced concrete infills. A more detailed description of the makeup of these modules is presented in Chapter 5. In current practice, the outer walls of such prefabricated modules are constructed of various lightweight materials, including thin steel sheets and sandwich panels. Berman & Bruneau (2005) have shown how thin steel sheets could enhance the stiffness of infill wall

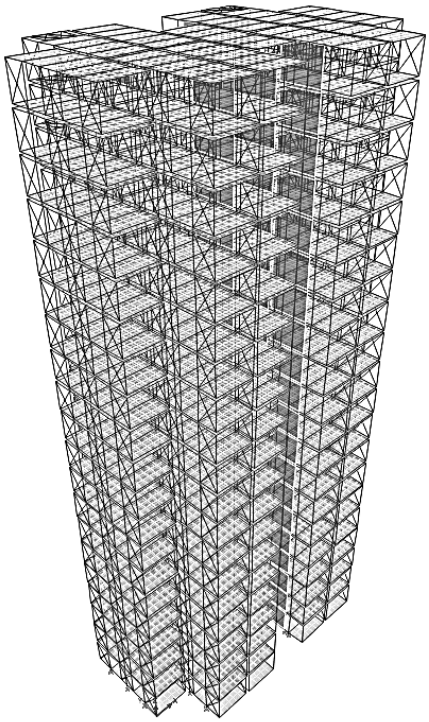

Figure 4. 4. 3D finite element model for the 20 storey structure (Note: only the load bearing elements are modelled)

panels. However, since the aim of this analysis was only to ascertain the adequacy of the introduced structural system, the modelling was kept simple, and only the load-bearing frame was considered. The weight of the wall panels was added to the supporting beam elements.

Columns and beams that constituted the load-transferring system were part of the prefabricated module, and their continuity was ensured through the stiffness of the bolted connection plates. The lateral connections were modelled as frame elements with equivalent stiffness and pinned at the common joint to allow independent rotation of the connected modules (Annan et al. 2009a). The method that was used to obtain the stiffness of these connections is explained in detail in Chapter 6.

To suit the particular structure considered, the stiffer modules (Type 1) were arranged in the three middle sets of modules (Figure 4.5). A set of modules with an opening that accommodates four elevator shafts (variation of Type 2) was located at the rear ends of the

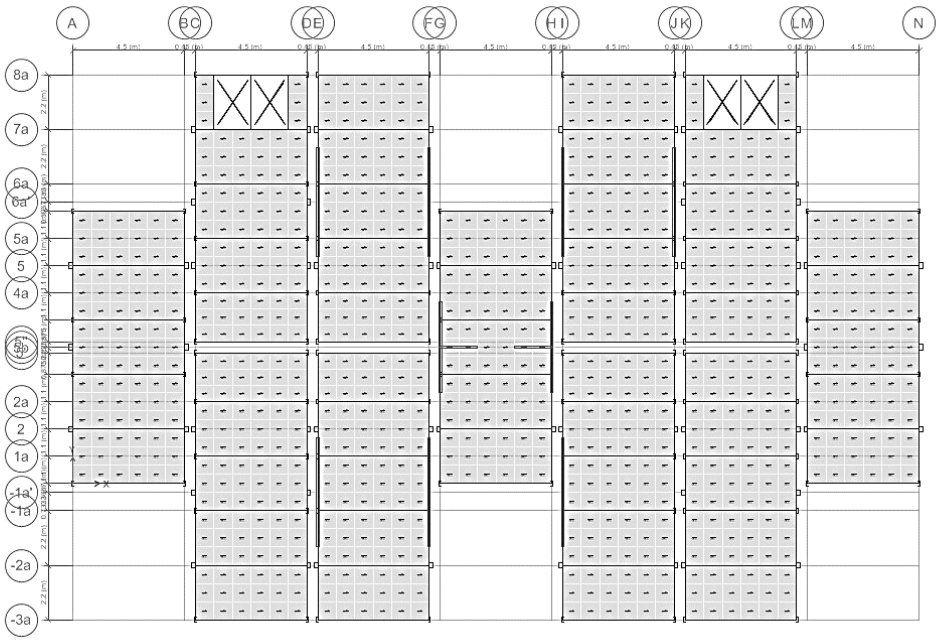

Figure 4. 5 Plan View of a typical floor of the 3D finite element model above. (Note: The 100mm thick wall elements in modules are shown with the thicker grey lines).

building. In practice, this module can be designed with the staircases and vertically run services that usually accompany a conventional lift core.

The structure was assessed in terms of its general structural stability, natural period, modes of vibration, and performance against lateral earthquake and wind loads. It was important to see the characteristics shown through the mode shapes to understand how the structure would behave dynamically under different loading conditions. The participation of these structural modes in the lateral response of the structure was calculated through the software ETABS by using the complete quadratic combination (CQC) method (Chapter 3, Eq. 3.15).

The structure was analysed with a dynamic earthquake response spectrum (Spec Y) according to the Australian Earthquake code, AS 1170.4 (2007), and a static wind load (Wind Y) according to the Australian Wind code, AS 1170.2 (2011). A hazard factor of 0.08 relating to the earthquake response spectrum was selected to match the subsoil conditions in Melbourne, Australia according to AS 1170.4 (2007), and the wind loads were calculated with a basic wind speed of 46 ms^{-1}. For simplicity, the results were analysed only in the critical Y-direction to obtain an initial idea of how structurally feasible the new system was. Once the concept is applied to high-rise structures, the lateral loads will become more critical. Therefore, an understanding of the structure's behaviour under earthquake and wind forces provides valuable insight into how the system can be modified for future high-rise use.

Further, to highlight the key benefit of this particular system, three different configurations (two in addition to the original one) of the elevator shafts were analysed to identify whether the centres of mass and stiffness varied drastically. These configurations are shown in Figure 4.6. The used ETABS version makes it possible to calculate centres of rigidity and mass for each floor (CSI Knowledge Base, 2014). Because the floors of the models were typical throughout, it was adequate to calculate the results for one floor.

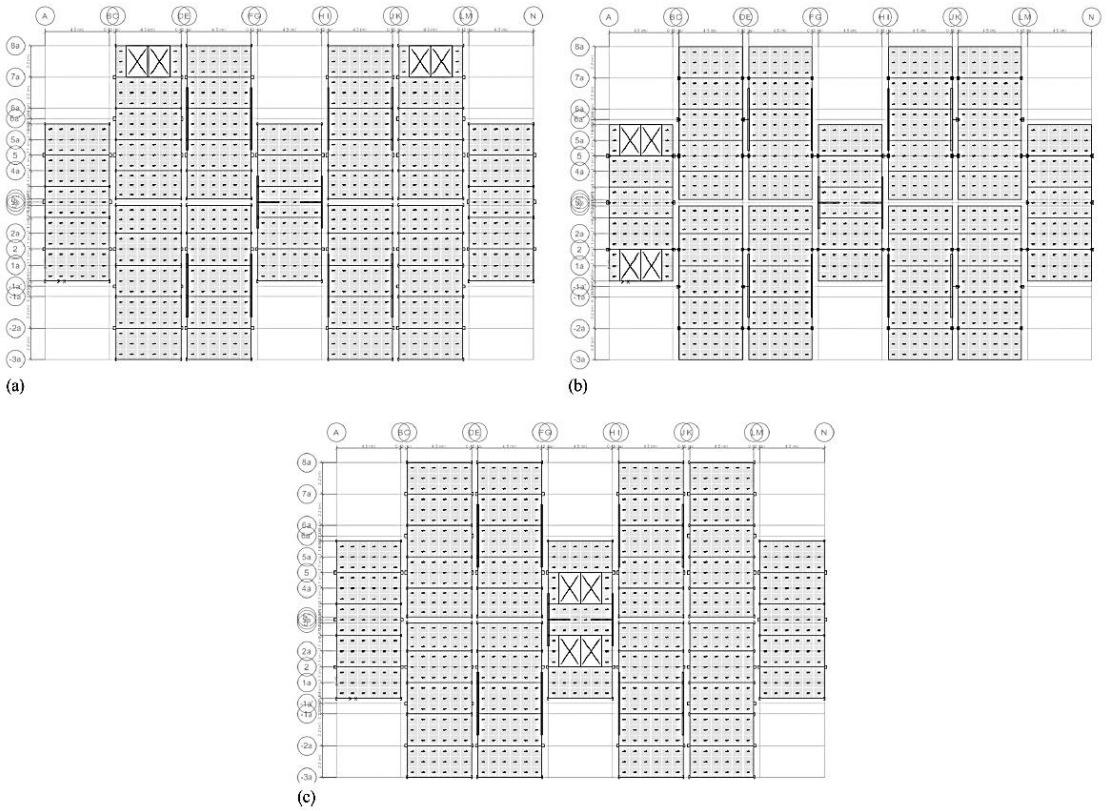

Figure 4. 6 Lift shafts: (a) placed in the rear (Configuration 1, the original configuration); (b) placed in the corner module (Configuration 2); (c) placed in the centre module (Configuration 3)

It is also expected that the system may present both geometric and material nonlinearities under more severe lateral loads. As a preliminary investigation into the performance of the introduced structural system under more severe earthquake loads, a nonlinear earthquake time-history analysis was carried out using ETABS by applying six time histories (Table 4.1) to the model with the original configuration. The lateral connections for this analysis were modelled as nonlinear link elements with equivalent stiffness. The maximum drift that would result from each record was observed. The analysis was carried out with and without P-Δ effects as two separate analyses.

Table 4. 1 Earthquake ground motion records applied for the nonlinear time history analysis

Record	Magnitude (Moment Magnitude Scale)	PGA	Duration
Chichi	7.63	0.278 g	90.0 s
Tabas	7.40	0.852 g	32.8 s
Dunzce	7.14	0.535 g	25.8 s
Kocaeli	7.40	0.312 g	21.1 s
Imperial Valley	6.90	0.519 g	40.0 s
Loma Prieta	7.10	0.371 g	60.0 s

4.3.2. Preliminary Findings

The results for structural period and modes of vibration are presented in Table 4.2. The modal mass participation factors provide an understanding of the influence of each mode of vibration on the behaviour of the building. Modes with higher participation are more easily excited by forces applied to the structure (Irvin, 2013). This, it is important to see which modes are prominent because this will indicate how the structure will behave when different loads are applied.

As summarized in Table 4.2, the fundamental period was 3.75 s. The fundamental mode was a translational mode with a rotational mode as the second. Results showed that the rotational modes can have considerable influence on the behaviour of the building. This result is important in analysing the behaviour against lateral loading, especially for high-rise applications.

The lateral loads were also within acceptable ranges for the member sizes used in the design of the structure. It was beyond the scope of this particular study to carry out a complete analysis of the structure against lateral loads, but the basic evaluation resulted in a favourable conclusion on the structural feasibility of the new system.

A summary of results against wind and earthquake forces is given in Table 4.3. As per AS 1170.4 (2007), the base shear of a structure is the "horizontal equivalent static shear force

acting at the base of a structure" resulting from horizontal forces such as wind and earthquake loads acting on the structure. The values of the base shears were of realistic and acceptable values, as shown in Table 4.3.

Table 4. 2 Modal frequencies and mass participation factors

Mode	Period (s)	Frequency (Hz)	UX	UY	RZ
1	3.75	0.27	73.2%	0.0%	0.0%
2	2.39	0.42	16.7%	0.2%	67.4%
3	1.79	0.56	6.9%	60.9%	0.1%

UX: Participation of the modal mass to translational movement in X direction
UY: Participation of the modal mass to translational movement in Y direction
RZ: Participation of the modal mass to rotational movement about Z (vertical) axis

Table 4. 3 Summary of results against lateral loads

Load Case	Base Shear (kN)	Maximum storey drift
Wind Y (Static)	5494	0.13%
Spec Y (Dynamic)	1232	1.20%

The story drift in a structure is the difference of displacements of the floors above and below, and is expressed as a percentage when it is given as a ratio to the height of the floor (Chopra, 2001). The story drifts resulting from the static wind and response spectrum analyses in this building were also within acceptable levels of below 1.5% as specified in AS 1170.4 (2007).

The maximum drifts that resulted from the nonlinear earthquake time-history analysis are presented in Table 4.4. Once the geometric nonlinearities were considered, the resulting drift values were slightly higher than the code-recommended 1.5% for two of the time histories analysed, whereas the others are still within acceptable limits.

Table 4. 4 Summary of maximum drift results from the nonlinear earthquake time history analysis

Ground motion record	Maximum Drift Without Considering P-Δ Effects	Maximum Drift Considering P-Δ Effects
Chichi	0.62%	1.69%
Tabas	0.63%	1.34%
Dunzce	1.24%	1.55%
Kocaeli	0.85%	0.99%
Imperial Valley	0.75%	1.43%
Loma Prieta	1.15%	1.17%

The results for centres of mass and rigidity of the three different elevator shaft configurations are shown in Tables 4.5–4.7. It is very evident that neither the centre of mass nor the centre of rigidity shifted considerably from the original configuration, although the position of the elevator shaft was changed. This is an indication that such an alteration will not cause any additional adverse twisting or torsion on the structure, thereby giving the full benefit of this new system, as expected

Table 4. 5 Centres of Mass and Rigidity for Configuration 1

Parameter	X (m)	Y (m)
Centre of Mass	17.10	5.33
Centre of Rigidity	17.10	5.05

Table 4. 6 Centres of Mass and Rigidity for Configuration 2

Parameter	X (m)	Y (m)	Change from Original Configuration	
			X (m)	Y (m)
Centre of Mass	17.35	5.35	+0.25	+0.02
Centre of Rigidity	17.10	5.50	0.00	+0.45

Table 4. 7 Centres of Mass and Rigidity for Configuration 3

Parameter	X (m)	Y (m)	Change from Original Configuration	
			X (m)	Y (m)
Centre of Mass	17.10	5.35	0.00	+0.02
Centre of Rigidity	17.10	5.50	0.00	+0.45

4.4. Discussion

Many structures around the world that have been classified as modular constructions in fact rely heavily on a conventional core structure as the primary lateral-load-resisting mechanism. This is a limitation that prevents the structure from enjoying the full benefits of modular construction.

The introduced advanced corner supported system is a step forward in designing low to medium-rise buildings as purely modular systems. The preliminary structural analysis showed that the system results in a structure that behaves within the parameters set out by design standards for conventional structures under normal loading conditions. The nonlinear earthquake time history analysis considered the possible geometric and material nonlinearities that may arise in the system when subject to more severe dynamic lateral loads. Although the resulting drift values were mostly within the specified limits, further studies were required to obtain a more detailed understanding on the failure mechanisms and redundancies of the system.

This study also confirmed that the newly introduced structural system allows the elevator shaft to be positioned in various arrangements without causing additional adverse torsional effects.

Although the advantages of the new system were proven to be desirable, further research was required to confirm the validity, especially for very tall buildings. Further, a detailed future study into the economic and sustainability aspects of this system will ensure that it is developed as a solid methodology to reap the full benefits of purely modular construction.

It is apparent that the basic idea behind the new system is feasible from a structural perspective. The added flexibility for designing with less consideration on maintaining a core structure at a fixed position makes the system very attractive for Architects as well.

The modules can be designed in such a way that they can replicate the use of a conventional core. For example, they can be used in collaboration with a smart system to support a crane and also support auto-climbing features.

One of the main attractions of this system as discussed previously is that it provides the opportunity to the Architects to design spaces without being restricted by a fixed positioning of the lift core. The lift core can be moved from one place to another along the height of the building. There are certain conceptual designs that have arisen with the need to move the position of the lift core as such and would largely benefit from a structural system like the Advanced Corner Supported Modular Structural System.

There is a clear demand and a studious interest in the construction industry to produce innovative elevator systems. A commendable step forward was taken by Thyssen Krupp (Higginbotham, 2015) to develop an innovative elevator system that can change direction (Figure 4.7). Although the system is still quite novel it appears that it could perform better without being dependent on being housed in a structural core. Structural systems such as the advanced corner supported system provide a useful conceptual base to assist such novel designs. It also opens a discussion on how modular technology can develop into creating service modules which can house vertical service pipe and duct networks that serve the purpose of the conventional lift core where many services and ducts run along the height of tall buildings.

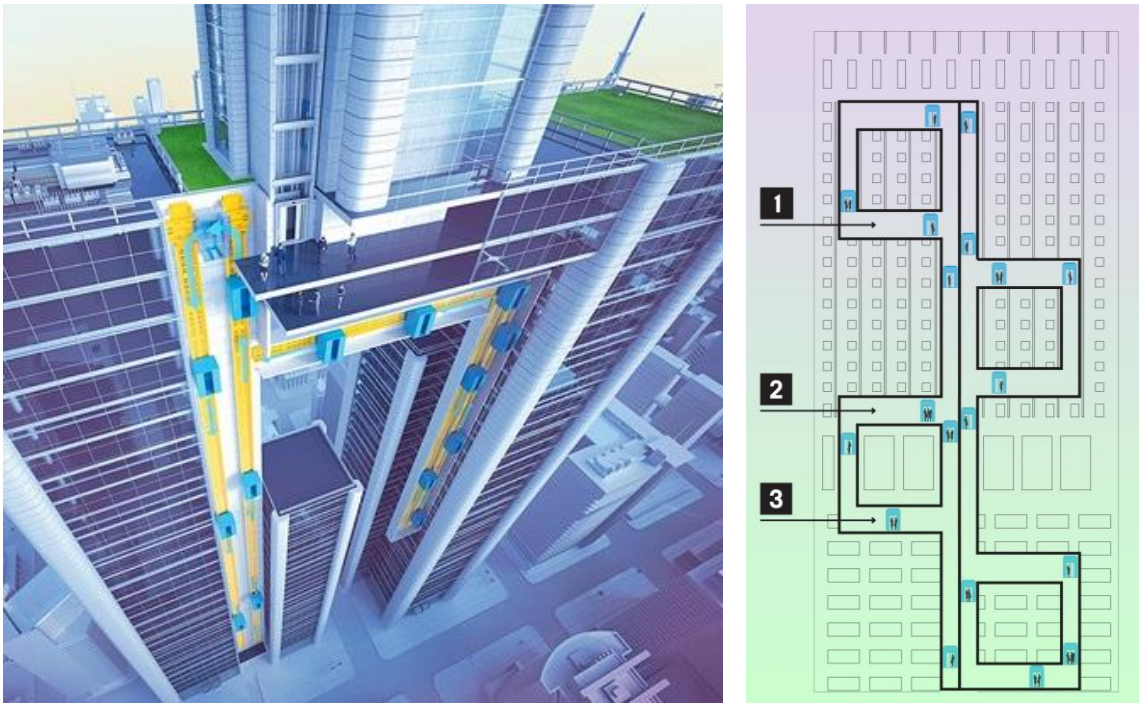

Figure 4. 7. The innovative elevator system that was invented by Thyssen Krupp to make elevators change direction through the height of the building (Higginbotham, 2015)

4.5. Summary

- This chapter introduces a new structural system concept for modular buildings in the form of the 'advanced corner supported modular structural system' with some preliminary analysis results on its structural behaviour.
- The advanced corner supported system presents designers with many attractive benefits including flexibility with arranging spaces without being restricted by an in-situ unmovable core. This prompts the need for this structural system to be investigated further on its structural behaviour against lateral loads in order to be used for medium to high rise structures.

- The preliminary results of the structural analysis using code based and ground motion based earthquake analyses provide a favourable outlook for this structural system. Further, there appears to be a developing trend in the construction industry for innovative and efficient engineering designs that would largely benefit from a structural system of this nature.
- Therefore, this thesis from herein will further investigate on the performance against lateral loads of the advanced corner supported system. The thesis will also investigate into the behaviour and key design requirements of the module to module connections that can be used within this structural system.

Chapter 5 Behaviour of Multi-storey Modular Buildings Subjected to Lateral Loads – A Case Study

5.1. Design of the Multi-storey Modular Building

A hypothetical ten-storey medium-rise building designed as a modular structure with the Advanced Corner Supported Modular Structural system which was introduced in Chapter 4 was considered for the analysis.

As explained in Chapter 4 the placement of the elevator shaft or a service core would not bear any implications on the behaviour of the main structure. However, for the purpose of obtaining useful results the structure is designed with a simple plan where the central module carries an opening for the elevator shafts and services. Each module is 4.2 metres wide and 10.8 metres long. These sizes are compatible with the size of transportable prefabricated modules that are used in the industry at present. The height of each module is taken as 2.8 metres, to be compatible with the storey height.

The building was modelled using the software RUAUMOKO 3D where a global structural analysis including non-linear time history analysis was carried out. The analysis was expected to provide more detailed analytical results of the behaviour of a modular building using the hybrid system which was introduced in Chapter 4. A plan view of the typical floor used for this model along with the layout of the prefabricated modules are presented in Figure 5.1.

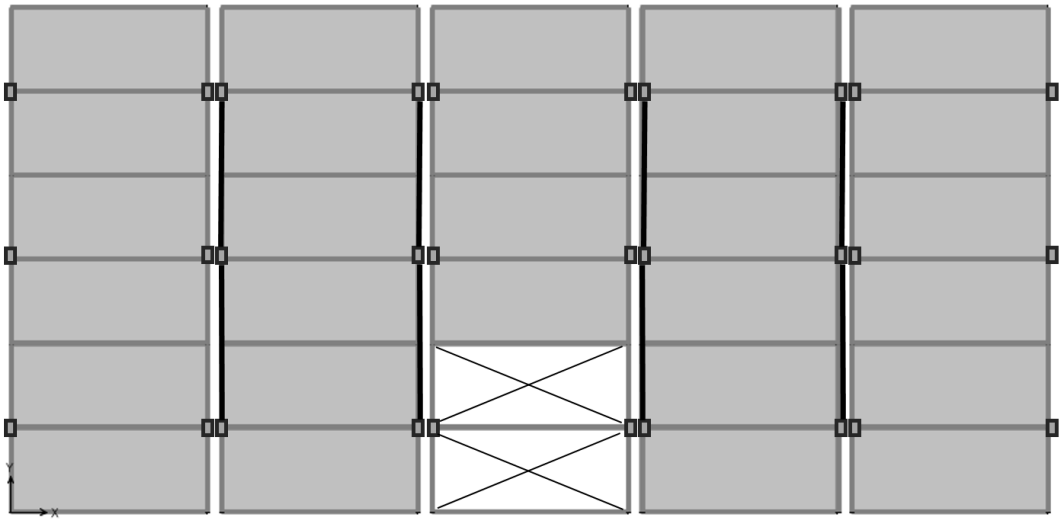

Figure 5. 1. A plan view of a typical floor of the ten storey modular building considered for the analysis

Additionally, the same structure was modelled using SAP2000 so that the results could be verified. The SAP2000 model was also subsequently used to obtain results such as modal mass participation factors that are not directly available as outputs in RUAUMOKO.

According to the Advanced Corner Supported system two types of modules were mainly used in the building where one type (Type 1 – Figure 5.2) has stiffer reinforced concrete walls of 100mm thickness and the other (Type 2 – Figure 5.3) without such reinforced concrete infills..

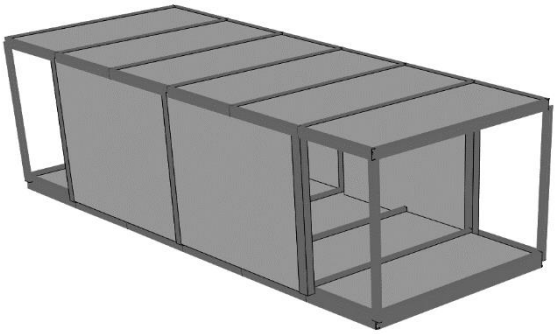

Figure 5. 2. Type 1 module with 100mm thick RC infill wall

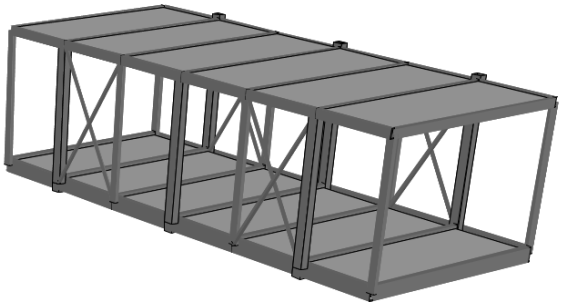

Figure 5. 3. Type 2 module (without infill walls)

For this particular design, these stiff walls are within the module and will not fill the void between two vertically adjacent modules. This will make sure that there are no wet joints in the construction, making the process much faster and convenient on-site.

The modules shown in Figures 5.2 and 5.3 are corner supported modules and their corner columns are rectangular hollows sections (RHS) of the size 220 mm x 150 mm x 14.2 mm. Each module consists of 6 main corner supporting columns as shown in Figure 5.1. Since the building is only 10 stories tall the columns size remains constant for all stories.

Each of Type 1 and Type 2 modules are made up with self-stabilised steel frames. The modules need to be structurally stable by their own since it is necessary for transportation and on-site handling. This internal frame includes internal columns made up of parallel flange channels (PFC) of the type 180 PFC. All of the floor beams in each module are spaced at 1.8 meters from each other and are made up of 300 PFC sections. The roof beams are also spaced at 1.8 meters from each other and are made up of 180 PFC sections. Type 2 modules also consist of steel bracings made up of universal angle sections (UA) of the type 75 UA. All these steel members were considered to be of grade 350 (Yield strength of 350 MPa).

The 3D visualisation of the computer model that was generated through RUAUMOKO 3D is shown in Figure 5.4. Since the graphical output of RUAUMOKO 3D is not the sharpest despite the software being highly regarded for its accuracy in earthquake analysis, the 3D image from SAP2000 model is also shown in Figure 5.5.

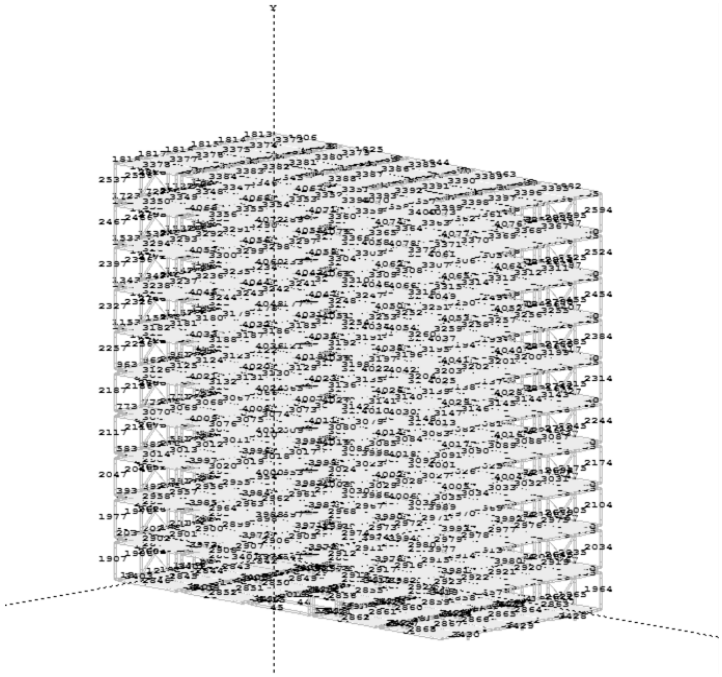

Figure 5. 4. 3D image of the ten storey modular building from RUAUMOKO 3D

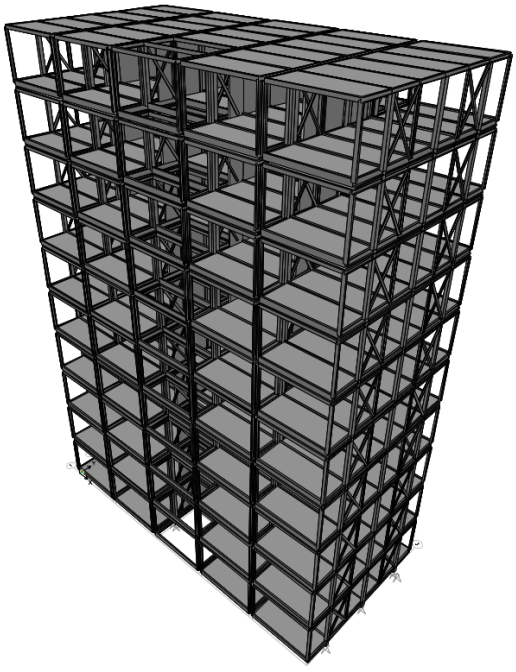

Figure 5. 5. 3D image of the ten storey modular building from SAP2000

5.2. Computer Generated Model and Structural Analysis

The building that was designed as explained in section 5.1 was modelled using RUAUMOKO 3D. This particular software was selected as it is based on advanced research on earthquake engineering at the University of Canterbury, New Zealand. As described in Chapter 4 the behaviour against earthquake forces are deemed to be the most critical for this system when used for low to medium-rise structures.

RUAUMOKO is a program that allows a building to be modelled in both 2D and 3D where the input can be created using either the batch mode or the interactive mode. For this particular analysis, the interactive mode was used where the input file was created separately with a word processor following the relevant input syntax of the software. The software package consists of its set of support software which includes the post processing software DYNAPLOT which runs the output file from RUAUMOKO 3D. The output file of RUAUMOKO can be read using a word processor to scan for any error or warning messages allowing a model to be run with a high level of accuracy.

A 3D frame model was created for the ten storey modular building introduced in section 5.1. All frame elements such as columns, beams and braces were modelled using the element type 'BEAM' (Carr, 2010). All 'BEAM' type elements follow the 'Giberson one-component beam model' (Sharpe, 1974). Parameters such as the end fixity, section properties and nonlinear behaviour are defined according to each frame member. An extract from the input file, where all critical inputs are shown, is given in Appendix A.

All floors, roofs and walls were modelled using the element type 'QUADRILATERAL' following a shell element definition. The module - module steel connections were modelled using the 'SPRING' elements with equivalent stiffness to the connection that is discussed in Chapter 6. These connections are pinned at the common joint to allow independent rotation of the connected modules (Annan et al., 2009a). These module-module connections are assumed

to be rigid connections for the purpose of forming the computer model as proposed by Annan et al. (2009a).

5.2.1. Expected Structural Behaviour

The gravity loads in the form of dead loads, live loads and super imposed loads (finishes, services etc.) that are imposed on the floors and roofs of each module will be transferred to the supporting corner columns through the floor and roof beams. The corner columns will transfer the gravity loads straight to the foundation. However, the transfer of lateral loads occur following a different mechanism.

A cross section of the module-module connection which transfers loads both vertically and horizontally, is sketched in Figure 5.6. The possible pinned connections are not shown in order to prevent confusion with the possible hinge locations shown in the diagram. One such connection would connect four supporting corner columns from four adjoining modules.

As shown in Figure 5.6 the module-module connection is intended to be facilitated with the use of a bolted plate connecting all four columns. A detailed analysis of a connection that can be used for this joint is presented in Chapter 6. This connection will transfer lateral loads as shear forces and therefore be designed to carry the ultimate shear force that occurs at its location. It is therefore unlikely that the initial hinge formation will occur at this connection during an earthquake. However, the connection is still a very important member of the overall system since it is the interface through which the lateral forces are shared among corner supporting columns.

Two of the possible hinge locations are marked in Figure 5.6. 'Hinge 1' which may form inside the floor beam of a module (or a roof beam if adequately loaded) would be a less likely scenario in the newly introduced structural system.

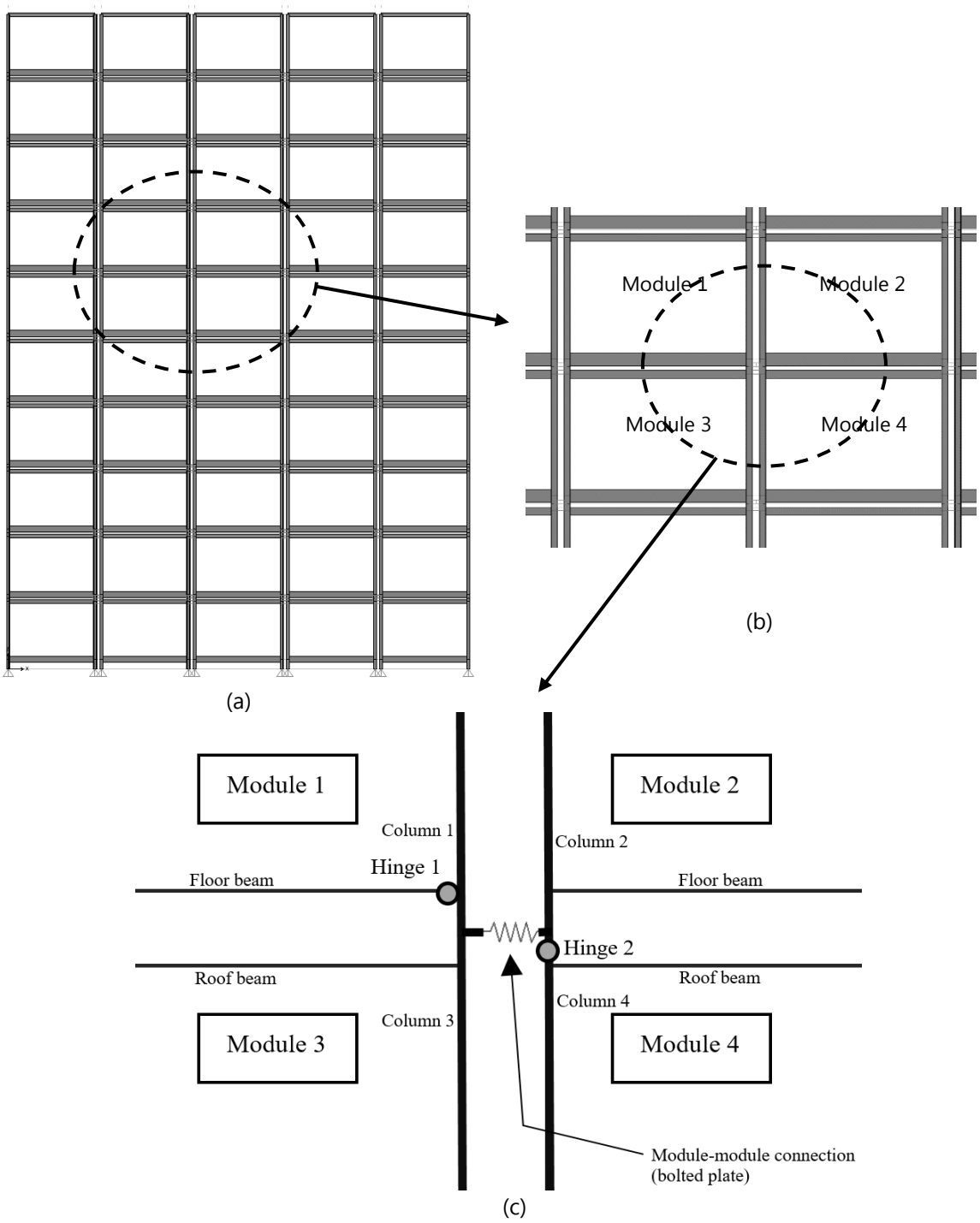

Figure 5. 6. An illustration of the module-module connection and possible hinge locations via (a) the view from the front elevation of the modular building, (b) a close-up of the elevation view of neighbouring modules and (c) the module-module connection

The infill concrete walls together with the roof and floor beams of the module would act as a deep beam of which the depth is the height of the module itself. Therefore this deep beam would be too strong to yield before the main column (Columns 1 to 4 in Figure 5.6). It is therefore expected that 'Hinge 2' which may form on the main corner column just below or above the module will be the more likely scenario of a hinge formation during an earthquake. This hypothesis is tested by means of a non-linear time history analysis.

5.2.2. Nonlinear Time History Analysis

A nonlinear time history analysis which is one of the most accurate methods to analyse the earthquake response as explained in Chapter 3, was carried out in order to identify which of the expected hinges would occur first and also to observe the moment curvature relationship of the critical main corner columns (Figure 5.6). This analysis would provide a more thorough understanding of the ductility of the columns under such earthquake loadings. All steel structural elements were specified with a bilinear hysteresis profile (Figure 5.7) as per the RUAUMOKO 3D Manual (Carr, 2010).

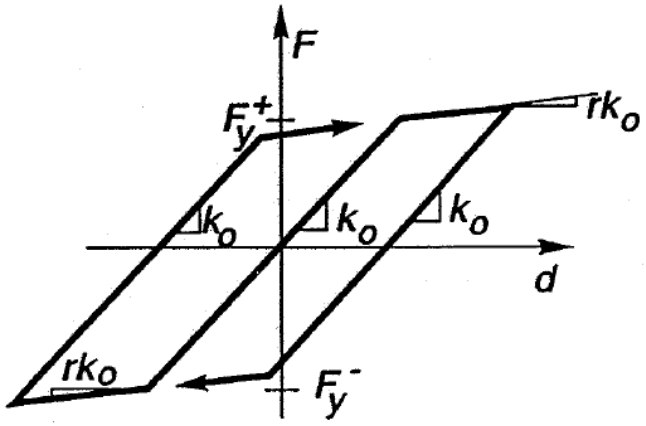

Figure 5. 7. Bilinear hysteresis model for steel (Carr, 2010)

The ductility of the column frame member will be evaluated in the form of curvature ductility (Carr, 2010) which is defined as;

Ductility (μ) = Maximum curvature (φ_m) / Yield curvature (φ_y) Eq. 5.1

In addition to the nonlinear time history analysis, a pushover analysis was also carried out in order to obtain the maximum yield curvatures of the columns where hinges were expected.

Six earthquake ground motion records were selected to be used for the nonlinear time history analysis where the maximum response can be considered for results.

These six records were selected to match the intensity of Type 1 earthquake as per EC8: 2004 with an assumed peak ground acceleration (PGA) of 0.4g and soil type C where the standard penetration test (SPT) number of blows ranges from 15 to 50. The six short duration earthquake records that were chosen for the time history analysis are shown below in Table 5.1.

Table 5. 1 Earthquake records used for the Nonlinear Time History Analysis

Earthquake Record	Magnitude (Moment Magnitude Scale)	Duration	Time Step	PGA	Scale
Chi chi	7.63	90.0 s	0.005 s	0.278 g	1
Düzce	7.14	25.8 s	0.005 s	0.535 g	1
Imperial Valley	6.90	40.0 s	0.005 s	0.519 g	1
Kocaeli	7.40	27.5 s	0.005 s	0.312 g	1
Loma Prieta	7.10	60.0 s	0.005 s	0.371 g	1
Tabas	7.40	16.0 s	0.005 s	0.852 g	1

The earthquake ground motions listed in Table 5.1 are presented graphically below in Figure 5.8;

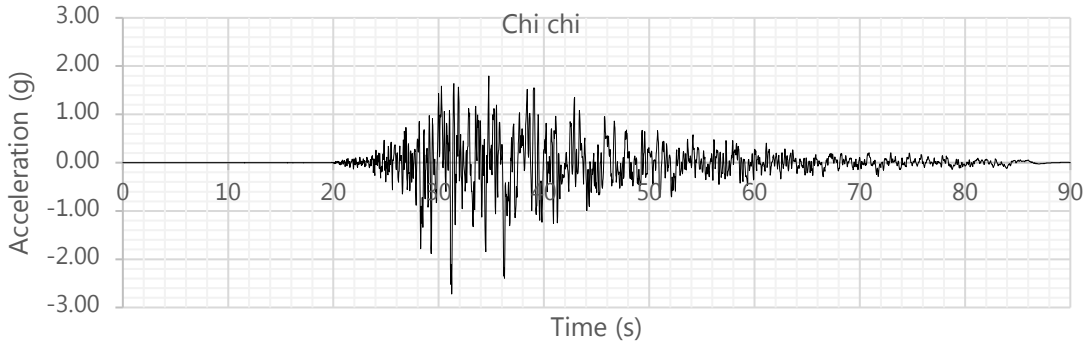
Chi chi
Acceleration (g)
3.00
2.00
1.00
0.00
-1.00
-2.00
-3.00
0
10
20
30
40
50
60
70
80
90
Time (s)

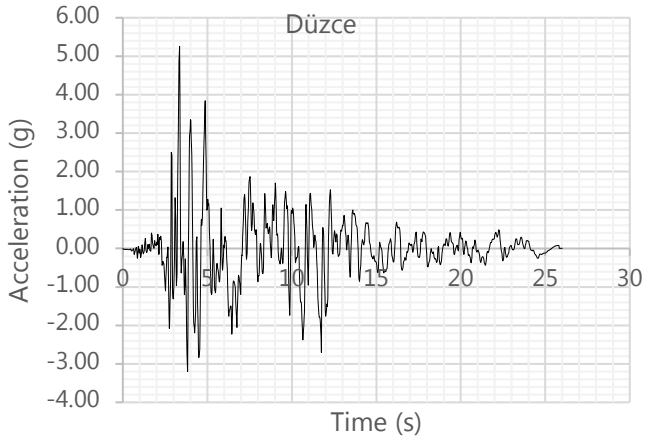
Düzce
Acceleration (g)
6.00
5.00
4.00
3.00
2.00
1.00
0.00
-1.00
-2.00
-3.00
-4.00
0
5
10
15
20
25
30
Time (s)

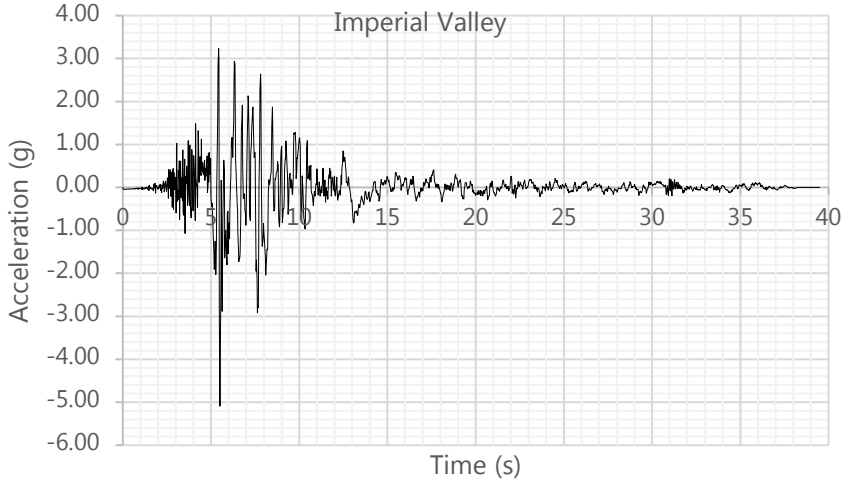
Imperial Valley
Acceleration (g)
4.00
3.00
2.00
1.00
0.00
-1.00
-2.00
-3.00
-4.00
-5.00
-6.00
0
5
10
15
20
25
30
35
40
Time (s)

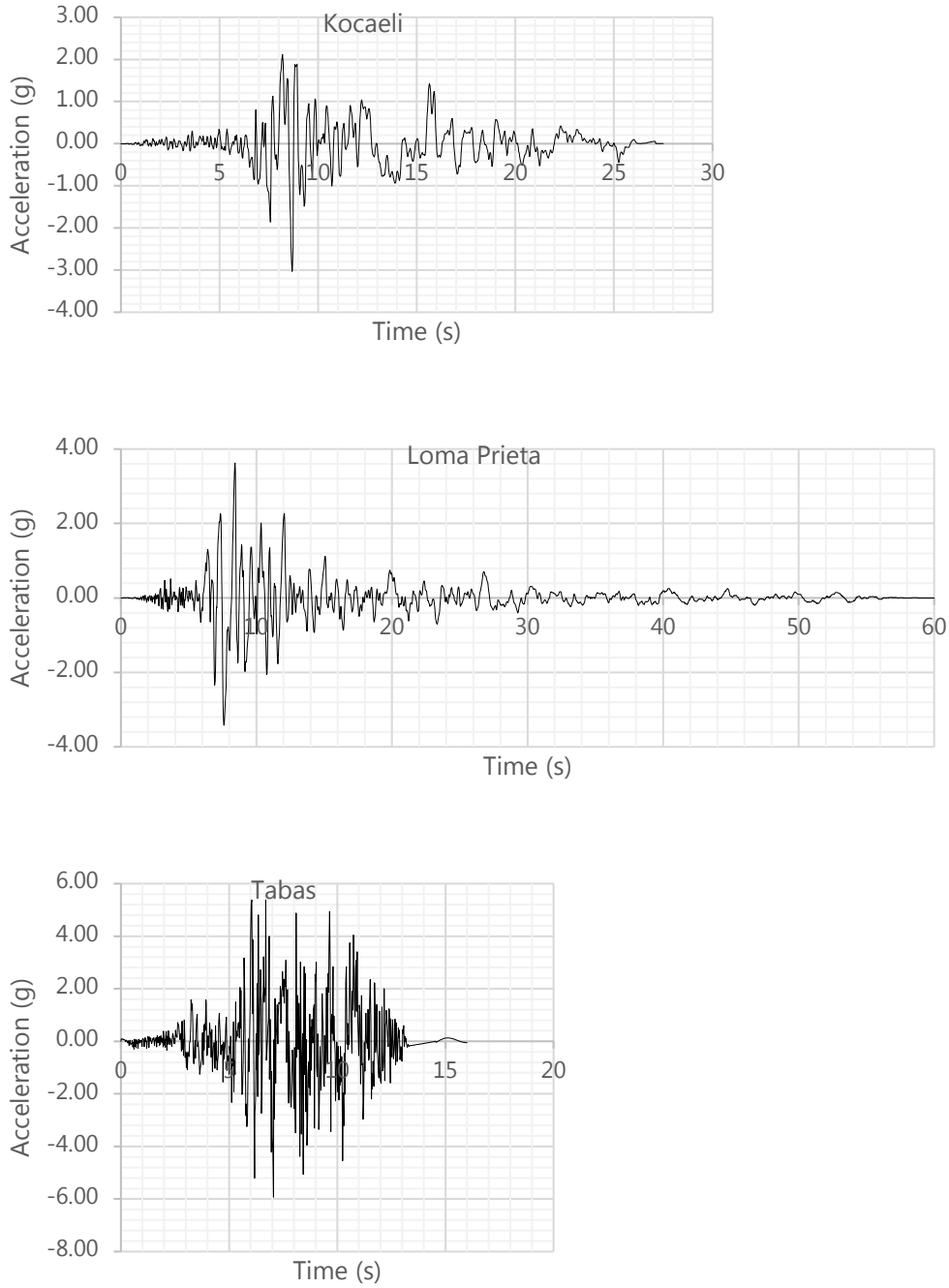

Figure 5. 8. Graphical presentation of the earthquake ground motions listed in Table 5.1

The above earthquake ground motions were applied on the ten storey modular building using RUAUMOKO 3D in a separate analysis. The resulting response of the structure is evaluated and discussed in section 5.3.

5.2.3. Static Nonlinear Pushover Analysis

A static nonlinear pushover analysis was carried out using the program RUAUMOKO 3D to develop an understanding of the seismic capacity of the analysed ten story building. Capacity Spectrum Method which is one of the simpler yet comparatively accurate methods in obtaining this result (as explained in Chapter 2), was used subsequent to generating the pushover curve from the computer model.

The capacity spectrum method was applied in order to generate a basic evaluation of the performance of the structure for a generic earthquake. The results generated here could be used as a benchmark in applying more specific earthquake conditions to building designs where the site location and the nature of the project is well defined.

5.3. Discussion of Results

5.3.1. Modal Results

An Eigen value analysis was carried out with the aid of RUAUMOKO 3D in determining the natural modes of vibration of the structure. The first two modes were found to be translational in the two principle horizontal directions where the third mode was a rotational mode about the vertical axis. These results were re-evaluated using the SAP2000 model. The results of the modal analysis for the first three modes are shown in Table 5.2 as follows;

Table 5. 2 Modal results generated for the 10 storey building

Mode	Nature	Period from RUAUMOKO	Period from SAP2000
1st	Translational	1.14 s	1.04 s
2nd	Translational	1.63 s	1.53 s
3rd	Rotational	0.81 s	0.78 s

The comparison model that was created on SAP2000 shows a close match to the results from the RUAUMOKO model and therefore it is reasonable to assume that it can be used for any further analysis.

The RUAUMOKO model is hereby used to generate results from the nonlinear time history analysis. Accordingly the hinge formation is observed through this nonlinear time history analysis and the results are discussed in section 5.3.2.

5.3.2. Hinge Formation at the Most Critical Column Element

It was observed through the nonlinear time history analysis that, as expected, the hinge formation occurs first on the supporting columns below the floor beam. In this regard it was observed that the columns below the 1st storey Type 1 modules were the most critical.

The hinge stiffness variation through the duration of the applied earthquakes indicates that the column forms hinges while the module-module connections and the floor beams remain elastic. Thus as per Figure 5.6, "Hinge 2" is where the hinge formation has occurred.

The stiffness curves are plotted for the most critical column (Column 3411) for each of the applied earthquake time histories in Fig 7. A continuous curve at 100% stiffness will show an element remaining elastic through the duration of the applied earthquake time history (Carr,

2010). However, the plotted curves (Figure 5.9) show the stiffness of the column at “Hinge 2” location dropping close to 0% which indicates that it has yielded.

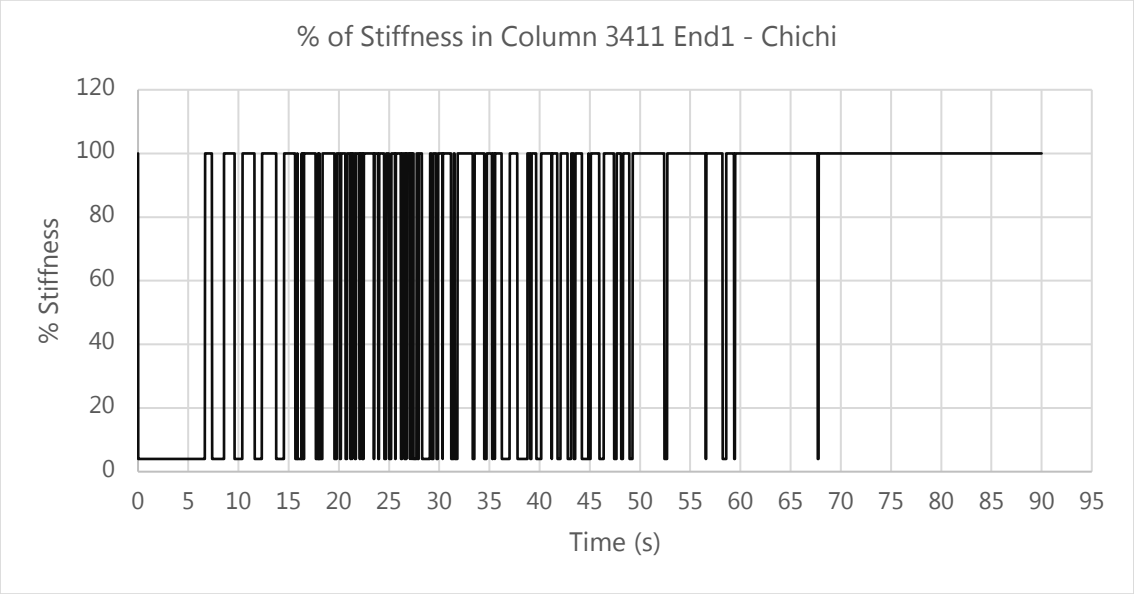

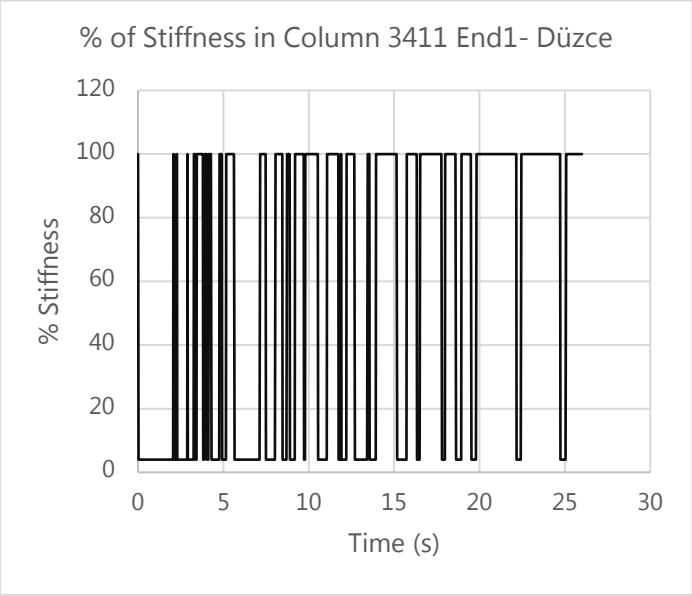

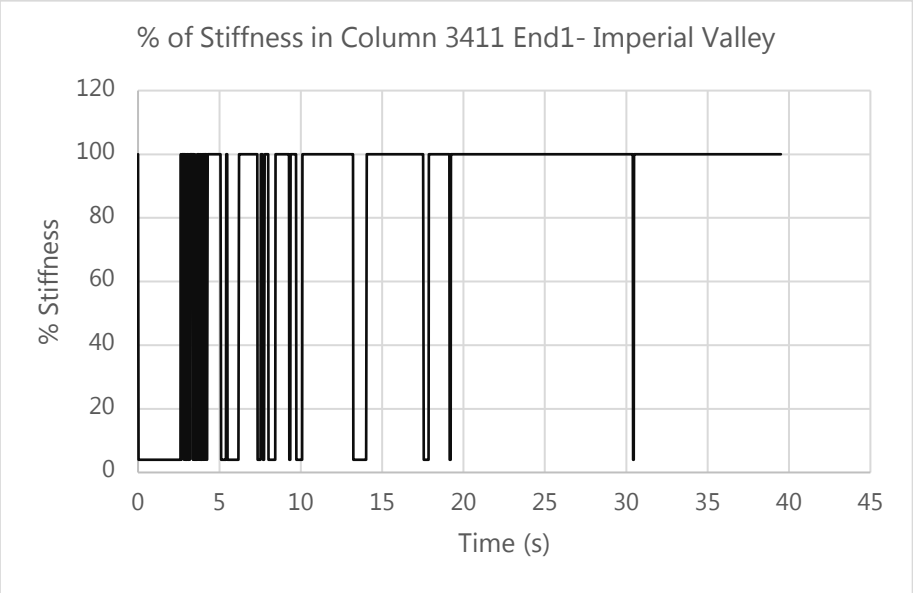
% of Stiffness in Column 3411 End1- Imperial Valley
% Stiffness
120
100
80
60
40
20
0
0
5
10
15
20
25
30
35
40
45
Time (s)

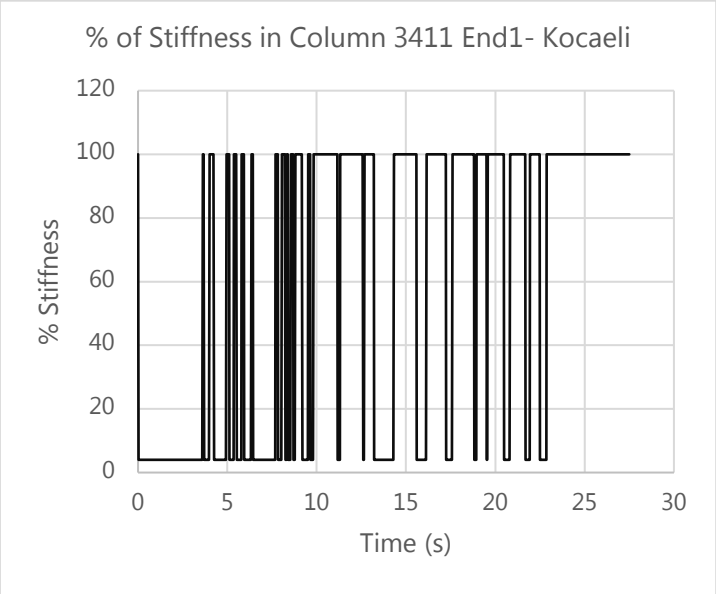
% of Stiffness in Column 3411 End1- Kocaeli
% Stiffness
120
100
80
60
40
20
0
0
5
10
15
20
25
30
Time (s)

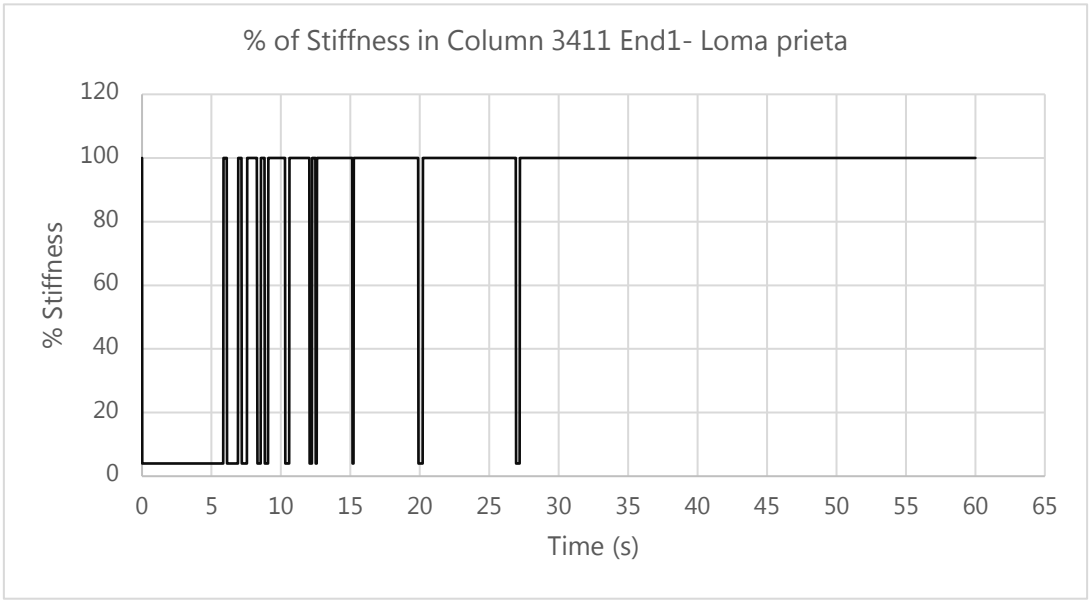

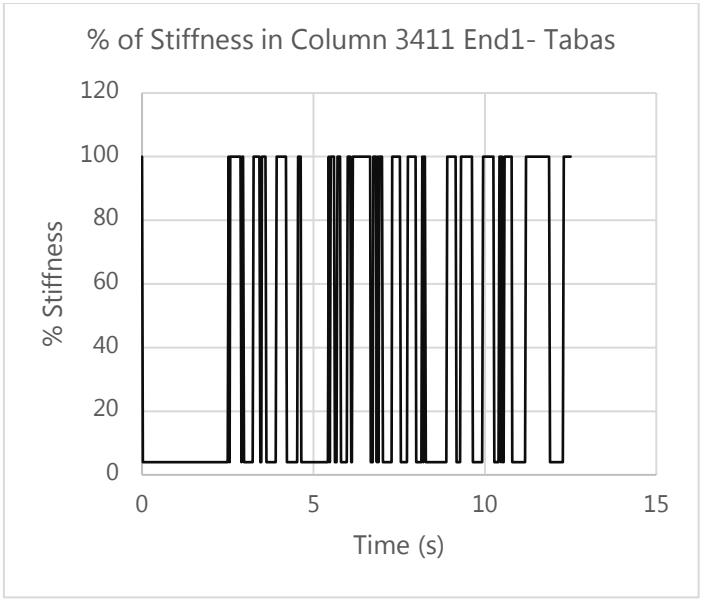

Figure 5. 9. Stiffness variation with time compared between the most critical column and the module-module bolted connection plate subject to the six earthquake time histories

5.3.3. Moment vs Curvature Results for the Most Critical Column Element

The moment curvature relationships that were generated for the critical column (of which the stiffness variation was shown through Figure 5.9) against the six earthquake time histories are shown below in Figure 5.10.

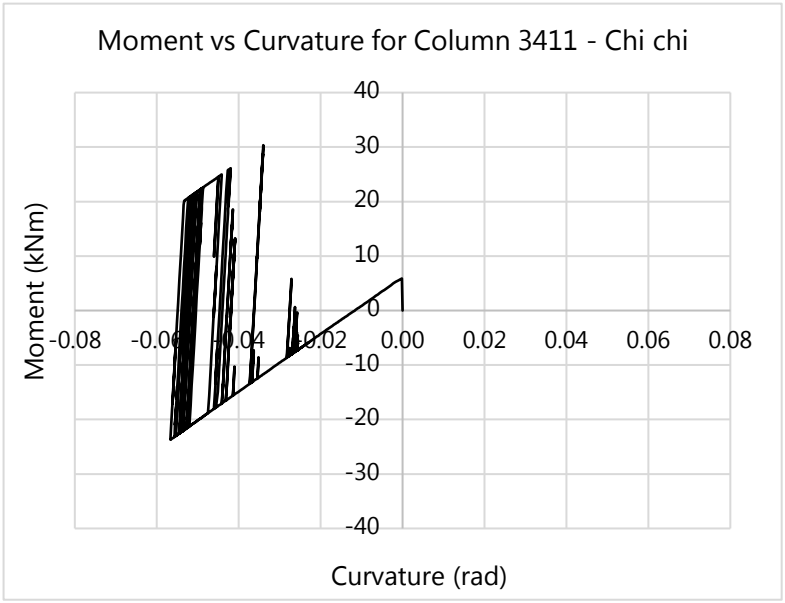

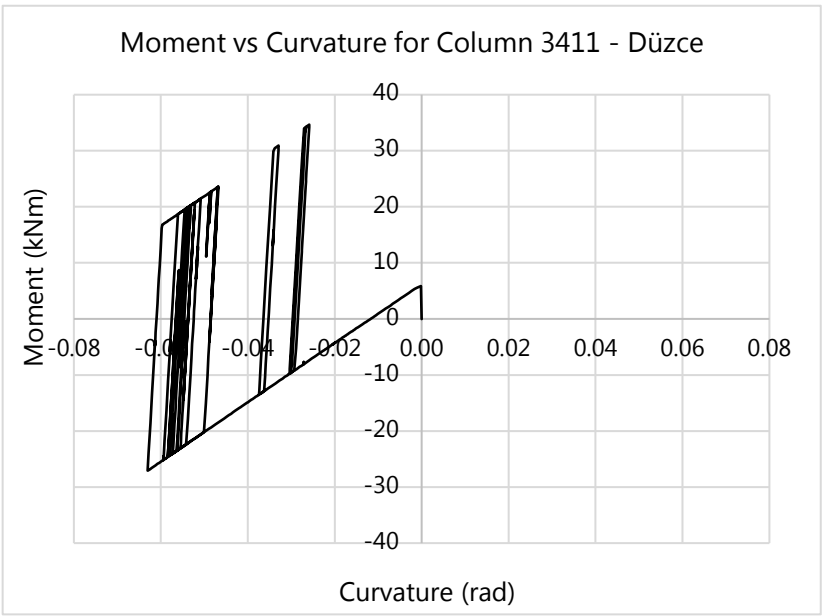

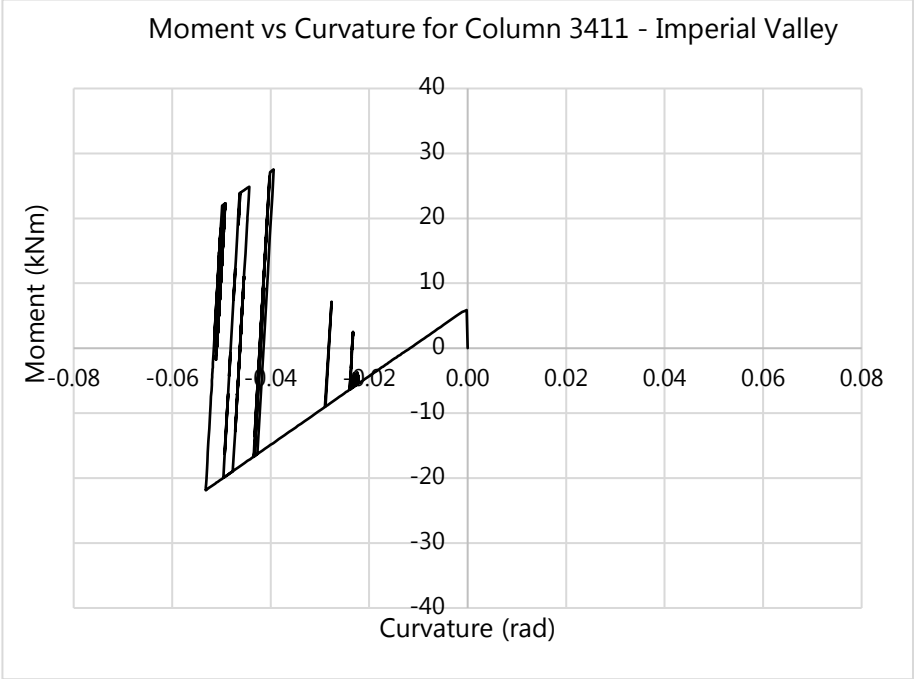
Moment vs Curvature for Column 3411 - Imperial Valley
Moment (kNm)
40
30
20
10
0
-10
-20
-30
-40
-0.08
-0.06
-0.04
-0.02
0.00
0.02
0.04
0.06
0.08
Curvature (rad)

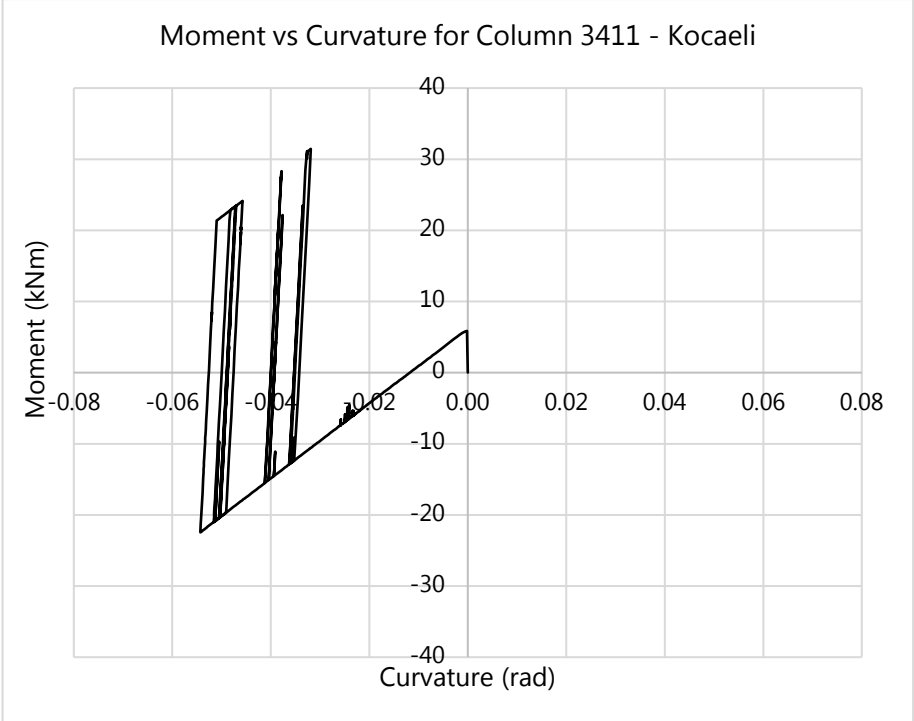
Moment vs Curvature for Column 3411 - Kocaeli
Moment (kNm)
40
30
20
10
0
-10
-20
-30
-40
-0.08
-0.06
-0.04
-0.02
0.00
0.02
0.04
0.06
0.08
Curvature (rad)

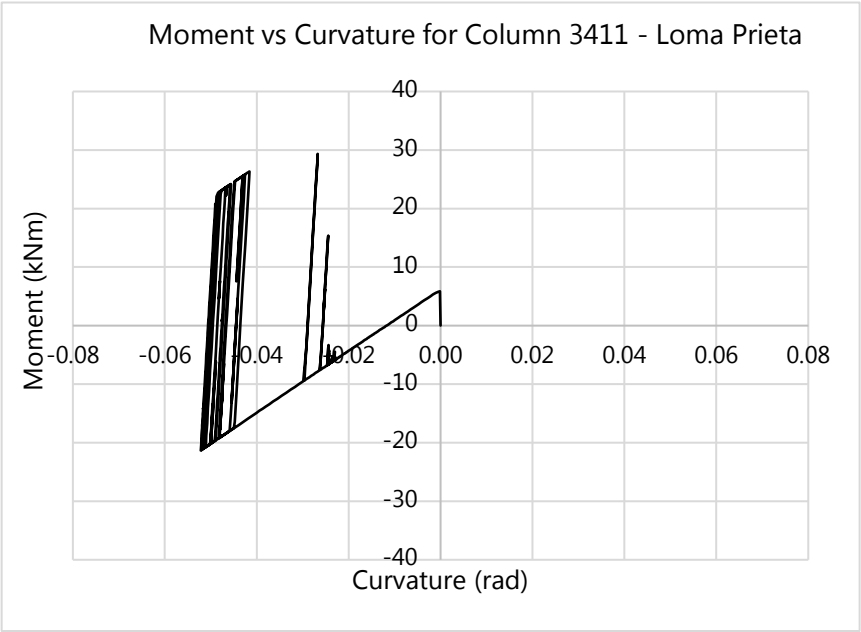

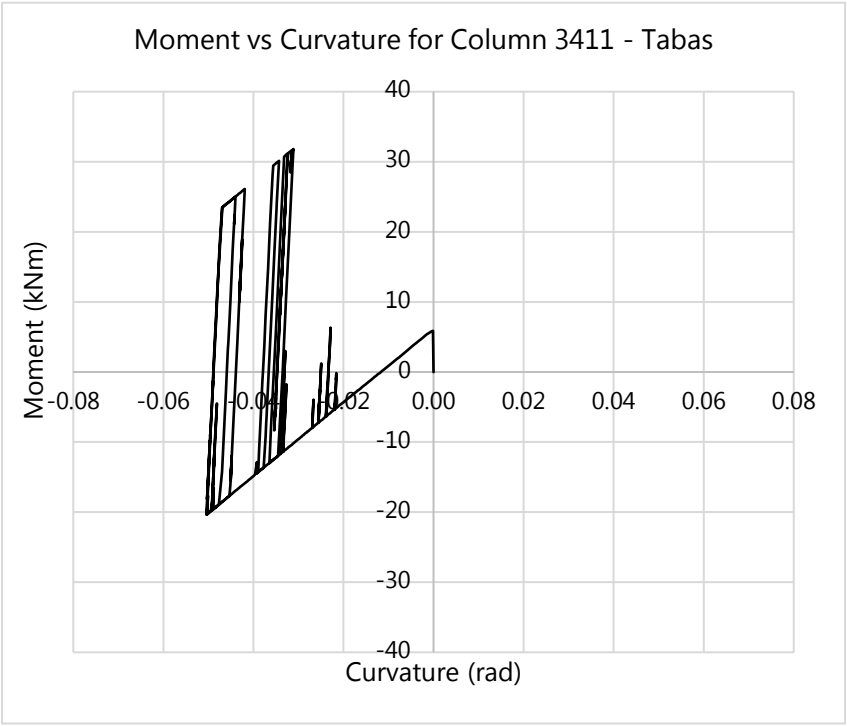

Figure 5. 10. Moment-curvature relationships for the most critical column subject to the six earthquake time histories

The gradient of the curve while the element is still elastic equals the value of elastic modulus (E) times the second moment of area about the bending axis (I). Therefore, where the curve changes its gradient shows where the value of EI has changed thus indicating yielding.

The column has deformed following the specified bilinear hysteresis rule and where the bi-linearity starts in each curve indicates the yield moment and yield curvature (φ_y) of the column. The value for yield curvature as observed is taken to be 0.02 rad.

Although ultimate failure cannot be observed here, a common maximum curvature can be observed at approximately 0.05 rad. Using the above observations, a ductility value of 2.5 (0.05 rad/0.02 rad – from Eq. 1) can be observed for the critical column.

5.3.4. Pushover Curve and Capacity Spectrum Analysis

The pushover curve generated is shown in Figure 5.11.

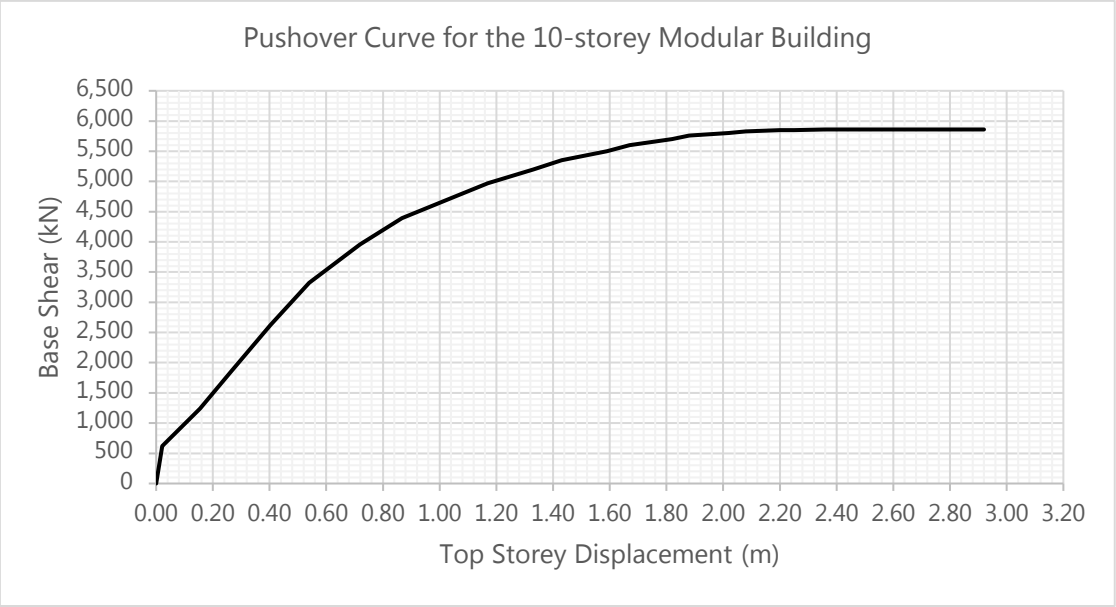

Figure 5. 11. Pushover Curve generated from the nonlinear static pushover analysis for the 10 storey building

The capacity spectrum method was subsequently applied on the pushover curve that is presented above to generate results on the seismic performance of the structures. The equations to convert the pushover curve to the ADRS format (Mahaney et al, 1993; Chopra et al., 1999) was discussed in Chapter 3.

The modal analysis results that were discussed previously were used in converting the pushover curve to the capacity curve in the ADRS format and the resulting capacity diagram is shown in Figure 5.12.

Subsequently the response of the structure to the applied earthquake accelerograms were extracted from the results of each of the RUAUMOKO models carried out for each earthquake loading. The response spectra for 5% damping were considered here to plot against the capacity curve as this is the damping value considered in most seismic design codes.

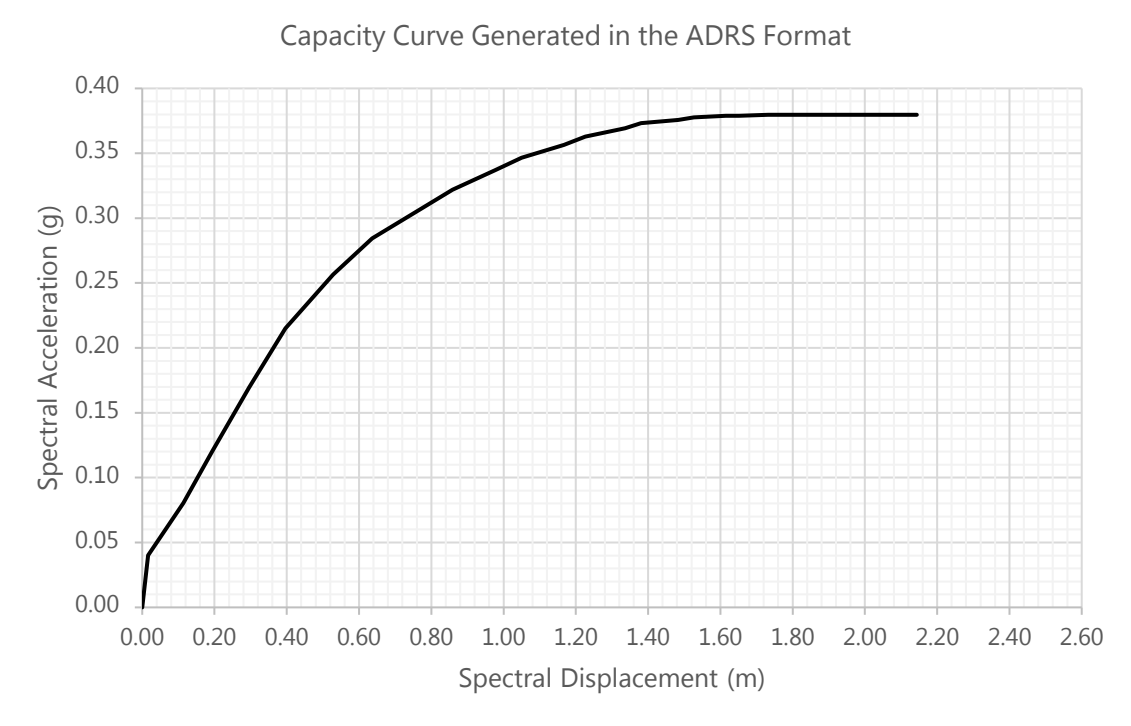

Figure 5. 12. Capacity Curve generated from the nonlinear static pushover analysis for the 10 storey building

A combined diagram of the 5% damped demand curves for all six considered earthquake records alongside the capacity curve of the building is shown below in Figure 5.13.

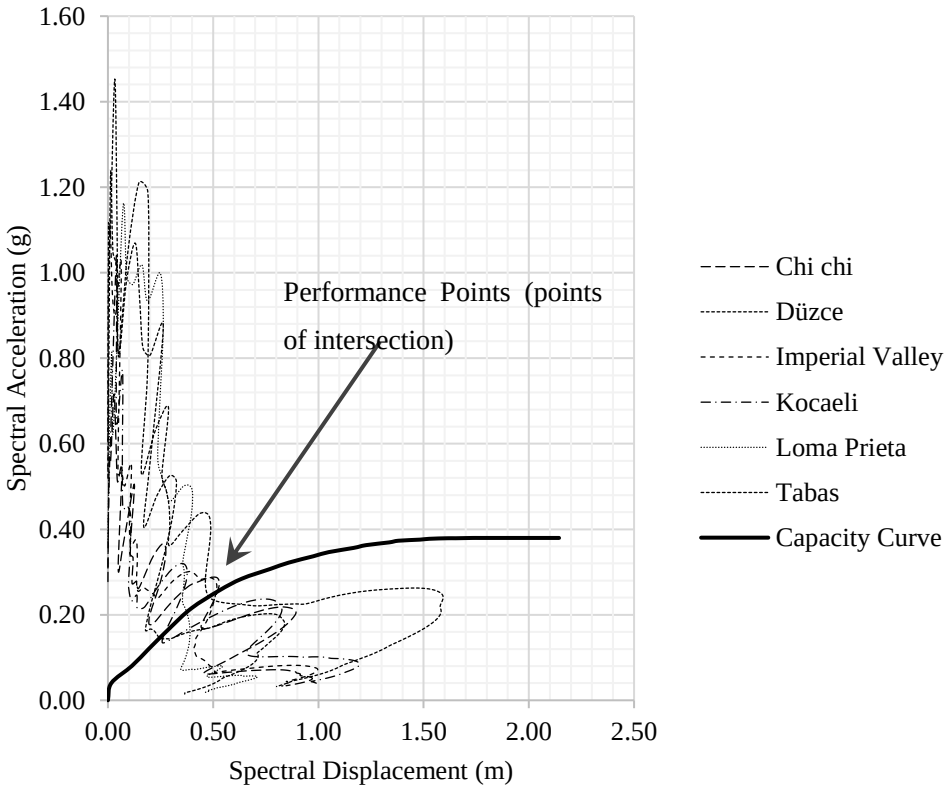

Figure 5. 13. Combined 5% damped demand curves against capacity spectrum

As per the 5% damped response spectra plotted against the capacity spectrum, it appears that the structure is past its linear deformation zone at its performance points against all six earthquake time histories. The performance points are also located further below the full capacity of the structure. Therefore, it can be deduced that the structure performs in the 'Life Safety' zone as per the ATC40 and SEAOC categorisations which were described in Chapter 3.

This is a valuable preliminary estimate of the performance of this structure against the earthquakes applied. Since the earthquakes are all with magnitudes greater than 6.5 in the Moment Magnitude scale it can be assumed as a stable structure under large earthquakes. This preliminary estimate can be used as a guidance in carrying out more exact performance based designs where site specific elastic design response spectra, which are scaled to match the required return periods representing the rarity of the earthquake as per the design, are applied on modular buildings.

5.4. Sensitivity Analyses

In addition to the detailed nonlinear analysis which was described previously, further investigation was carried out into the ten storey building to understand the contribution of the stiff modules to the overall behaviour of the structure.

This further analysis was carried out in two main avenues as follows;

1. A sensitivity analysis to establish the properties of the walls that affect the contribution of the stiff modules in resisting the earthquake loads
2. A sensitivity analysis carried out to establish extents of the drift profile and displacement profile of the building to varying wall depth inside the module

The dynamic linear earthquake analysis suggested in AS 1170.4 (2007) was used for the purpose of the above mentioned sensitivity analyses. A hazard factor of 0.08 which is consistent with the value for Melbourne, Australia was used along with a return period of 2500 years which results in a k_p factor of 1.3. The earthquake is applied only in the critical Y direction. Soil class D is assumed in order to achieve a larger base shear since a ten-story building would not amount to a very large seismic weight. A response spectrum analysis was

carried out considering the above parameters to obtain the earlier mentioned sensitivity results.

5.4.1. Contribution of the Stiffer Modules to Earthquake Resistance

The contribution of the stiff modules is measured as the percentage of the base shear carried by the foundation of each of the stiff module stacks. The contribution of the stiff modules as explained above was measured against varying wall properties. The most critical property of the wall to be changed is its depth since it has the largest proportional effect on the stiffness of the wall in the considered direction.

The first sensitivity analysis is therefore carried out by changing the depth of the wall. The base model was developed keeping the wall depth at 5.4m in each side of the module's exterior wall. It was then analysed by changing the wall depths to 1.8m, 3.6m, 7.2m and 9.0.

The resulting contributions of the stiff modules to each of these wall depths is presented in Table 5.3 below.

Table 5. 3 Sensitivity of the Contribution of Stiff Modules in Resisting the Earthquake Base Shear to Varying Wall Depth

Wall Depth	Full Base Shear in Y Direction	Contribution by Stiff Modules	% Increase in Contribution from the no-walls condition
1.8 m	775 kN	42 %	5.0 %
3.6 m	789 kN	58 %	45.0 %
5.4 m	918 kN	82 %	105.0 %
7.2 m	1053 kN	91 %	127.5 %
9.0 m	1113 kN	90 %	125.0 %

The contribution of the stiffer modules seem to be largely sensitive to the depth of the wall built in the module. This effect seems to null out when the depth reaches 9.0m out of the 10.8m of full depth. A half depth wall with a depth of 5.4 m appears to have achieved an optimum amount of contribution. It is therefore interesting to observe how the change of wall depth affects the drift performance and the overall lateral deflections of the building.

As per the graph shown in Figure 5.14 smaller wall depths of 3.6m and 1.8m attract large drifts at the bottom levels of the structure. Having a half depth wall of 5.4 m again seems to have resulted in a reasonable performance for the building. The deflection profile of the building is plotted in Figure 5.15. A typical earthquake displacement profile is observed for

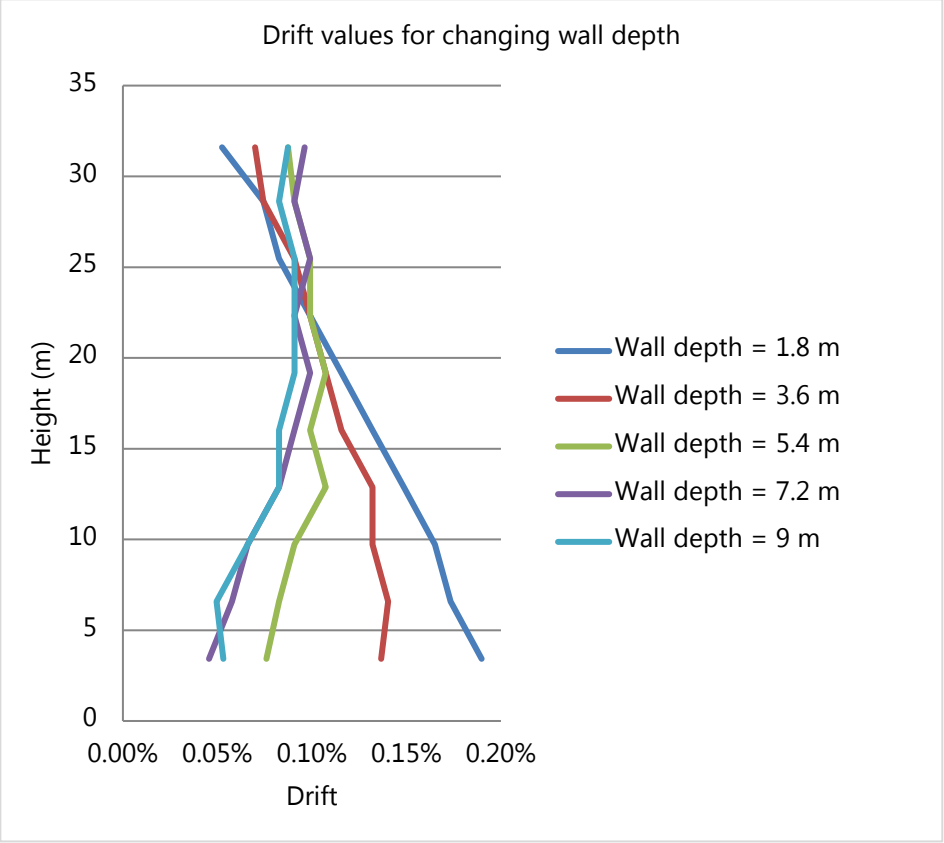

Figure 5. 14. Sensitivity of the drift values to changing wall depth inside the module

each analysis and shows that the overall deformation can be largely affected by altering the wall depth.

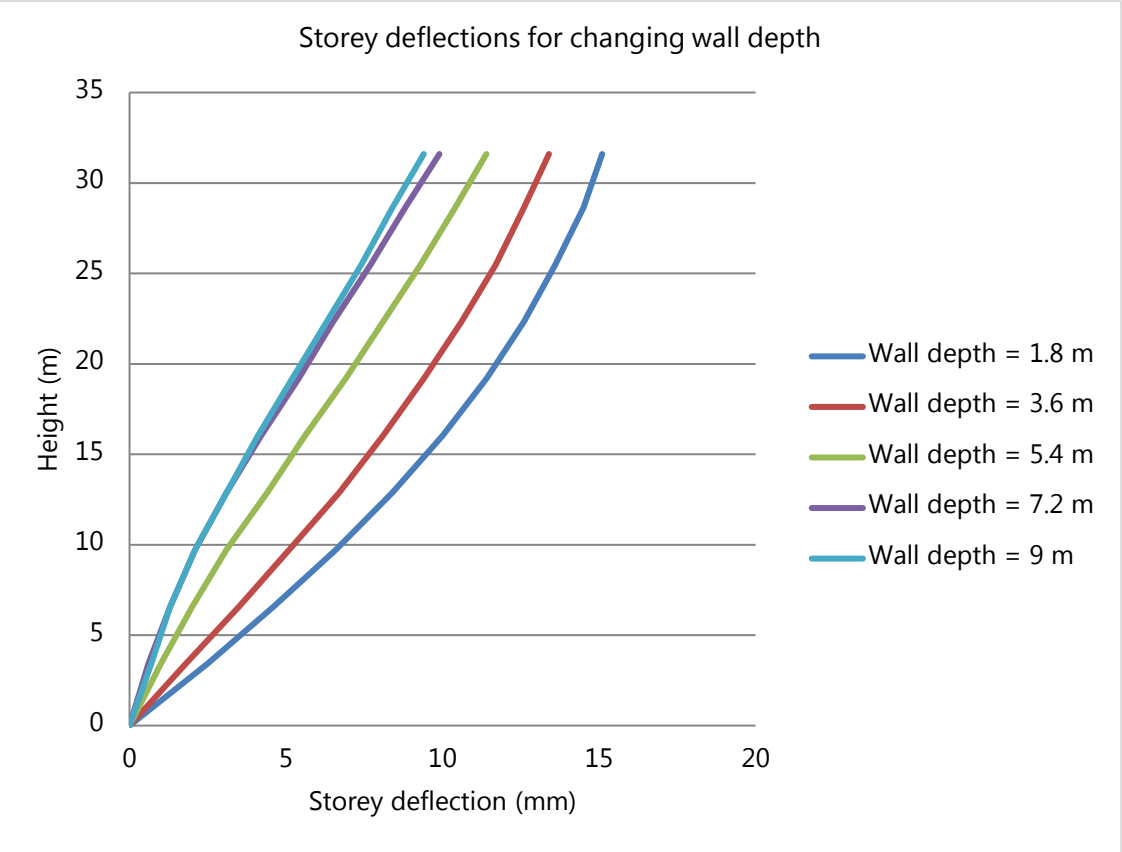

Figure 5. 15. Sensitivity of the storey deflections to changing wall depth inside the module

5.5. Summary

- It is important to investigate the behaviour of the elements that join at the module-module connection as they play a critical role in how the advanced corner supported system performs. A ten storey modular building that is constructed with the advanced

corner supported system is analysed in this chapter with applied earthquake time histories. The behaviour of the system is analysed through nonlinear time-history analysis and nonlinear static pushover analysis. The performance is then evaluated using the Capacity Spectrum method.

- Possible hinge formations are identified at the critical module to module connection and its connecting elements where the results for the more likely outcome are observed from the nonlinear time history analysis. A hinge formation in the main corner column just under the floor beam or above the roof beam ("Hinge 2" as per Fig 5.6) proves to be the most likely scenario out of the possibilities hypothesised. It was further observed through the Capacity Spectrum analysis that the system can perform at 'Life Safety' levels in the applied earthquake conditions.
- In addition to the above, a simpler analysis is performed to evaluate the sensitivity of storey deflections and drifts to the depth of the walls that are in the stiffer modules. The contribution of these stiffer modules in transferring lateral loads is also evaluated. It was observed that for the 10.8 meter long modules an approximate wall depth of 5.4m (half of the length) would be the optimum level in controlling deflections and in contributing to the lateral load transfer.
- Conclusions on the observed results are presented later in Chapter 8.

Chapter 6 Finite Element Analysis and Laboratory Testing of a Module to Module Steel Connection

6.1. Introduction

The global analysis of the ten storey modular building as discussed in Chapter 5 has produced valuable results in order to understand the overall behaviour of the structural system against dynamic earthquake forces. In this regard, when considering medium to high-rise buildings the lateral load transfer mechanisms are highly significant.

It is understood that the module to module connections transfer the applied lateral loads from the point of application to the stiffer modules. The interface through which this load transfer occurs is the bolted steel connection that connects two adjacent corner columns of two neighbouring modules. Although corner supported modules built and joined with such connections have already been used in practice, they have not effectively participated in the lateral load resisting system due to over-conservative designs and lack of knowledge about their actual behaviour, as discussed in Chapter 4.

A connection as such was designed solely for the purpose of this research. The make-up of the connection was intended to be as generic as possible so that any Engineer could follow the findings and recommendations of this study and create their own unique connection

design. Uniqueness of each designer's product has been a key criteria in acquiring a larger market share in the modular construction industry. The design of the connection which is considered for this analysis is illustrated in figure 6.1 below.

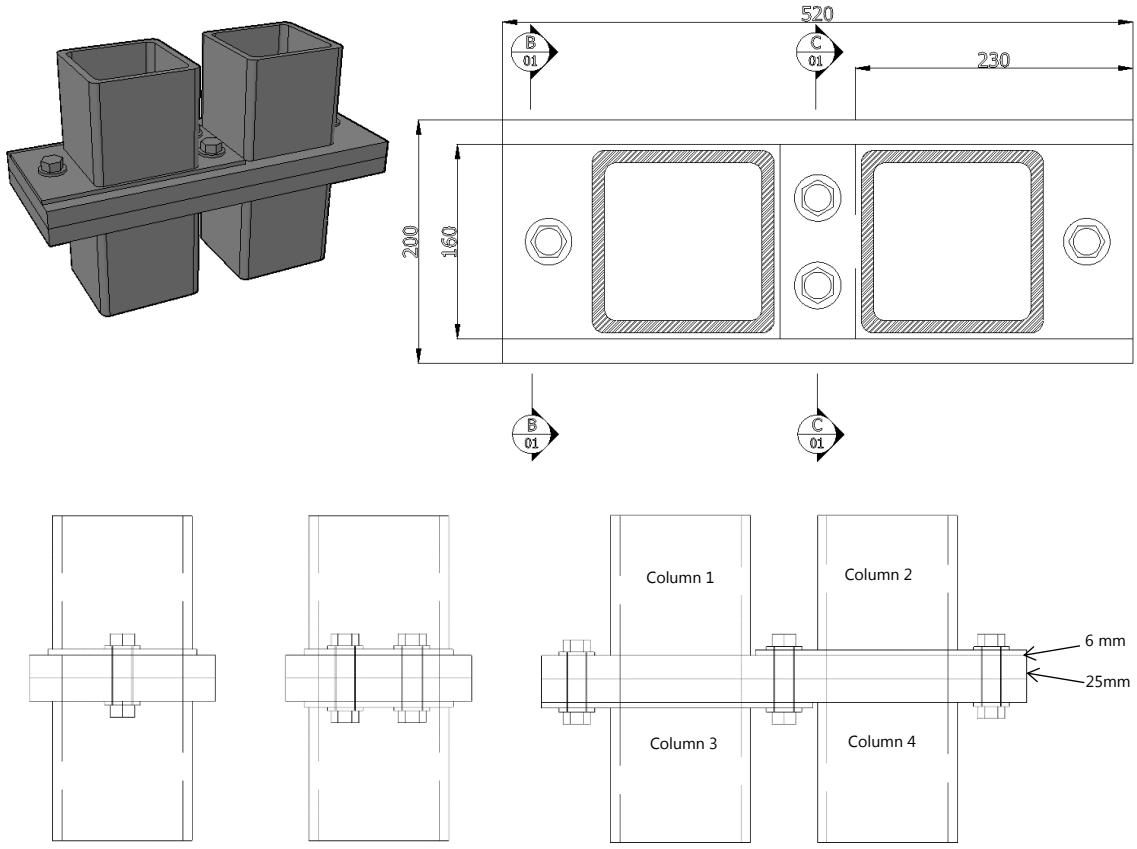

Figure 6. 1. The Steel Connection designed for the purpose of this research; the connection will connect two adjacent corner supporting columns of two neighbouring modules (Note: the structure where this connection is applied is shown in Figure 5.6)

This connection is modelled using the finite element software ANSYS (version 16.0) to assess its behaviour more accurately against an applied lateral load. Since this connection would transfer shear forces resulting from both wind and earthquake forces, a general monotonic lateral load is applied to study its basic behaviour to laterally applied loads.

A laboratory experiment was conducted in order to validate the results of the computer model which was generated through ANSYS. The experiment was designed in a manner that would accommodate the available equipment and their capacities. The design of the connection was to be exactly the same as what was modelled in ANSYS.

6.2. The Module to Module Connection

The connection is designed to transfer loads both horizontally and vertically as this is expected from a corner supported system. One such unit of these connections would connect four neighbouring modules (Figure 5.6), both vertically and horizontally. The four square hollow sections represent the four corner columns that connect at this joint.

Three variations of this module to module connection design were considered for the finite element analysis and the experimental validation. The parameters that were different in the three designs were only the size of the bolts and the type and size of the bolt holes. All other properties were kept constant. The three designs and the parameters that were different in each of them are shown in Table 6.1.

Table 6. 1 Connection designs and their varied parameters used for the finite element analysis and the laboratory experiments

Connection Design	Bolt diameter	Bolt Hole diameter and type
C1	12 mm	14 mm round
C2	16 mm	18 mm round
C3	16 mm	18 mm slotted

An image from the 3D finite element model created on ANSYS is shown in Figure 6.2. Three separate models were created on ANSYS to analyse the three connection designs C1, C2 and C3 respectively. The basic procedure that was carried out in designing each of the connection designs is explained in section 6.2.1.

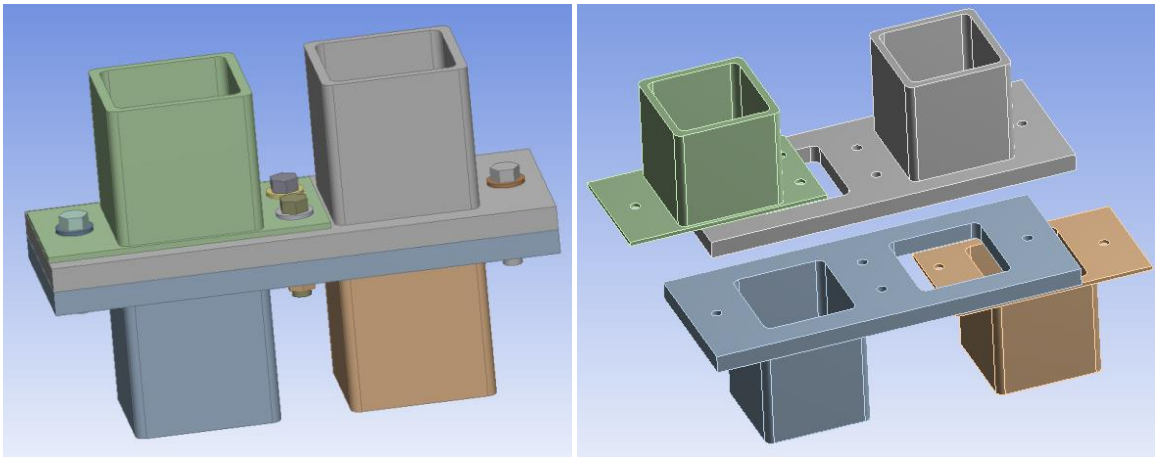

Figure 6. 2. Images of a 3D computer model of the module to module connection and an exploded view showing the four main parts that comprise the connection

6.2.1. Structural Design of the Module to Module Connection

Prior to carrying out the finite element analysis and the laboratory test, the connection designs required to be checked for adequacy in resisting the loads that were to be applied. A code based design was followed to establish this criteria. The strength and serviceability limit states for each connection design was calculated following the Australian steel design standard AS 4100 (1998). The complete design calculation is shown here for connection design C1 where the same procedure was followed in designing connection designs C2 and C3. The supporting guidelines provided by Gorenc et al. (2005) was also followed in the design calculations in addition to the design standard AS 4100 (1998).

Calculation of Nominal Shear Capacity (V_f)

The nominal shear capacity is calculated using the guidance given in clause 9.3.2 of AS 4100 (1998). The calculation demands the understanding of the number of shear planes that each bolt covers. As far as the actual connection employed in a real building is concerned, the two bolts in the middle would cover 3 shear planes each and the two bolts in the corners would cover 2 shear planes each. This action is illustrated in Figure 6.3 below.

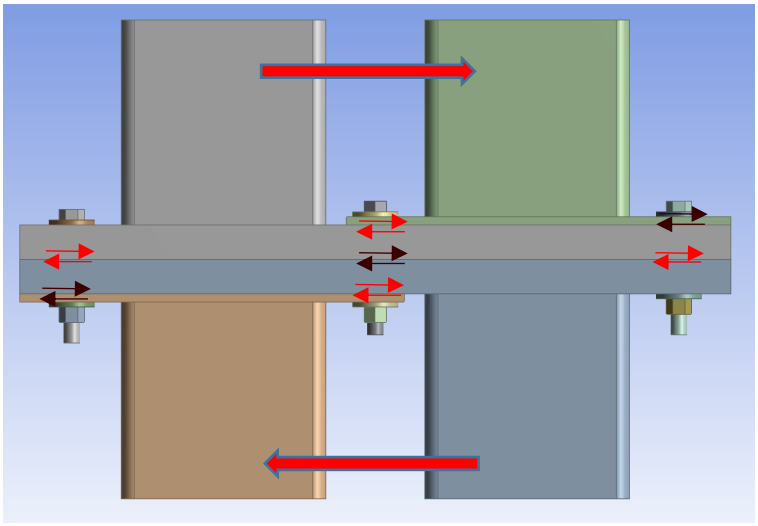

Figure 6. 3. Existing shear planes in the connection when columns are axially loaded

However, the columns were not to be axially restrained during the planned experiment which is described in section 6.4 and are free to move along the direction of any lateral load that is applied. Since the load cell would only be connected to one plate at the connection, the shear plane for all bolts will only lie at the common interface of the two 25 mm thick plates they connect as shown in Figure 6.4. Therefore, for the purpose of the laboratory experiment and the finite element analysis only one shear plane would be considered for the design of this connection and all three of its variations.

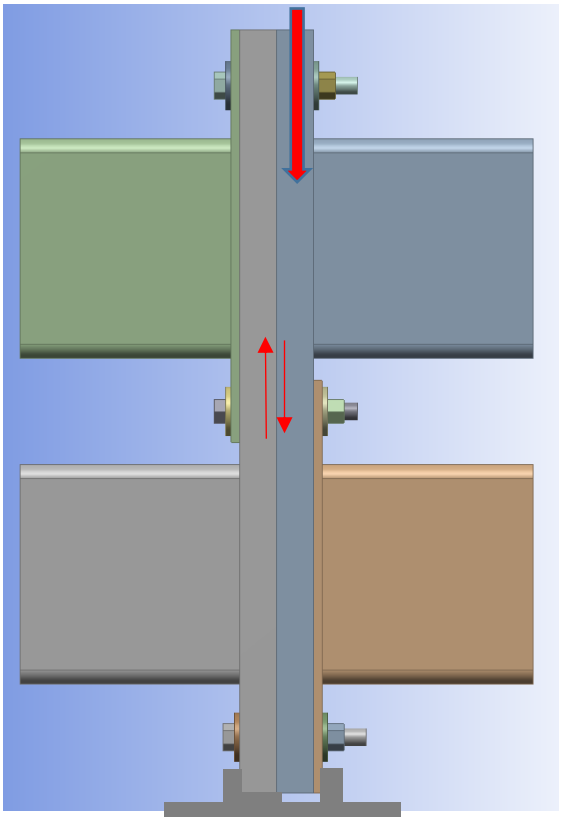

Figure 6. 4. Existing shear planes in the connection when columns are not axially restrained (design for the Experiment)

Considering no shear planes in the threaded region;

$$V_f = 0.62 k_r f_{uf} n_x A_0 \qquad \text{Eq. 6.1}$$

Where;

$k_r = Reduction\ factor\ for\ length\ of\ bolt\ line\ (bears\ a\ value\ of\ 1.0\ for\ connections\ other\ than\ lap\ connections)$
$f_{uf} = Minimum\ tensile\ strength\ of\ the\ bolt$
$n_x = Number\ of\ shear\ planes\ in\ the\ unthreaded\ region$
$A_0 = Bolt\ shank\ area$

The calculation for one bolt is as follows;

$$V_f = 0.62 \times 1 \times 800 \frac{N}{mm^2} \times 1 \times 113.1\ mm^2 \times 10^{-3}$$

$$= 56.1\ kN$$

Therefore, the shear capacity of all four bolts would be 224.4 kN (56.1 kN x 4). Although the above value is considered for the experiment, a capacity reduction factor of 0.8 applies over this value for the design shear capacity of the connection as per AS 4100 (1998).

Although shear failure is anticipated to be critical for this connection, the following checks for bearing (crushing) and tear-out are also carried out for the design of the plies. The 6mm thick ply is considered the most critical one for these checks. Tensile strength of the steel with 350 MPa yield strength is considered to be 450 MPa for these calculations.

Check for bearing (V_b) is as follows;

$$V_b = 3.2 t_p d_f f_{up} \qquad \text{Eq. 6.2}$$

Where;

$t_p = Thickness\ of\ the\ ply$
$f_{up} = Minimum\ tensile\ strength\ of\ the\ ply$
$d_f = Bolt\ diameter$

The calculation for one of the 6 mm plies for crushing under the pre-tension of one of the bolts is as follows;

$$V_b = 3.2 \times 6\ mm \times 12\ mm \times 450\ N/mm^2$$

$$= 103.7\ kN$$

Therefore, all bolt pre-tensions applied need to be less than 103.7 kN each.

Check for tear-out failure (V_p) is as follows;

$$V_p = a_e t_p f_{up} \qquad \text{Eq. 6.3}$$

Where;

$$a_e = Minimum\ distance\ from\ the\ ply\ edge\ to\ the\ centre\ of\ the\ hole\ in\ the\ direction\ of\ the\ bearing\ load$$

The calculation for one of the 6 mm plies for tear-out near one of the bolts is as follows;

$$V_p = 35\ mm \times 6\ mm \times 450\ N/mm^2$$

$$= 94.5\ kN$$

Therefore the tear-out capacity of the full connection would be 378 kN (94.5 kN x 4). Since this value is higher than the shear capacity of the connection, it is therefore deduced that considering shear capacity would satisfy other two failure criteria as well.

Calculation of Slip Resistance (V_{sf}/ $F_{s,RD}$)

This connection shall be treated as a 'Slip Critical' connection due to the geometric position of the connection in the structure and the type of loads that it would undergo during an earthquake. The Australian standard AS 4100 (1998) addresses slip failure as a serviceability limit criteria and is calculated as follows;

$$V_{sf} = \mu n_{ei} N_{ti} k_b \qquad \text{Eq. 6.4}$$

Where;

$$\mu = Coefficient\ of\ friction\ between\ plies$$
$$n_{ei} = Number\ of\ shear\ planes$$
$$N_{ti} = Minimum\ pretension\ imparted\ on\ the\ bolts\ during\ installation$$
$$k_b = Factor\ for\ hole\ type\ (1.0\ for\ standard\ holes, 0.85\ for\ oversize\ holes\ and$$

$short\ slots\ and\ 0.70\ for\ long\ slotted\ holes)$

Following the AJAX Fastener Handbook (1999), a value of 31.8 kN is considered for N_{ti} and the calculation for slip resistance is as follows;

$$V_{sf} = 0.2 \times 1 \times 31.8\ kN \times 1 = 6.36\ kN$$

The slip would therefore occur at a load of 6.36 kN for one bolt in the connection. The total slip resistance of the entire connection is therefore 25.44 kN (6.36 x 4).

Similar calculation procedure is followed for the design of both C2 and C3 connection designs and the results of the design calculations are presented in a tabular form in Table 6.2 as follows;

Table 6. 2 Design Capacities for the three connection designs considered for the laboratory test and finite element analysis

Connection Design	Shear Capacity	Maximum Bolt Pretension allowed per bolt	Slip Capacity (Serviceability)
C1	224.4 kN	103.7 kN	25.4 kN
C2	398.9 kN	138.2 kN	47.4 kN
C3	398.9 kN	138.2 kN	40.3 kN

6.3. Finite Element Analysis

Three models were created using ANSYS to carry out finite element analyses on the three connection designs which were mentioned in Table 6.1 previously. The 'Transient Structural' module of ANSYS was used to carry out the analyses for all three models. The exact setup that was planned for the laboratory experiment was used in the finite element analysis in defining the boundary conditions and loading.

The common properties that were considered for the models in general are as follows (Refer to Figure 6.1 for column numbers mentioned below);

Four hollow section columns	: 150x150x9 Square Hollow sections with a yield strength of 350 MPa
Bottom and top plates of Columns 1 & 4	: 25 mm thick steel plates with a yield strength of 350 MPa
Bottom and top plates of Columns 2 & 3	: 6mm thick steel plates with a yield strength of 350 MPa
Grade of bolts	: Grade 8.8 with a yield strength of 660 MPa
Minimum Tensile strength of Grade 8.8 bolts	: 800 MPa (AJAX, 1999)
Washers	: 4mm thick stainless steel washers
Young's modulus of Steel	: 200000 MPa
Shear modulus of Steel	: 80 GPa

While the common properties are as those mentioned above, the three different models created to represent the connection designs C1, C2 and C3 have the properties mentioned below that differ them from one another. The AJAX Fastener Handbook (AJAX, 1999) was used as a reference to all the bolt and nut details and also their fastening specifications.

Figure 6.5 explains the notations used to characterise the bolt geometry. Table 6.3 lists out the geometric properties of each connection design.

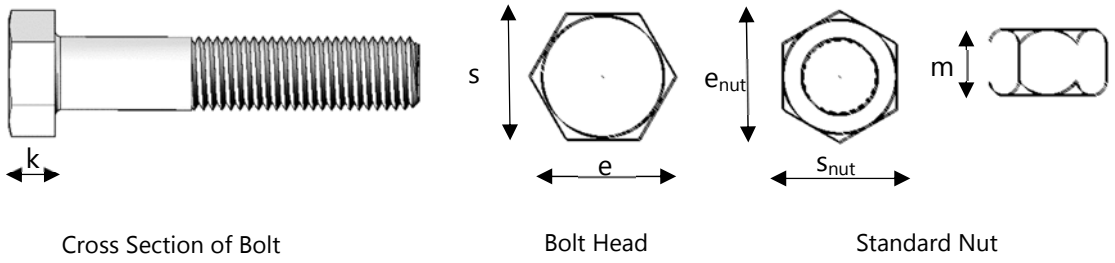

Figure 6. 5. Dimensions of the bolts and nuts used to model the steel connections

Notations (compatible with the notations used in AJAX (1999))

k : Thickness of bolt head

s : Width across flats

e : Width across corners

m : Thickness of standard nut

s_{nut} : Width across flats of the nut

e_{nut} : Width across corners of the nut

Table 6. 3 Details of the bolts and nuts used for the ANSYS models representing the connection designs

Property	Value in each connection design		
	C1	C2	C3
Bolt diameter	12 mm	16 mm	16 mm
Hole type and diameter	14 mm round	18 mm round	18 mm slotted
Pitch of threads	1.75 mm	2.0 mm	2.0 mm
k	7.5 mm	10.0 mm	10.0 mm
s	18 mm	24 mm	24 mm

e	20.03 mm	26.75 mm	26.75 mm
m	10.58 mm	14.45 mm	14.45 mm
s_{nut}	18 mm	24 mm	24 mm
e_{nut}	20.03 mm	26.75 mm	26.75 mm
Bolt pre-tension	31.8 kN	59.2 kN	59.2 kN

Each of the models are loaded with a similar loading to that of what was applied during the laboratory experiment. Details of the loading will be discussed with reference to the laboratory experiment under section 6.4.

6.4. Laboratory Experiment

As previously discussed, a laboratory experiment with three connection specimens manufactured to the same designs was setup to validate the finite element analysis. Where the main intent of the laboratory experiment was to validate the computer generated models, the experiment would also provide a valuable insight into the actual behaviour of the connections when subjected to a shearing action.

6.4.1. Experiment Setup

A vertical load cell with a loading capacity of 500 kN was used for the experiment. The specimens were placed on a steel table which was placed directly under the load cell. A schematic of the laboratory setup is shown in Figure 6.6.

The apparatus was setup in the laboratory to make best use of the available equipment. As a result, the specimen was kept parallel to the vertical axis so that the compressive load applied

from the vertical load cell would act as a horizontal-equivalent shearing force on the bolted joint as shown in Figure 6.6.

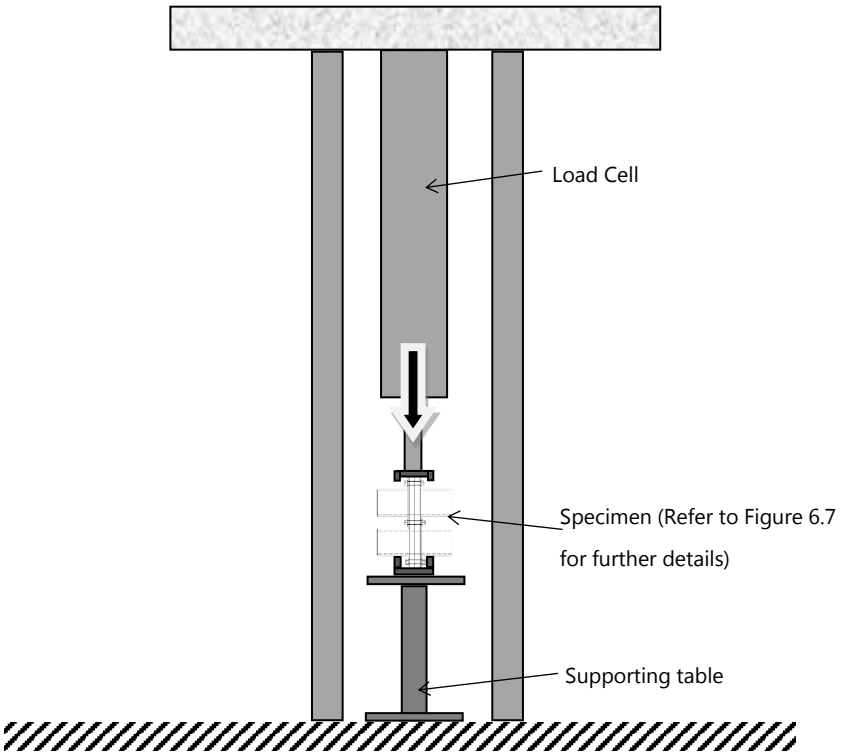

Figure 6. 6. Sketch of the setup for laboratory experiment

A close-up view of the supporting block that allows the shearing action is shown in figure 6.7. While it blocks one plate from moving down it allows the other to freely move. Another similar block is kept at the top of the specimen as well where it allows the movement of the opposite plate to freely move while holding the other from moving.

Figure 6. 7. A close up view of the supporting block used for the experiment (Left) and a schematic diagram of the same (Right) for a clear view

A contactless measurement system (ARAMIS) was used in this experiment to obtain the required strain values. This assisted in obtaining accurate strain values while not obstructing the experiment with strain gauges and other equipment that would otherwise require to be physically attached to the specimens. The ARAMIS system measures strains in both 2D and 3D environments with the use of high definition photogrammetry. Once each specimen was setup under the load cell the ARAMIS camera was calibrated to the depth of the target area from the place of the camera. Figure 6.8 shows the first specimen after being placed under the load cell.

The target area was sprayed with a special paint as required by the ARAMIS manual and Figure 6.9 shows how one of the specimens was prepared accordingly. A further description of the contactless measurement system ARAMIS is provided in section 6.4.2.

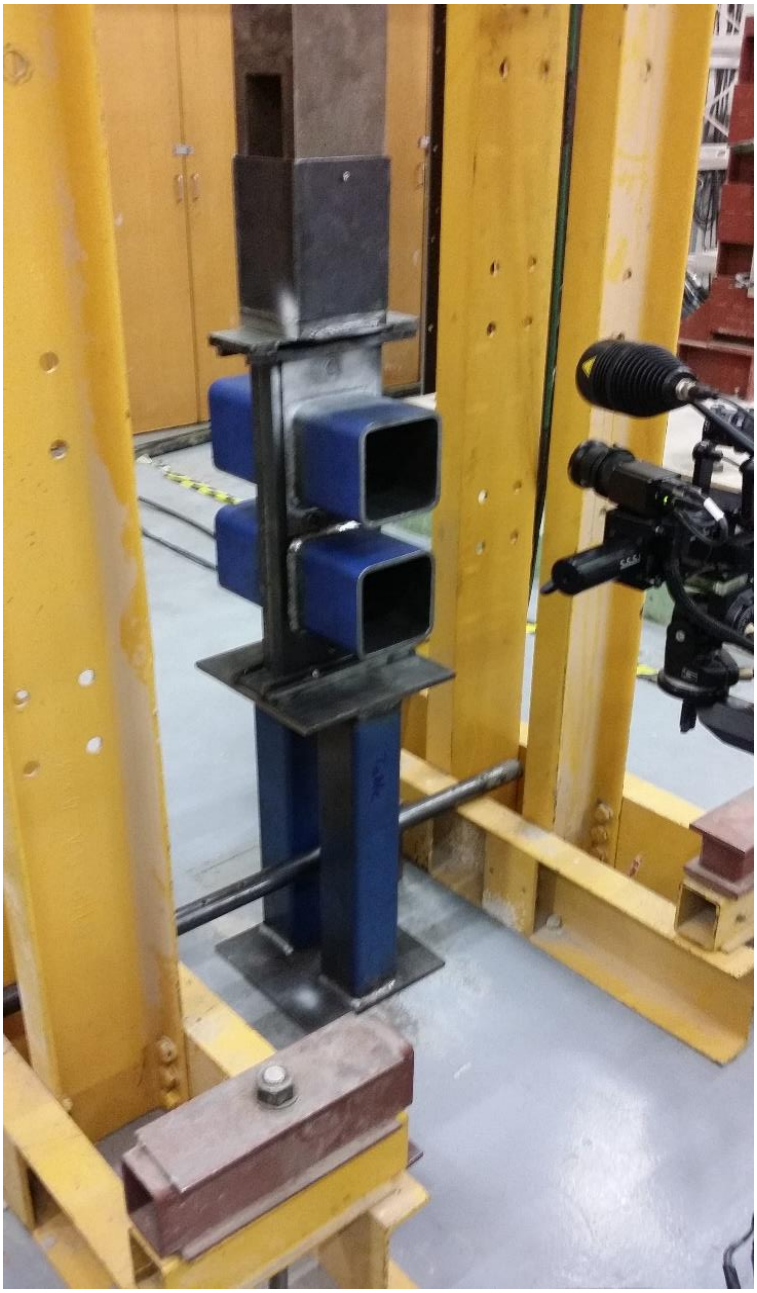

Figure 6. 8. A specimen set up under the load cell ready to be loaded

6.4.2. Setup for Contactless Measurements

The sophisticated contactless measurement system named ARAMIS was used to measure the strains on the specimens. By definition, ARAMIS is a 3D non-contact deformation measuring system. Depending on the expected range of deformations an area on the specimen must be selected for the camera to focus before taking measurements. The area around the first bolt immediately under the load cell was chosen as a suitable area from which to take the strain measurements. A special paint mixture was then sprayed on to the target area of each specimen and was allowed to dry for 90 minutes as specified (Figure 6.9).

The camera and the sensors were fully calibrated before each of the three experiments using the special calibration kit that is provided with the product and care was taken to ensure that the apparatus was fixed without any undue movements which may tamper with the measurements. Lighting around the target area of the specimen was keenly adjusted to receive the sharpest and cleanest possible image on the monitor as shown in Figure 6.10.

Figure 6. 9. The special paint applied around the area of the first bolt before focusing the camera of the ARAMIS system for strain measurements

Some of the main features of the ARAMIS system are specifically intended to obtain strain measurements and validate finite element models (ARAMIS, 2008). Such features together with the efficiency and user friendliness of the system made it desirable to be used for the experiment.

The loading and displacement values were obtained directly from the data logger of the load cell. Since the experiment was conducted as a slow load rate application the load was applied as a displacement based load at a displacement rate of 0.1 mm/min.

Figure 6. 10. Focusing the camera of the ARAMIS system to the target area around the first bolt, before applying the load on the specimen

6.5. Comparison of Results from the Laboratory Experiment against the Analysis Results

6.5.1. Load vs Deformation Relationships

The results to the finite element analysis as well as the corresponding experiments are compared here for the purpose of validating the finite element models. Gorenc et al. (2005) provide the diagram shown in Figure 6.11 to explain the expected behaviour of a clamping bolt similar to those used in the specimens.

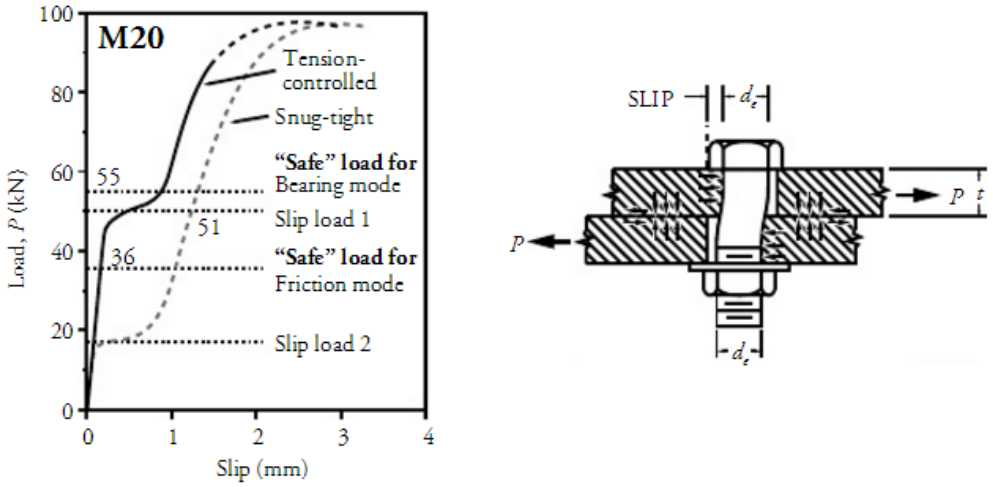

Figure 6. 11. Behaviour of high-strength structural bolts undergoing combined shear and bearing stresses following a slip (Gorenc et al., 2005)

As the figure explains, the bolts will deform under the 'Friction Mode' until the deformation pushes the bolts to the edge of their clearance hole. Afterwards the bolts will begin to experience shear deformation while also resisting the axial forces that are generated through the bearing against the wall of the clearance hole. A firmly tightened bolt is expected to undergo its deformation similar to the curve with the solid line as shown in Figure 6.11 and a snug-tight bolt would follow the dotted line in the same figure.

The specimens that were manufactured for the experiment were specified to have tightened bolts applied with an equivalent torque to ensure the specified bolt pre-stresses as per the AJAX (1999).

The results for load deformation were measured directly from the load cell's data logging software during the experiment and the resulting values were obtained in the form of a data file in the text format for each of the specimens. The data in the text files were then developed into useful graphical representations of Load vs Deformation relationships as shown in Figures 6.12 to 6.14.

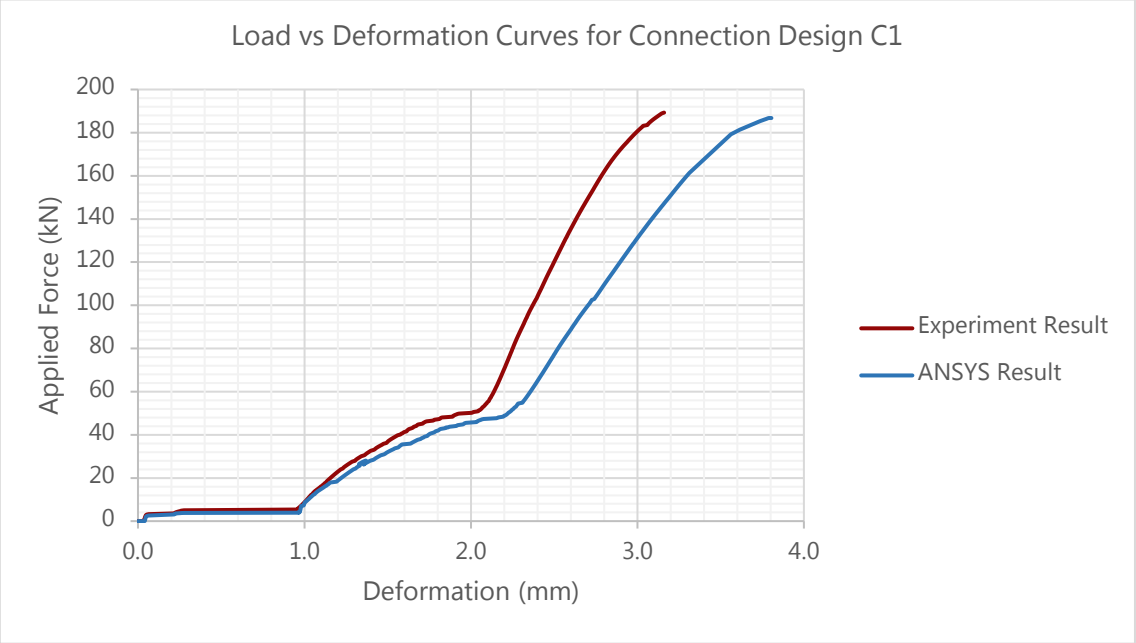

Figure 6. 12. Comparison of Load vs Deformation Curves from the Experiment against those from the ANSYS model for Connection Design C1

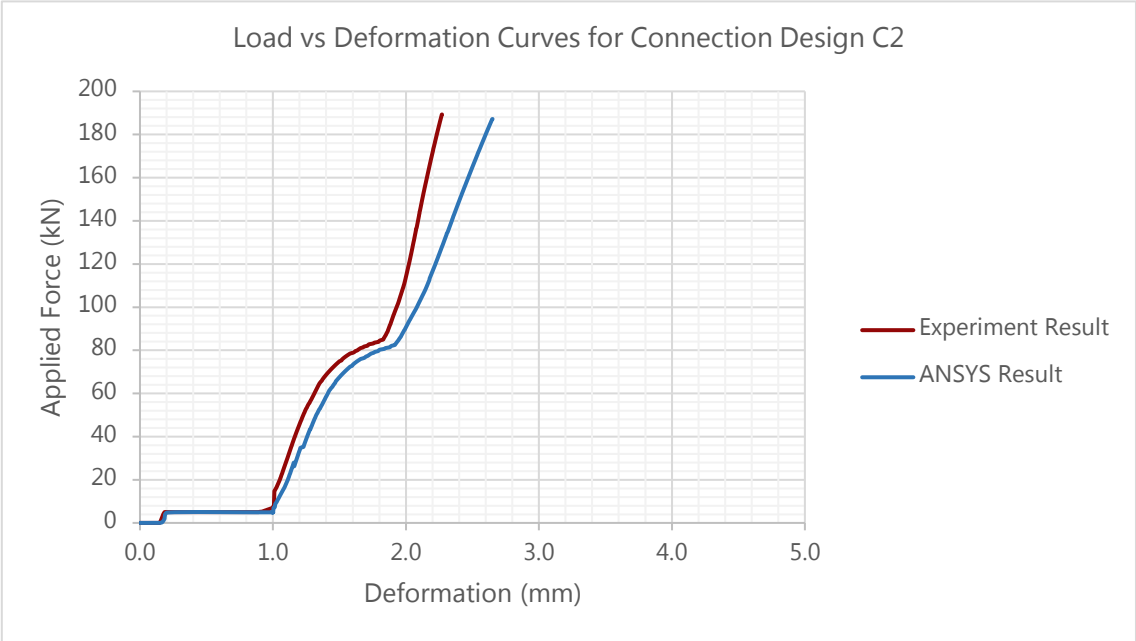

Figure 6. 13. Comparison of Load vs Deformation Curves from the Experiment against those from the ANSYS model for Connection Design C2

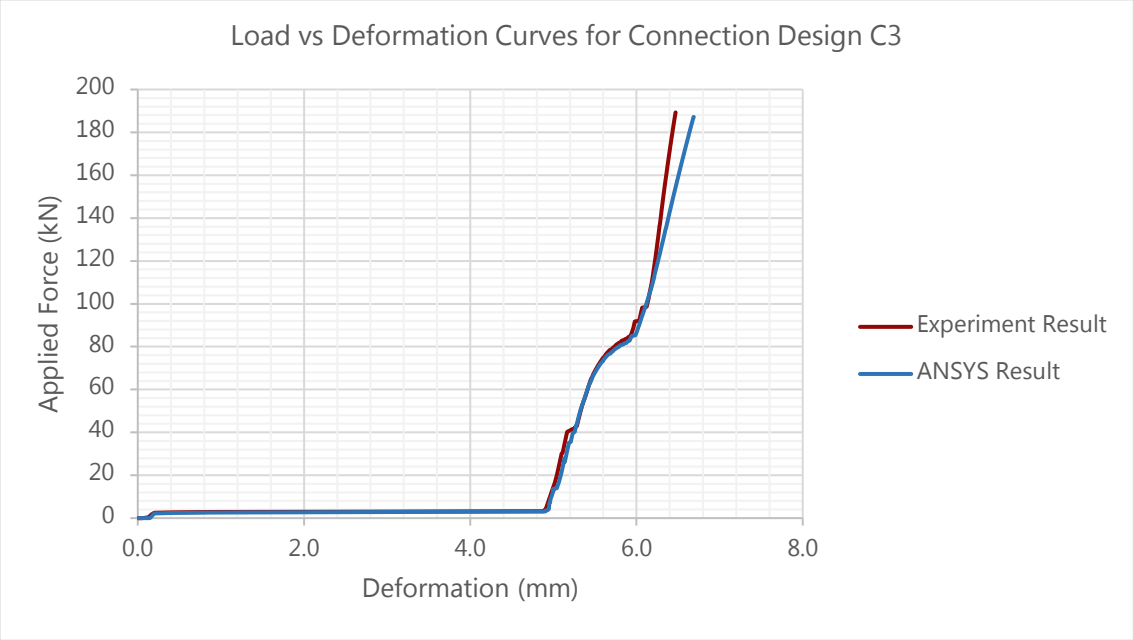

Figure 6. 13. Comparison of Load vs Deformation Curves from the Experiment against those from the ANSYS model for Connection Design C3

The load vs deformation curves for the three connection designs show a very close match in the different stages of the deformation. The pattern of the curves as a whole show very close resemblance to each other.

When studying the curves for connection designs C1 and C2, three distinct stages of deformation can be identified. The initial part of the curve shows a rapid deformation until the deformation reaches a value of approximately 1mm. This can be identified as the initial slip of the connection until the first bolt starts to touch the edge of its clearance hole. Since the bolt hole diameter is 2mm greater than the diameter of the bolt, there is a 1mm wide empty space between the bolt and the outer edge of the bolt hole at the beginning of loading. Similarly connection design C3 also undergoes the same stages with a higher initial slip of approximately 5mm which matches with the slot size of 26mm for the M16 bolt.

This free space is uniform in the ANSYS model thus shown very distinctly in each of the deformation curves for connection designs C1, C2 and C3. However, the connections that were made for the laboratory experiment may have had a slight misalignment from the centre. Therefore, although hardly noticeable, the laboratory specimens attain values slightly higher or lower than the values that resulted from the ANSYS model for this first stage of deformation. This is the initial slip of the connection where the slip failure occurs at only one bolt.

Once the first bolt has settled into the edge of its bolt hole the overall stiffness of the connection is modified. The connection would now facilitate the action of that bolt fully in resisting the lateral force. The other bolts too similarly and gradually undergo slip failure and settle into their bolt holes and fully contribute to the overall lateral stiffness of the connection. This transformation is depicted in the second stage of deformation shown in the curves. The loads that correspond to the end of the second stage are matched with the overall slip resistance calculated in section 6.2.

Table 6. 4 Comparison of slip resistance of the analytical model and the experimental results

Connection Design	Slip Capacity for μ=0.20 (Serviceability Design)	Slip resistance of the ANSYS model	Slip resistance of the laboratory specimen
C1	25.4 kN	48.5 kN	51.8 kN
C2	47.4 kN	81.5 kN	84.0 kN
C3	40.3 kN	81.0 kN	83.5 kN

The third stage of deformation is quite clear in all three connection designs. This is the stage where all components of the connection act together as one unit to resist the lateral force. The stiffness shown in this region of the curves is therefore representative of the overall lateral stiffness of the respective connection design. In this stage the bolts undergo bearing and shear deformation. Therefore, the stiffness of the bolts calculated to resist bearing and shear should represent the overall elastic stiffness of the connection. This assumption is discussed further with calculations later in this Chapter.

Further validation of the ANSYS model is obtained through the strain values obtained with the contactless measurement system ARAMIS. The strain values are plotted throughout the time history of the loading for five selected points on the ARAMIS map. The same five points are selected from the ANSYS model for its strain values and compared with the former. The comparison of results for the three connection designs is as follows;

6.5.2. Strain Measurements

The contactless strain measurements that were taken with the aid of the ARAMIS system is compared here against the results from the ANSYS model. To increase accuracy of the comparison process, five nodes were selected from the ARAMIS results where the measurements were clear for the total duration of the experiment. The same five points were marked out on the ANSYS model. The strain values for all five of those points were compared throughout the time duration of the experiment for all three connection designs.

Connection Design C1

The five points that were marked to measure the strain results through the duration of the test is illustrated in Figure 6.15. The marked points A, B, C, D and E are at similar locations to the stage points 0, 1, 2, 3 and 4 from the ARAMIS strain measurement. A sample strain result plot output from ARAMIS is demonstrated in Figure 6.16.

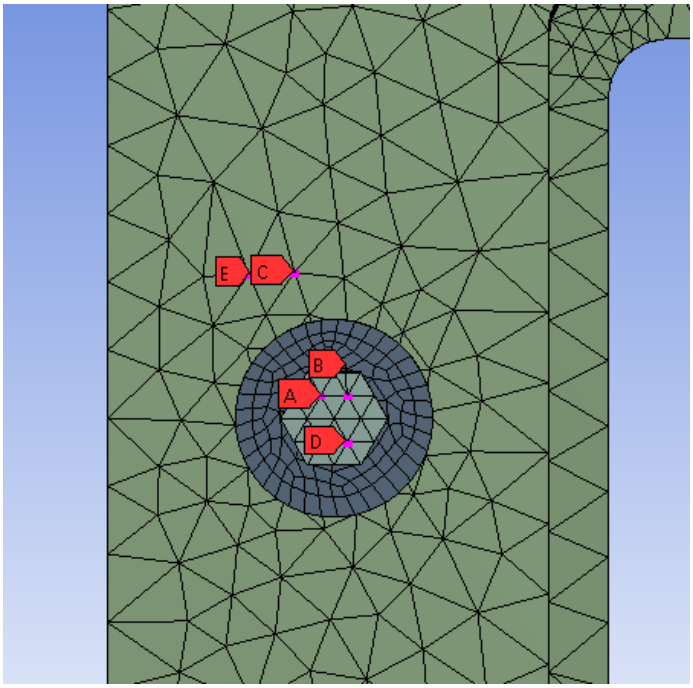

Figure 6. 14. Five points marked on the ANSYS model to measure von Mises strains

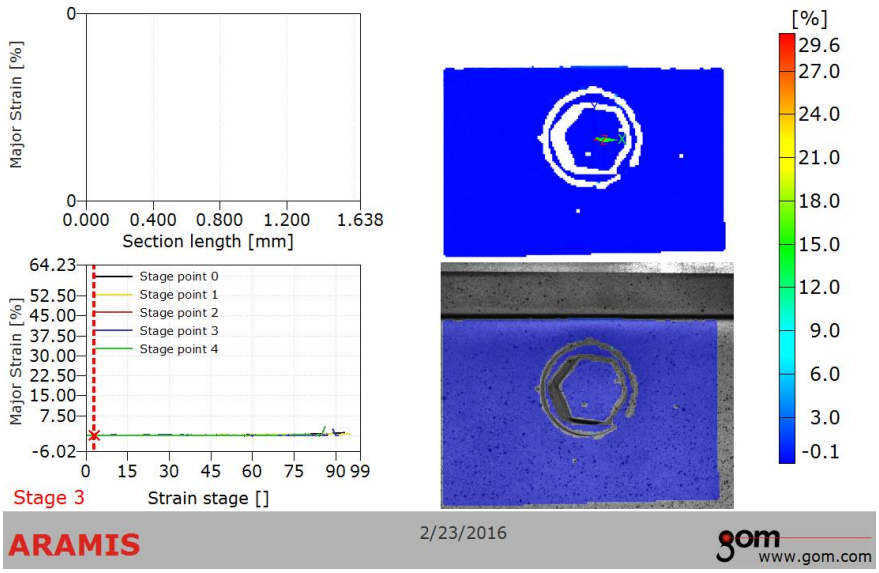

Figure 6. 15. A sample strain results plot from ARAMIS for a time at the initial part of the loading

The von Mises strain results plotted for each of the 'stage points' mentioned above and their comparison with the ANSYS analysis for connection design C1 are shown below from Figures 6.17 to 6.31.

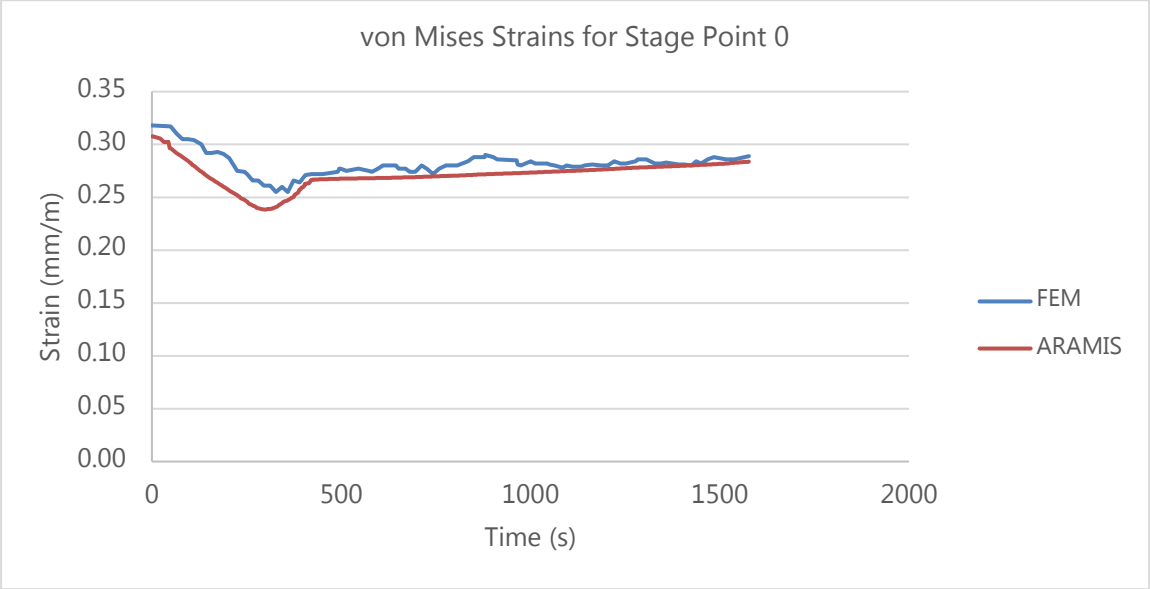

Figure 6. 16. Resulting von Mises strains for Stage Point 0 from FEM (Finite Element Model) and ARAMIS measurements

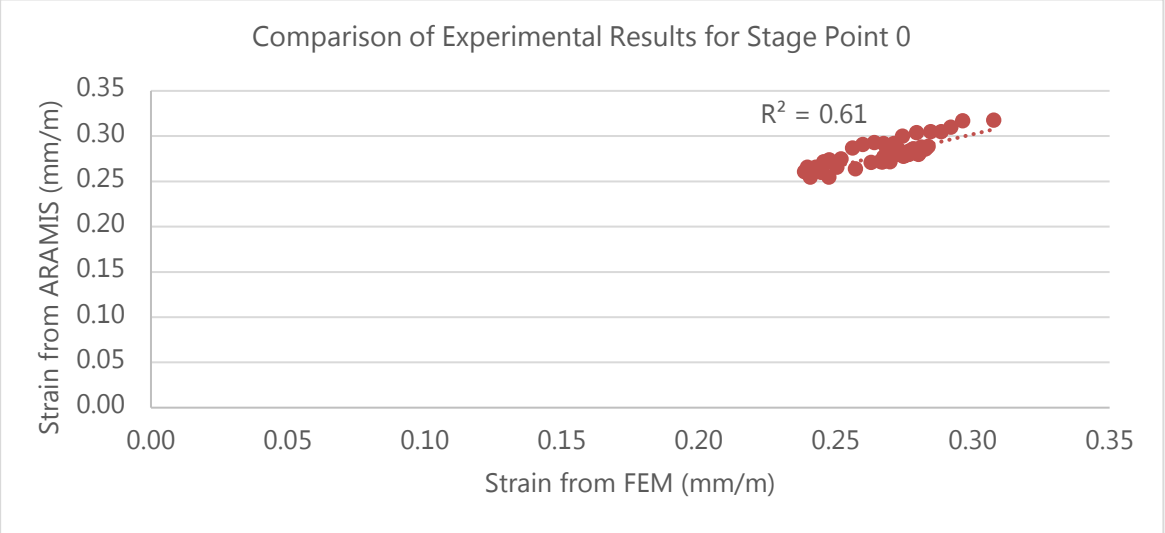

Figure 6. 17. Comparison by R^2 value of von Mises strains from FEM (Finite Element Model) with ARAMIS measurements for Stage Point 0

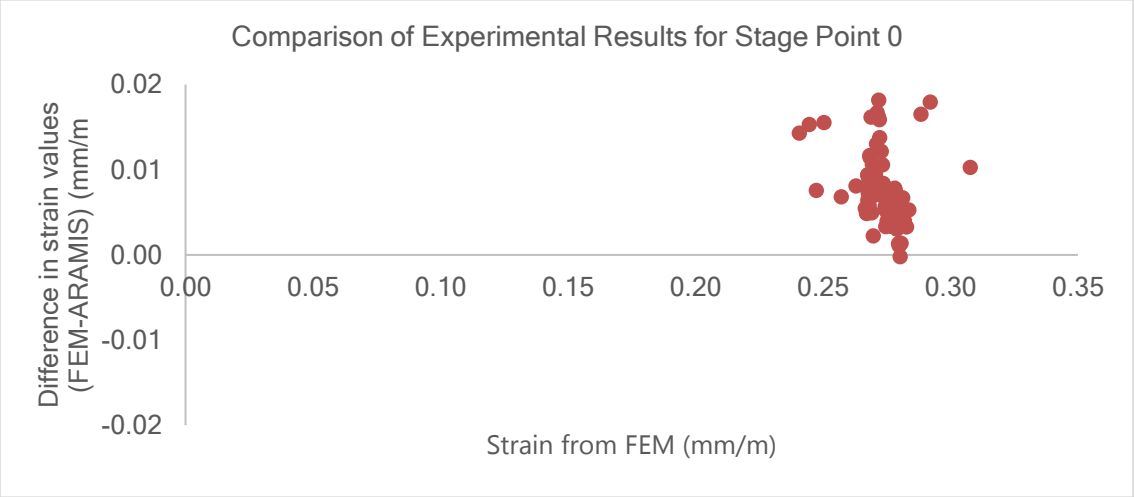

Figure 6. 18. Comparison by scatter diagram of von Mises strains from FEM (Finite Element Model) with ARAMIS measurements for Stage Point 0

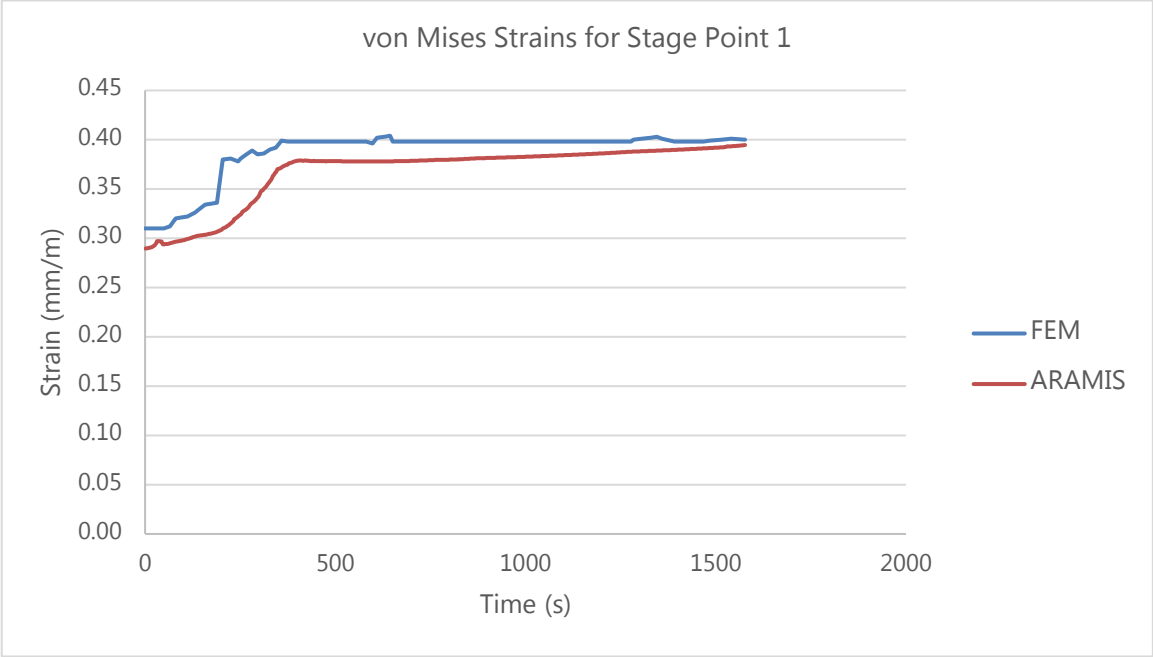

Figure 6. 19. Resulting von Mises strains for Stage Point 1 from FEM (Finite Element Model) and ARAMIS measurements

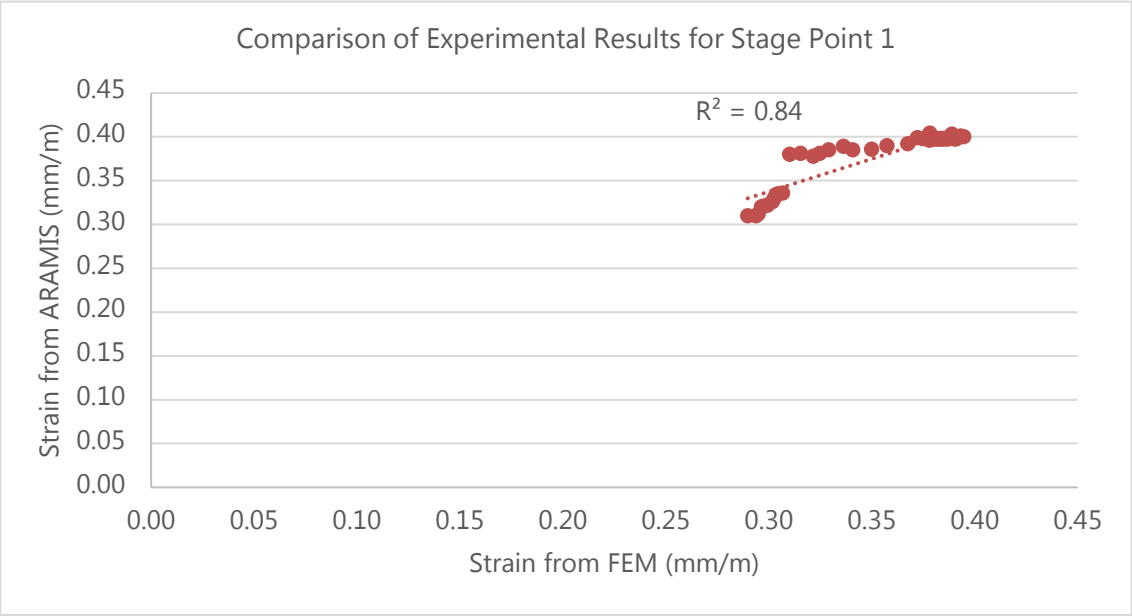

Figure 6. 20. Comparison by R^2 value of von Mises strains from FEM (Finite Element Model) with ARAMIS measurements for Stage Point 1

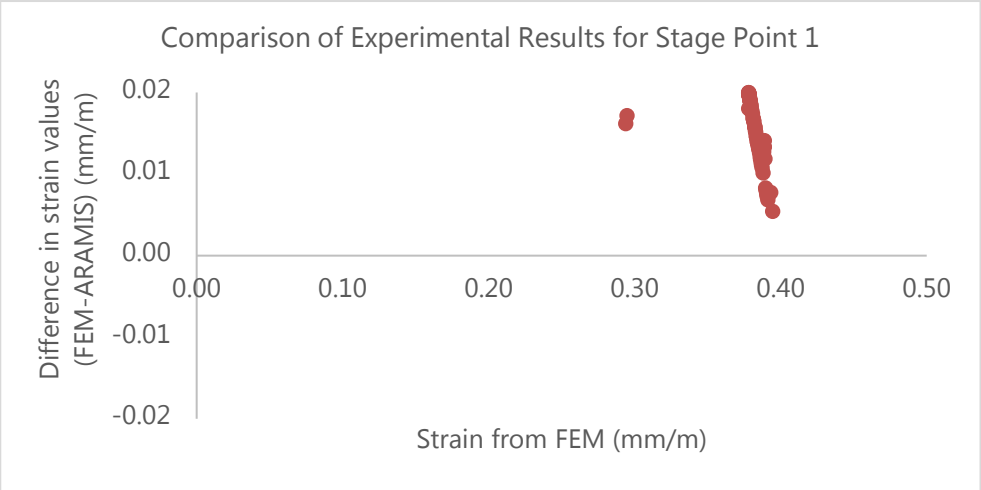

Figure 6. 21. Comparison by scatter diagram of von Mises strains from FEM (Finite Element Model) with ARAMIS measurements for Stage Point 1

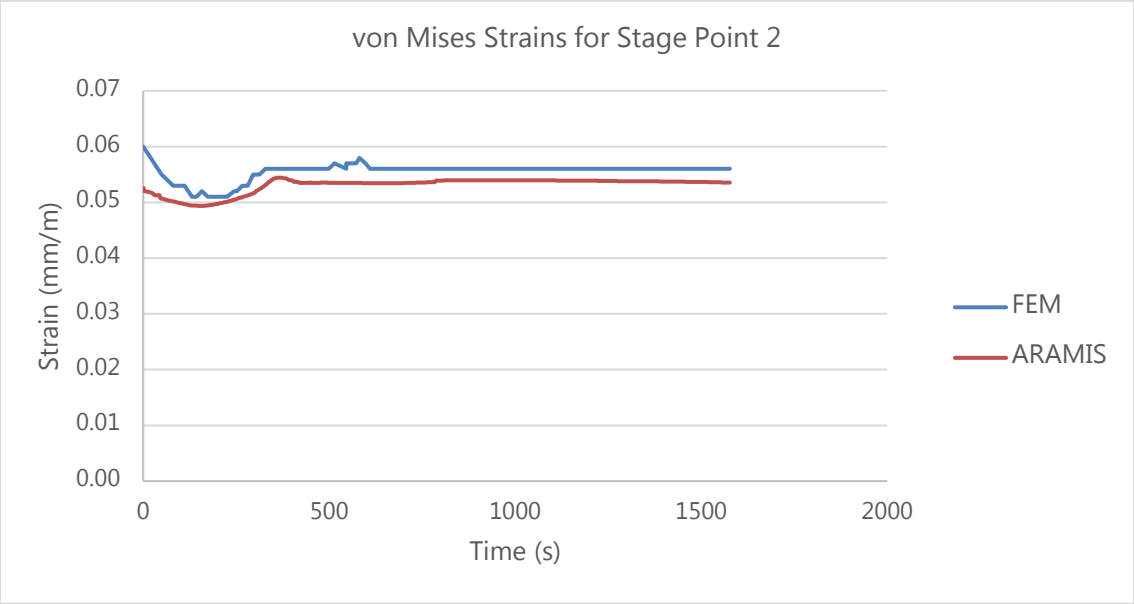

Figure 6. 22. Resulting von Mises strains for Stage Point 2 from ANSYS model and ARAMIS measurements

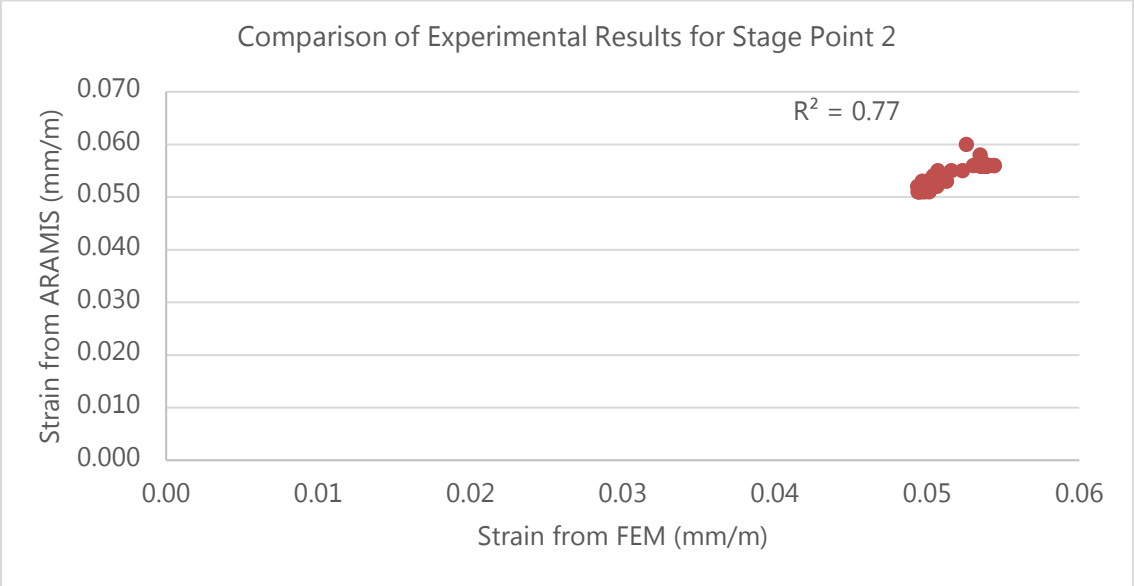

Figure 6. 23. Comparison by R^2 value of von Mises strains from FEM (Finite Element Model) with ARAMIS measurements for Stage Point 2

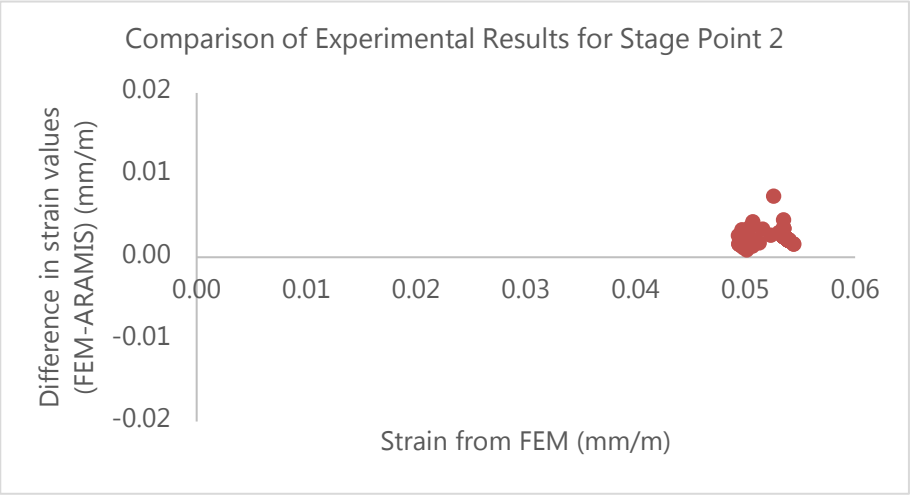

Figure 6. 24. Comparison by scatter diagram of von Mises strains from FEM (Finite Element Model) with ARAMIS measurements for Stage Point 2

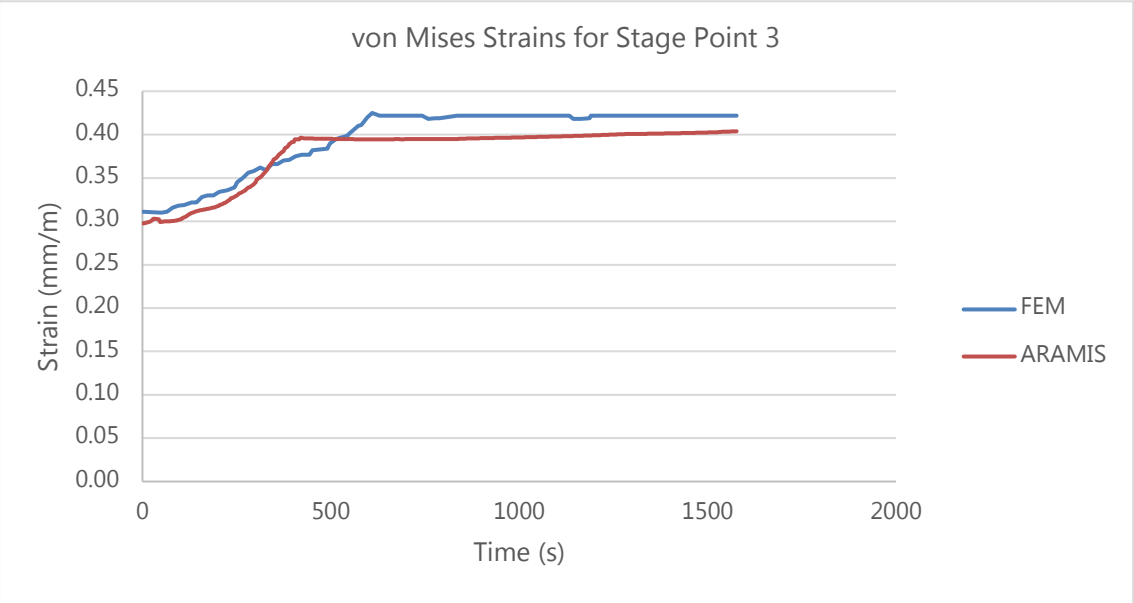

Figure 6. 25. Resulting von Mises strains for Stage Point 3 from ANSYS model and ARAMIS measurements

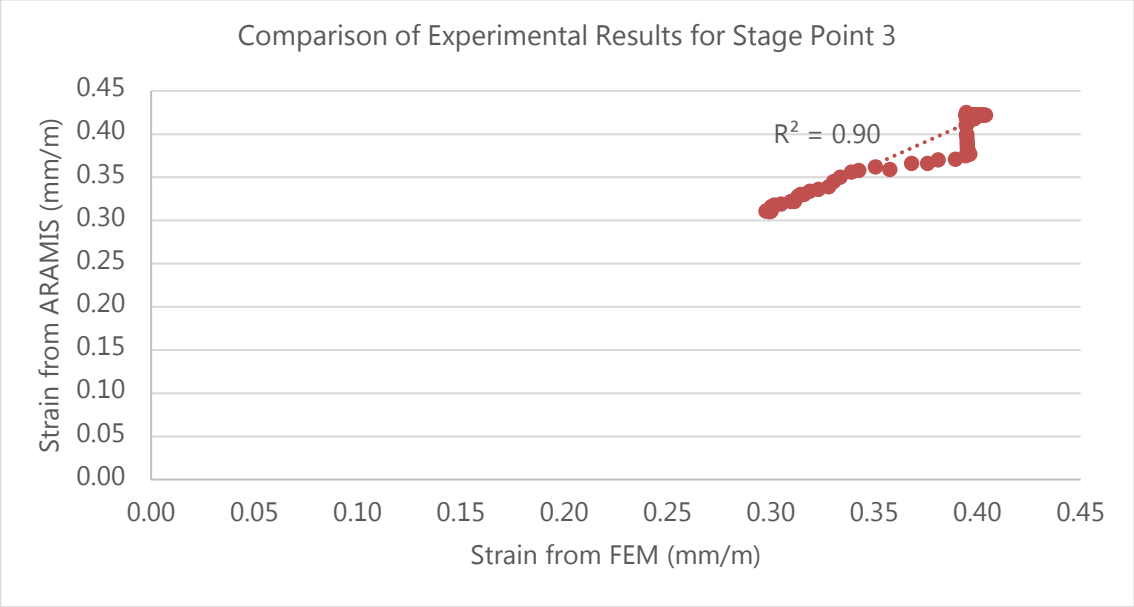

Figure 6. 26. Comparison by R^2 value of von Mises strains from FEM (Finite Element Model) with ARAMIS measurements for Stage Point 3

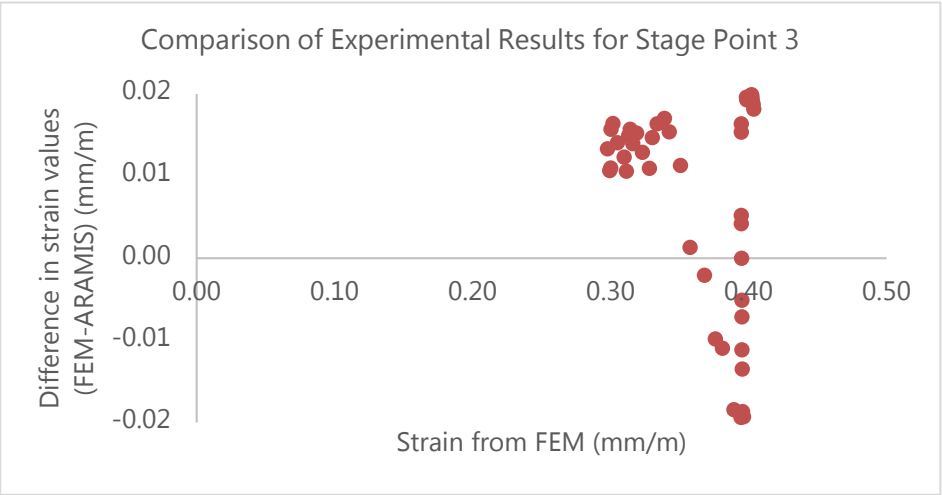

Figure 6. 27. Comparison by scatter diagram of von Mises strains from FEM (Finite Element Model) with ARAMIS measurements for Stage Point3

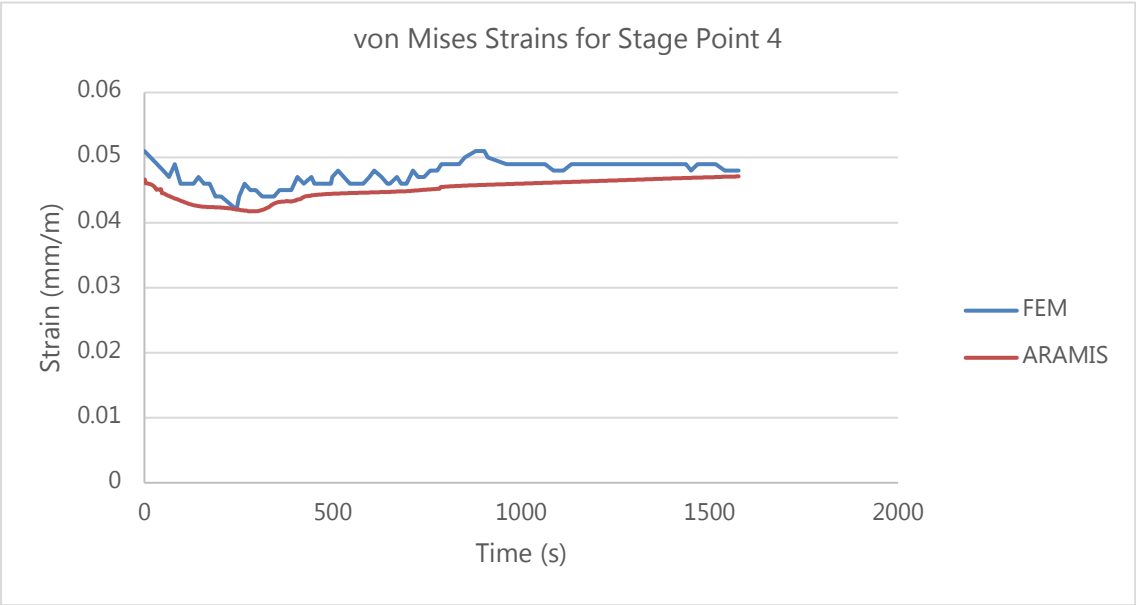

Figure 6. 28. Resulting von Mises strains for Stage Point 4 from ANSYS model and ARAMIS measurements

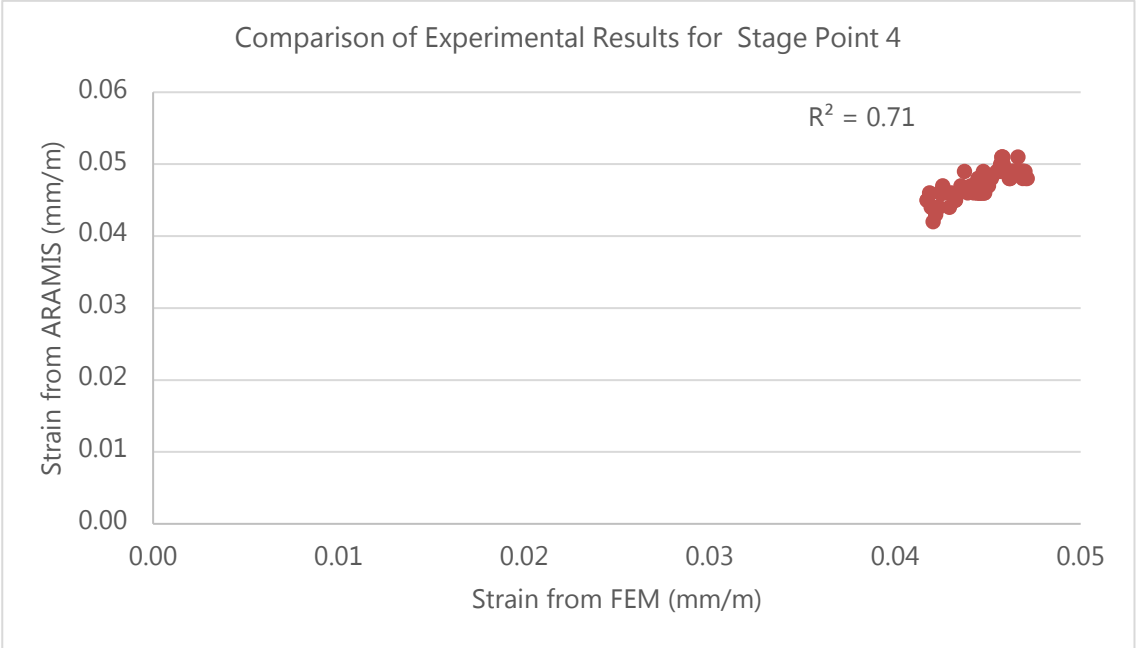

Figure 6. 29. Comparison by R^2 value of von Mises strains from FEM (Finite Element Model) with ARAMIS measurements for Stage Point 4

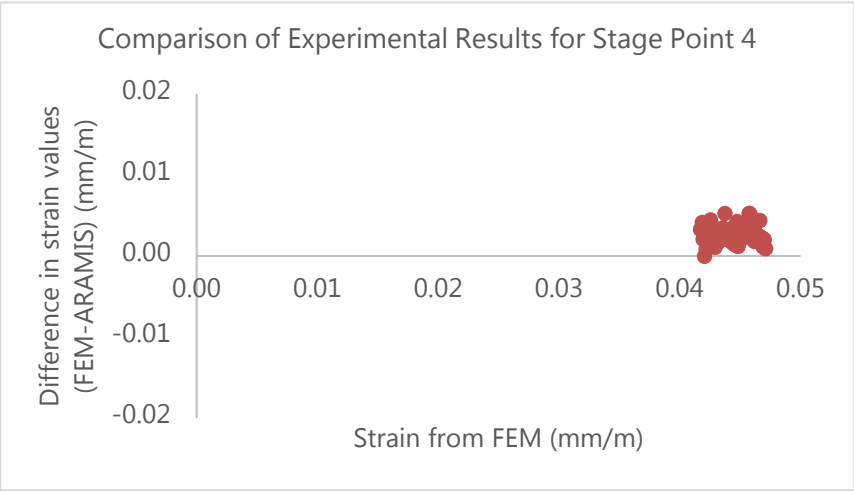

Figure 6. 30. Comparison by scatter diagram of von Mises strains from FEM (Finite Element Model) with ARAMIS measurements for Stage Point 4

The values for von Mises strain at stage points 0 to 4 show a close similarity mainly in terms of the pattern in which the strains have developed through the loading history. The resulting coefficients of determination (R^2) range from 0.61 to 0.90. Since the scatter diagrams show a clear bias where the strains from the laboratory experiment are consistently lower than the resulting strains from the ANSYS model, the coefficients of determination estimated for connection design C1 can be regarded as satisfactory. It also shows that the ANSYS analysis was conservative compared to the experimental results.

Connection Design C2

The five points that were marked to measure the strain results for connection design C2 through the duration of the test is illustrated in Figure 6.32. The marked points A, B, C, D and E are at similar locations to the stage points 0, 1, 2, 3 and 4 from the ARAMIS strain measurement. A sample strain results plot output from the ARAMIS software is shown in Figure 6.33.

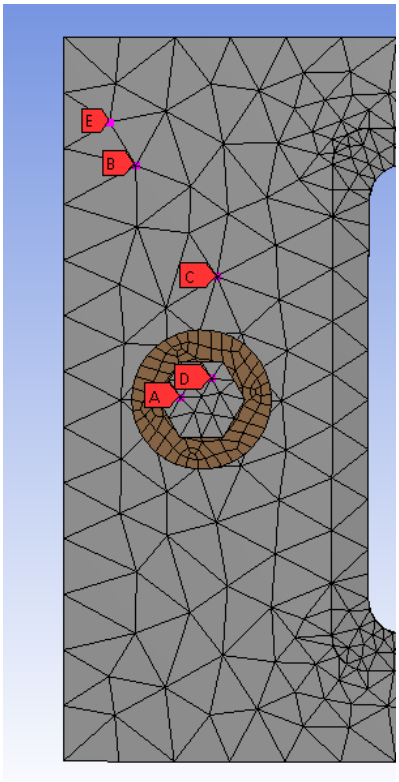

Figure 6. 31. Five points marked on the ANSYS model (Left) to measure von Mises strains for connection design C2

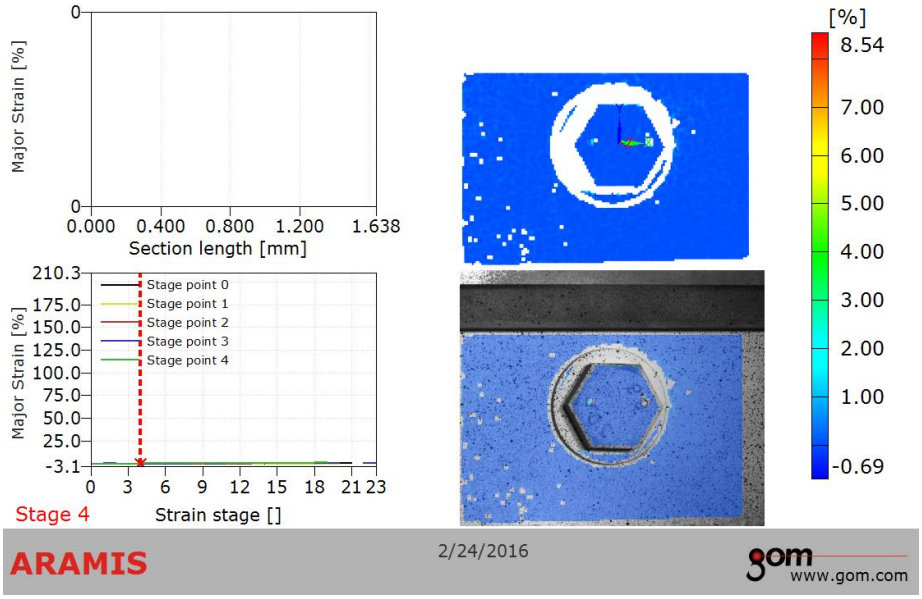

Figure 6. 32. A sample strain results plot from ARAMIS for a time at the initial part of the loading

The von Mises strain results plotted for each of the 'stage points' mentioned above and their comparison with the ANSYS analysis for connection design C2 are shown below from Figures 6.34 to 6.48;

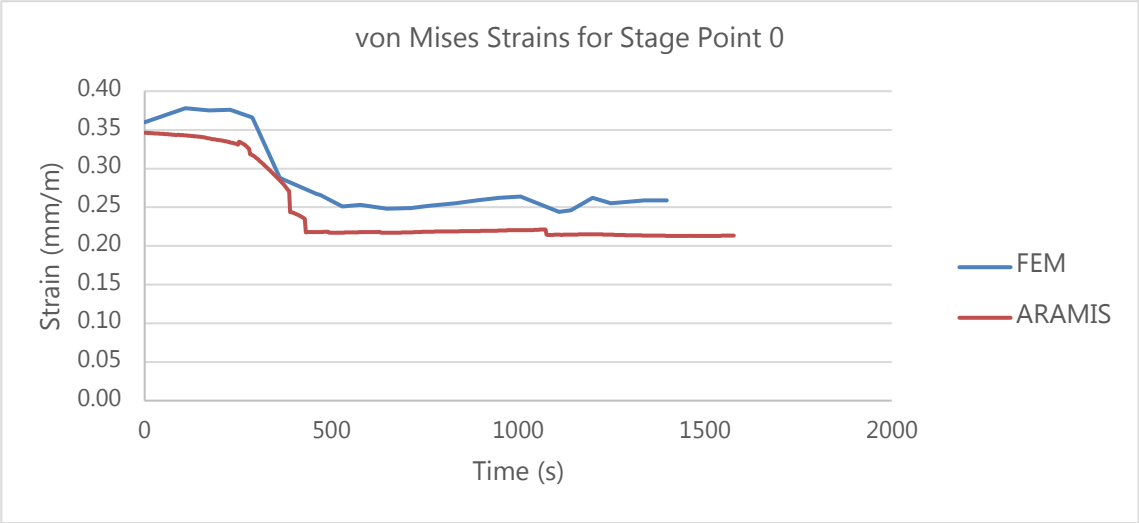

Figure 6. 33. Resulting von Mises strains for Stage Point 0 from ANSYS model and ARAMIS measurements

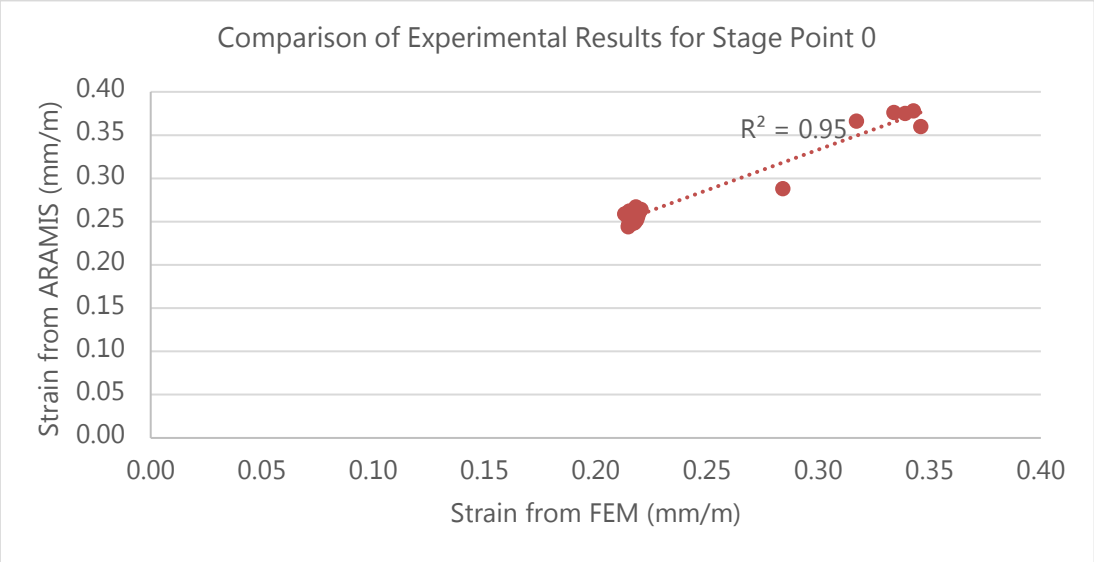

Figure 6. 34. Comparison by R^2 value of von Mises strains from FEM (Finite Element Model) with ARAMIS measurements for Stage Point 0

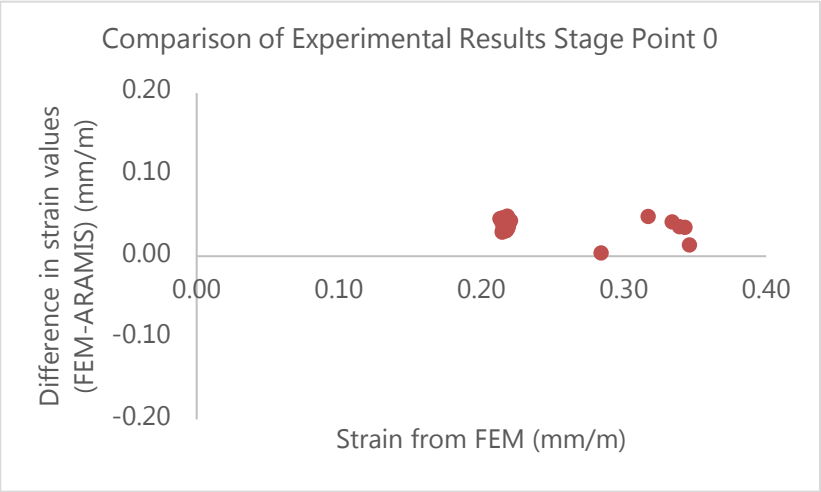

Figure 6. 35. Comparison by scatter diagram of von Mises strains from FEM (Finite Element Model) with ARAMIS measurements for Stage Point 0

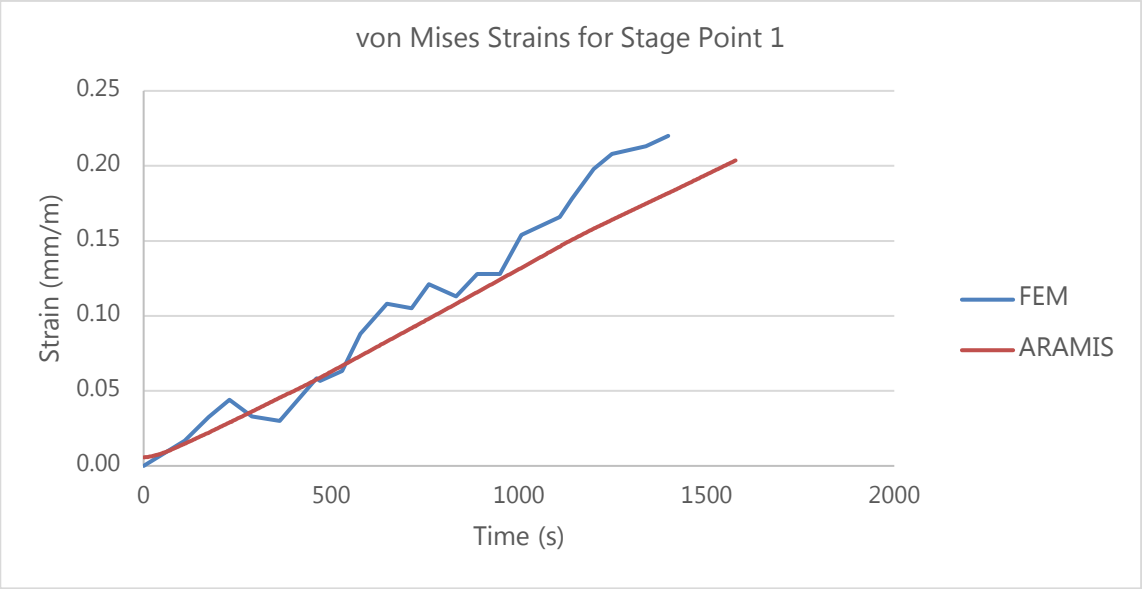

Figure 6. 36. Resulting von Mises strains for Stage Point 1 from ANSYS model and ARAMIS measurements

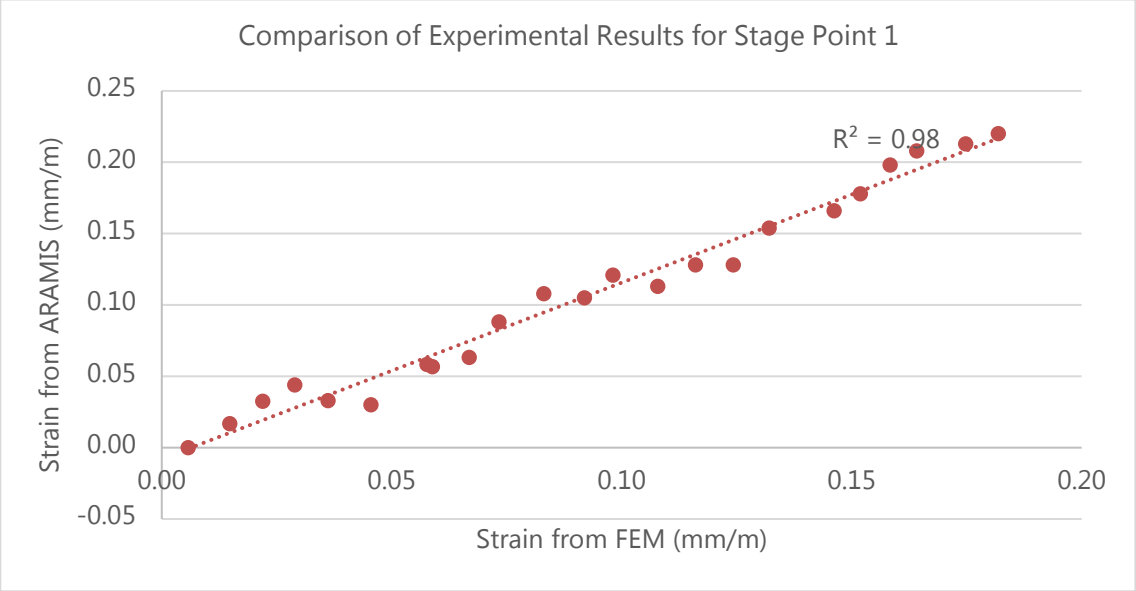

Figure 6. 37. Comparison by R^2 value of von Mises strains from FEM (Finite Element Model) with ARAMIS measurements for Stage Point 1

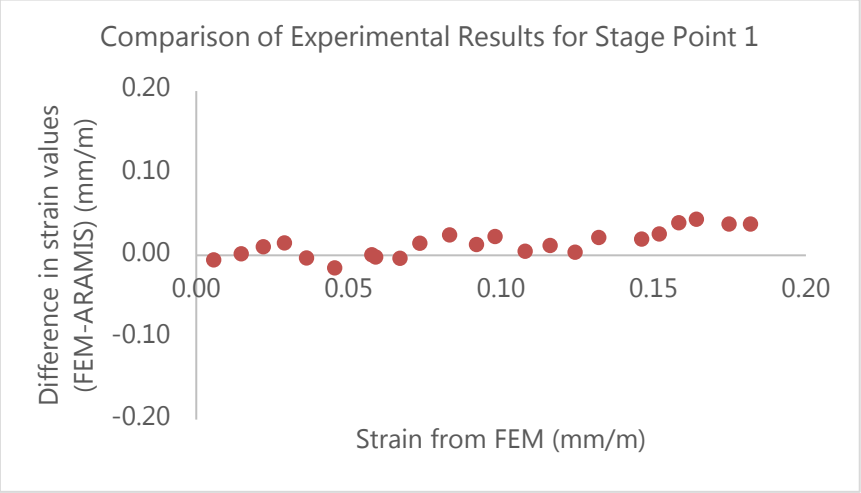

Figure 6. 38. Comparison by scatter diagram of von Mises strains from FEM (Finite Element Model) with ARAMIS measurements for Stage Point 1

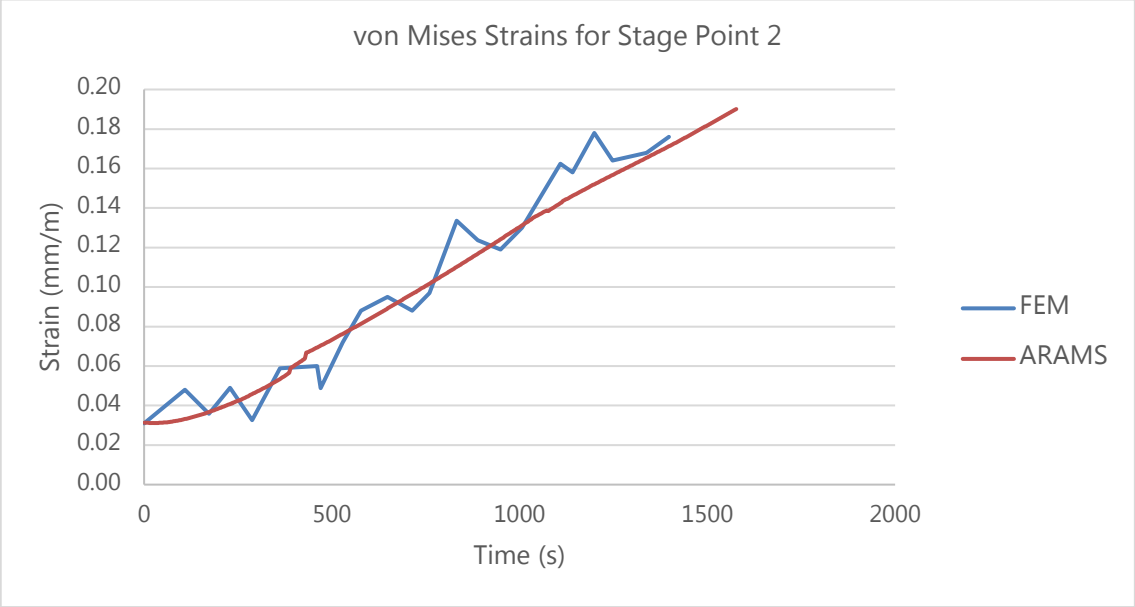

Figure 6. 39. Resulting von Mises strains for Stage Point 2 from ANSYS model and ARAMIS measurements

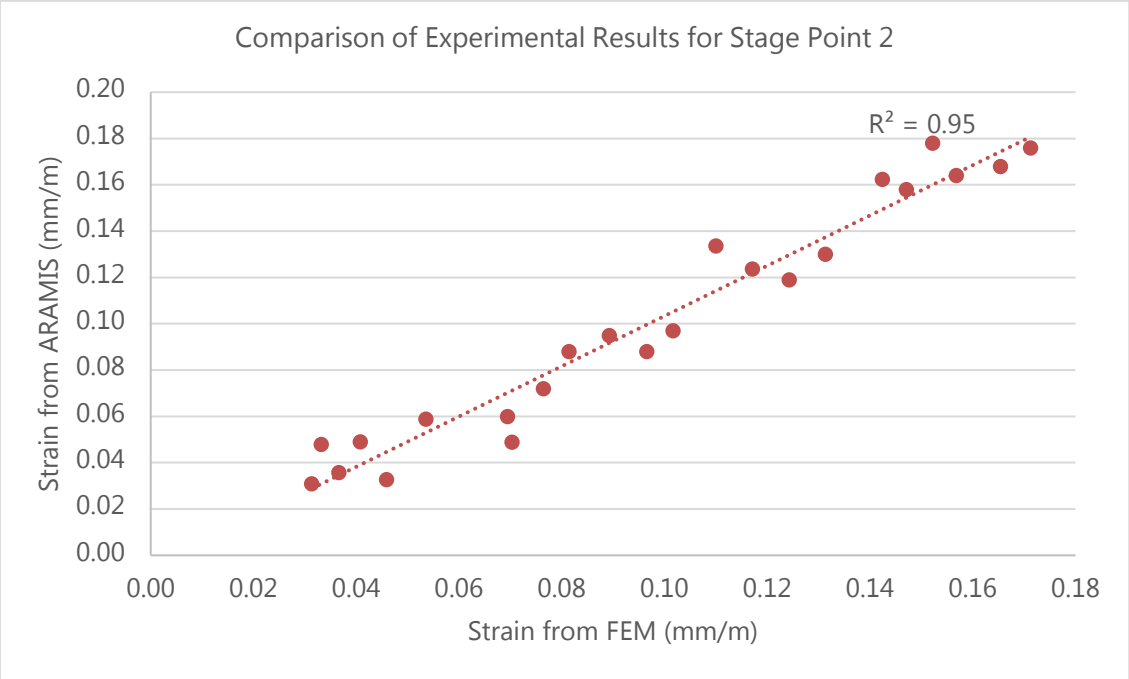

Figure 6. 40. Comparison by R^2 value of von Mises strains from FEM (Finite Element Model) with ARAMIS measurements for Stage Point 2

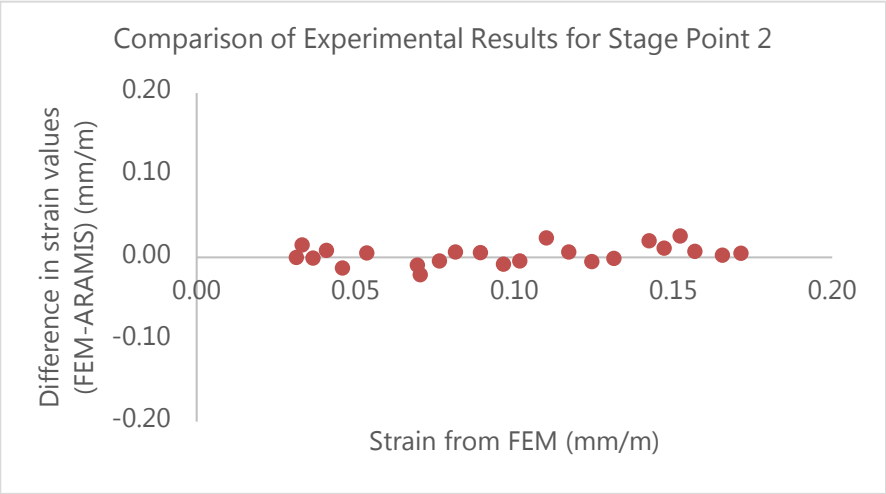

Figure 6. 41. Comparison by scatter diagram of von Mises strains from FEM (Finite Element Model) with ARAMIS measurements for Stage Point 2

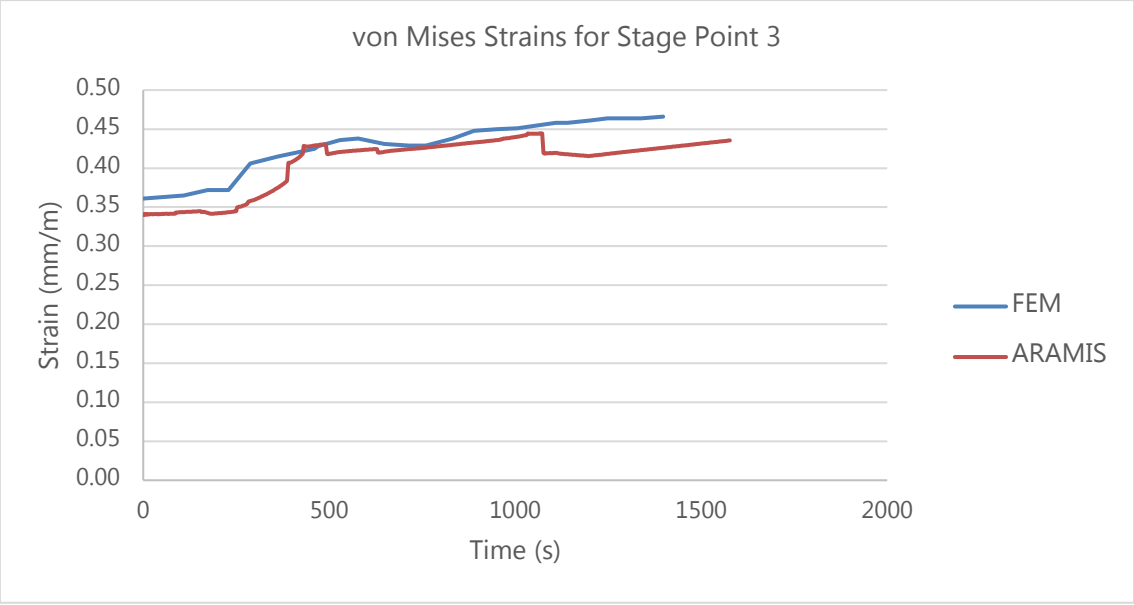

Figure 6. 42. Resulting von Mises strains for Stage Point 3 from ANSYS model and ARAMIS measurements

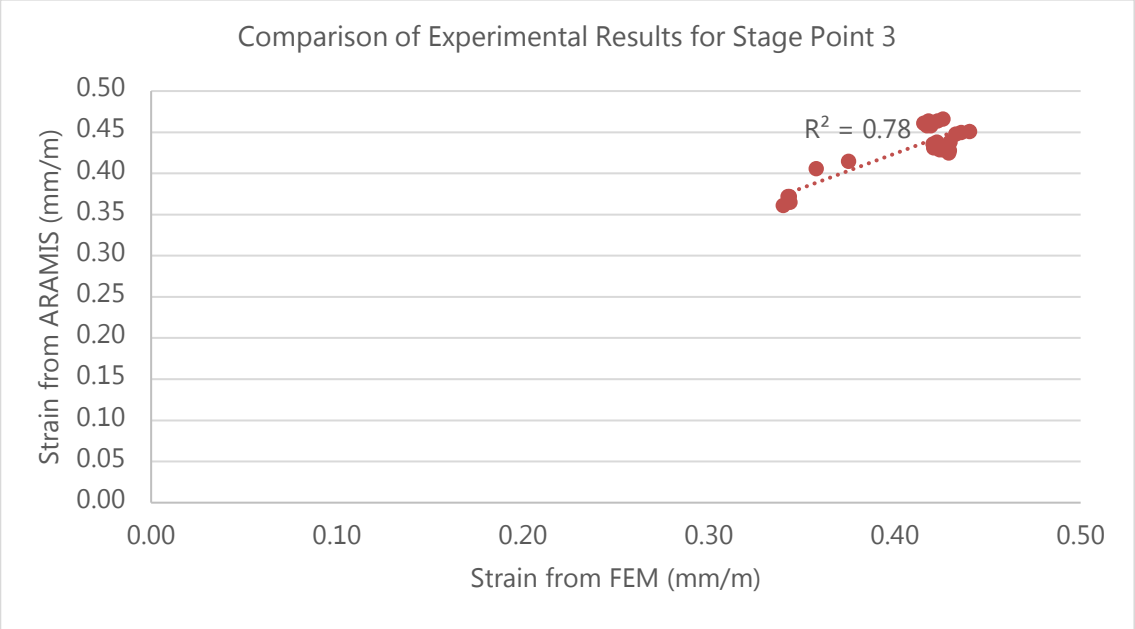

Figure 6. 43. Comparison by R^2 value of von Mises strains from FEM (Finite Element Model) with ARAMIS measurements for Stage Point 3

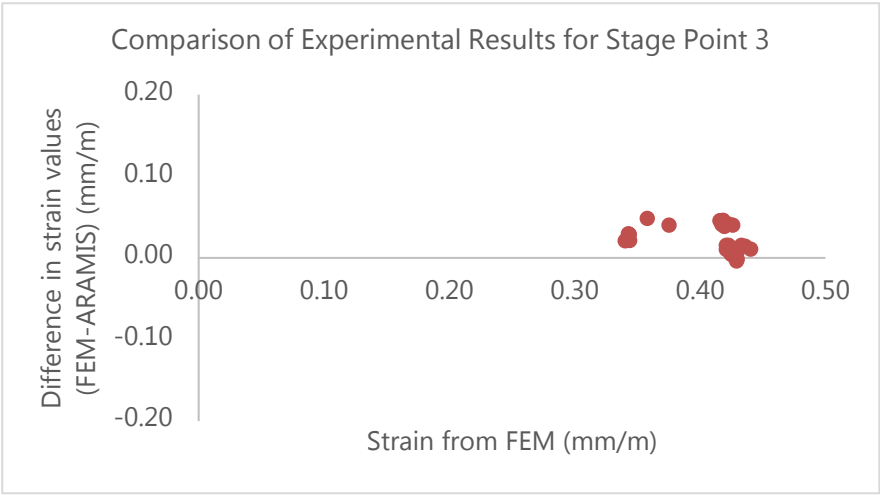

Figure 6. 44. Comparison by scatter diagram of von Mises strains from FEM (Finite Element Model) with ARAMIS measurements for Stage Point 3

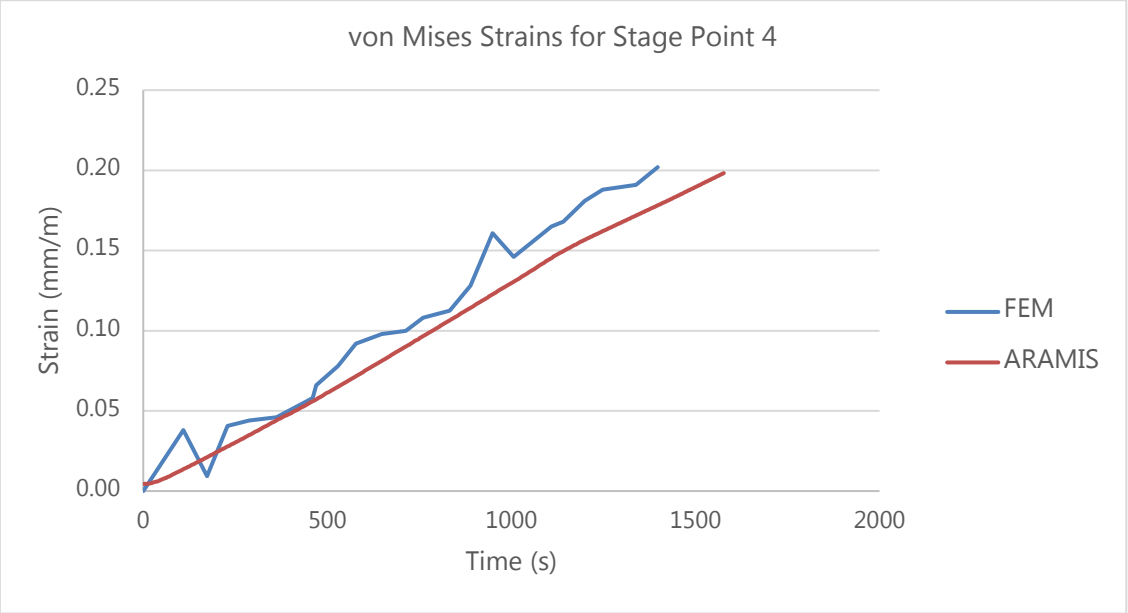

Figure 6. 45. Resulting von Mises strains for Stage Point 4 from ANSYS model and ARAMIS measurements

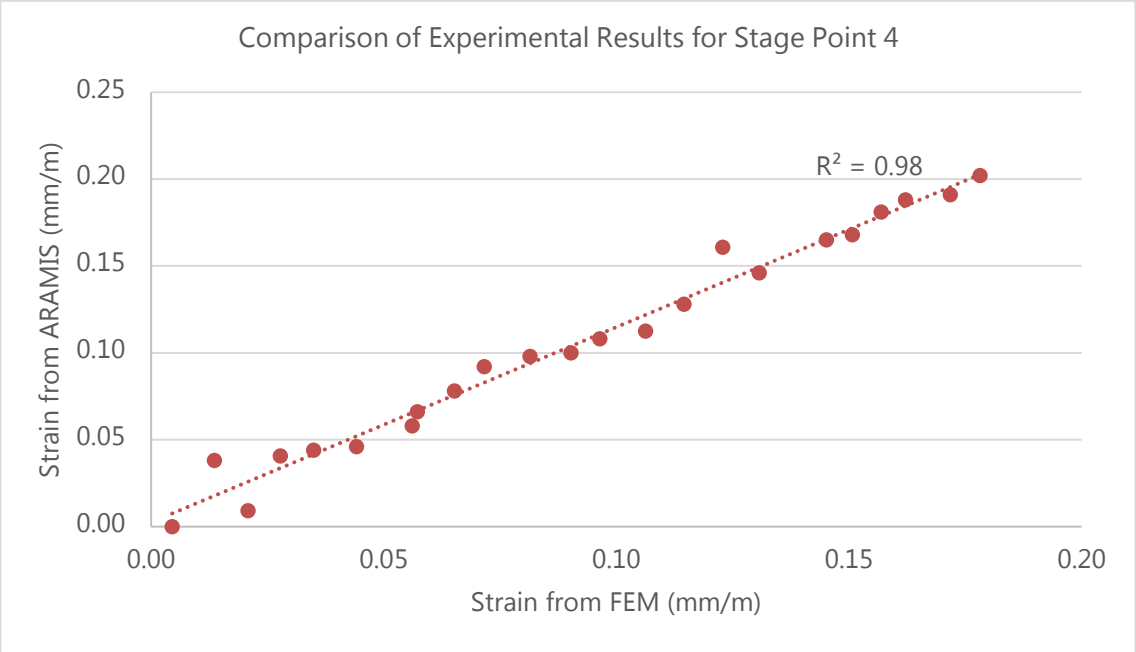

Figure 6. 46. Comparison by R^2 value of von Mises strains from FEM (Finite Element Model) with ARAMIS measurements for Stage Point 4

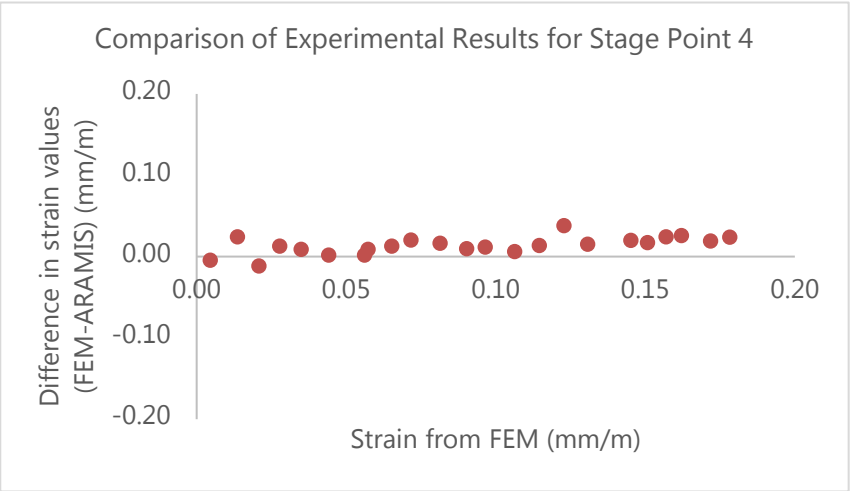

Figure 6. 47. Comparison by scatter diagram of von Mises strains from FEM (Finite Element Model) with ARAMIS measurements for Stage Point 4

The values for von Mises strain at stage points 0 to 4 show a close similarity mainly in terms of the pattern in which the strains have developed through the loading history. The resulting coefficients of determination (R^2) range from 0.78 to 0.98. Since the scatter diagrams show a clear bias where the strains from the laboratory experiment are consistently lower than the resulting strains from the ANSYS model, the coefficients of determination estimated for connection design C2 can be regarded as satisfactory and shows that the ANSYS analysis was conservative compared to the laboratory experiment.

Connection Design C3

The five points that were marked to measure the strain results for connection design C2 through the duration of the test is illustrated in Figure 6.49. The marked points A, B, C, D and E are at similar locations to the stage points 0, 1, 2, 3 and 4 from the ARAMIS strain measurement. A sample strain results plot output from the ARAMIS software is shown in Figure 6.50.

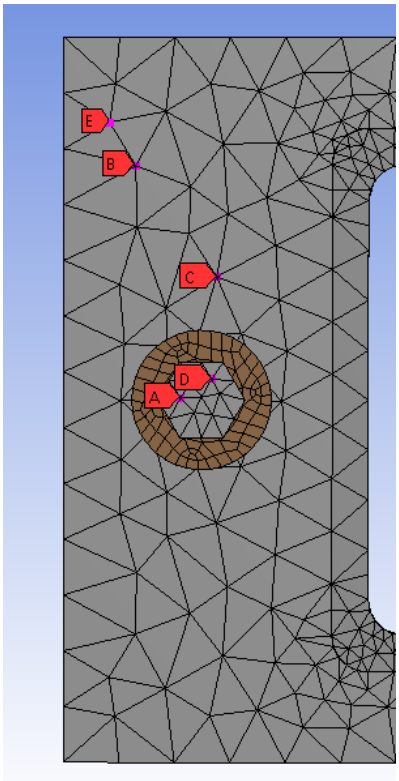

Figure 6. 48. Five points marked on the ANSYS model (Left) to measure von Mises strains for connection design C3

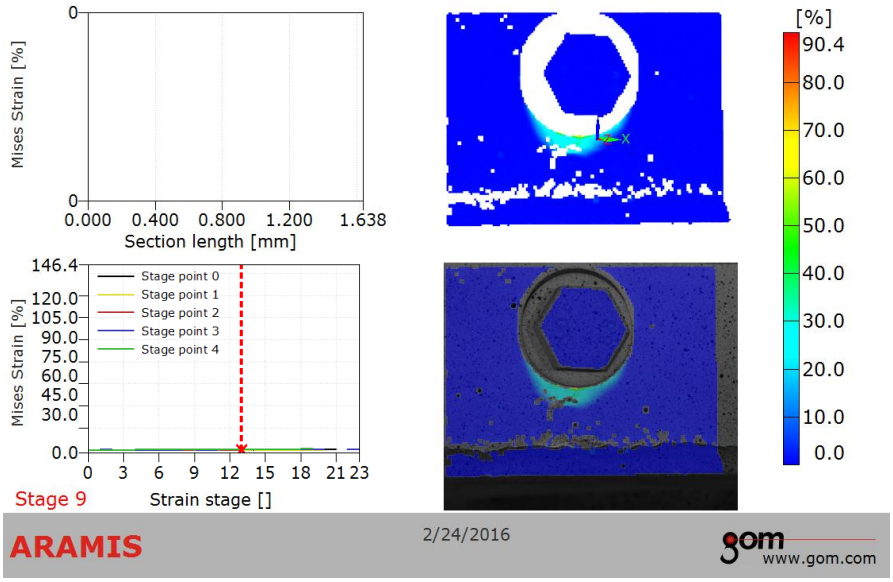

Figure 6. 49. A sample strain results plot from ARAMIS for a time at the initial part of the loading

The von Mises strain results plotted for each of the 'stage points' mentioned above and their comparison with the ANSYS analysis for connection design C3 are shown below from Figures 6.51 to 6.65.

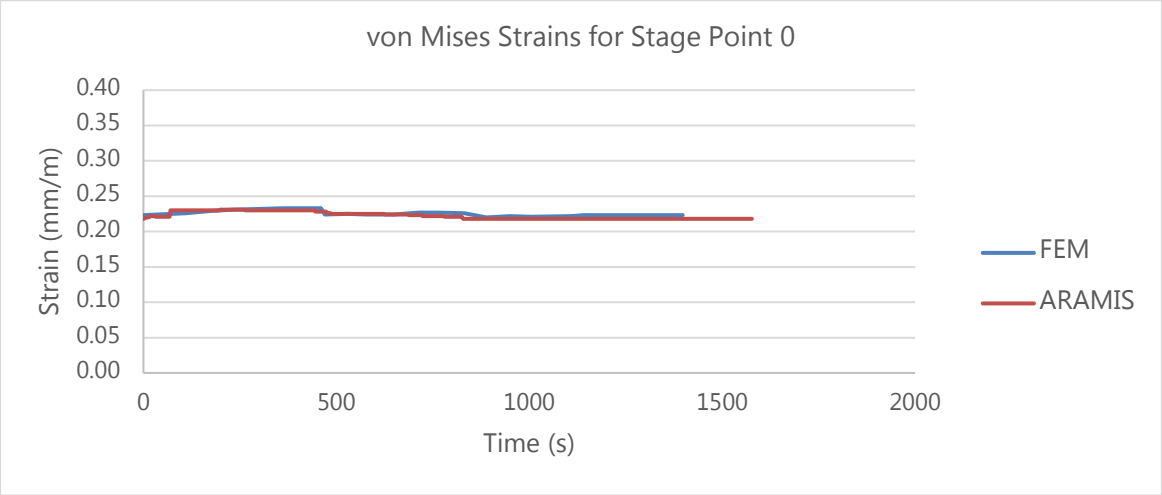

Figure 6. 50. Resulting von Mises strains for Stage Point 0 from ANSYS model and ARAMIS measurements

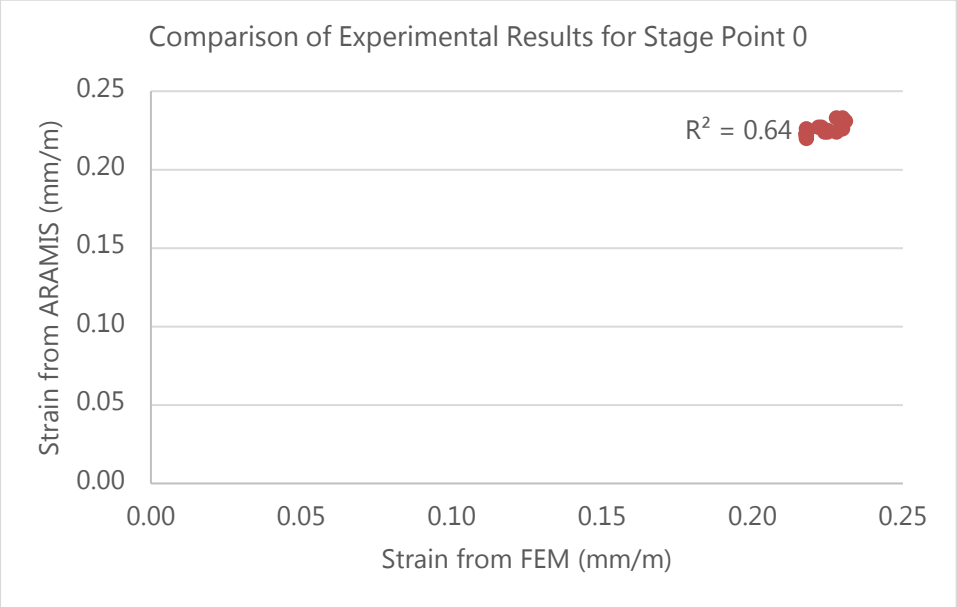

Figure 6. 51. Comparison by R^2 value of von Mises strains from FEM (Finite Element Model) with ARAMIS measurements for Stage Point 0

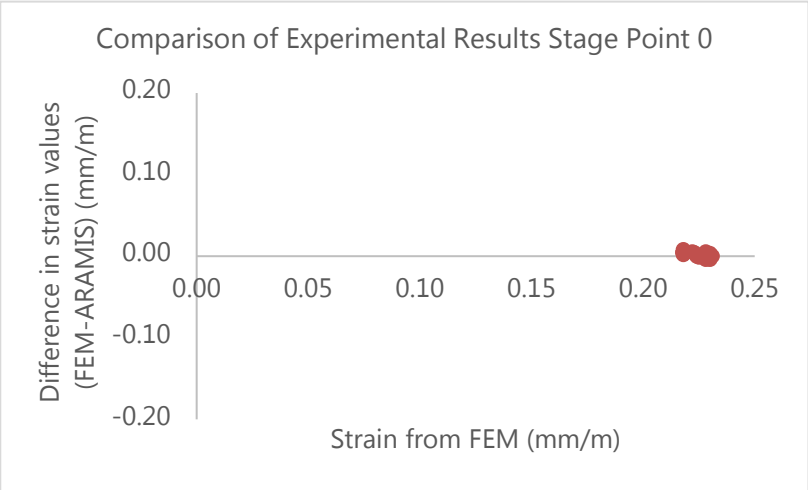

Figure 6. 52. Comparison by scatter diagram of von Mises strains from FEM (Finite Element Model) with ARAMIS measurements for Stage Point 0

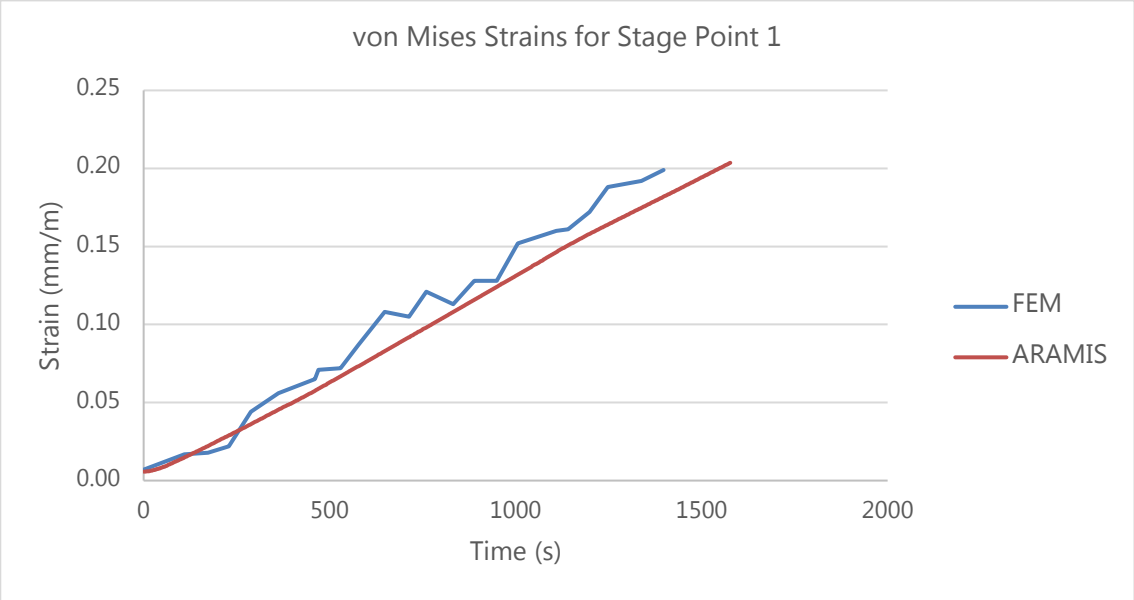

Figure 6. 53. Resulting von Mises strains for Stage Point 1 from ANSYS model and ARAMIS measurements

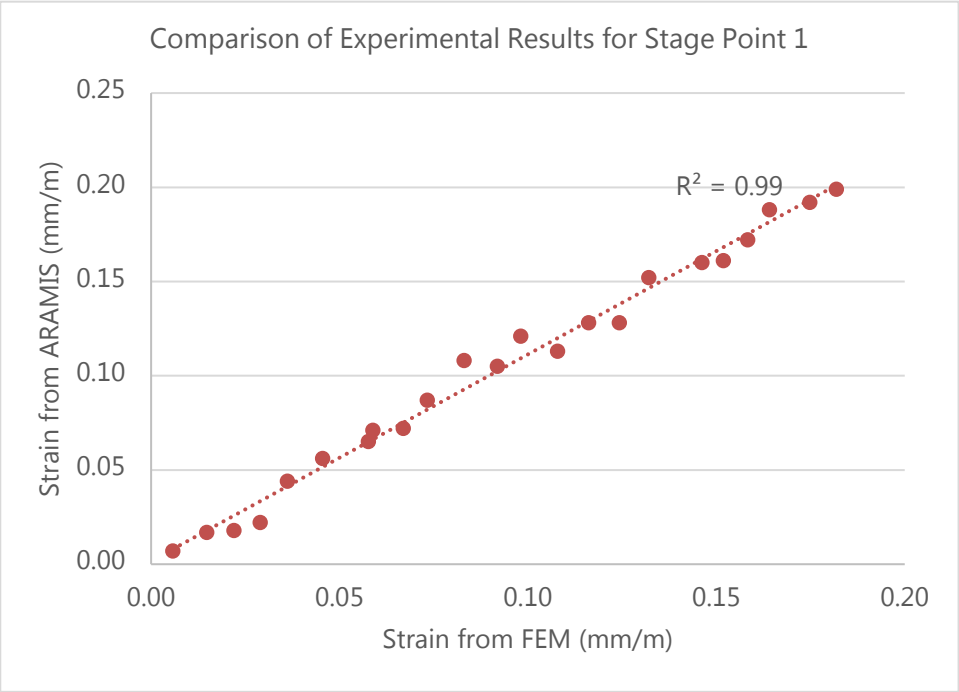

Figure 6. 54. Comparison by R^2 value of von Mises strains from FEM (Finite Element Model) with ARAMIS measurements for Stage Point 1

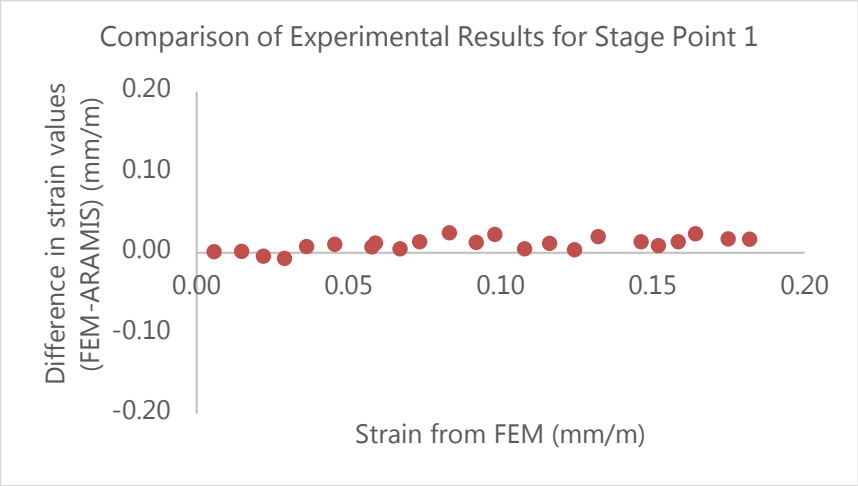

Figure 6. 55. Comparison by scatter diagram of von Mises strains from FEM (Finite Element Model) with ARAMIS measurements for Stage Point 1

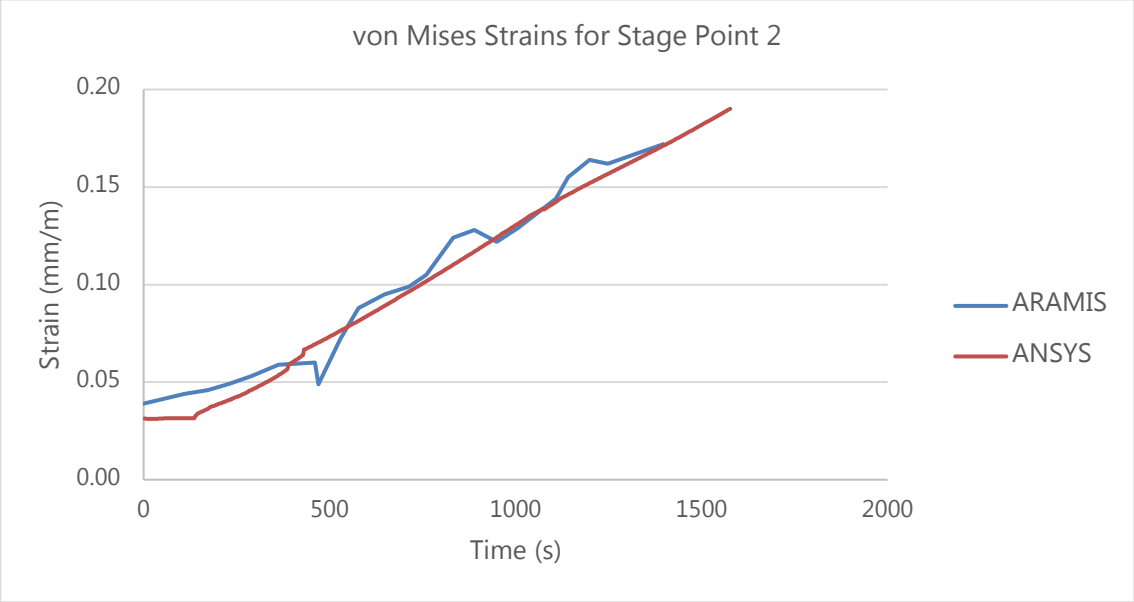

Figure 6. 56. Resulting von Mises strains for Stage Point 2 from ANSYS model and ARAMIS measurements

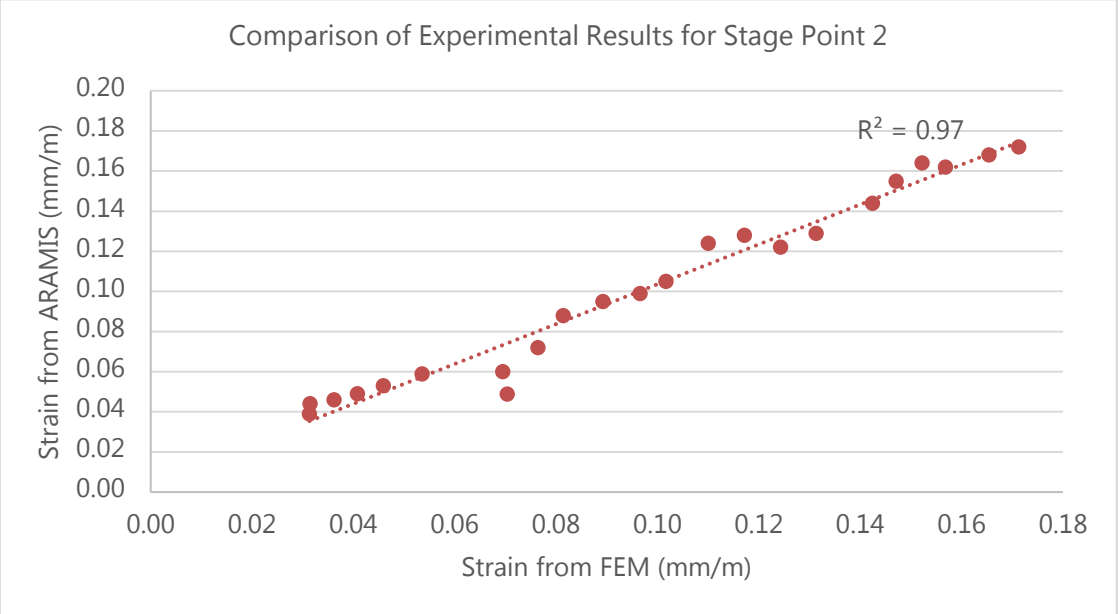

Figure 6. 57. Comparison by R^2 value of von Mises strains from FEM (Finite Element Model) with ARAMIS measurements for Stage Point 2

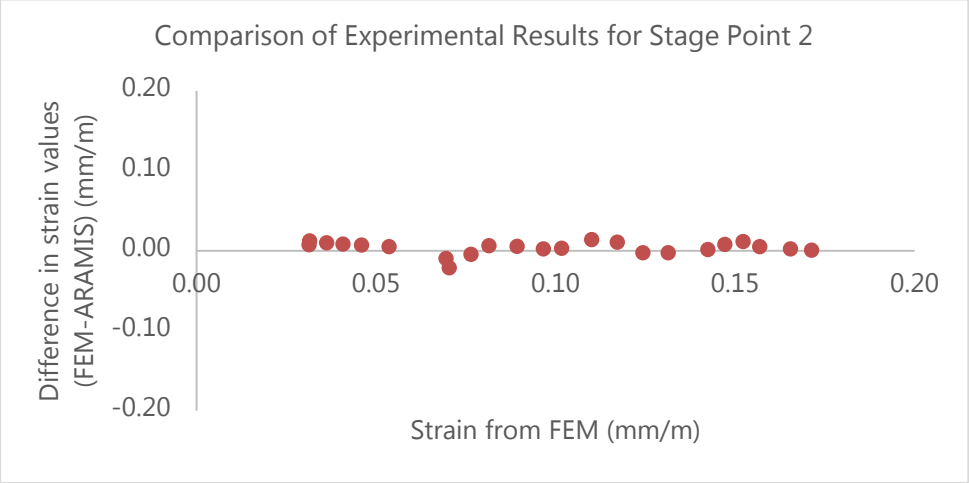

Figure 6. 58. Comparison by scatter diagram of von Mises strains from FEM (Finite Element Model) with ARAMIS measurements for Stage Point 2

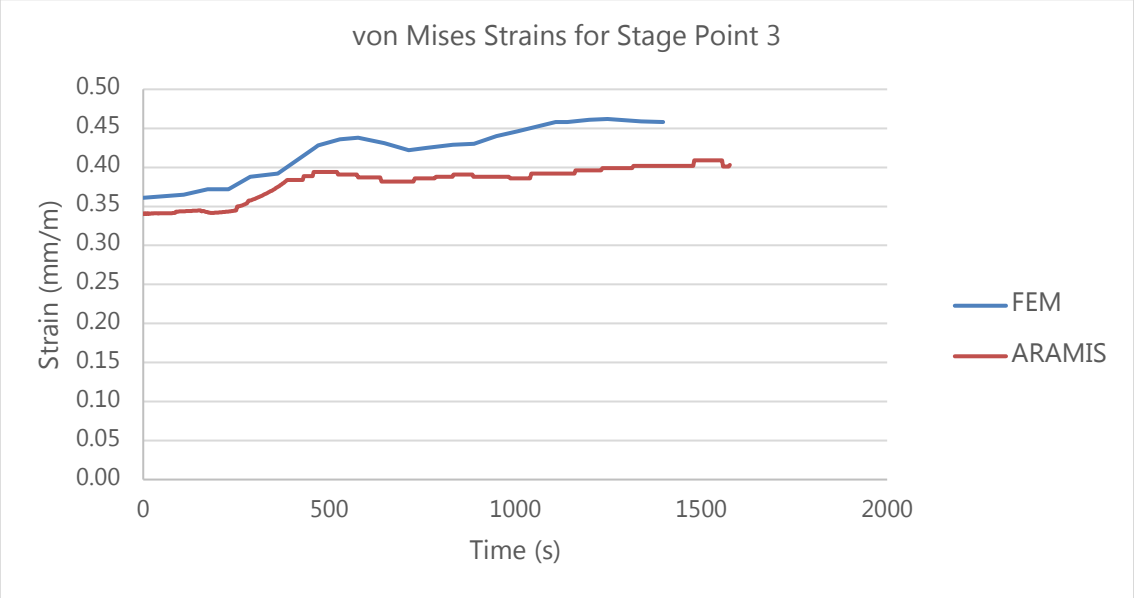

Figure 6. 59. Resulting von Mises strains for Stage Point 3 from ANSYS model and ARAMIS measurements

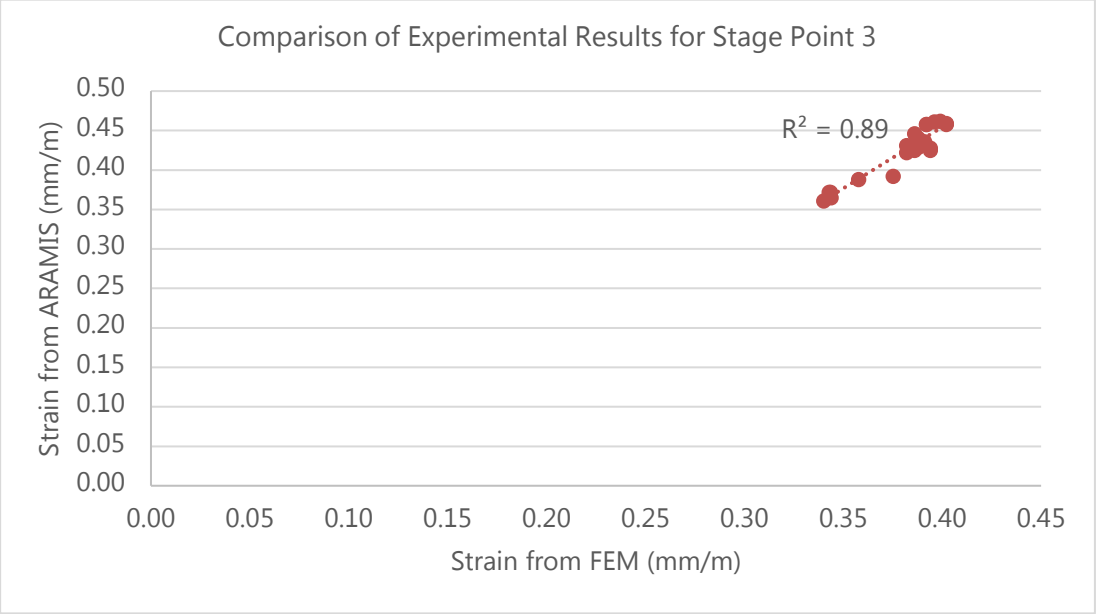

Figure 6. 60. Comparison by R^2 value of von Mises strains from FEM (Finite Element Model) with ARAMIS measurements for Stage Point 3

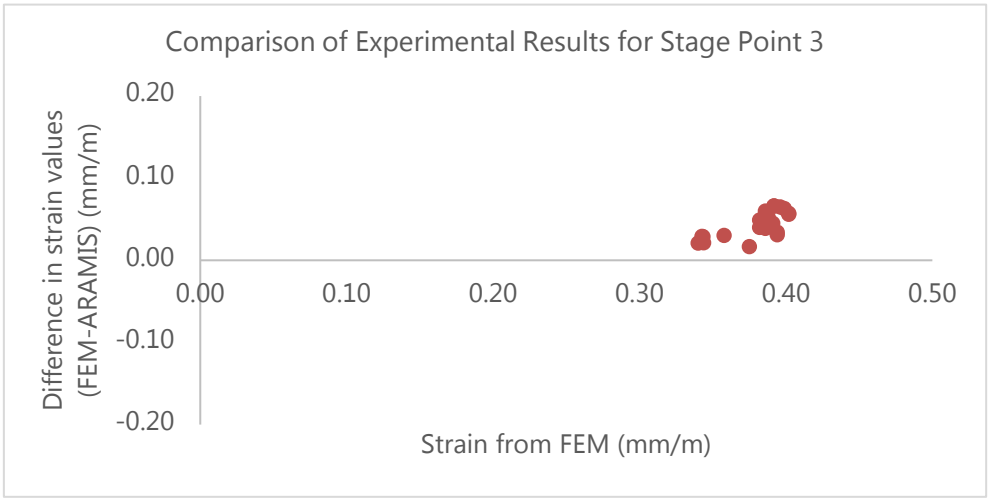

Figure 6. 61. Comparison by scatter diagram of von Mises strains from FEM (Finite Element Model) with ARAMIS measurements for Stage Point 3

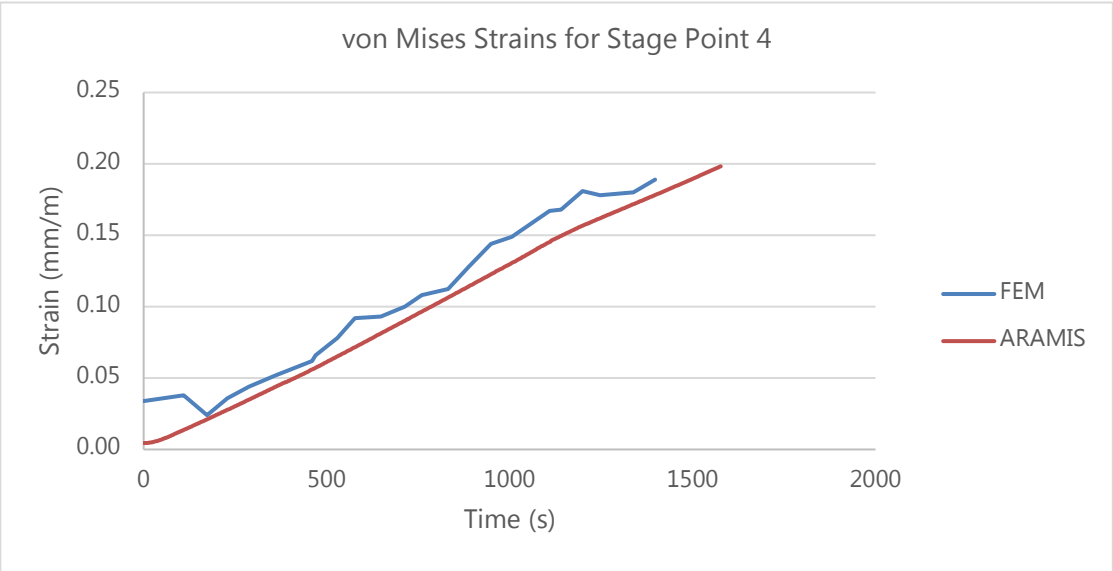

Figure 6. 62. Resulting von Mises strains for Stage Point 4 from ANSYS model and ARAMIS measurements

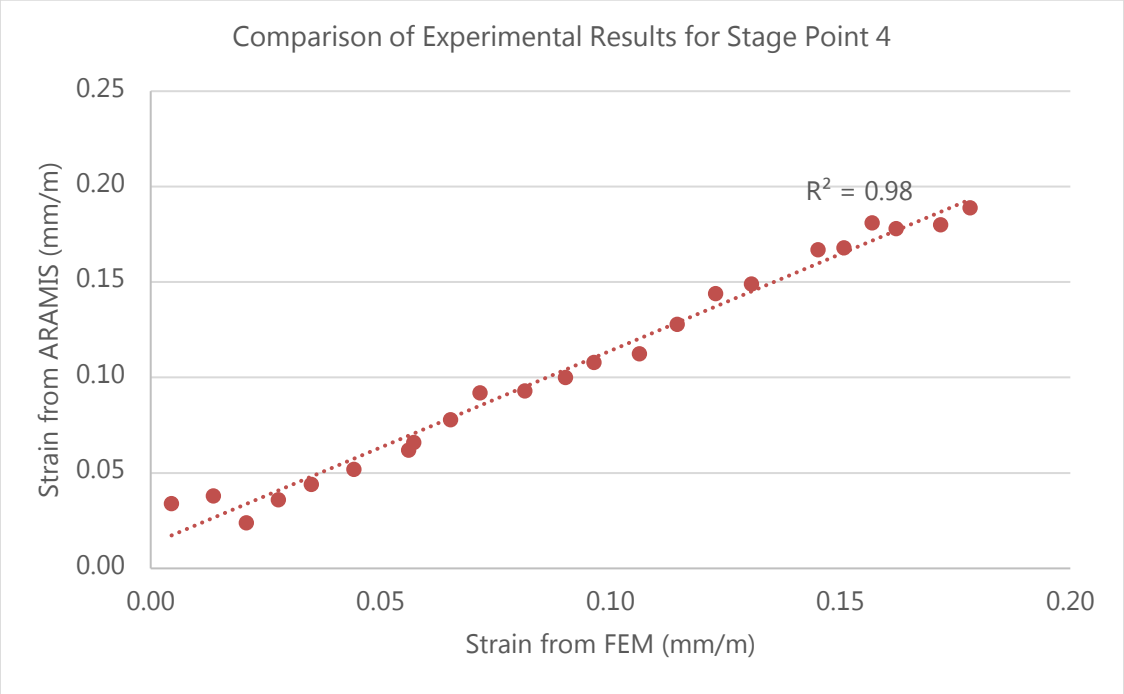

Figure 6. 63. Comparison by R^2 value of von Mises strains from FEM (Finite Element Model) with ARAMIS measurements for Stage Point 4

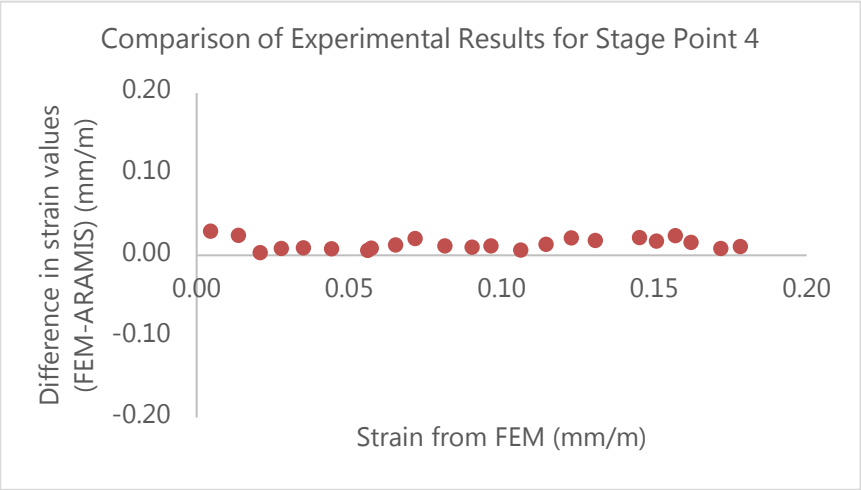

Figure 6. 64. Comparison by scatter diagram of von Mises strains from FEM (Finite Element Model) with ARAMIS measurements for Stage Point 4

The values for von Mises strain at stage points 0 to 4 show a close similarity mainly in terms of the pattern in which the strains have developed through the loading history. The resulting coefficients of determination (R^2) range from 0.64 to 0.99. Since the scatter diagrams again show a clear bias where the strains from the laboratory experiment are consistently lower than the resulting strains from the ANSYS model, the coefficients of determination estimated for connection design C3 can be regarded as satisfactory. Similar to the other two connections C1 and C2, the ANSYS model proves to be conservative compared to the experimental results.

6.6. Estimating the Stiffness of the Connection

It is important that there is an accurate estimate for the stiffness of the module to module connection and that a proper method is established in numerically estimating it. The significance of this value is mostly related to the modelling of the structural system in a global computer model. This value can be used in modelling the connection as a spring or link type element with a spring stiffness equal to that of the connection of the stiffness estimated here. As the intent of this exercise is to find a value of stiffness for the eventual design of the member, only the elastic stiffness is taken into consideration.

Stiffness, by definition is the extent of resistance of a given member to an applied force, and is formulated as the force needed to move the member by a unit displacement in a given direction for a given mode of deformation. The bolts in the connection showed that it goes through two distinct stages of deformation namely, the initial slip and then the shear deformation. Therefore, the stiffness is calculated for both these stages separately.

The stiffness values are estimated separately for each bolt and combined afterwards assuming that the combined resistance of the bolts act as shown below in Figure 6. 66;

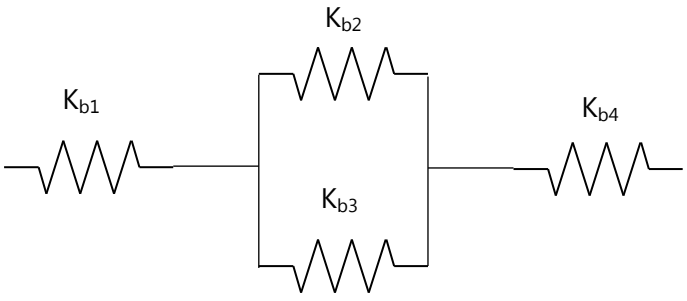

Figure 6. 65. A schematic representation of the stiffness of each bolt that can be combined to result in the overall stiffness of the connection

As illustrated the two bolts in the middle are considered to be acting in parallel and the combined stiffness of them would act in series with the two corner bolts. The resultant stiffness would therefore be;

$$\frac{1}{k} = \frac{1}{k_{b1}} + \frac{1}{(k_{b2}+k_{b3})} + \frac{1}{k_{b4}} \qquad \text{Eq. 6.5}$$

The formulae given in Chapter 3 (Eq. 3.17 and Eq. 3.18) are used here to calculate the stiffness of the overall connection at the slip and shearing stages.

Stiffness for Slip (k_{slip})

The slip capacity for the entire connection was calculated to be the stiffness for elastic slip stage calculation for the whole connection is carried out as follows;

$$k_{slip} = {}^{P_{slip}}\!/_{\Delta_{slip}} \qquad \text{Eq. 6.6}$$

Slip stiffness for one bolt considering the 1mm slip to the edge of the clearance hole;

$$k_{slip} = {}^{6.36\ kN}\!/_{1\ mm} = 6.36\ kN/mm$$

Overall stiffness of all four bolts;

$$\frac{1}{k_{slip}} = \frac{1}{6.36} + \frac{1}{2 \times 6.36} + \frac{1}{6.36}$$

$$k_{slip} = 2.54\ kN/mm$$

Similarly the stiffness is calculated for connection designs C2 and C3 to be 4.74 kN/mm and 4.03 kN/mm respectively.

Stiffness against combined Shear and Tension (k_{br})

Using the principles of Hooke's law the shear stiffness can be expressed as follows where A_s is the tensile stress area of the bolt (van Gaasbeek, 2015);

$$k_\tau = {GA_s}/{L} \qquad \text{Eq. 6.7}$$

For a single bolt;

$$k_\tau = {80000\ Nmm^{-2} \times 84.3\ mm^2}/{31\ mm} = 217.5\ kN/mm$$

Shear stiffness of the overall connection;

$$\frac{1}{k_\tau} = \frac{1}{217.5} + \frac{1}{2 \times 217.5} + \frac{1}{217.5}$$

$$k_\tau = 87.0\ kN/mm$$

Following Eq. 3.17 presented in Chapter 3, the stiffness of the connection against tension is calculated as follows;

$$k_m = AEd\mathrm{e}^{B({d}/{L})}$$

For corner bolts;

As per Wileman et al. (1991) the stiffness of each plate in the connection that is connected through a single bolt is calculated separately and then combined in series.

The stiffness of the joint where 6mm plate is connected by the corner bolt is calculated as follows;

$$k_{m(6mm)} = 0.78715 \times 200000 \times 14 \times \mathrm{e}^{0.62873({14}/{6})} = 9557.4\ kN/mm$$

Similarly for each 25mm plate;

$$k_{m(25mm)} = 3240.8\ kN/mm$$

The resultant clamped member stiffness at the 1st bolt;

$$\frac{1}{k_{m1}} = \frac{1}{9557.4} + \frac{1}{3240.8} + \frac{1}{3240.8}$$

$$k_{m1} = 1385.5\ kN/mm$$

Calculated similarly, the stiffness (k_m) of middle bolts result in a value of 1220.2 kN/mm

Therefore, the overall stiffness in tension is calculated as;

$$\frac{1}{k_m} = \frac{1}{1385.5} + \frac{1}{2 \times 1220.2} + \frac{1}{1385.5}$$

$$k_m = 539.6\ kN/mm$$

The stiffness for combined tension and shear can therefore be estimated as;

$$\frac{1}{k_{br}} = \frac{1}{k_m} + \frac{1}{k_\tau}$$

$$\frac{1}{k_{br}} = \frac{1}{539.6} + \frac{1}{87.0}$$

$$k_{br} = 74.9\ kN/mm$$

Similarly the stiffness is calculated for connection designs C2 and C3 to be 134.9 kN/mm each.

The above shown theoretical estimation of stiffness was compared with the experimental and analytical results by studying a representative part from the elastic region of the force vs deformation curve for each connection. The resulting values are tabulated in Table 6.5 as follows;

Table 6. 5 Design Capacities for the three connection designs considered for the laboratory test and finite element analysis

Connection Design	Theoretical Connection Stiffness	Analytical Connection Stiffness	Experimental Connection Stiffness
C1	74.9 kN/mm	102.6 kN/mm	137.9 kN/mm
C2	134.9 kN/mm	148.4 kN/mm	225.0 kN/mm
C3	134.9 kN/mm	152.0 kN/mm	285.0 kN/mm

The literature based theoretical calculations of stiffness show a closer match with the values of stiffness that result from the ANSYS model than to those of the experimental results. This may be a result of the ANSYS models being more controlled simulations where all parameters are as expected whereas the laboratory experiments are dependent on many such parameters that can vary from the expected values. Variations in the size of the bolt holes, thickness of clamping plates are examples for such parameters that could have impacted the variation of stiffness values from the laboratory experiment.

6.7. Summary

- As discussed in Chapter 5, the module to module connection is vital in the performance of the lateral load transfer mechanism of the advanced corner supported system. This chapter evaluated the behaviour of this connection by analysing three variations of its design by means of finite element analysis and a laboratory experiment. The laboratory experiment is intended to validate the results of the finite element analysis and further to provide a physical observation of the behaviour of the connection when it undergoes lateral loads.
- The load vs deformation relationships for the three connections designs show three distinct stages of deformation. The initial slip where the first bolt slips to the edge of

its clearance hole was seen as the first stage. The transformation stage where the other three bolts gradually slip while the first bolt undergoes shear and bearing deformations is the second stage. The four bolts undergo shear and bearing together as a complete connection and demonstrates the overall stiffness of the connection in the third stage of deformation.

- All three connection designs C1 to C3 demonstrated the behaviour of a slip critical connection where the slip stage is reached at quite an early stage in each of the loading histories. Therefore, this must be considered for the design of the connection.
- This chapter also provides the basis in which the stiffness of the connection can be calculated. This method can be adopted in calculating spring stiffness values for similar module to module connections in order to be used in global structural models where the connections can be modelled as 'spring' or 'link' type elements depending on how the relevant software defines them.
- The experimental results measured through the contactless measurement system ARAMIS showed a close match to the analytical results output from ANSYS. A satisfactory comparison was achieved by measuring the strains of selected points on a target area of the specimens.
- The ANSYS model for each of the connection designs was successfully validated through the laboratory experiment. The ANSYS models could hereafter be used confidently to extract further analytical results.

Chapter 7 Failure Modes and Design Criteria for Module to Module Connections

7.1. Further Findings from the Finite Element Analysis

Since the results from finite element model showed a close comparison with the experimental results, it is reasonable to use the observations from the model to pursue further findings. These findings are useful in establishing the grounds for the approach to design these connections and identifying which failure modes would be critical when resisting lateral loads.

The failure criteria requires to be identified for the purpose of setting out a clear design procedure. A bolted steel connection may face failure through shear in bolts, tension in bolts, bearing of the bolts, bearing of the plates, tear-out of bolt holes or a combination of these. The results from the finite element analysis is therefore critically evaluated here to identify which of these failure criteria is critical for the design of the connection and the structure as a whole.

7.2. Stress and Strain Behaviour of Bolts

As observed from the force vs deformation relationships discussed in Chapter 6, it is evident that the connection behaves as a 'slip critical' connection where the bolts will carry bulk of the applied shear force. This shear force will be resisted by the friction in bolts until it reaches the slip stage and from thereon be resisted as a bearing force on the bolts against the plies (plates).

Since there are a number of stresses acting on each bolt, either one of them or a combination can cause failure. The overall failure of the bolts can be studied by following the von Mises stresses as per the 'Distortion Energy Theory'. The equivalent (von Mises) stresses that resulted from the ANSYS model for each of the connections C1 to C3 for each bolt are shown from Figures 7.1 to 7.3.

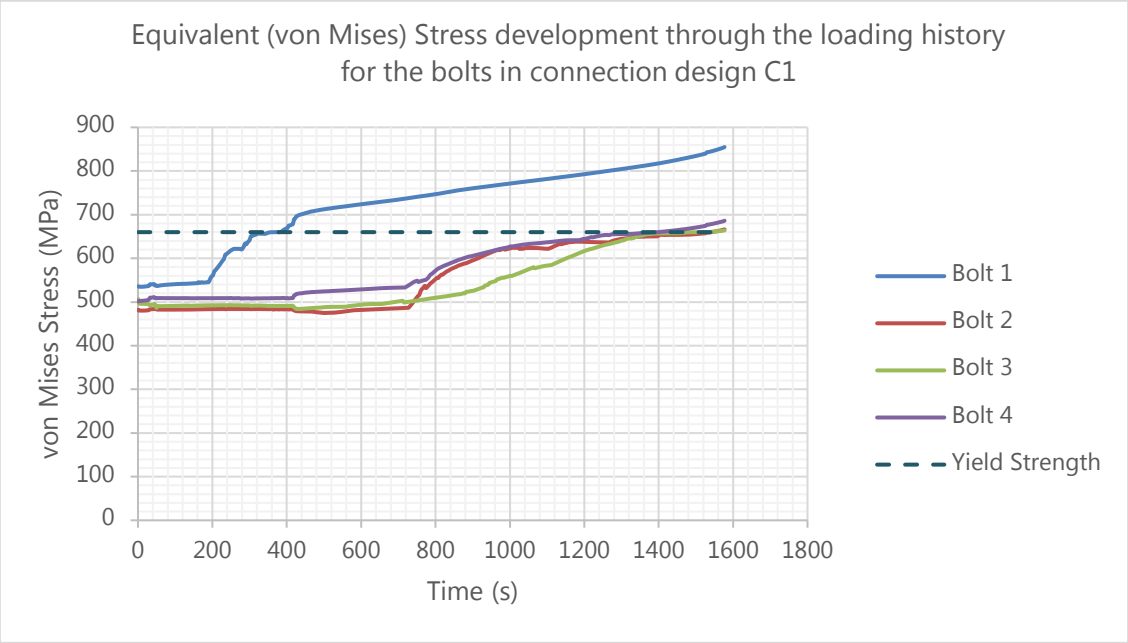

Figure 7. 1. Equivalent (von Mises) stress development through the loading history for the bolts in connection design C1

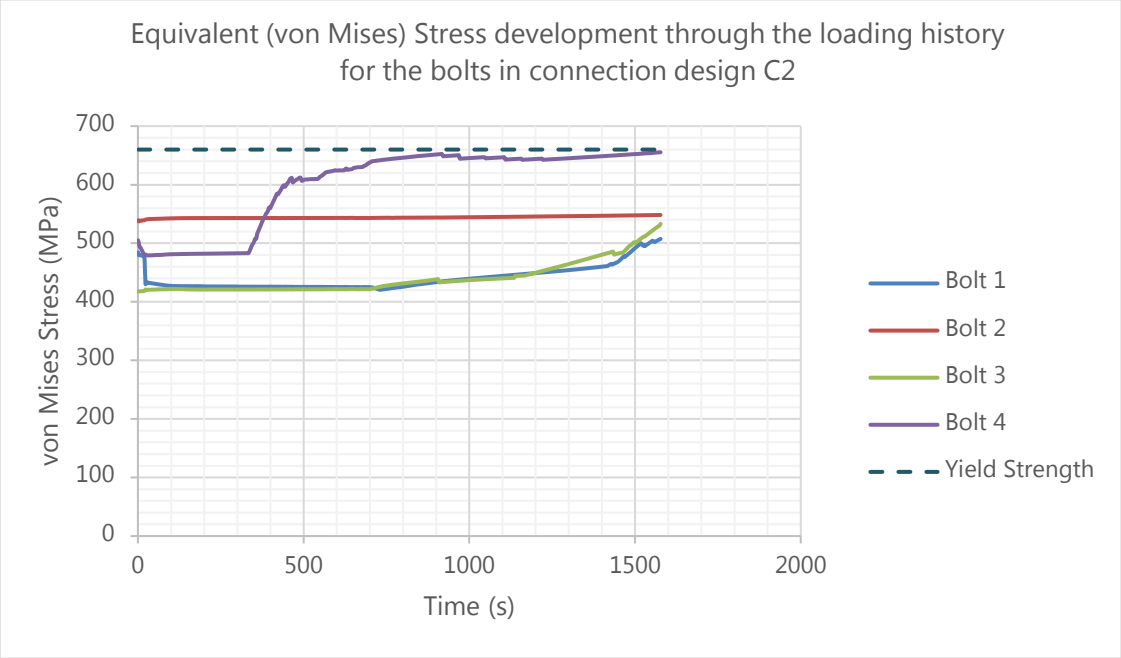

Figure 7. 2. Equivalent (von Mises) stress development through the loading history for the bolts in connection design C2

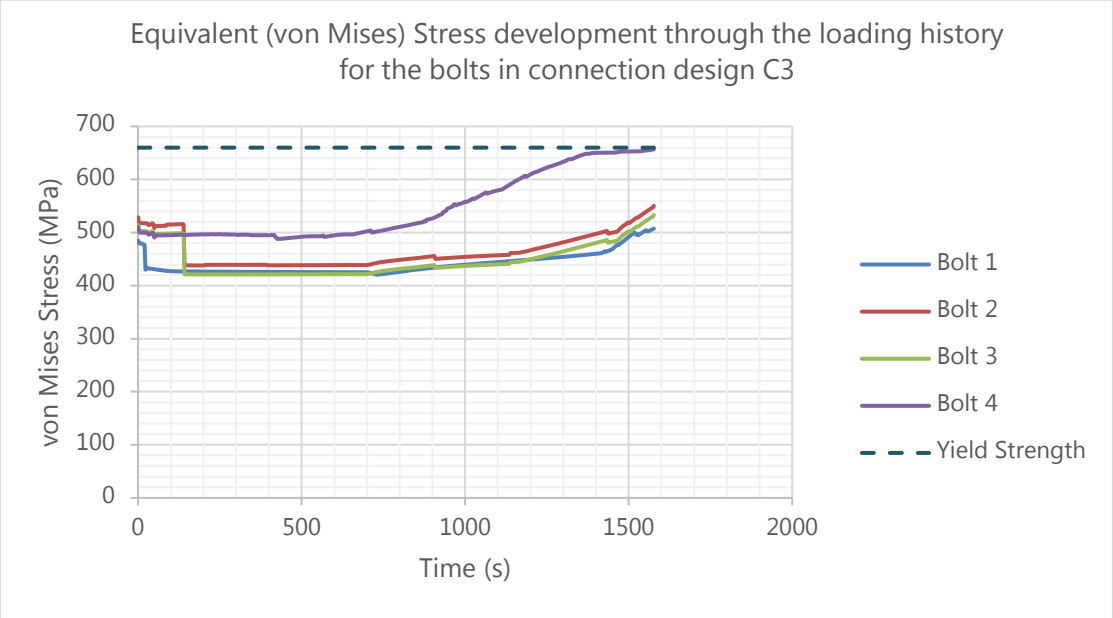

Figure 7. 3. Equivalent (von Mises) stress development through the loading history for the bolts in connection design C3

As discussed previously in Chapter 3, the Distortion Energy Theory is a simple and accurate method to observe the behaviour of the overall connection. In that regard, only connection design C1 appears to be yielding through bolt 1 initially and then through the remaining three bolts towards the end of the loading history.

Bolt 4, which is the closest to the bottom support appears to have developed the largest amount of strains in both connections designs C2 and C3 although neither of them have yielded.

Although this preliminary overview of the behaviour of the connection provides a clear observation of the overall failure of the connection, it fails to elaborate on the mode of failure and whether the yielding occurs due to one action or a combination of actions.

Therefore, each possible failure criteria was separately investigated for each connection design. The results are discussed in the following sections.

7.2.1. Evaluation of Shear Stresses

The shear stress generation is observed here against the shear strains that develop in each bolt for all three connection designs. The generated graphs are presented from Figures 7.4 to 7.6.

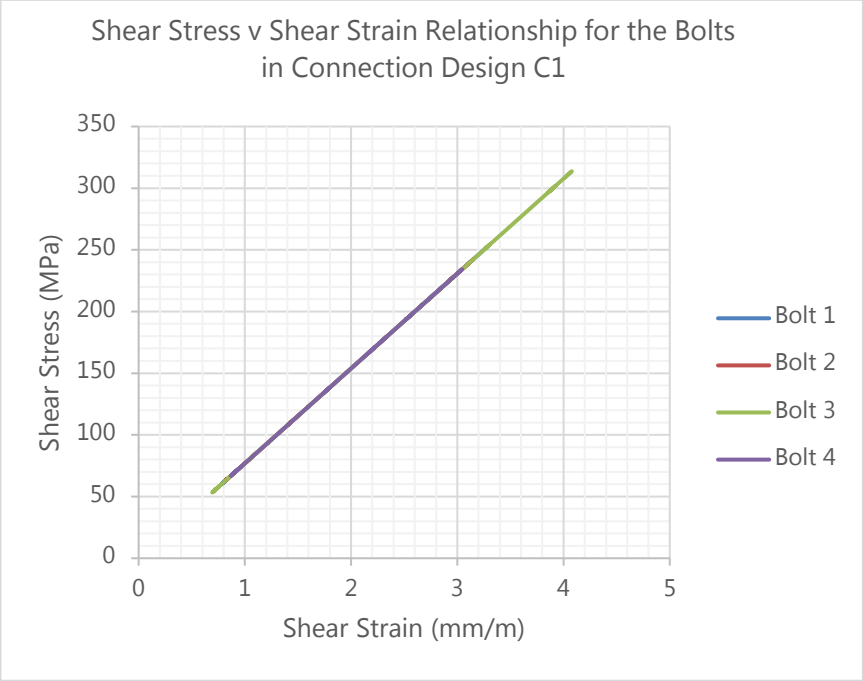

Figure 7. 4. Shear stress vs shear strain relationship for the bolts in connection design C1

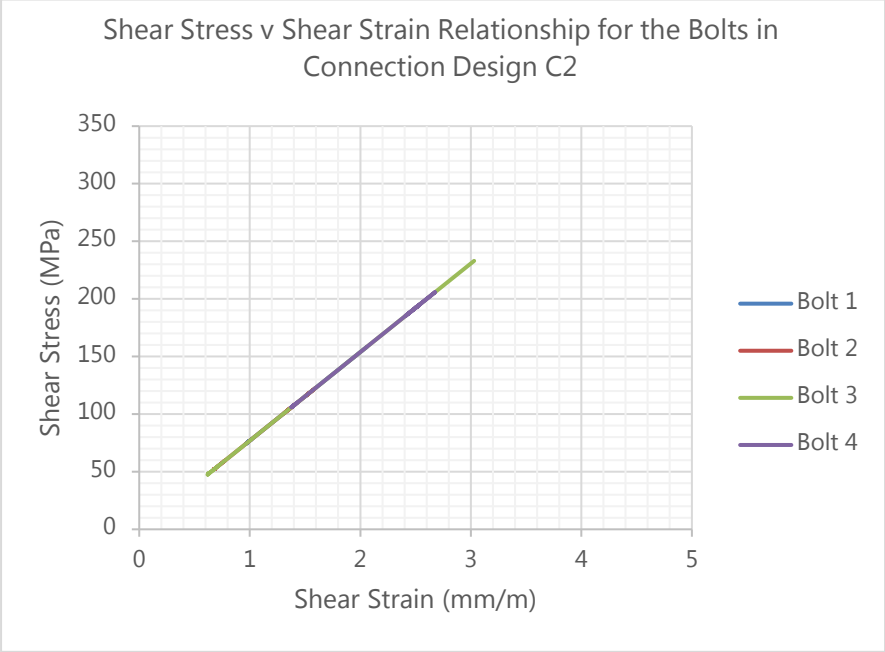

Figure 7. 5. Shear stress vs shear strain relationship for the bolts in connection design C2

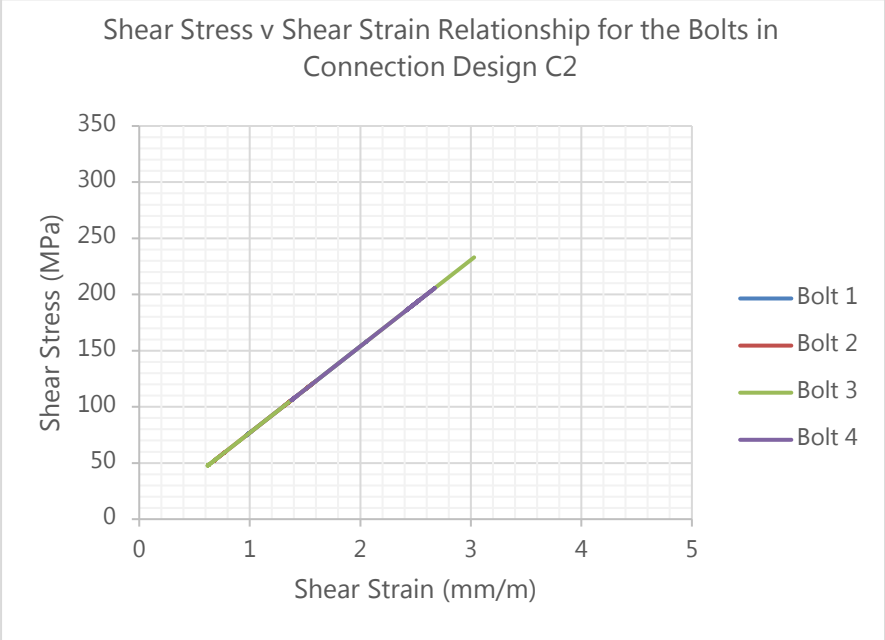

Figure 7. 6. Shear stress vs shear strain relationship for the bolts in connection design C3

All three diagrams for the shear stress vs shear strain behaviour show that none of the connections face pure shear failure. The generated stresses and strains vary from one bolt to the other in each of the connections which shows how the shear stress is not equally born by all four bolts. This is an interesting observation to note as most design codes including the Australian code would recommend assuming that all bolts bear the shear force equally. However, guidelines such as AISC (1980) suggest that shear forces born by individual bolts in a bolted connection vary with their distance to each other as well as the distance from where the load is applied. It must be noted here that the straight lines in each of the curves presented in figures 7.4 to 7.6 has a gradient equal to the shear modulus of the material. Each of the curves resulted in a gradient of approximately 76.9 GPa.

Although a pure shear failure is not observed, there still was some nonlinearity that was shown from force vs deformation relationship of the C1 connection as presented in Chapter 6. The shear stress values plotted against the full deformation of the bolt in the direction of the applied load would show evidence of any yielding that occurs while the shear stresses are generated.

A plot of a similar analysis of the shear stress vs deformation relationship for a steel bolt is shown through the research carried out by Kulak et al. (1987) and is shown in Figure 7.7. The graph would highlight the slip deformation as well as any yielding through the nonlinearity in the curve and also the very evident change in the gradient.

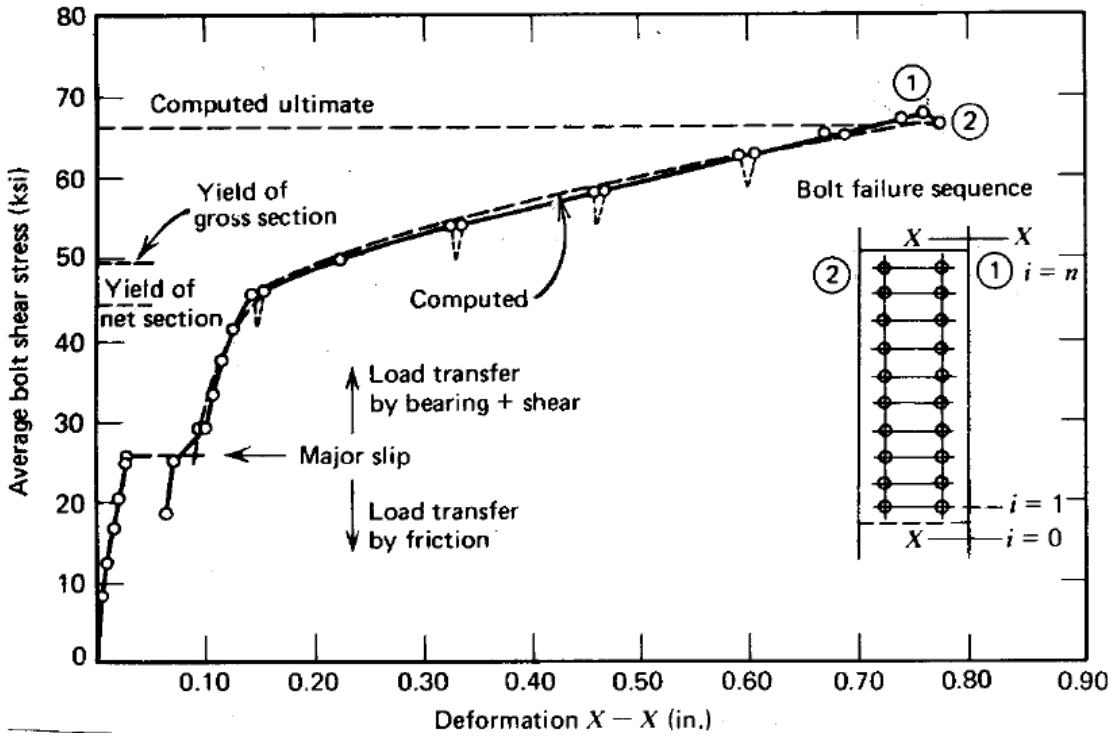

Figure 7. 7. A plot of theoretical and experimental results for a shear stress vs deformation relationship for a slip critical bolt (Kulak et al. 1987)

The shear stresses were plotted against the deformation of the bolt in the direction of the load application. The generated graphs are presented in Figures 7.8 to 7.10.

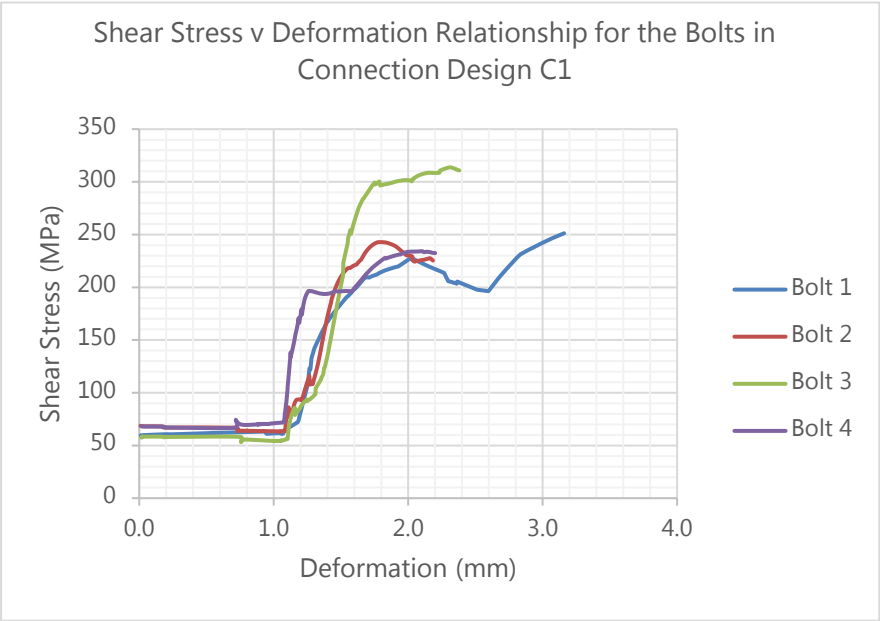

Figure 7. 8. Shear stress vs deformation in the direction of the applied load for the bolts in connection design C1

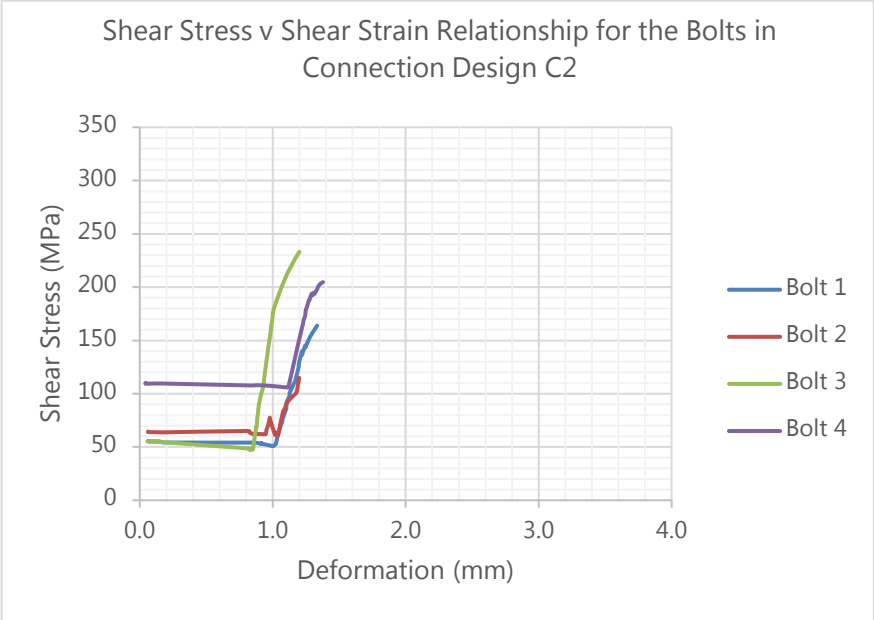

Figure 7. 9. Shear stress vs deformation in the direction of the applied load for the bolts in connection design C2

Figure 7. 10. Shear stress vs deformation in the direction of the applied load for the bolts in connection design C2

It appears that the bolts undergo yielding in connection design C1 in after the slip has occurred while the shear stresses develop. The slip of 1mm bolt clearance in the connection designs C1 and C2 and that of 5mm of the connection design C3 is quite evident in these graphs. They also clearly show how the shear stresses start developing immediately after the slip failure. This is the advantage of viewing the stress vs deformation relationship in addition to the stress vs strain relationship where the slip failure would not be evident.

It is also noted that the shear stress values do not start from zero, and that there is a shear stress at the beginning of loading. This is due to the fact that during the experiment the sample is kept parallel to the vertical axis and the self-weight of the full connection acts as a shear load on the bolts before any load is applied from the load cell. This shear stress value is a constant that remains on the bolts until they go through the slip failure and enter into bearing mode where they start developing additional shear stresses. This is evident from the

fact that it is 'Bolt 4', which is the closest to the bottom support and furthest from the point of application of the load that has the largest shear stress at the beginning, since it would experience the largest proportion of the self-weight of the connection.

7.2.2. Evaluation of Principle Stresses

To further investigate into the failure mode of the bolts, the stress vs strain relationships are also plotted for all three connection designs and are shown in Figures 7.11 to 7.13.

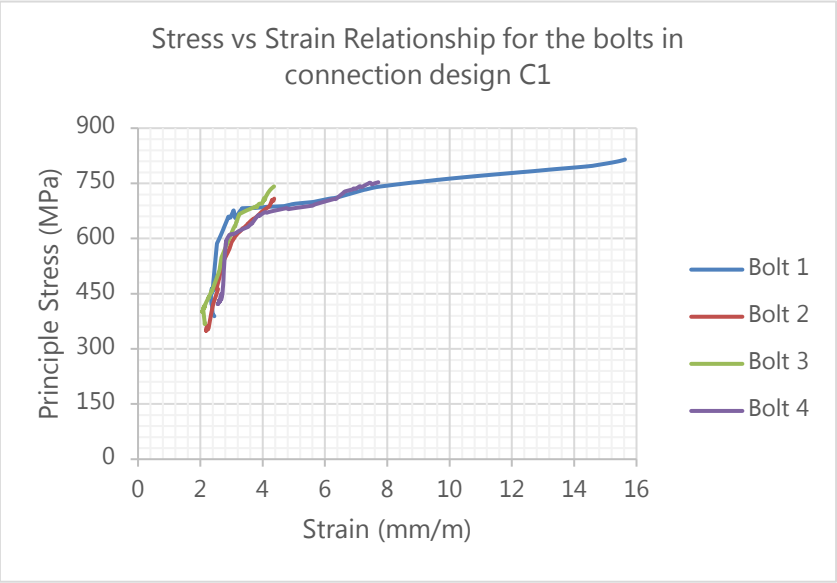

Figure 7. 11. Shear stress vs deformation in the direction of the applied load for the bolts in connection design C1

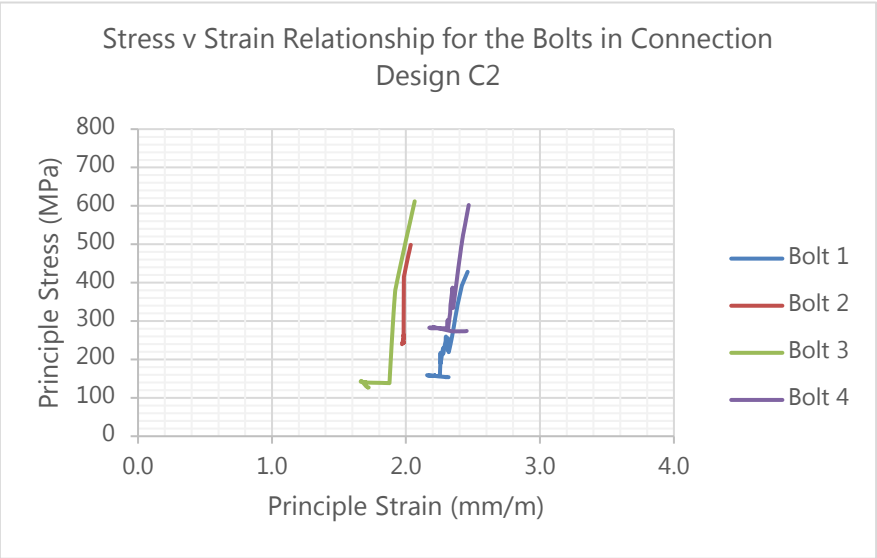

Figure 7. 12. Shear stress vs deformation in the direction of the applied load for the bolts in connection design C2

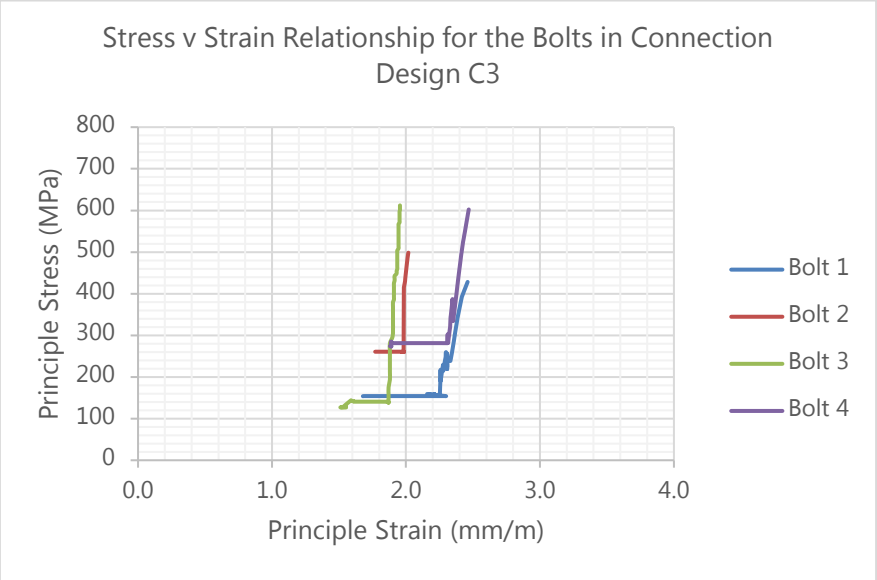

Figure 7. 13. Shear stress vs deformation in the direction of the applied load for the bolts in connection design C3

The principal stresses for connection design C1 show a clear nonlinearity for all four bolts. However, no nonlinearity was observed for either connection design C2 or C3. As discussed in Chapter 3, Maximum Principal Stress Theory is not the best estimate of yielding behaviour for bolted connections. However, it provides an indication that large axial stresses have developed in each of the bolts in all three connections. However, further results need to be observed to clearly identify the behaviour of the connection.

7.2.3. Evaluation of the Combined Effect of Shear and Tension

The combined effect of shear and tension is critical for this connection as all three connection designs appeared to have undergone slip failure quite early in their loading histories. Therefore, the combined effect as of shear and tension is checked against its capacity which was estimated through Eq. 3.25 provided in Chapter 3. The combined behaviour is plotted and presented from Figures 7.14 to 7.16.

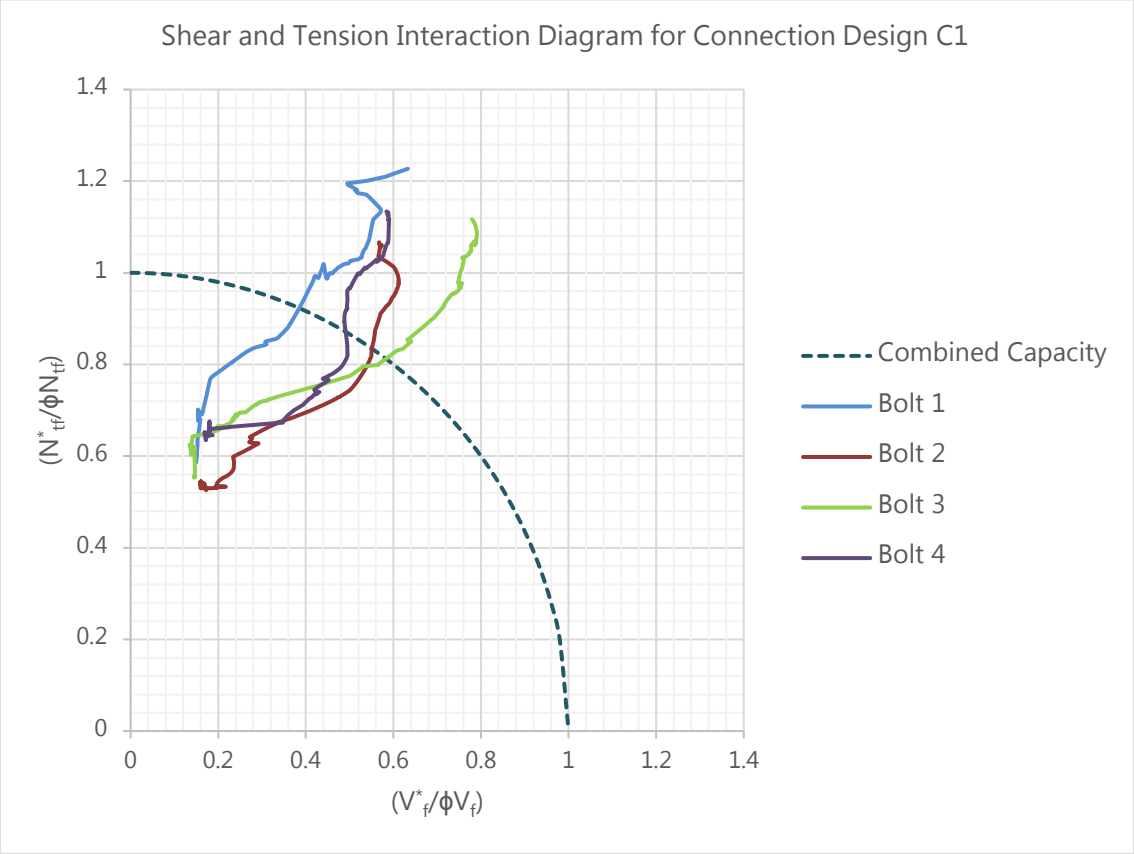

Figure 7. 14. Shear and tension interaction diagram for connection design C1

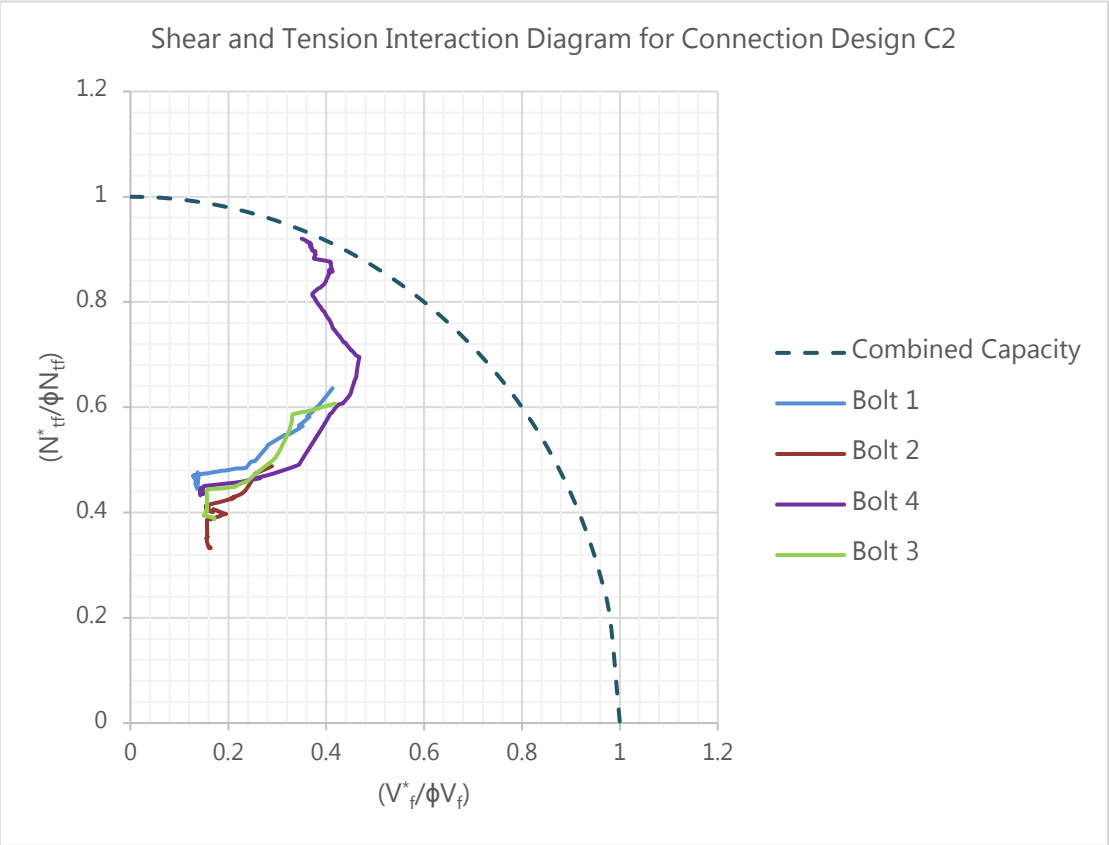

Figure 7. 15. Shear and tension interaction diagram for connection design C2

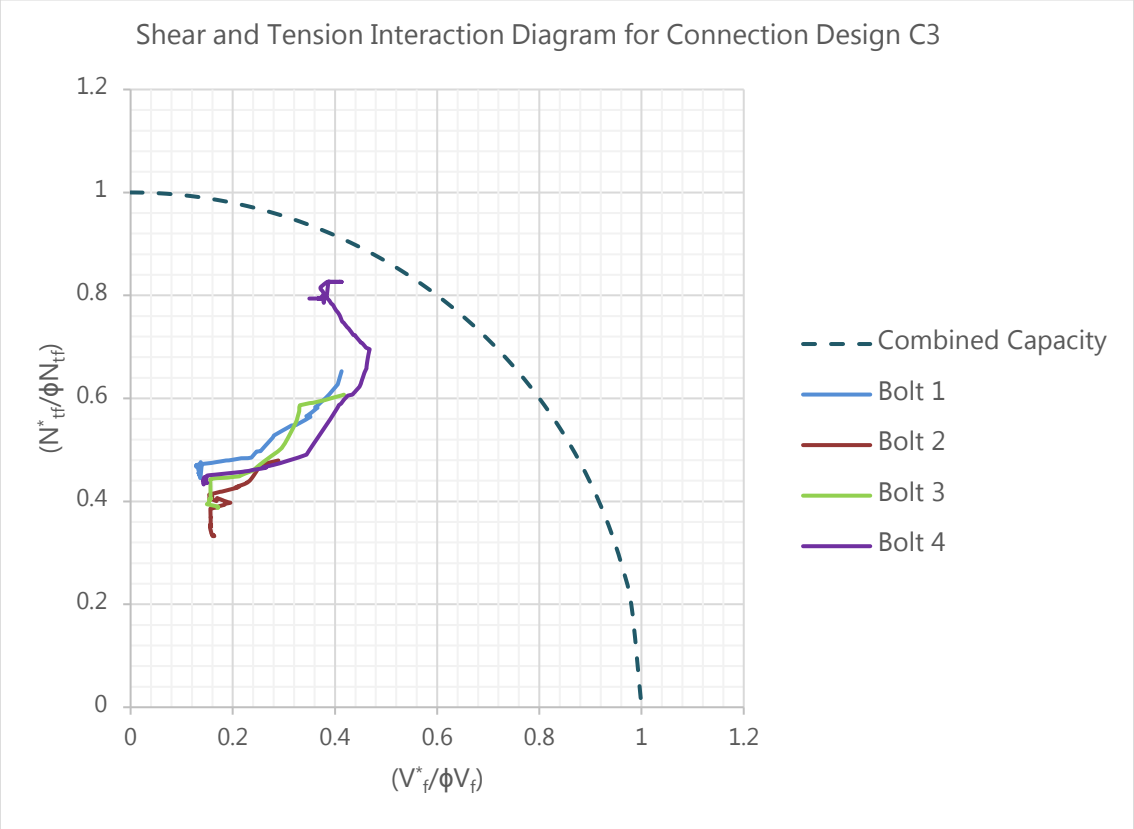

Figure 7. 16. Shear and tension interaction diagram for connection design C2

This is further evidence that the connection design C1 has yielding bolts and none can be found in connection designs C2 and C3. It is also evident that both shear and the axial stresses generated through bearing has caused these bolts to fail. AS 4100 (1998) provides an interaction relationship to calculate the combined action of shear and axial tension as discussed in Chapter 3 (Eq. 3.25). The hypothesis developed through the above graphs that the failure of bolts in these connection is more likely due to the combined effect of shear and bearing can be proven by plotting the tensile and shear combined stresses in an interaction diagram. Figures 7.14 to 7.16 present these interaction diagrams for each of the connection designs.

These interaction diagrams confirm the view that failure mode of is a combination of shear and tension. Due to the extent of the applied loads, only connection design C1 has shown yielding of the bolts through combined shear and tension. This failure pattern is further illustrated through the images captured from the finite element model carried out on ANSYS and presented in Figures 7.17 to 7.19.

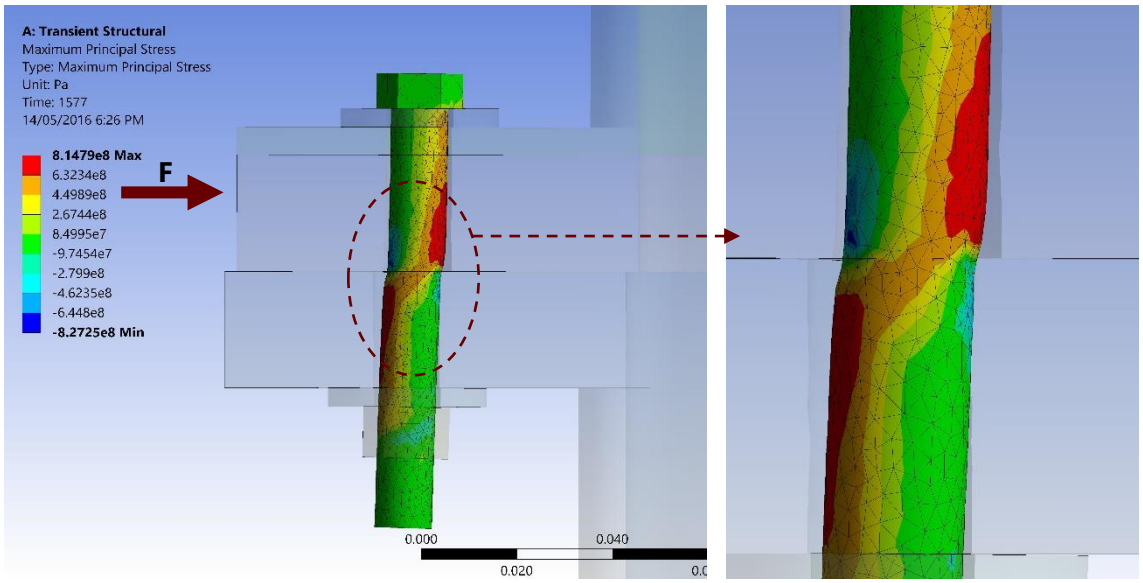

Figure 7. 17. Failure mode of Bolt 1 of connection design C1 (Left) and a close-up image of the failure zone (Right)

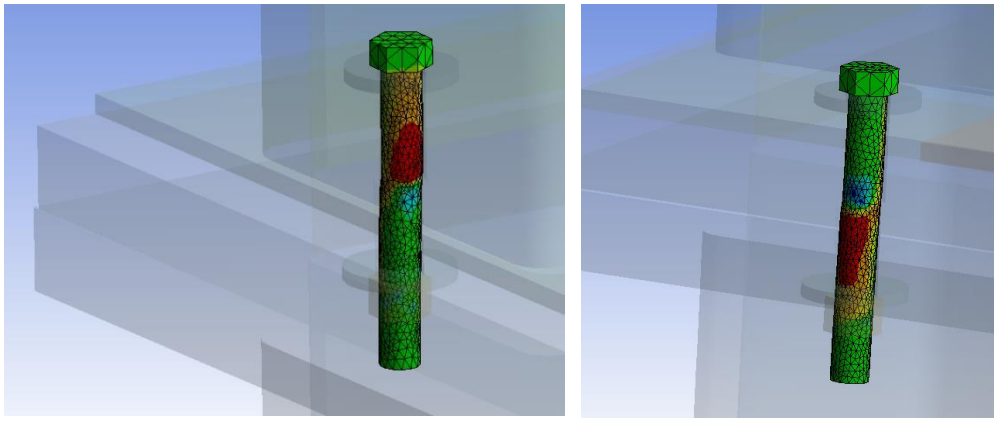

Figure 7. 18. Failure mode of Bolt 1 of connection design shown from two different angles

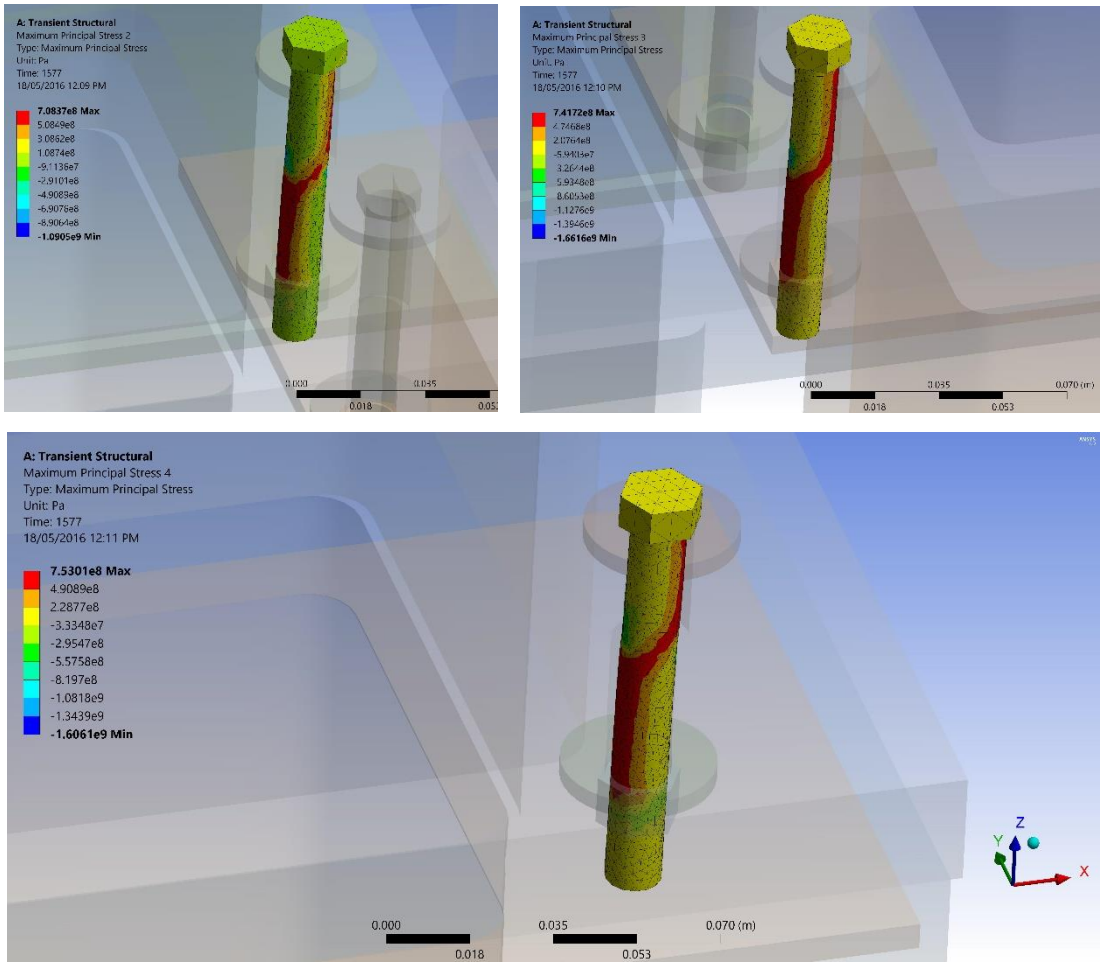

Figure 7. 19. Failure mode of Bolts 2, 3 and 4 of connection design C1

7.3. Suitable Design Approach

As observed from each of the stress and strain assessments in this chapter, the connections show distinct failure mechanisms that can be directly addressed through a design. Most international design standards including those in Australia still follow limit state design as opposed to the newer trends towards performance based design.

This section will address both these design approaches in order to fulfil one of the main objectives of this research. The Australian steel design standard AS 4100 (1998) provides for 'Strength Limit State' and 'Serviceability Limit State' for the design of steel bolted connections. The connections discussed in this thesis will also follow the same limit states as follows;

7.3.1. Serviceability Limit State

It was observed that all three connection designs underwent slip failure quite early in the loading history. Therefore the connection needs to be considered as a 'slip critical' joint for the purpose of design.

Even though only one shear plane was considered in the calculations presented in Chapter 6 due to the nature of the laboratory setup, all applicable shear planes as shown in Figure 6.4 need to be considered in estimating the slip resistance for this connection when applied to a real building.

It would also be prudent to consider a low coefficient of friction to anticipate the worst case slip scenario. In reality, the connection too would have protective coatings that ensure the durability of the component. Such paints can result in a lower coefficient of friction in all slip planes. It would not be advisable to sacrifice durability to achieve a higher resistance to slip by simply preparing the interface rough. However, innovative techniques can be applied here

to provide a solution through various methods such as durable and resilient paints with a rough texture or a geometric change of the surfaces that prevent slip failure. As a more conservative solution, a larger bolt size can also be used since it would require a higher bolt pre-tension.

7.3.2. Strength Limit State

Subsequent to slip failure, it was observed that the bolts of each of the connections transfer into a stage where they resist a combined shear and bearing action. Therefore, the check for combined shear and tension is the critical design criterion.

7.3.3. Earthquake Design

The connection can be modelled as a pin joint for the connecting columns vertically and a spring (or link element with equivalent spring stiffness according to the element definitions of software such as ETABS and SAP2000) for the horizontal component of the connection with a stiffness that can be calculated using the method explained in Chapter 6.

The inter-storey drift is an important result to check for both wind and earthquake designs. This value is uniquely different for corner supported modular structural systems as every modular floor has two different structural elements as the roof/soffit of the lower storey and the floor of the upper storey. In contrast, a regular building would have both these components represented by a single slab element. Therefore the inter-storey height is defined as the height between two consecutive module to module connections as illustrated in Figure 7.20.

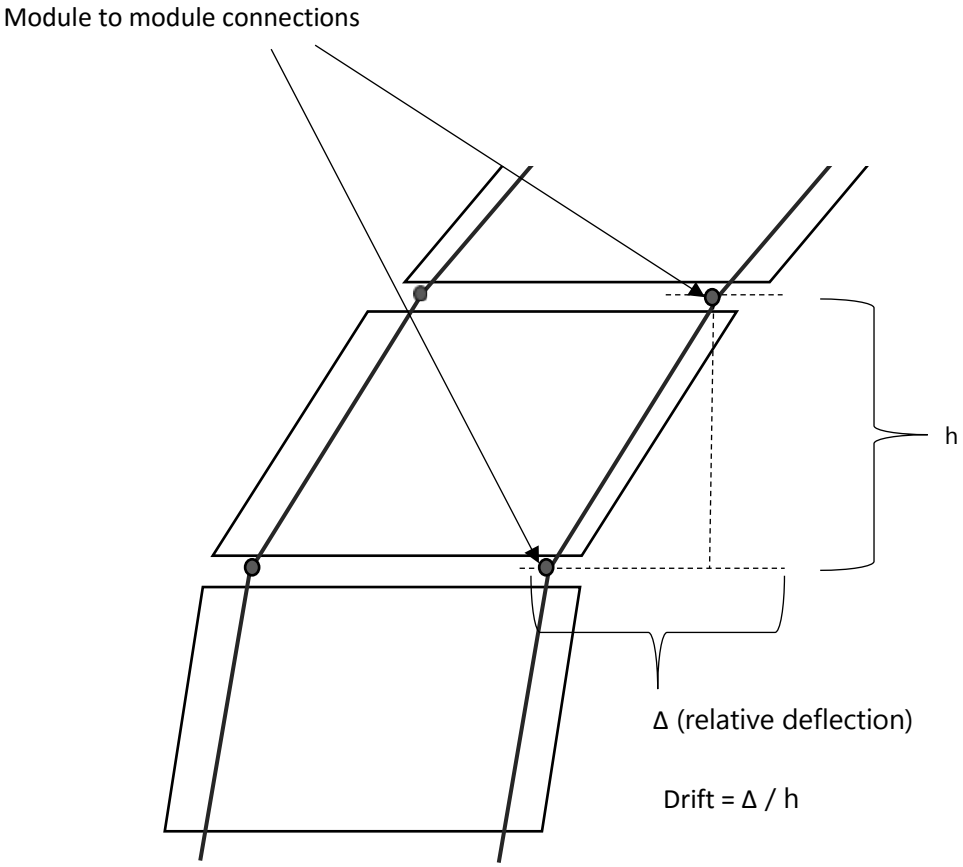

Figure 7. 20. An illustration for the definition of inter-storey drift for corner supported modules as used in this research

Once the global structure is analysed as such, the connection design can be approached as discussed in section 7.3. While addressing the slip as a serviceability limit, designers must note that slip failure can occur easily in these connections during moderate to large earthquakes. Therefore, as mentioned earlier, the combined bearing and shear capacity of the connection shall be the most critical design criterion to achieve.

It must also be noted here that as explained in Chapter 5, the design must at all times ensure that the connection remains elastic and any plastic hinge formation occurs in the supporting column. To ensure that this happens, designers may conservatively choose to over-design

the connection with bolt sizes and numbers higher than required to satisfy the code requirements. Since steel by nature is a ductile material, over-designing the connection would not make it brittle or prone to other types of failure. This concept must not be overlooked as if the failure occurs in the connection before anywhere else, collapse of the structure may be imminent.

While a conventional design may address the above mentioned criteria, designers may also choose to follow a performance based design.

On this regard, the Australian wind code AS 1170.2 (2011) can be regarded as a performance based design guide for wind when it is applied together with the 'human perception of motion' criteria proposed by Mendis et al. (2007). Wind accelerations calculated for the structure can be checked with the acceptable limits set out by Mendis et al. (2007) as shown in Figure 7.21.

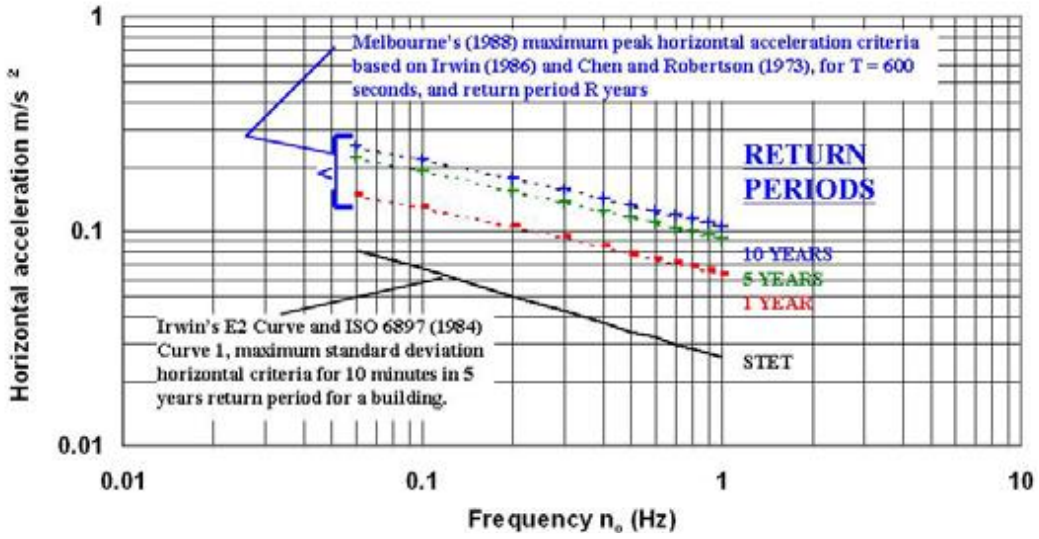

Figure 7. 21. Human comfort criteria against wind accelerations - human perception of motion (Mendis et al., 2007)

As far as earthquake design is considered, performance based designs can follow many available practice guidelines as discussed in Chapter 3. A nonlinear time history analysis or a nonlinear static analysis (pushover analysis) would be required for a comprehensive performance assessment against earthquake loads. The Capacity Spectrum method which was carried out for the analysis presented in Chapter 5 is a quick and safe estimate which can be used for this purpose.

However, where the structure is safely expected to follow a linear elastic behaviour for the level of earthquakes expected in a particular site, the guideline produced by SEAOC (1995) can be used as a framework to arrive at a preliminary estimate of the performance level of the structure. This framework is presented in Table 7.1. The inter-storey drifts needed for this assessment can be found out by a code based response spectrum analysis following the modelling basics discussed here. The drifts in this regard can be calculated following the definition introduced in Figure 7.20.

Table 7. 1 Preliminary Estimate of Performance Levels (SEAOC, 1995)

Performance Level	Apparent Damage	Limiting Inter-storey Drift
Fully Operational	Negligible Negligible structural and non-structural damage Continuous service Facility operates and functions after earthquake.	0.2 %
Immediate Occupancy	Light Negligible structural and light non-structural damage Most operations and functions can resume immediately Repair is required to restore some non-essential services Structure is safe for occupancy immediately after earthquake Essential operations are protected, non-essential operations are disrupted.	0.5 %
Life Safety	Moderate	1.5 %

	Structural damage is light to moderate Non-structural damage is moderate to severe Selected building systems, features or contents may be protected from damage Life-safety is generally protected Structure is damaged, but remains stable Potential falling hazards remain secure.	
Collapse Prevention	Severe Structural damage is severe, but collapse is prevented Non-structural elements may fail.	2.5 %
Collapse	Complete portions of primary structural system collapse Or Complete structural collapse.	> 2.5%

7.4.Summary

- This chapter discusses further results from the finite element models that were carried out using ANSYS for the three connection designs C1, C2 and C3 which were subsequently validated through laboratory experiments.
- By studying the shear stress vs shear strain curves for all three connections, it is evident that the most critical failure criteria could not be purely by shear.
- Yielding of bolts in connection design C1 is shown through the shear stress vs deformation relationship as well as the stress vs strain relationships of the bolts.
- However, the interaction diagrams drawn for the combined effect of shear and tension clearly demonstrate that the failure occurs by the stresses generated by the bearing of the bolts against the plates while undergoing shear stresses.
- Slip failure is evident in all three connections at a very low lateral load and therefore requires the connection to be designed for serviceability as a 'slip critical' connection.

- As far as the strength design criteria is concerned, the combined effect of shear and tension needs to be checked as the most critical design check in carrying out the design calculation for module to module connection of this type.

Chapter 8 Conclusions and Recommendations

8.1. Conclusions on the Introduced Advanced Corner Supported Modular Structural System

Most multi storey modular buildings that use corner supported systems, rely heavily on a central core which is more often than not, a cast in-situ reinforced concrete wall system. In addition to that, many of those buildings would have the modules permanently fixed by pouring concrete to the empty space between two stories of modules and form a non-removable slab. These techniques have thus far prevented modular designs from enjoying the full set of benefits that modular construction offers, especially in the form of reusability and complete off-site manufacturing.

The Advanced Corner Supported Modular Structural System provides a promising scope for designing low to medium rise structures as a purely modular construction. The preliminary analysis which is presented in Chapter 4 of this thesis shows that the system makes the structure behave within parameters set out by design standards for conventional structures under normal loading conditions.

The outcomes of this pave way for further analysis and experiments as carried out to a greater extent through this research and presented through Chapters 5, 6 and 7 of this thesis.

It is also established by this thesis that the newly introduced Advanced Corner Supported system allows the lift shafts to be positioned in innovative arrangements without causing additional adverse torsional effects. There is an increasing interest in the industry for such innovation as it provides both aesthetic as well as practical advantages.

It is envisioned that this technology will develop further to be used widely for high rise applications. The system is adequately versatile to allow for different variations of the Advanced Corner Supported system to be developed to achieve the specific requirements of such projects. Different materials such as high strength steels and concrete and composites with various mechanical properties can be evaluated to be used in connections and walls in the stiffer modules.

The modules can be designed in such a way that it can replicate the use of a conventional core during construction. For example, they can be collaborated with a smart system to support a crane and also support auto-climbing features. Compact service modules which are also manufactured as sub-modules in a controlled factory environment can also be used to house different mechanical, electrical and plumbing networks.

With an increasing interest and drive from the industry, this technology will provide a very desirable solution to designers, builders, developers and dwellers.

8.2. Conclusions from Global Structural Analysis

The elements that join at the module to module connection play a critical role in lateral load resisting system in a modular building. Therefore, these connections need to be designed to take the full shear force generated by the lateral loads. They also need to stay elastic while other hinge locations yield since if any failure occurred at the connection the entire structure would collapse.

By the results observed from the nonlinear time history analysis, a hinge formation in the main corner column just under the floor beam or above the roof beam ("Hinge 2" as per Figure 5.6) proves to be the most likely scenario out of the possibilities discussed. The formation of such hinges in a main column is not a desirable scenario as it may lead to collapse during a large earthquake. However, prevention of these hinges from forming may not always be possible under large earthquakes. Alternatively the structure could be designed in such a way that the hinge formation occurs elsewhere, possibly on the floor beams of less stiff modules that do not carry concrete walls. A unique advantage of a purely modular building is the ability to remove damaged modules and have them replaced. The removed modules can also be repaired and reused elsewhere on other suitable projects.

The ductility of the corner columns is also a critical criterion to maintain in order to achieve a better performance under high seismic loads. Although yielding may occur, high ductile columns may still prevent collapse and assist the horizontal members to redistribute the loads among neighbouring modules.

However, in a severe earthquake, it may prove very difficult to prevent the columns from forming hinges. As such, the immediate investigation into the condition of the structure after a large earthquake is highly important. Structural Health Monitoring (SHM) techniques therefore can plays a key role in improving the seismic performance of such structures and also assist in improving the understanding of the behaviour of these structures under dynamic earthquake loads.

In conclusion, it must be noted that this structural system has many advantages which ensure highly profitable outcomes to both builders and developers. However, where such buildings are required to be constructed in high seismic areas special care must be taken to ensure that the critical columns are not vulnerable to hinge formations. The unique reusability characteristics of modular construction allows for a better chance at designing to sacrifice less critical elements in a large earthquake and safeguard human lives by preventing collapse.

8.3. Conclusions from Finite Element Analysis and Laboratory Experiment

The module to module connection play a critical role in how lateral loads are transferred and resisted in a modular building. The bolted steel plates that connect neighbouring modules are the key elements that transfer the lateral loads from weaker modules to stiffer modules. Therefore, it is vital that there is a better understanding about their behaviour when subjected to lateral loads.

The finite element analysis that was carried out using the software ANSYS was successfully validated through a set of laboratory experiments which were conducted on three different connection designs. The experiments and the validated model resulted in a valuable understanding on how the connection would behave under lateral loads. Since the ANSYS model proved to demonstrate conservative results compared to the experiment, it can be utilised for further analytical work to understand the behaviour of these connections under more scenarios.

The analysis on all three connection designs show that slip failure is inevitable for large horizontal forces, the likes of which can be expected in earthquakes. Although slip failure is not catastrophic, it transforms the connection to a 'bearing' type connection thereafter.

Therefore, slipping of bolts needs to be expected in an earthquake. As a result, large slots are not advisable to modular building with a large building height, as accumulated slips can result in a very large lateral deflection which combined with P-Δ effects can cause severe damages to the supporting columns. Having slotted holes do appeal a lot for modular construction as it allows for a larger margin of tolerance while placing the modules to align with the bolt holes of the modules that are already fixed in the structure. However, designers need to bear in mind that, if slotted holes are still required they are properly designed to delay the slip

failure as much as possible. This can be achieved by having larger bolt sizes than necessary. However, this practice is not advisable in high seismic regions.

An alternative to provide for this need during installation of modules is to use advanced machinery such as specially designed mobile rigs to support the module while being put into place accurately. This would minimise human errors and also provide a safer working environment during the installations of modules, while enabling the installation of modules with much smaller tolerances.

The findings from the finite element analysis combined with the findings from the global analysis forms a solid methodology to be used for the structural design of modular buildings that would be built with a corner supported or advanced corner supported system. This approach is explained with recommendations in section 8.4.

8.4. Recommended Approach to the Design of a Modular Building with the Advanced Corner Supported System

As any building design, the design to a modular building will commence with the concept designs of Architectural, Structural Engineering and Mechanical, Electrical & Plumbing (MEP) Engineering disciplines. The key to an efficient modular building design lies in the geometric layout of the building plan. Once the initial Architectural concept is developed, the plans need to be studied to develop the best suited layout of modules.

The conceptual sizing of the modules is mainly constrained by the dimensions that are allowed by their transport. If modules are to be transported on land they would need to abide by road width and allowable height regulations. Other factors such as available member sizes, factory capacity and of course financial limitations would also affect the conceptual design of the modular building.

Once a conceptual design is developed, the structure can be analysed and designed in detail using the knowledge gained through this research. The established method of calculating the stiffness of the connection is vital in developing global structural models for practical applications using commercial software such as ETABS. The analytical results produced in this thesis can be used as a benchmark to compare with for any such global analysis.

The infill walls and the module to module connection are the two most important components of the Advanced Corner Supported Modular Structural system. The walls are purely intended to provide superior stiffness to a select set of modules. The infill material and the dimensions of the walls need to be decided upon this concept. Therefore, engineers have the liberty to experiment with innovative materials as longs as it provides the required stiffness. Lightweight concretes, phase changing materials, aerated concretes, innovative composite materials are a few to mention. While maintaining the main purpose of providing a higher stiffness, designers can aim to achieve further efficiencies through these walls. As an example, composites can be developed to provide the required stiffness as well as other advantages such as thermal insulation, fire resistance and sound insulation.

The conceptual design of the connections must also be aligned with the strategy to install the modules on site. Workers need to have safe and easy access to the connections during installation to ensure that the bolts are properly tightened.

All these components of the structural design together with the fabrication specifications need to be efficiently organised to ensure the complete procedure takes place with time and cost efficiency as intended by pure modular construction. Modern design techniques such as Building Information Modelling (BIM) can be used to ensure such efficiency and that the coordination of all parties are well managed.

8.5. Recommendations for Future Research

While developing a sound understanding on the behaviour of corner supported modular buildings and their module to module connections under applied lateral loads, this research creates opportunities for further academic and industry research.

Some of the topics with noteworthiness for future research that can arise from the findings of this research can be broadly identified in the following areas;

Variations to the Advanced Corner Supported Modular Structural System

This thesis introduced the conceptual framework for the development of the proposed 'Advanced Corner Supported Modular Structural System'. The proposed design is a generic design that provided an efficient analysis for this research. However, this can be further modified with complex geometric arrangements and usage of modern innovative materials.

Further, the infill walls and corner columns can also be redesigned as cavity walls and hollow columns which can be filled with high performance and high strength concretes subsequent to installation, especially for taller buildings. Further research should look into ways of developing smart column to column and wall to wall connections that would not compromise the reusability of modules.

Development of Service Modules to house MEP Services for Multi-storey Buildings

Multi-storey buildings typically contain building services networks that connect vertically via a service core. With modular technology it is possible to create prefabricated and compact service modules that can house such services and still provide the capability of being efficiently connected as modules both vertically and horizontally.

Future research should investigate in detail into what services are readily convertible to this system and which others would require further development. This shall lead into further advancement in modular technology.

Further Experimental Studies and Finite Element Analyses

The experiment carried out and presented in this thesis is a useful investigation into the behaviour of the module to module connections against lateral loads and it provided a fair validation to the finite element analysis. In this regard, further experiments and analysis are suggested to investigate more severe earthquake conditions. Cyclic loading tests on either scaled or full-scaled specimens need to be carried out in order to physically observe and determine the behaviour and failure mechanisms of these connections under severe dynamic loading conditions. Further finite element analyses can carry the results presented in this thesis much further in analysing many more loading conditions as well as many more connection designs in order to establish a complete understanding of modular type connections.

References

1. ACT 40 (1996). *Seismic Evaluation and Retrofit of Concrete Buildings*. California, USA, Applied Technology Council.

2. AISC: 1980: *Specification for the Design, Fabrication, and Erection of Structural Steel for Buildings*, American Institute of Steel Construction, Chicago.

3. AJAX (1999). *Fastener Handbook: Bolt Products*. AJAX Technical Advice Centre (ATAC).

4. Al-Huniti, N. S. (2005). Computation of Member Stiffness in Bolted Connections Using the Finite Element Analysis. *Mechanics Based Design of Structures & Machines*, *33(3/4),* 331-342.

5. Annan, C. D., Youssef, M. A. & El Naggar, M. H. (2009a). Seismic Vulnerability Assessment of Modular Steel Buildings, *Journal of Earthquake Engineering, 13(8)*, 1065-1088.

6. Annan, C. D., Youssef, M. A. & El Naggar, M. H. (2009b). Effect of Directly Welded Stringer-to-Beam Connections on the Analysis and Design of Modular Steel Building Floors. *Advances in Structural Engineering, 12(3),* 373-383.

7. ARAMIS (2008). *ARAMIS User Information - Hardware*, Gesellschaft für Optische Messtechnik (GOM), Germany

8. Arshad, S. & Athar, S. (2013). Rural Housing Reconstruction Program Post-2005 Earthquake: Learning from the Pakistan Experience. *A Manual for Post-Disaster Housing Program Managers*. Washington D.C., World Bank.

9. AS 1170.2: 2011: *Structural Design Actions. Part 2: Wind Actions*, Standards Australia, New South Wales.

10. AS 1170.4: 2007: *Structural Design Actions. Part 4: Earthquake Actions in Australia*, Standards Australia, New South Wales.

11. AS 4100: 1998 (Reconfirmed in 2016): *Steel Structures*. Standards Australia, New South Wales.

12. ASCE 7: 2010: *Minimum Design Loads for Buildings and Other Structures*. American Society of Civil Engineers (Ed.) ASCE 7-10. Reston, VA

13. Aye, L., Ngo, T., Crawford, R. H., Gammampila, R. & Herath, N. (2012). Life Cycle Greenhouse Gas Emissions and Energy Analysis of Prefabricated Reusable Building Modules. *Energy and Buildings*, *47(0)*, 159-168

14. Baker, J. W. (2005). *Vector-valued Ground Motion Intensity Measures for Probabilistic Seismic Demand Analysis*. Stanford University.

15. Berman, J. W. & Bruneau, M. (2005). Experimental Investigation of Light-Gauge Steel Plate Shear Walls. *Journal of Structural Engineering*, American Society of Civil Engineers, 259-267.

16. Bezler, P., Curreri, J. R., Wang, Y. K. & Gupta A. K. (1990). *Alternate Modal Combination Methods in Response Spectrum Analysis,* United States Nuclear Regulatory Commission, Washington D.C.

17. Bruneau, M., Sabelli, R., & Uang, C. (2011). *Ductile Design of Steel Structures*. New York: McGraw-Hill, c2011.

18. Carr, A. J. (2010), *RUAUMOKO Manual: User Manual for the 3 Dimensional Version Ruaumoko 3D*, Unversity of Cantebury, Christchurch, NZ

19. Chopra, A. K. & Goel, R. K. (1999). Capacity Demand Diagram Methods Based on Inelastic Design Spectrum. *Earthquake Spectra, 15***,** 637-656.

20. Chopra, A. K. & Goel, R. K. (2000). *Application of Inelastic Design Spectrum to Capacity-Demand-Diagram Methods. Proceedings of Structures Congress.*

21. Chopra, A. K. & Goel, R. K. (2002). A Modal Pushover Analysis Procedure for Estimating Seismic Demands for Buildings. *Earthquake Engineering and Structural Dynamics, 31***,** 561-582.

22. Chopra, A. K. & Goel, R. K. (2004) A Modal Pushover Analysis Procedure to Estimate Seismic Demand For Unsymmetric-Plan Buildings. *Earthquake Engineering and Structural Dynamics, 33***,** 903-927.

23. Chopra, A. K. (2001). *Dynamics of Structures*, Prentice Hall, New Jersey, USA

24. Chopra, A. K., Goel, R. K. & Chintanapakdee, C. (2004) Evaluation of a Modified MPA Procedure Assuming Higher Modes as Elastic to Estimate Seismic Demands. *Earthquake Spectra, 20***,** 757-778.

25. CSI Knowledge Base. (2014) <https://wiki.csiamerica.com/display/etabs/Center+of+rigidity>.

26. Dalal Sejal P., Vasanwala S., & Desai, A. (2011). Performance Based Seismic Design of Structure: A Review. *International Journal of Civil & Structural Engineering, 1(4),* 795-803

27. Der Kiureghian, A. (1980). *A Response Spectrum Method for Random Vibrations*, University of California at Berkeley.

28. Dowrick, D. J. (2009)*. Earthquake Resistant Design and Risk Reduction, 2nd Edition.* Wiley.

29. EC 8: 2004: *Design of Structures for Earthquake Resistance*. *Part 1: General rules, Seismic actions and rules for buildings.* Brussels, Belgium.

30. Fajfar, P. & Gaspersic, P. (1996). The N2 Method for the Seismic Damage Analysis of RC Buildings. *Earthquake engineering and structural dynamics*, 25**,** 31-46.

31. Fajfar, P. (1999). Capacity Spectrum Method Based on Inelastic Demand Spectra. *Earthquake engineering and structural dynamics, 28***,** 979-993.

32. FEMA 273: 1997: *NEHRP Guidelines for the Seismic Rehabilitation of Buildings*, Washington, USA.

33. FEMA 450: 2003: *NEHRP Recommended Provisions for Seismic Regulation of Buildings and Other Structures*, prepared by the Building Seismic Safety Council for the Federal Emergency Management Agency, Washington, D.C.

34. Freeman, S. A. (1998). *The Capacity Spectrum Method as a Tool for Seismic Design. 11th European Conference on Earthquake Engineering.* Paris, France.

35. Freeman, S. A. (2004). Review of the Development of the Capacity Spectrum Method. *ISET Journal of Earthquake Technology, 41***,** 1-13.

36. Freeman, S. A., Nicoletti, J. P., & Tyrell, J. V. (1975). *Evaluations of Existing Buildings for Seismic Risk—a Case Study of Puget Sound Naval Shipyard. Proceedings of the 1st U.S. National Conference on Earthquake Engineering.* Bremerton, Washington.

37. Gilmartin, U. M., Freeman, S. A. & Rihal, S. (1998). *Using Earthquake Strong Motion Records to Assess the Structural and Non-structural Response of the 7-Story Van Nuys Hotel to the Northridge Earthquake of January 17, 1994. 6th US National Conference on Earthquake Engineering*. Seattle, Washington, U.S.A.

38. Goel, R. K. & Chopra, A. K. (2004) Evaluation of Modal and FEMA Pushover Analysis: SAC Buildings. *Earthquake engineering and structural dynamics, 20***,** 225-254.

39. Goltabar A. M., Kami R. S. & Ebad, A. (2008). Study of Impact between Adjacent Structures during of Earthquake and their Effective Parameters, *American Journal of Engineering and Applied Sciences 1 (3),* 210-218

40. Gorenc, B. E., Tinyou, R., & Syam, A. (2005). *Steel Designers Handbook*. Sydney: University of New South Wales Press.

41. Grierson, D. E. (2006). Optimal Performance-Based Seismic Design Using Modal Pushover Analysis. *Journal of Earthquake Engineering, 10***,** 73-96.

42. Gunawardena, T., Mendis, P. & Ngo, T., (2016). Innovative Flexible Structural System Using Prefabricated Modules. *Journal of Architectural Engineering, 22(2)*, American Society of Civil Engineers.

43. Gupta A. K. & Cordero K. (1981*). Combination of Modal Responses, Transactions of the 6th International Conference on Structural Mechanics in Reactor Technology*, Paper No. K7/5, Paris, France, North-Holland Publishing Company, for the Commission of the European Communities.

44. Gupta, B. & Kunnath, S. (2000). Adaptive Spectra based Pushover Procedure for Seismic Evaluation of Structures. *Earthquake Spectra, 16***,** 367-391.

45. Guyader, A. C. & Iwan, W. D. (2006). Determining Equivalent Linear Parameters for Use in a Capacity Spectrum Method of Analysis. *Journal of structural engineering, 132***,** 59-67.

46. Haidar, N. (2011). Mathematical Representation of Bolted-Joint Stiffness: A New Suggested Model. *KSME journal 25(11),* 2827.

47. Herath, N. (2011). *Behaviour of Outrigger Braced Tall Buildings Subjected to Earthquake Loads*. (Doctoral Thesis), The University of Melbourne.

48. Hickory Group (2014). Retrieved December 20, 2014, from http://www.hickory.com.au/ projects/one9-apartments

49. Higginbotham, A. (2015, November 4). *Lift off: When will elevators finally reach the 21st century?* Retrieved July 09, 2016, from http://www.wired.co.uk/article/21st-century-lift-can-navigate-buildings

50. Hong, S.G., Cho, B.H., Chung, K.S. & Moon, J.H. (2011), Behaviour of Framed Modular Building System with Double Skin Steel Panels. *Journal of Constructional Steel Research, 67,* 936-946.

51. IBC: 2009: *International Building Code*, International Code Council, Falls Church, Virginia.

52. Idriss, I. M. (1990). *Response of soft soils during earthquakes. Proceedings HB Seed Memori.*

53. Irvin, T. (2013). Effective Modal Mass and Modal Participation Factors, Revision H, <http://www.vibrationdata.com/tutorials/ModalMass.pdf>, (Dec 10, 2014)

54. IrwinConsult Engineering Consultants. (n.d.). Retrieved August 27, 2016, from http://www.irwinconsult.com.au/

55. Jaillon, L., Poon, C. S. & Chiang, Y. H. (2009). Quantifying the Waste Reduction Potential of Using Prefabrication in Building Construction in Hong Kong. *Waste Management*, *29(1),* 309-320.

56. Jan, T. S., Liu, M. W. & Kao, Y. C. (2004). An Upper-bound Pushover Analysis Procedure for Estimating the Seismic Demands of High-Rise Buildings. *Engineering Structures, 26*, 117-128. *al symposium.* University of California, Berkeley.

57. Jie, Z. Z.-X., Zhao W., Zhu H., & Zhou C. (2007). Safety Analysis of Optimal Outriggers Location in High Rise Building Structures. *Journal of Zhejiang Science A, 8*, 264-269.

58. Kalkan, E. & Kunnath, S. K. (2006). Adaptive Modal Combination Procedure for Nonlinear Static Analysis of Building Structures. *Journal of Structural Engineering, 132*, 1721-1731.

59. Kappos A. J. & Panagopoulos, G. (2004), Performance-Based Seismic Design of 3d R/C Buildings Using Inelastic Static and Dynamic Analysis Procedures, *ISET Journal of Earthquake Technology, Paper No. 444, Vol. 41, No. 1,* March 2004, pp. 141-158

60. Kulak, G. L., Fisher, J. W., & Struik, J. A. (1987). *Guide to Design Criteria for Bolted and Riveted Joints*. New York: Wiley.

61. Lawson, M., Byfield, M., Popo-Ola, S. & Grubb, J. (2008), Robustness of Light Steel Frames and Modular Construction, *Structures & Buildings*, *161*, 3-16.

62. Lawson, R. M. & Richards, J. (2010), Modular Design for High-Rise Buildings, *Structures & Buildings*, *163,* 151-164.

63. Lawson, R. M., Ogden, R. G. and Bergin, R. (2012). "Application of Modular Construction in High-rise Buildings", *Journal of Architectural Engineering*, American Society of Civil Engineers, 148-154.

64. Lee, J. (2011). *Blind Bolted Connections for Steel Hollow Section Columns in Low Rise Structures* (Doctoral Thesis), The University of Melbourne.

65. Lew, M., Naeim, F., Hudson, M. B. & Korin, B. O. (2008). *Challenges in specifying Ground Motions for Design of Tall Buildings in High Seismic Regions of the United States. The 14th World Conference on Earthquake Engineering.* Beijing, China.

66. Lin, Y. Y. & Miranda, E. (2004). Non Iterative Capacity Spectrum Method Based on Equivalent Linearization for Estimating Inelastic Deformation Demands of Buildings. *Journal of Structural Mechanics and Earthquake Engineering, 21***,** 113-119.

67. Luco, N. & Bazzurro, P. (2004). *Effects of Earthquake Record Scaling on Nonlinear Structural Response. Report on PEERLL Program Task 1G00*, Pacific Earthquake Engineering Research

68. Lusby-Taylor, P., Morrison, S., Ainger, C. & Ogden, R. (2004), Design and Modern Methods of Construction, *The Commission for Architecture and the Built Environment (CABE),* London

69. Mahaney, J., Paret, T. F., Kehoe, B. E. & Freeman, S. A. (1993). *The Capacity Spectrum Method for Evaluating Structural Response during the Loma Prieta Earthquake. National Earthquake Conference*, Oakland, CA, U.S.A, Earthquake Engineering Research Institute.

70. Martino, R. & Kingsley, E. S. G. (2004). *Nonlinear Pushover Analysis of RC Structures*. ASCE.

71. McIntosh, J. (2013), The Implications of Post Disaster Recovery for Affordable Housing. Tiefenbacher, J. (ed.) Approaches to Disaster Management: Examining the Implications of Hazards, Emergencies and Disasters. Rijeka (Croatia), Intechation, *Waste and Resource Management, 2(1),* 65-72.

72. Mendis, P. Ngo, T. Haritos, N. Hira, A, Samali, B. & Cheung, J. (2007). Wind Loading on Tall Buildings, *EJSE Special Issue: Loading on Structures.* http://www.ejse.org/Archives.htm

73. Moehile, J. P. (2006). Seismic Analysis, Design, and Review for Tall Buildings. *The Structural Design of Tall and Special Buildings, 15***,** 495-513.

74. Moghada, A. S. (2002). *Pushover Procedure for Tall Buildings. Proceedings of the 12th European Conference on Earthquake Engineering.* London, UK, Elsevier Science Ltd.

75. Mohraz, B. (1976). A Study of Earthquake Response Spectra for Different Geological Conditions. *Bulletin of the Seismological Society of America*, *66*, 915-935.

76. Musto J. C. & Konkle N. R. (2006). Computation of Member Stiffness in the Design of Bolted Joints. *ASME Journal of Mechanical Design. 2005; 128(6),* 1357-1360.

77. Newmark, N. M. & Hall, W. J. (1982). *Earthquake Spectra and Design*. California, USA, Earthquake Engineering Research Institute.

78. Nukala, P. K. (1999). *Implementation of Modal Combination Rules for Response Spectrum Analysis using GEMINI.* US Department of Commerce

79. Osmani, M., Glass, J. & Price, A. (2006). Architect and Contractor Attitudes to Waste Minimisation, *Waste and Resource Management*, *2(1),* 65-72.

80. Oxfam (2003). *Guidelines for Post Disaster Housing, Version 1*. Oxford, Oxfam.

81. Paret, T. F., Sasaki, K. K., Eilbeck, D. H. & Freeman, S. A. (1996). *Approximate Inelastic Procedures to Identify Failure Mechanisms from Higher Mode Effects. 11th World Conference on Earthquake Engineering*

82. Paulay, T. & Priestley, M. J. N. (1992). *Seismic Design of Reinforced Concrete and Masonry Buildings*, New York, John Wiley and sons, Inc.

83. PEER (2014). PEER Ground Motion Database. Pacific Earthquake Engineering Research Center, University of California, Berkeley.

84. Poursha, M., Khoshnoudian, F. & Moghadam, A. S. (2009). A Consecutive Modal Pushover Procedure for Estimating the Seismic Demands of Tall Buildings. *Engineering Structures, 31***,** 591-599.

85. Poursha, M., Khoshnoudian, F. & Moghadam, A. S. (2010). Assessment of Modal Pushover Analysis and Conventional Nonlinear Static Procedure with Load Distributions of Federal Emergency Management Agency for High Rise Buildings. *The structural design of tall and special buildings, 19***,** 291-308.

86. Powell, G. H. (2013). Static Pushover Methods - Explanation, Comparison and Implementation. Retrieved on August 29, 2016 from https://wiki.csiamerica.com/display/perform/Static+pushover+methods+-+explanation,+comparison+and+implementation

87. Priestley, M. J. N., Calvi, G. M. & Kowalsky, M. J. (2007) *Displacement Based Seismic Design of Structures,* Pavia, Italy, IUSS Press.

88. Rakesh, K. G. & Chopra, A. K. (2004). Evaluation of Modal and FEMA Pushover Analyses: SAC Buildings. *Earthquake Spectra, 20***,** 225-254.

89. Rakesh, K. G., & Chopra, A. K. (2005). Extension of Modal Pushover Analysis to Compute Member Forces. *Earthquake Spectra*, *21***,** 125-139.

90. Roosli, R., Vebry, M., Othuman M., Azree M. & Ismail, M. (2012). Building and Planning of Post-Disaster Rehabilitation and Reconstruction, *International Journal of Academic Research; Jan2012*, *Vol. 4 Issue 1*, p194

91. Rosenblueth, E., & Elorduy, J. (1969). *Responses of Linear Systems to Certain Transient Disturbances*, *Proceedings of the Fourth World Conference on Earthquake Engineering,* Santiago, Chile.

92. SAC/FEMA 350: 2000: *Recommended Seismic Design Criteria for New Steel Moment-Frame Buildings*. Washington, D.C.,

93. Sasaki, K. K., Freeman, S. A., & Paret T. F. (1998). *Multi Mode Pushover Procedure (MMP)- A Method to Identify The Effect of Higher Modes in a Pushover Analysis*. *6th U S National Conference of Earthquake Engineering.* Seattle, W A.

94. SEAOC: 1995: *Performance Based Seismic Engineering for Buildings*. In California, E. A. O. (ed.) Vision 2000. Sacramento, CA.

95. SEAOC: 1999: *Recommended Lateral Force Requirements and Commentary, 7th Edition*, Appendices G and I.

96. SEAW (Structural Engineers Association, Washington) (2011). Great East Japan (Tohoku) Earthquake and Tsunami. *The Japan Journal*, December, 2011.

97. Seed, H. B., Ugas, C. & Lysmer, J. (1974). *Site Dependent Spectra for Earthquake Resistant Design.* Report EERC 74-12. Berkeley, USA, University of California

98. Sharpe, R.D. (1974). *The Seismic Response of Inelastic Structures*, (Doctoral Thesis), Department of Civil Engineering, University of Canterbury

99. Shigley J. E. and Mischke C. R. (2006). *Mechanical Engineering Design, Eighth Ed.,* McGraw-Hill, New York, USA.

100. Stewart, J. P., Chiou, S. J., Bray, J. D., Grave, S. R. W., Somerville, P. G. & Abrahamso, N. A. (2001). *Ground Motion Evaluation Procedures for Performance-Based Design*. *PEER-2001/09.* University of California: Berkeley, CA, Pacific Earthquake Engineering Research Center.

101. Sullivan, T. J., Priestley, M. J. N. & Calvi, G. M. (2006). Seismic *Design of Frame-Wall Structure.* ROSE Research Report No 2006/02. Pavia.

102. Taranath, B. S. (1988). *Structural Analysis and Design of Tall Buildings*, New York: McGraw-Hill.

103. Tas, N., Tas, M. & Cosgun, N. (2010). Study on Permanent Housing Production after 1999 Earthquake in Kocaeli (Turkey), *Disaster Prevention and Management*, *Vol. 19 Iss: 1*, pp.6 - 19

104. Tas, N., Tas, M. & Cosgun, N. (2011). Permanent Housing Production Process after 17 August 1999 Marmara Earthquake in Turkey. *International Journal of Strategic Property Management*, *15,* 312-328

105. UPSeis. (n.d.). Retrieved August 06, 2016, from http://www.geo.mtu.edu/UPSeis/Mercalli.html

106. USGS. (1989). Retrieved August 08, 2016, from https://earthquake.usgs.gov/learn/topics/measure.php

107. USGS. (2012). Retrieved 18 December 2012, from http://earthquake.usgs.gov/earthquakes/eqarchives/year/eqstats.php

108. VanGaasbeek C. J. (2011). *Numerical Modeling of Bolted Joints. An Applied Finite Element Analysis Approach* (Masters Thesis), Polytechnic Institute, Connecticut, USA

109. Whitaker, A., Constantinou, M., & Tsopelas, P. (1998). Displacement Estimates for Performance Based Seismic Design. *ASCE, Journal of Structural Engineering, 124*, 905-912.

110. Wileman, J., Choudhury, M., & Green, I. (1991). Computation of Member Stiffness in Bolted Connections, *ASME Journal of Mechanical Design, 113*, pp. 432–437.

111. Willford, M., Whittaker, A. & Klemencic, R. (2008). *Recommendations for the Seismic Design of High-Rise Buildings.* Council on Tall Buildings and Urban Habitat.

112. Wilson, J. L. (2000). *Earthquake Design And Analysis Of Tall Reinforced Concrete Chimneys. Department of Civil and Environmental Engineering*, The University of Melbourne.

113. Yan, C., Wilkinson, S., Potangaroa, R. & Seville, E. (2010). Resourcing Challenges for Post-Disaster Housing Reconstruction: A Comparative Analysis. *Building Research & Information*, 38, 247-264

114. Yan, C., Wilkinson, S., Potangaroa, R. & Seville, E. (2011). Identifying Factors Affecting Resource Availability for Post-Disaster Reconstruction: A Case Study in China, *Construction Management & Economics*, *29,* 37-48.

Appendix A – RUAUMOKO Model

An extract from the input file for the RUAUMOKO model is given below for further reference. (Since the text entered for the entire model is too long to be included in the thesis, only key inputs are shown).

```
10 Storey Modular Building with Earthquake Time Histories
2       1       0       0       1       0       0       0       1       0       ! Control Parameters
0       0       1       ! EQ Directions
1700    4078    11      12      1       2       9.81    5       5       0.005   26      1       ! Input
5       5       10      1.1     10      10      10      0       0       0       1       0       ! Output
DEFAULT
0       0       0.00001 0       0       0       0       0       0       0       0       ! Iterations

NODES   0
1       0       0       1.8     1       1       1       0       0       0       0       0
2       0       0       5.4     1       1       1       0       0       0       0       0
3       0       0       9       1       1       1       0       0       0       0       0
4       4.2     0       1.8     1       1       1       0       0       0       0       0
```

```
5       4.2     0       5.4     1       1       1       0       0       0       0       0
.
.
.
ELEMENTS        0
1       2       31      38      0       0       z
2       2       32      39      0       0       z
3       2       33      40      0       0       z
4       2       34      41      0       0       z
5       2       35      42      0       0       z
6       2       36      43      0       0       z
7       2       37      44      0       0       z
8       2       31      32      0       0       x
9       2       32      33      0       0       x
10      2       33      34      0       0       x
11      2       34      35      0       0       x
12      2       35      36      0       0       x
13      2       36      37      0       0       x
14      2       38      39      0       0       x
15      2       39      40      0       0       x
.
.
.
PROPS
1       BEAM "180 PFC"
1       4       0       0       0       2       0       0       0       0
2.00E+08        7.69E+07        2.66E-03 8.10E-08 1.41E-05 1.51E-06 1.65E-03 1.08E-03 6.42E-02 0       0.20748
0
0       0       0.04    0.04
```

0 0 0 0
1197 -1197 0 0 2 0
81.9 -81.9 24.2 -24.2

2 BEAM "300 PFC"
1 4 0 0 0 2 0 0 0 0
2.00E+08 7.69E+07 5.11E-03 2.90E-07 7.24E-05 4.04E-06 2.88E-03 2.40E-03 7.47E-02 0 0.39858
0
0 0 0.04 0.04
0 0 0 0
2069 -2069 0 0 2 0
253.8 -253.8 52.7 -52.7

3 BEAM "180 PFC-col"
1 4 0 0 0 2 0 0 0 0
2.00E+08 7.69E+07 2.66E-03 8.10E-08 1.41E-05 1.51E-06 1.65E-03 1.08E-03 6.42E-02 0 0.20748
0
0 0 0.04 0.04
0 0 0 0
1197 -1197 0 0 2 0
81.9 -81.9 24.2 -24.2

4 BEAM "100x75x8 UA"
1 4 3 3 0 0 0 0 0 0
2.00E+08 7.69E+07 1.31E-03 2.80E-08 1.30E-06 6.26E-07 5.85E-04 7.80E-04 3.340E-02 -4.530E-02 0.10218
0

5 QUADRILATERAL "Slab 125"
0 0 3.30E+07 0.2 0.125 40.25 2 0 0 0

```
6       QUADRILATERAL  "Slab 100"
0       0       3.30E+07        0.2     0.100   25.2    2       0       0       0

7       BEAM “100 infill Wall”
1       4       0       0       0       0       0       0       0       0
3.3E+07 1.38E+10        0.18    5.79E-04 1.5E-04 4.86E-02 0.15  0.15    0       0       4.32
0

8       SPRING  "Connection"
2       1       0       0       0       0       0
700000  500000  700000  700000  700000  700000  3.06    1       1
480     -480    480     -480    480     -480    1
4146    -4146   613     -613    4146    -4146   2

9       BEAM "220x150x14.2 SHS Column"
1       4       0       0       0       2       0       0       0       0
2.10E+08        8.08E+07        9.82E-03 6.80E-05 6.30E-05 3.53E-05 4.37E-03 6.25E-03 0       0       0.77087
0
0       0       0.04    0.04
0       0       0       0
3435.25 -3435.25 0      0       1.5     0
248.75  -248.75 192.045 -192.045

10      BEAM "220x150x14.2 SHS Column"
1       4       0       0       0       2       0       0       0       0
2.10E+08        8.08E+07        9.82E-03 6.80E-05 6.30E-05 3.53E-05 4.37E-03 6.25E-03 0       0       0.77087
0
0       0       0.04    0.04
```

```
0          0          0          0
3435.25    -3435.25   0          0          1.5        0
248.75     -248.75    192.045    -192.045

11         BEAM "220x150x14.2 SHS Column"
1          4          1          1          0          2          0          0          0          0
2.10E+08              8.08E+07              9.82E-03   6.80E-05   6.30E-05   3.53E-05   4.37E-03   6.25E-03   0          0          0.77087
0
0          0          0.04       0.04
0          0          0          0
3435.25    -3435.25   0          0          1.5        0
248.75     -248.75    192.045    -192.045

WEIGHTS              0          ! 'S.Dead + 0.3 Live' has been added to the weight of the slabs
1          0          0          0          0          0          0
1700       0          0          0          0          0          0

LOADS
1          0          0          0          0          0          0
1700       0          0          0          0          0          0

EQUAKE
6          4          0.005      1          -1
```

Appendix B – Sample Design of a Module to Module Connection

The sample design is carried out for the connection shown below. All steel members are considered to be having a yield strength of 350 MPa and the bolts are all considered to be of Class 8.8.

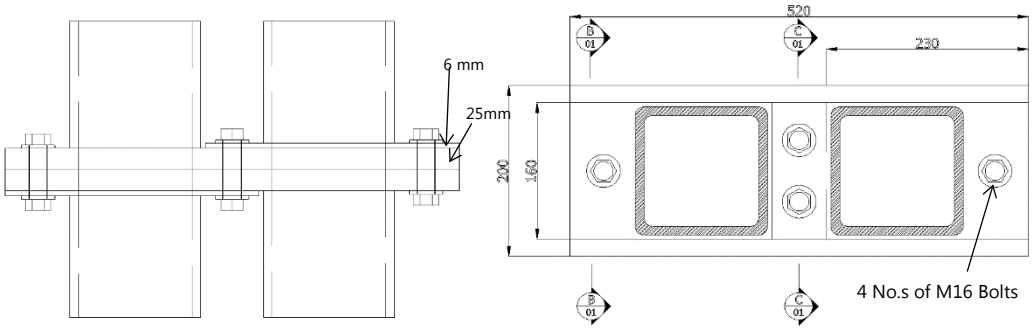

The design capacities of this connection can be calculated as follows;

Reference	Calculation	Result
AS 4100: 1998	Number of shear planes considered are as follows; Bolts in the middle = 3 (assume 1 shear plane in the threaded region) Bolts in the corners = 2 (assume 1 shear plane in the threaded region for only one of the corner bolts)	
C 9.3.2.1	$V_f = 0.62 k_r f_{uf} (n_n A_c + n_x A_0)$ Strength Limit State: Calculation of Nominal Shear Capacity The calculation for one middle bolt is as follows; $V_f = 0.62 \times 1 \times 800\ N/mm^2 \times (1 \times 144\ mm^2 + 2 \times 201\ mm^2)$ $= 270.8\ kN$ $\emptyset V_f = 0.8 \times 270.8 = 216.6\ kN$	For one middle bolt; $\emptyset V_f = 216.6\ kN$
C9.3.2.4	Check for bearing (V_b) is as follows; $V_b = 3.2 t_p d_f f_{up}$ The calculation for one of the 6 mm plies for crushing under the pretension of one of the bolts is as follows; $V_b = 3.2 \times 6\ mm \times 16\ mm \times 450\ N/mm^2$ $= 138.2\ kN$ $\emptyset V_b = 0.9 \times 138.2 = 124.4\ kN$ Therefore, all bolt pretensions applied need to be less than 138.2 kN each.	For one 6mm ply; $\emptyset V_b = 124.4\ kN$

	Check for tear-out failure (V_p) is as follows; $V_p = a_e t_p f_{up}$ The calculation for one of the 6 mm plies for tear-out near one of the bolts is as follows; $V_p = 35\ mm \times 6\ mm \times 450\ N/mm^2$ $= 94.5\ kN$ $\emptyset V_p = 0.9 \times 94.5 = 85.1\ kN$ Therefore the tear-out capacity of the full connection would be 340 kN (85.1 kN x 4).	For one 6mm ply at one bolt; $\emptyset V_p = 85.1\ kN$
9.3.3.3	The combined capacity for shear and tensile bearing shall be checked for the design values as follows; $\left(\frac{V_f^*}{\emptyset V_f}\right)^2 + \left(\frac{N_{tf}^*}{\emptyset N_{tf}}\right)^2 \leq 1$	
9.3.3.1	Serviceability Limit: Calculation of Slip Resistance (V_{sf}/ $F_{s,RD}$) This connection shall be addressed as a 'Slip Critical' connection; $V_{sf} = \mu n_{ei} N_{ti} k_b$ Following the AJAX Fastener Handbook (1999), a value of 59.2 kN is considered for N_{ti} and the calculation for slip resistance for one of the corner bolts that has just one shear plane is as follows; $V_{sf} = 0.2 \times 1 \times 59.2\ kN \times 1 = 11.8\ kN$	

	$\emptyset V_{sf} = 0.7 \times 11.8 = 8.26\ kN$ The slip would therefore occur at a load of 8.26 kN for the first bolt which has the lowest number of shear planes.	For the corner bolt with one shear plane; $\emptyset V_{sf} = 8.26\ kN$